TECHNISCHE UNIVERSITÄT
CHEMNITZ

(Ethynyl-)Ferrocenyl Phosphine Palladium Complexes and (Bis-)Phosphinoimidazol(e/ium) Compounds and their Application in Homogeneous Catalysis

von der Fakultät für Naturwissenschaften der Technischen Universität Chemnitz

genehmigte Dissertation zur Erlangung des akademischen Grades

doctor rerum naturalium

(Dr. rer. nat.)

vorgelegt von Diplom-Chemikerin Bianca Milde

geboren am 17. August 1983 in Lichtenstein

eingereicht am: 03. April 2012

Erstgutachter: Prof. Dr. Heinich Lang

Zweitgutachter: Prof. Dr. Stefan Spange

Tag der Verteidigung: 09. Juli 2012

Bibliographische Beschreibung und Referat

Bianca Milde

(Ethynyl-)Ferrocenyl Phosphine Palladium Complexes and (Bis-)Phosphino-imidazol(e/ium) Compounds and their Application in Homogeneous Catalysis

Technische Universität Chemnitz, Fakultät für Naturwissenschaften

Dissertation 2012, 239 Seiten

Die vorliegende Dissertation beschäftigt sich mit der Synthese, der Charakterisierung und der Anwendung neuartiger Phosphane in homogenkatalytischen Reaktionen. Dabei wurden die Ferrocenyl- und Ferrocenylethinylphosphan-Palladium und Ferrocenylethinylphosphan-Ruthenium Komplexe in der Palladium-vermittelten Mizoroki-Heck- und Suzuki-Miyaura-Reaktion sowie der Ruthenium-katalysierten Synthese von *β*-Oxopropylestern verwendet. Der Schwerpunkt lag dabei auf der Untersuchung des Einflusses der elektronischen und räumlichen Eigenschaften der Phosphanliganden auf die Aktivität und Produktivität der entsprechenden Katalysatoren in den homogenkatalytischen Reaktionen.

Weiterhin beschäftigt sich die vorliegende Arbeit mit der Synthese und Charakterisierung von funktionalisierten (Phosphino)Imidazol und (Phosphino)Imidazolium Salzen und deren Anwendung in der Suzuki-Miyaura-Reaktion. Dabei wurde neben der Untersuchung des Einflusses der Position der Phosphanylgruppe und der unterschiedlichen Substituenten ebenfalls die Auswirkung von elektronenziehenden und -schiebenden Gruppen am Phosphanrest untersucht. Die neutralen Mono- und Diphosphane wurden außerdem in der Kreuzkupplung von Arylhalogeniden und in der Synthese räumlich anspruchsvoller Biaryle verwendet. Des Weiteren wurden die (Phosphino)Imidazolium-Salze als Liganden in der Suzuki-Miyaura-Reaktion in ionischen Flüssigkeiten als Reaktionsmedium angewendet, um die Möglichkeit des Recyclings der Katalysatorphase zu untersuchen.

Stichworte: Kreuzkupplung, Mizoroki-Heck-Reaktion, Suzuki-Miyaura-Reaktion, β-Oxopropylester, (Ethinyl)Ferrocen, Palladium, Ruthenium, Phosphan, Imidazol(ium), (Spektro-)Elektrochemie.

Präambel

Im Rahmen der Promotionsarbeit an der Professur für Anorganische Chemie der Technischen Universität Chemnitz konnten fünf, das Thema der Promotion betreffende, Publikationen erstellt werden. Diese sind bereits veröffentlicht, im Druck, zur Veröffentlichung angenommen bzw. eingereicht. Alle Publikationen wurden unter Anleitung von Herrn Prof. Dr. Heinrich Lang selbstständig und in englischer Sprache verfasst. Im Falle von Publikationen, welche in arbeitsgruppeninterner Kooperation erstellt wurden, wird an entsprechender Stelle verwiesen.

Alle diese Promotionsschrift betreffenden Manuskripte sind in inhaltlich unveränderter Form als Kapitel C bis G eingefügt worden. Die Kapitel A Einleitung (Introduction), Kapitel B Kenntnisstand (State of Knowledge) und Kapitel H Zusammenfassung (Summary) sowie die Abschnitte Inhaltsverzeichnis (Table of Contents), Abkürzungen (List of Abbreviations) und Anhang (Appendix) sind in englischer Sprache erstellt worden. Weiterhin erfolgt die Nummerierung der in der Dissertationsschrift aufgeführten chemischen Verbindungen gemäß der Bezeichnung des Manuskriptes, in welchem die wissenschaftlichen Ergebnisse veröffentlicht wurden.

Die vorliegende Promotionsarbeit wurde in der Zeit von Oktober 2007 bis Dezember 2011 unter Leitung von Herrn Prof. Dr. Heinrich Lang am Lehrstuhl für Anorganische Chemie der Technischen Universität Chemnitz durchgeführt.

Herrn Prof. Dr. Heinrich Lang

danke ich für die gewährten Freiheiten bei der Bearbeitung des Themas, die anregenden Diskussionen sowie für die großzügige Unterstützung dieser Arbeit und das mir entgegengebrachte Vertrauen.

„Wer all seine Ziele erreicht hat,

hat sie sich als zu niedrig ausgewählt.“

(Herbert von Karajan)

Table of Contents

List of Abbreviations

Å	Angstrom
Ac	Acetyl, CH_3CO
Acac	Acetylacetonate, $C_5H_7O_2$
Ad	Adamantyl, $C_{10}H_{15}$
Ar	Aryl
Eq	Equivalent
BDMIM	1-*n*-Butyl-2,3-dimethyl imidazolium, $C_9H_{17}N_2$
BMIM	1-*n*-Butyl-3-methyl imidazolium, $C_8H_{15}N_2$
bpy	2,2'-Bipyridine, $C_{10}H_8N_2$
n-Bu	*n*-Butyl, *n*-C_4H_9
t-Bu	*t*-Butyl, *t*-C_4H_9
Cod	Cyclo-1,5-octadiene, C_8H_{12}
Cy	Cyclohexyl, $^cC_6H_{11}$
p-cymene	1-Methyl-4-*i*-propyl benzene, 1-CH_3-4-*i*-Pr-C_6H_4
dba	Dibenzylideneacetone, $C_{17}H_{14}O$
dcpe	1,2-Bis(dicyclohexylphosphino)ethane
dec.	Decomposition
dippb	1,4-Bis(di-*i*-propylphosphino)butane
dippf	1,1'-Bis(di-*i*-propylphosphino)ferrocene, $Fe(\eta^5\text{-}C_5H_4P(i\text{-}Pr)_2)_2$
dippp	1,3-Bis(di-*i*-propylphosphino)propane
DMIM	1,3-Dimethyl imidazolium, $C_5H_9N_2$
DMF	*N*,*N*-Dimethylformamide, $(CH_3)_2NCHO$
dppe	1,2-Bis(diphenylphosphino)ethane
dppp	1,3-Bis(diphenylphosphino)propane
dppf	1,1'-Bis-(diphenylphosphino)ferrocene, $Fe(\eta^5\text{-}C_5H_4PPh_2)_2$
dtbpf	1,1'-Bis-(di-*t*-butylphosphino)ferrocene, $Fe(\eta^5\text{-}C_5H_4P(t\text{-}Bu)_2)_2$
Et	Ethyl, C_2H_5
Fc	Ferrocenyl, $Fe(\eta^5\text{-}C_5H_4)(\eta^5\text{-}C_5H_5)$
Fur	2-Furyl, $^cC_4H_3O$
IUPAC	International Union of Pure and Applied Chemistry
Irrev.	Irreversible
L	Ligand

m	*meta*-Position
M	Metal
MCM-41	Mobil Composition of Matter No. 41
Me	Methyl, CH_3
Mes	Mesityl, 2,4,6-trimethylphenyl, 2,4,6-$(CH_3)_3C_6H_2$
Mp	Melting point
NHC	*N*-heterocyclic carbene
n-Oct	*n*-Octyl, *n*-C_8H_{17}
o	*ortho*-Position
p	*para*-Position
Ph	Phenyl, C_6H_5
i-Pr	*i*-Propyl, *i*-C_3H_7
R	Single-bonded organic group
r.m.s.	Root mean square
Rc	Ruthenocenyl, Ru(η^5-C_5H_4)(η^5-C_5H_5)
S	Solvent
sc	*Supercritical*
SRPC	Slow-Release Precatalyst
Tf	Triflyl, Trifluoromethanesulfonyl, CF_3SO_2
TFA	Trifluoroacetate, CF_3CO_2
thf	Tetrahydrofuran, $^cC_4H_8O$
TMS	Trimethylsilyl, $Si(CH_3)_3$
TOF	Turnover frequency [mol product / (mol catalyst · h)]
o-Tol	*o*-Tolyl, 2-$CH_3C_6H_4$
TON	Turnover number [mol product / mol catalyst]
Ts	Tosyl, 4-Toluenesulfonyl, 4-$CH_3C_6H_4SO_2$
X	Halide (F, Cl, Br, I)

EA	**Elemental Analysis**
Anal. Calc.	Calculated values
Found	Found values

FT-IR	**Fourier Transformed Infrared** spectroscopy
$\tilde{\upsilon}$	Wave number / cm^{-1}

m	Middle intensity
s	Strong intensity
vs	Very strong intensity
w	Weak intensity
v	Stretching vibration
δ	Bending vibration

MS	**Mass Spectrometry**
ESI	Electrospray Ionization
HR	High resolution
$[M]^+$	Molecular-ion peak
m/z	Mass-to-charge ratio
TOF	Time-of-Flight

NMR	**Nuclear Magnetic Resonance** spectroscopy
δ	Chemical shift / ppm
d	Doublet
HSQC	Heteronuclear Single Quantum Coherence
HMBC	Heteronuclear Multiple Bond Correlation
$^nJ_{XY}$	Coupling constant over *n* bonds between core X and core Y / Hz
m	Multiplet
ppm	Parts per million
pt	Pseudotriplet
s	Singlet
sept	Septet
t	Triplet

UV/Vis	**Ultraviolet/Visible light** spectroscopy
ε	Coefficient of extinction / $L \cdot mol^{-1} \cdot cm^{-1}$
λ	Wavelength / nm

NIR	**Near Infrared** spectroscopy
IVCT	Intervalence Charge Transfer
LMCT	Ligand to Metal Charge Transfer

$\Delta\nu_{1/2}$	Band-width at half height / cm^{-1}
$(\Delta\nu_{1/2})_{theo}$	Theoretical band-width at half height / cm^{-1}
ε_{max}	Extinction coefficient at the band maximum / $L \cdot mol^{-1} \cdot cm^{-1}$
ν_{max}	Maximum value of the absorption / cm^{-1}
Γ	Electronic coupling parameter

CV	**Cyclic Voltammetry**
LSV	Linear Sweep Voltammetry
SWV	Square Wave Voltammetry
E^0	Redox potential, $E^0 = \frac{E_{pa}+E_{pc}}{2}$
E_1^0	Potential of the 1st redox process
E_2^0	Potential of the 2nd redox process
ΔE_p	Difference between oxidation and reduction potential, $\Delta E_p = (E_{pa} - E_{pc})$
ΔE^0	Potential difference between two redox processes
$E_{ox\text{-}irrev}$	Irreversible oxidation potential
E_{pa}	Anodic peak potential
E_{pc}	Cathodic peak potential
$E_{red\text{-}irrev}$	Irreversible reduction potential
OTTLE	Optically Transparent Thin-Layer Electrode
SCE	Saturated Calomel Electrode

A Introduction

1 Homogeneous Catalysis

Catalysis is the key for successful sustainable synthetical methods in industrial chemistry. [A1] It is indispensable for the synthesis of various bulk and fine chemicals as well as natural products and specialty chemicals. [A1,A2] The term "catalysis" (greek, *καταλισισ*: dissolution) leads back to Jöns Jakob Berzelius in 1836, when he proposed the existence of a "catalytic force" during a systematical investigation of observations reported by other scientists. [A2b,A3] Later, in 1894, Wilhelm Ostwald gave the modern definition for catalysis which is still generally accepted:

"Catalysis is the acceleration of a chemical reaction, which proceeds slowly, by the presence of a foreign substance." [A4]

Furthermore, he defined the term "catalyst" in 1902:

"A catalyst is a substance that changes the velocity of a reaction without itself being changed by the process." [A2b,A3g;A5a]

In 1909 Ostwald received the Nobel Prize in chemistry *"in recognition of his work on catalysis and for his investigations into the fundamental principles governing chemical equilibria and rates of reaction".* [A5] Thus, he was the pioneer who strongly influenced the developments in the field of catalysis for decades.

In general, catalysis can be classified, for example by the reaction medium, into two main categories: heterogeneous (multiphasic) and homogeneous (monophasic) catalysis. [A1c,A2a,d,A3f,g,A6] Moreover, in recent years, various transition forms between homogeneous and heterogeneous catalysis developed rapidly, *e. g.* phase transfer catalysis, immobilized homogeneous catalysts, stabilized nanoparticles or biological catalysis (Scheme A1). [A2b,A3f,A7]

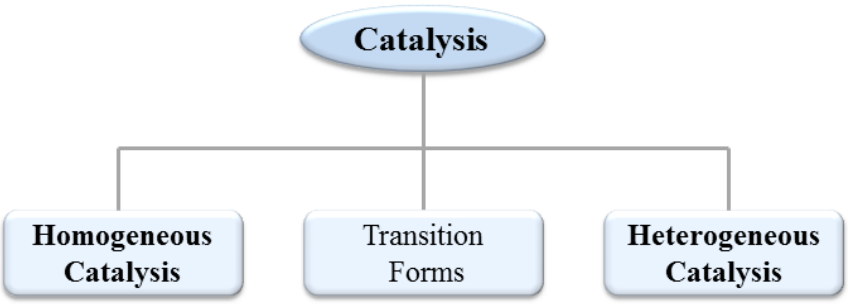

Scheme A1. Categories of catalysis.

The advantages of monophasic homogeneous catalysis in respect to multiphasic heterogeneous catalysis are the higher activities and selectivities of the catalysts as well as low catalyst concentrations and mild reaction conditions. Furthermore, it is possible to customize the ligands on the catalytically active metal center to attune them to special synthetic problems. However, the major drawbacks of homogeneous catalysts are the difficult and hence expensive separation from the product and the low thermal stability. [A1a,c,A6a,b,A8] In Table A1 the most important advantages and disadvantages of both categories are summarized.

Table A1. Comparison of homogeneous and heterogeneous catalysis. [A1a,c,A6a,b,A8]

	Homogeneous Catalysis	**Heterogeneous Catalysis**
active centers	all metal atoms	only surface atoms
catalyst concentration	low	high
selectivity	high	low
diffusion issues	uncommon	existing
reaction conditions	mild	harsh
sensitivity toward catalyst poisoning	low	high
structure / stoichiometry	defined	undefined
variation of steric and electronic properties	possible	not possible
mechanistic understanding	plausible	difficult
thermal stability	low	high
recycling	expensive	unnecessary

Nowadays, 85 – 90 % of all chemical processes are using catalysts, whereby the more widely used ones are of heterogeneous nature. [A2b,d,A6c,d] Especially homogeneous catalysts developed fast in the last 50 years and are present in approximately 15 % of all catalytical processes (Scheme A2).

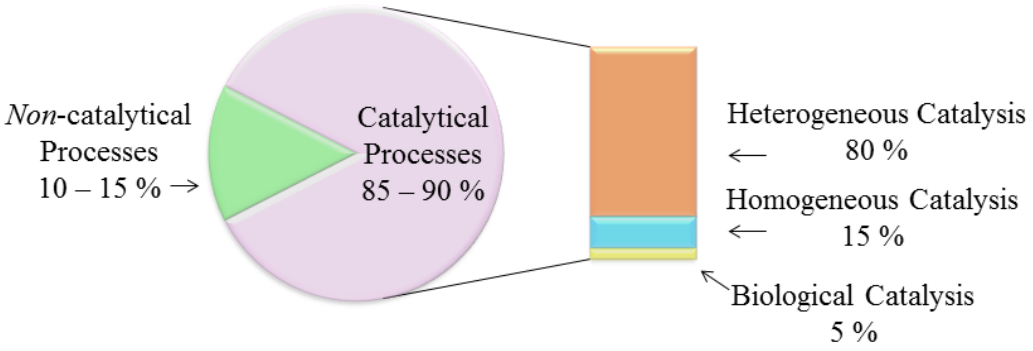

Scheme A2. Catalytic reactions in chemical industry. [A2b]

Despite the fact that heterogeneous catalysts are favored in industrial applications, the focus of research concentrates currently on homogeneous catalysts due to the better mechanistic understanding and the possibility to synthesize new *single-site* tailor-made catalysts for particular problems. [A2e,A8b] Thereby, the ligands and their electronic and steric properties, which are responsible for the catalytic activity, selectivity and stability, are of interest. [A3f,g] Furthermore, the sustainability is a major topic, since increasing environmental concerns and dwindling resources force the chemical industry to use cleaner processes. [A6b] New approaches include the recovery and recycling of the catalyst by means of immobilization of homogeneous catalysts on solid surfaces or on a soluble carrier and the use of "green solvents", for example, ionic liquids or *sc*CO_2. [A2b,A3f,A6a,A7,A9] In addition, commercializing of new processess including, for example, *C,C* cross-couplings for fine-chemical synthesis has improved in the last 20 years, due to readily available starting materials, tolerance of the catalysts toward functional groups and the generality and simplicity of the used methods. [A2d] In Scheme A3 some of the most important industrial applications of homogeneous catalysis are summarized.

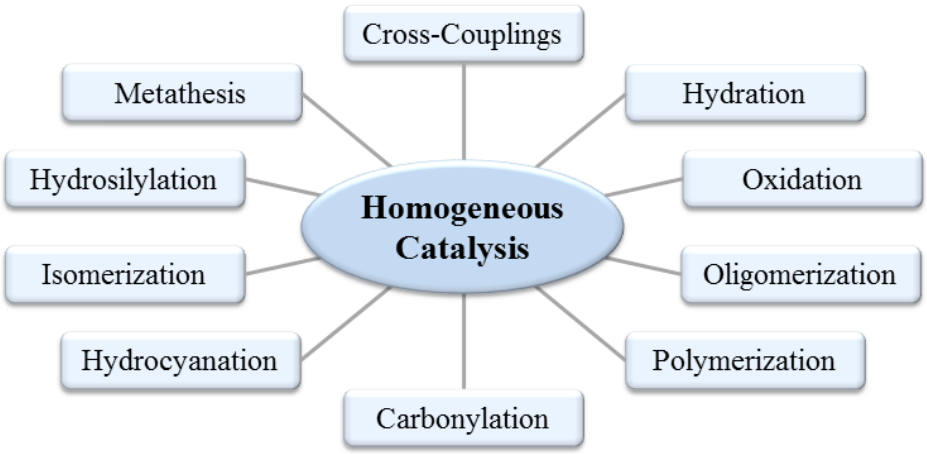

Scheme A3. Selected industrial reactions of homogeneous catalysis. [A2d]

2 References

[A1] a) M. Röper *Chem. unserer Zeit* **2006**, *40*, 126; b) M. Baerns *Basic Principles in Applied Catalysis*, *Springer-Verlag*, Berlin, Heidelberg, New York, **2004**; c) G. Emig *Chem. unserer Zeit* **1987**, *4*, 128.

[A2] For example: a) M. Beller, C. Bolm *Transition Metals for Organic Synthesis 2nd Edition, Wiley-VCH*, Weinheim **2004**; b) J. Weitkamp *Katalyse* in *Chemische Technik: Prozesse und Produkte*, ed. R. Dittmeyer, W. Keim, G. Kreysa, A.

Oberholz, *Wiley-VCH*, Weinheim, **2004**; c) L. H. Gade *Chem. unserer Zeit* **2006**, *40*, 83; d) M. Beller *Chemie, Ingenieur, Technik* **2006**, *78*, 1061; e) S. Bhaduri, D. Mukesh *Homogeneous Catalysis: Mechanisms and Industrial Applications, Wiley-Interscience*, New York, **2000**.

[A3] a) B. Lindström, L. J. Pettersson *Cattech.* **2003**, *7*, 130; b) *History of Catalysis*, URL: http://alexandria.tue.nl/repository/freearticles/591529.pdf (09.03.2012); c) A. J. B. Robertson *Platinum Metals Rev.* **1975**, *19* (2), 64; d) A. Hergesell *Ph. D. Thesis*, RWTH Aachen University, **2011**; e) G. Ertl, T. Gloyna *Z. Phys. Chem*. **2003**, *217*, 1207; f) A. Behr *Angewandte Homogene Katalyse*, *Wiley-VCH*, Weinheim, **2008**; g) D. Steinborn *Grundlagen der metallorganischen Komplexchemie*, *Teubner*, Wiesbaden, **2007**.

[A4] W. Ostwald, Abstract for *Z. phys. Chem.* **1894**, *15*, 705.

[A5] a) H. Hildebrandt *The Nobel Prize in Chemistry 1909*, URL: http://www.nobelprize.org/nobel_prizes/chemistry/laureates/1909/ (09.03.2012); b) D. Steinborn *Fundamentals of Organometallic Catalysis*, *Wiley-VCH*, Weinheim, **2012**.

[A6] a) B. Cornils, W. A. Herrmann *Applied Homogeneous Catalysis with Organometallic Compounds, VCH*, Weinheim, **1996**; b) D. J. Cole-Hamilton, R. P. Tooze *Catalyst Separation, Recovery and Recycling*, *Springer*, Dordrecht, **2006**; c) B. Cornils, W. A. Herrmann *J. Catal*. **2003**, *216*, 23; d) S. Bhaduri, D. Mukesh *Homogeneous Catalysis: Mechanisms and Industrial Applications, Wiley-Interscience*, New York, **2000**.

[A7] D. Astruc *Organometallic Chemistry and Catalysis*, *Springer*, Berlin, Heidelberg, New York, **2007**.

[A8] a) N. J. Ronde *Ph. D. Thesis*, Eindhoven University of Technology, **2004**; b) W. A. Herrmann, B. Cornils *Angew. Chem. Int. Ed. Engl.* **1997**, *36*, 1048;

[A9] For example: a) P. Wasserscheidt, T. Welton *Ionic Liquids in Organic Synthesis*, *Wiley-VCH*, Weinheim, **2003**; b) P. J. Dyson, T. J. Geldbach *Metal Catalyzed Reactions in Ionic Liquids*, *Springer*, Dordrecht, **2005**.

B State of Knowledge

1 Transition Metal-Catalyzed *C,C* Cross-Coupling Reactions

Transition metal-catalyzed cross-coupling reactions of organic electrophiles with organometallic reagents represent one of the most important ways for the formation of carbon-carbon and carbon-heteroatom bonds, respectively. [B1] A variety of organometallic reagents and organic halides, including aryl, alkyl, allyl, alkenyl and alkynyl groups, can be applied (Scheme B1). [B1a,B2] The advantages of cross-couplings over classical organic reactions are the easily accessible and inexpensive starting materials, versatile coupling methods, high productivity and selectivity as well as the tolerance concerning various functional groups and shorter reaction sequences. [B1a,B2a,B3]

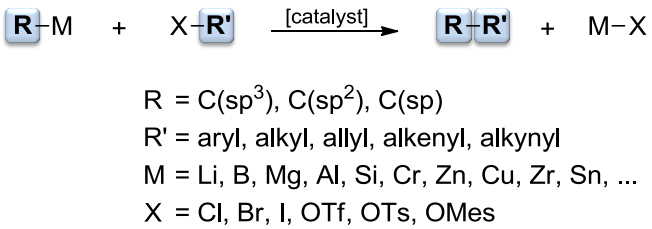

Scheme B1. Transition metal-catalyzed cross-coupling reactions.

In addition, *C,C* cross-coupling reactions are useful tools for the synthesis of complex structures, fine chemicals and natural products. However, the success of these transformations is highly dependent on the applied transition metal catalyst. [B2a] As catalysts, typically late transition metals (*e. g*. Ni, Pd, Cu) are used and especially palladium attracted much attention during the last 50 years. [B4] The advantages of palladium compared to other metals are its *non*-toxicity, its insensitivity toward oxygen and moisture and its tolerance toward numerous functional groups. [B4a] In initial research studies the most commonly applied catalysts were $[PdCl_2(PPh_3)_2]$ and $[Pd(PPh_3)_4]$. [B1c,B3a,b,B5] However, the use of stable zerovalent palladium complexes requires the dissociation of ligands which may be slow and the equilibrium may be unfavorable, thus reducing the efficiency of the catalyst. [B1c] When using palladium(II) compounds the formation of the active palladium(0) species is the crucial step, which can be accomplished by transmetalation with M-R' whereby a small amount of homo-coupled by-product R'-R' will be formed. [B1c] If using less strong alkylation agents based on boron or silicium an activating base is required, which is usually the same as in the reaction. [B1c] Nevertheless, the formed by-products may still influence the catalysis even if present in only small amounts. [B1c] However, the choice of the ligand is the key step toward a successful catalytic reaction, thus, directly influencing the catalytic cycle (Scheme B2).

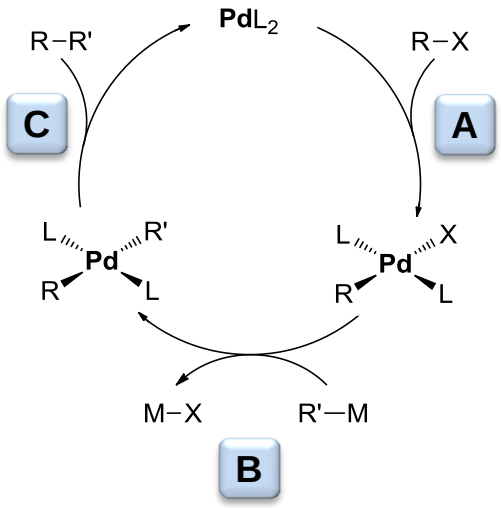

Scheme B2. General reaction mechanism for *C,C* cross-couplings utilizing a palladium catalyst.

The common mechanism of *C,C* cross-coupling reactions involves sequential oxidative addition (**A**), transmetalation (**B**), and reductive elimination (**C**). [B2a,b,B3a,B6] In general, the oxidative addition, usually the rate determining step, is favored by strong σ donating ligands which increase the electron density at the palladium and accelerate the reaction. [B1c,B7] Furthermore, electron poor aromatic halides are preferred with a decrease of reactivity of X in the order I > Br ≈ OTf >> Cl. [B2a,B7] The transmetalation is favored by electron-rich groups R' and a low steric congestion of R and R'. [B1c,B7] The reductive elimination can be influenced by weak σ donating and bulky ligands which destabilize the formed intermediate complex. [B1c,B7]

The importance and excellence of palladium-catalyzed *C,C* cross-coupling reactions in modern organic synthesis resulted in the awarding of the 2010 Nobel Prize in Chemistry for Richard F. Heck, Ei-ichi Negishi and Akira Suzuki. [B4a,B5,B9] In addition to those reactions, named after their developers, many more cross-couplings were established in the last 40 – 50 years, for example the Sonogashira, Stille or Kumada reaction. [B2c] The most important cross-coupling reactions, including the year of their first publication are depicted in Scheme B3.

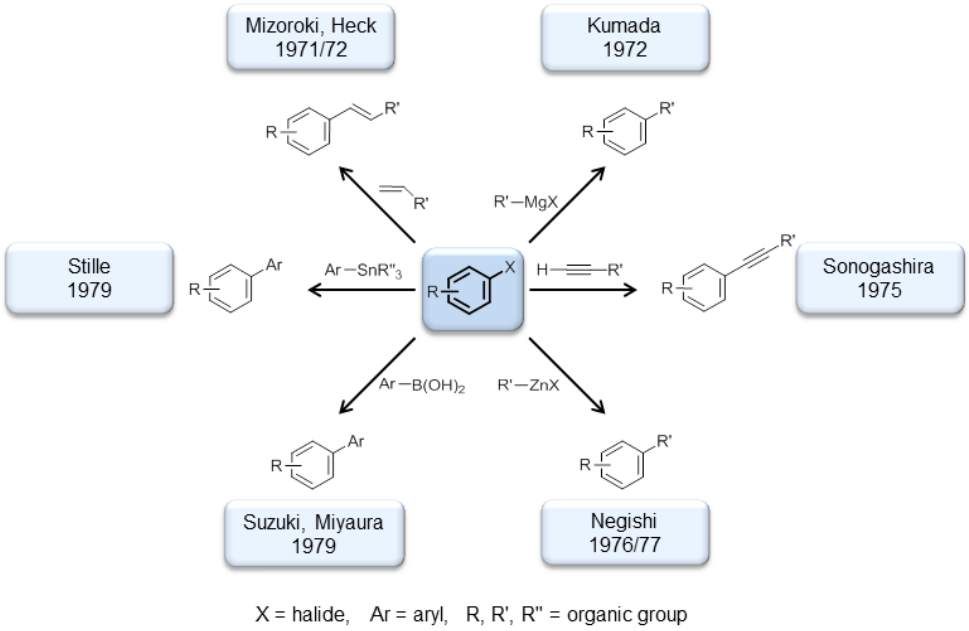

Scheme B3. Selected examples of Pd-catalyzed cross-coupling reactions.

In view of industrial application, the depicted cross-coupling reactions offer a promising opportunity of more selective routes and shorter reaction times to fine chemicals compared to classical organic synthesis. Hence, it is not surprising that since the early 1990s more and more palladium-catalyzed reactions were transferred from academic to industrial scale. [B2c] One example is the synthesis of Losartan (Scheme B4), the first angiotensin II receptor antagonist, used for the treatment of hypertension (high blood pressure) which is synthesized *via* Suzuki-Miyaura reaction and marketed by Merck & Co. Inc. [B3b]

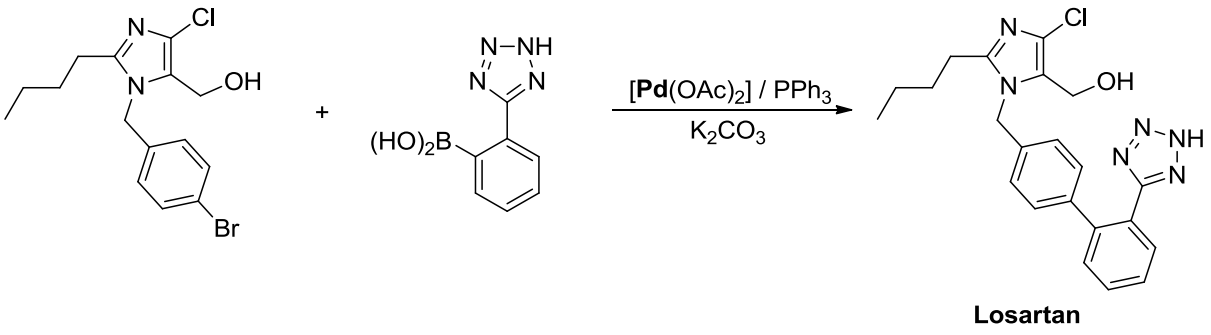

Scheme B4. Synthesis of Losartan *via* Suzuki-Miyaura cross-coupling. [B3b]

2 Mizoroki-Heck Reaction

The palladium-catalyzed cross-coupling of arylated and vinylated halides with olefins in the presence of a base is among the most important and widely used reactions in organic and organometallic synthesis. [B1a,B2a,B9] Using this reaction (Scheme B5), it is possible to couple electron-rich or electron-poor, mono-substituted olefins as well as di-substituted or cyclic olefins. [B1a,B2a,B2e,B3a,B10] In general, the Mizoroki-Heck reaction proceeds with high stereo- and regioselectivity, which makes it an indispensable tool for the synthesis of pharmaceuticals and agrochemicals, *e. g*. Naproxen (anti-inflammatory drug) or Prosulfuron (herbicide). [B1c]

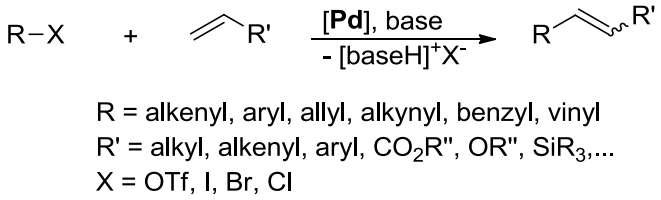

Scheme B5. The Mizoroki-Heck reaction. [B1a]

The first publications on this reaction were almost simultaneously made by Tsutomu Mizoroki [B11a] and Richard F. Heck [B11b], but it was Heck who first described a mechanism, demonstrated its usefulness and continued the research in this field of chemistry. [B10] However, the Mizoroki-Heck reaction follows a slightly different pathway than the other *C,C* cross-coupling reactions, having merely the oxidative addition and reductive elimination in common. [B1c] The mechanism initially proposed by Heck is depicted in Scheme B6.

Before entering the catalytic cycle it is necessary to form the catalytically active palladium(0) species, which is either generated from palladium(0) complexes *via* ligand dissociation or formed *in situ* by reduction of a palladium(II) source *via* the base, the olefin or the commonly applied phosphine ligands. [B12]

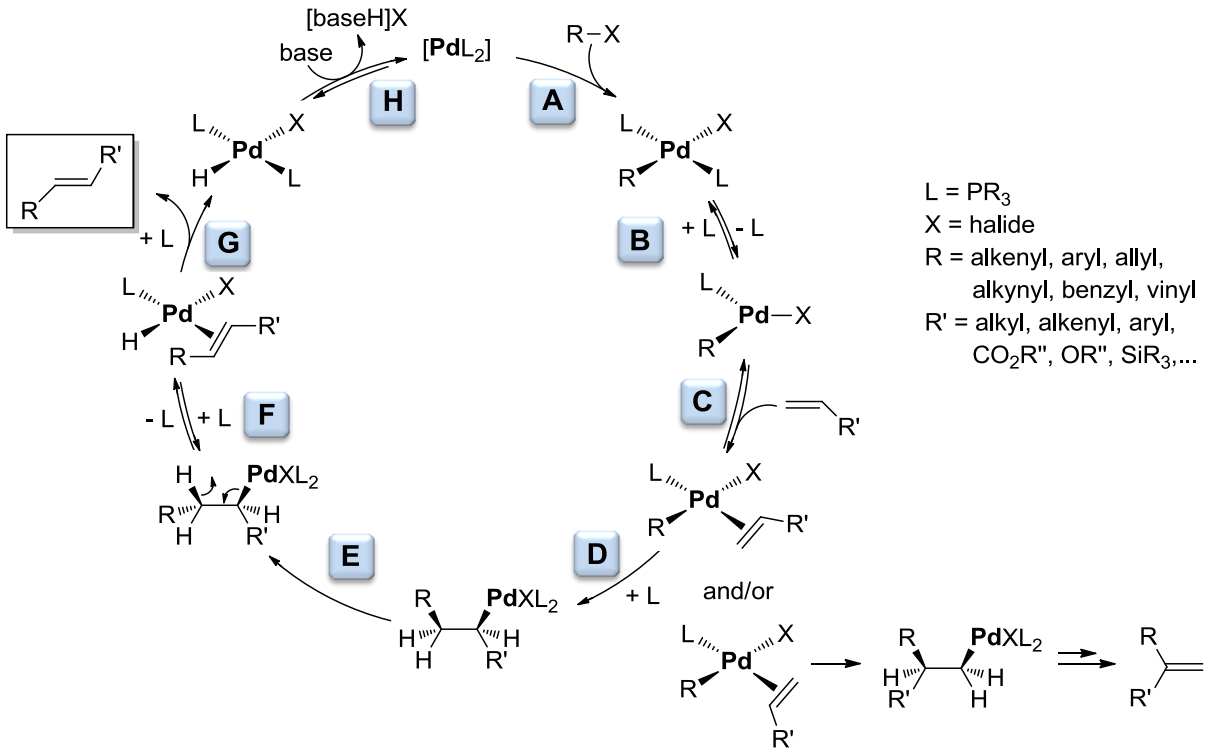

Scheme B6. Mechanism of the Mizoroki-Heck reaction proposed by Heck in 1974. [B10]

The first step of the catalytic cycle is the oxidative addition of an aryl (vinyl) halide to a coordinatively unsaturated 14-electron-palladium(0) complex, forming after *cis*-*trans* isomerization a *trans*-palladium(II) complex (**A**). Afterward, one ligand dissociates (**B**) and the alkene R'CH=CH_2 η^2-coordinates to palladium(II) (**C**) followed by a *syn*-insertion of the alkene which leads to an alkyl-palladium(II) complex (**D**). In this step two isomers may be formed *via* α- or β-arylation leading to the linear or branched arylated alkene. After intramolecular *C*-*C* bond rotation (**E**), a *syn*-β-hydride elimination gives the respective hydrido-palladium(II) complex which is η^2-coordinated by the arylated alkene (**F**). After dissociation of the alkene (**G**), the hydrido-palladium(II) complex undergoes reductive elimination to regenerate the active palladium(0) species and to release H-X, which is then quenched by the base (**H**). [B1a,B2a,B10]

The rate determining step is usually referred to be the oxidative addition due to the reactivity order of the aryl halide: Ar-I > Ar-Br >> Ar-Cl, which proves to be true for less reactive halides. However, for more reactive ones, the complexation/insertion step is considered to be rate determining. [B10]

In recent studies, it could be confirmed that the mechanism in its main steps proposed by Heck is correct. [B10] However, due to its complexity, the catalytic cycle may involve intermediates which differ from the originally proposed ones, depending on the catalytic

precursor (Pd(0) complexes, $[Pd(OAc)_2]$, palladacycles), the ligand (mono- or diphosphines, carbenes, bulky monophosphines), the additives (halides, acetates), the aryl compound (halide, triflate), the alkenes (electron-rich *vs*. electron-deficient) and the base. Depending on the experimental conditions and the resulting active species, the cycle may include palladium nanoparticles, anionic $[PdL_2(OAc)]^-$ (L = monophosphine; L_2 = diphosphine), neutral $[PdL_2]$ (L = carbene, monophosphine) or [PdL] (L = bulky phosphine or carbene) complexes as well as cationic $[ArPdL_2S]^+$ (S = solvent, L = monophosphine, monocarbene or L_2 = bidentate diphosphine) or T-shaped complexes [ArPdXL] (L = bulky phosphine). [B10]

During the last years, many modifications and improvements of the catalyst systems have been reported, which can be classified into four different types. [B10]

Type I systems (classical Mizoroki-Heck systems) are very robust regarding the deviation of parameters of a process and the active species are mostly palladium particles. [B10] They allow versatile reaction conditions for the coupling of aryl iodides and activated aryl bromides and very high TON and TOF values are characteristic. [B10] However, these reactions proceed slowly at ambient temperature and the addition of phosphines or other strongly coordinating ligands often retard the reaction. [B10] Type I systems can be generated from almost any palladium-containing precursor which possesses labile or hemi-labile ligands, *i. e*. $[Pd(OAc)_2]$ or $[PdCl_2]$, by gently warming of the palladium(II) salt in thf in the presence of an excess of $[(n\text{-}Bu)_4N][RCO_2]$ which functions as a reducing and stabilizing agent. [B10] In addition, the use of additives are known to facilitate the reaction by balancing the rate of palladium(0) formation, oxidative addition and nucleation of the particles and hence allowing the performance at ambient temperature and mild reaction conditions (Scheme B7). [B10] The use of tetraalkylammonium salts as additives was first reported by Jeffery [B13], however, the most impressive example for the usage of additives in association with a simple palladium precursor ($[Pd(OAc)_2]$) was described by Beletskaya and co-workers. [B1a,B10,B14] They demonstrated that water-soluble aryl iodides and bromides can be coupled quantitatively in aqueous medium using only 0.0005 mol% palladium, which led to the term "homeopathic" dose. [B14,B15]

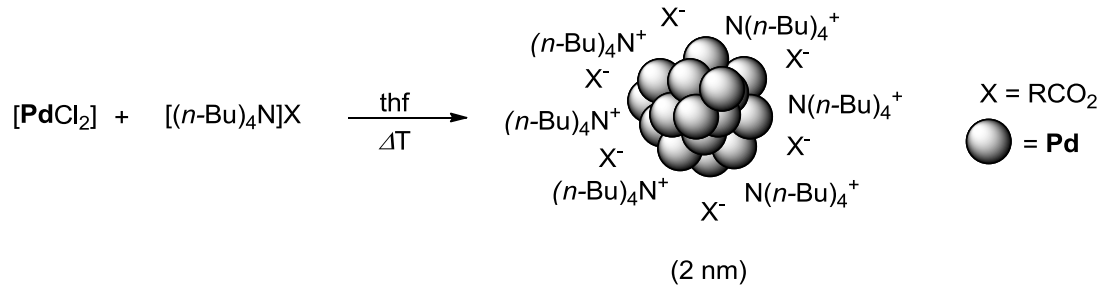

Scheme B7. Thermal preparation of palladium colloids stabilized by $[(n\text{-}Bu)_4N]Cl$. [B15]

Another type of highly active Type I catalysts, so called PCP pincer complexes, was reported by Milstein *et. al*. (Scheme B8). [B2a,B9c,B10] These complexes also show high thermal stability (decomposition > 180 °C) and insensitivity toward oxygen. Additionally, the catalyst shows an exceptional longevity and upon addition of new substrates, a continuation of the catalytic reaction. In the coupling of iodo benzene with methyl acrylate quantitative conversions and TON values of 500000 could be achieved. Even in the coupling of bromo benzene TONs of 132900 were obtained with catalyst loadings as low as 0.000035 mmol. However, ligand-acceleration effects were not observed. [B9c]

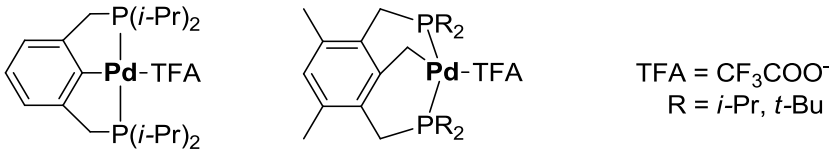

Scheme B8. PCP pincer complexes. [B9c]

In general, **Type II** systems are very sensitive. [B10] That means each substrate combination, concentration and experimental realization must be optimized separately. [B10] They are usually applied in the coupling of *non*-activated aryl bromides, activated aryl chlorides and sterically hindered alkenes, but are very sensitive toward a change of parameters. [B10] Furthermore, these couplings need high reaction temperatures, polar and high boiling solvents and palladium loadings between 0.05 – 0.5 mol%. [B10] The difference to Type I systems is the strong dependency of the initial palladium loading revealing an optimal concentration, which means that higher or lower starting concentrations lead to a deactivation of the catalyst due to the formation of clusters, nanoparticles or palladium black (bulk material). [B10] To achieve Type II systems, two different methodologies can be applied. The first one is the addition of a palladium salt or complex to the reaction mixture in the presence of a stabilizing additive. [B10] In the second methodology the palladium is bound in a stable complex which releases the active species slowly during the course of the reaction by means of thermal decomposition or reaction with compounds of the reaction system. [B10] Such types of compounds are called “slow-release precatalysts” (SRPCs) and can be used preformed or formed *in situ* from an easily accessible palladium source and a strong coordinating ligand. [B10] They are stable at high temperatures but react slowly and no considerable ligand acceleration effects can be observed. [B10] Prominent examples of SRPCs include phosphapalladacycles which were first introduced by Herrmann and Beller (Scheme B9). [B1a,B2a,e,B10,B12,B16] Their palladacycle (R = *o*-Tol; X = OAc) was the prototype of this class of catalysts and is the only representative that has found application in various synthesis

protocols. [B10] Palladacycles are thermally stable and decompose above 250 °C. [B16c] Furthermore, they exhibit long-term stability, avert P-C cleavage of the phosphine ligands which depletes the system of the phosphine and leads to by-products. [B16c] The Herrmann-Beller palladacycle is able to quantitatively couple 4-bromo benzaldehyde at 135 °C with TONs up to 200000 (TOF: 5000 – 50000 h^{-1}) and even 4-chloro benzaldehyde with a conversion of 80 % and TON values in the range of 600 – 800. [B16c]

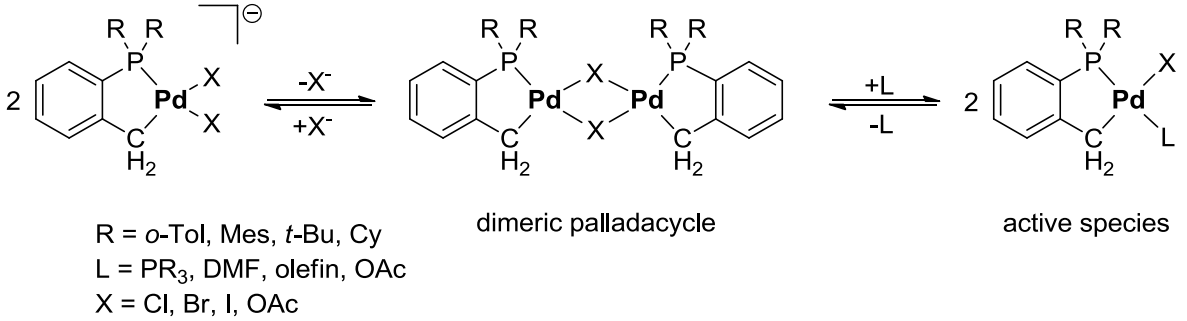

Scheme B9. Phosphapalladacycles.

Another important class of highly active Type II catalysts represent *N*-heterocyclic carbene (NHC) complexes. [B10] Bulky electron-rich carbenes provide some advantages compared to classical phosphine ligands by avoiding critical properties such as high toxicity, flammability and high costs. [B10] Furthermore, they provide high longtime thermal stability due to their bulkiness and are stable toward air and moisture. [B2a,B10,B17] The first examples of NHC palladium complexes in Mizoroki-Heck reactions were reported by Herrmann *et al.* in 1995 (Scheme B10). [B17] They demonstrated the efficiency of this catalyst in the coupling of 4-bromo acetophenone with *n*-butyl acrylate leading to TON values of 250000 without palladium precipitation. [B17] Furthermore, they could achive turnover frequencies of 15000 h^{-1} in the coupling of desactivated aryl bromides and were able to quantitatively couple 4-chloro benzaldehyde and 4-chloro nitrobenzene at 130 °C using [(*n*-Bu)$_4$N]Br as additive. [B17] However, at the beginning of the reactions the activity is lower, when compared to palladacyclic systems due to a slow activation (reduction) of the catalyst. [B17]

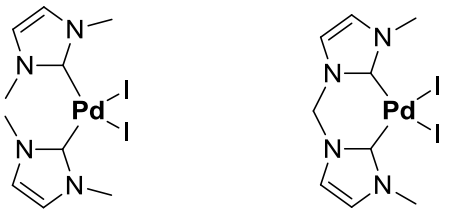

Scheme B10. NHC palladium complexes by Herrmann. [B17]

Recently, Herrmann and co-workers combined the advantages of both catalyst systems, resulting in a new class: NHC-substituted phosphapalladacycles (Scheme B11). [B16b] This new type combines the extraordinary stability of the palladacycles as well as the high σ donor ability and bulkiness of the *N*-heterocyclic carbene. [B16b] Using these catalysts, TON values up to 343000 could be obtained in the coupling of less active aryl bromides with styrene at 130 °C. [B16b] The advantage of this catalyst compared to others is its high activity in the coupling of 4-chloro acetophenone with styrene at 130 °C leading to a TON of 10800, which is much higher than the results achieved with the simple palladacycle. [B16b] Hence, for optimal catalytic results, these new complexes should feature one bulky, strongly σ donating carbene ligand and a less Lewis-basic cyclometallated phosphine to increase the activity. [B16b]

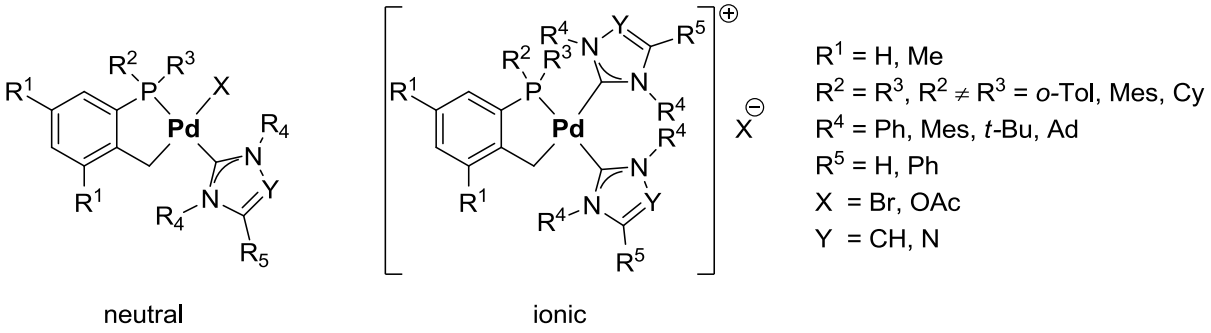

Scheme B11. NHC-substituted phosphapalladacycles. [B16b]

Type III and **Type IV** catalytic systems are stable and robust against air and moisture and can be applied in the reaction of *non*-activated aryl bromides and chlorides (Type III) as well as in the coupling of aryl halides and aryl triflates (Type IV). [B10] However, achieving high TON and TOF values is complicated because of high catalyst loadings (rarely less than 0.5 mol%) and the synthetic effort leads to high catalyst costs. [B10] Nevertheless, aryl chlorides cannot reliably be coupled in reasonable yields using Type I or II systems, the use of tailor-made ligands is mandatory, which leads to ligand-accelerated processes. [B10] True Type III ligand-accelerated processes are characterized by considerable milder reaction conditions (80 – 120 °C) and the use of polar solvents, nucleophilic bases and other coordinating additives should be avoided. [B10] Furthermore, the applied protocols should feature electron-rich and bulky ancilliary ligands, which are required for the formation of the coordinatively unsaturated, active palladium species. [B10] However, ligand-accelerated systems are much slower and less effective than Type I or II systems because most of the palladium remains in an inactive form due to a less effective preactivation at lower temperatures. [B10] If the temperature is increased, deligation of the palladium complex would lead to *non*-ligated

unsupported palladium(0) which is not able to activate less reactive substrates (see Type I and II systems). [B10]

One of the first attempts to develop a suitable system for the coupling of unactivated aryl chlorides was reported by Milstein and co-workers. [B10,B18] They applied dippp (1,3-bis(di-*i*-propylphosphino)propane) and dippb (1,4-bis(di-*i*-propylphosphino)butane) featuring electron-rich and bulky *i*-propyl groups in the reaction of substituted aryl halides with styrenes. However, these reactions cannot be referred to be truly ligand accelerated because of the applied polar solvent (DMF) and reaction temperatures above 120 °C. [B10] Hartwig and co-workers reported that less reactive substrates can be coupled in the presence of electron-rich and bulky monophosphines P(*t*-Bu)$_2$R (R = *t*-Bu, Ph, Fc) and [Pd$_2$(dba)$_3$] in DMF at 110 °C. [B10,B19] At the same time, Littke and Fu published a similar protocol for the coupling of *non*-activated aryl chlorides in which they applied P(*t*-Bu)$_3$ and [Pd$_2$(dba)$_3$] in 1,4-dioxane between 100 – 120 °C using Cs_2CO_3 as base. [B10,B20b] In addition, when using the sterically hindered amine Cy_2NMe as base the coupling of activated aryl chlorides and all kinds of aryl bromides at ambient temperature is possible, requiring 0.5 – 1.5 mol% palladium. [B10,B12,B20a,c] As an alternative to the highly air sensitive P(*t*-Bu)$_3$ also the stable salt [P(*t*-Bu)$_3$H]BF$_4$ can be employed. [B10, B20c] To this day, there are only a few other ligands that can compete with the P(*t*-Bu)$_3$ system by Hartwig and Fu. [B10] One example is the sterically hindered triphenylphosphino derivative reported by Tsuji *et al.* which shows quantitative conversion in the reaction of chloro benzene with methyl acrylate at 100 °C using 1.5 mol% [Pd$_2$(dba)$_3$] (for comparison: P(^{t}Bu)$_3$: 63 %) (Scheme B12). [B21] A true ligand-acceleration effect could be observed by Dyson *et al*. for an electron-rich aminophosphine, which forms a four-membered ring with palladium (Scheme B12). [B10,B22] These complexes are able to quantitatively couple all types of aryl bromides with styrene at only 80 °C. [B10,B22] However, the coupling of aryl chlorides is not reported. In spite of all the improvements made, a general protocol for the Mizoroki-Heck reaction of aryl chlorides is still unavailable. [B10]

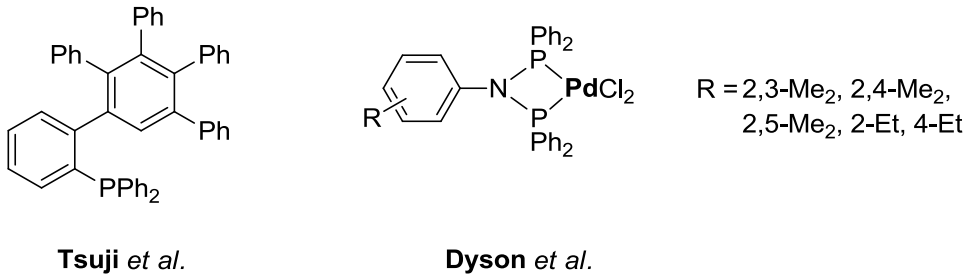

Tsuji *et al.* **Dyson** *et al.*

Scheme B12. Type III catalyst systems by Tsuji and Dyson. [B10,B21,B22]

Type IV catalytic reactions require mild reaction conditions and typically bidentate ligands are used. [B10] The main feature of the catalytic cycle is the dissociation of an anionic ligand from the palladium in order to obtain a free coordination site for the alkene. [B10] Therefore, this type of reaction is often referred as the polar pathway. [B10] The most important function of the ligand is the restriction of all potential transformations to a single selective pathway and thereby the suppression of unwanted side reactions. [B10] In addition, the design of the ligand should avoid the formation of chemically inert complexes due to bis-chelation. [B10] However, usually a decrease in the reaction rates is observed, when bidentate ligands are used. [B10] In contrast, Shaw and co-workers showed that high yields and TON values up to 225000 could be obtained in the coupling of iodo benzene with styrene applying bidentate $[PdL_2Cl_2]$ complexes (*e. g.* L_2 = dppe, dppp) (Scheme B13). [B10,B23] In general, bidentate phosphines are mostly exclusively used in asymmetric Mizoroki-Heck reactions and they play an important role as ancillary ligands in many regio- and stereoselective protocols. [B10]

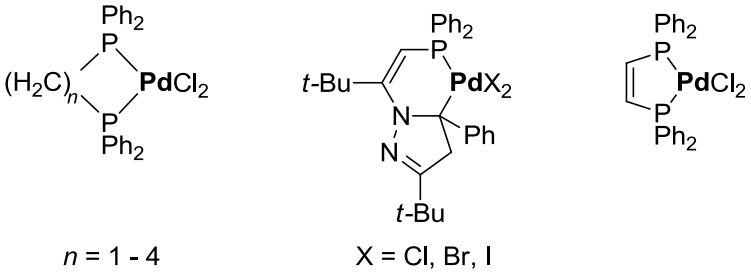

Scheme B13. Bidentate $[PdCl_2L_2]$ complexes synthesized by Shaw. [B10,B23]

3 Suzuki-Miyaura Reaction

The palladium-catalyzed cross-coupling of organo halides (or triflates) with nucleophilic organoboron reagents is one of the most versatile reactions in organic synthesis (Scheme B14). [B2a,B24] While this reaction is usually used in the synthesis of unsymmetric biaryls, it can also be effectively applied in the coupling of alkyl, alkenyl and alkynyl as well as aryl boronic acids. [B1,B2a,B24c,B24f,B25] Based on its versatility, the Suzuki-Miyaura reaction is a powerful tool not only for academic research but also for industrial synthesis of, for example, fine chemicals, natural products, pharmaceuticals and agrochemicals. [B24b,c,g,B25a]

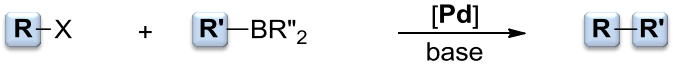

R, R' = aryl, alkenyl, alkynyl, alkyl
R" = OH, OR, alkyl
X = Cl, Br, I, OTf

Scheme B14. The Suzuki-Miyaura reaction.

Arylboronic acids are suitable reagents as they can be easily prepared by hydroboration of alkenes or alkynes, by the reaction of trialkylborates with Grignard or organolithium compounds, the palladium-catalyzed reaction of aryl halides with (di)boranes or direct transition metal-catalyzed borylation of arenes *via* C-H activation. [B1a,B2a,B25b] Furthermore, they exhibit a high thermal, air and moisture stability, low toxicity and a high tolerance toward various functional groups. [B1a,B2a,B24b-d,g]

The Suzuki-Miyaura reaction follows a similar catalytic cycle to that of other cross-coupling reactions (*vide supra*), involving oxidative addition (**A**), transmetalation (**C**), reductive elimination (**E**) and two isomerization steps (**B**, **D**) (Scheme B15). [B2e]

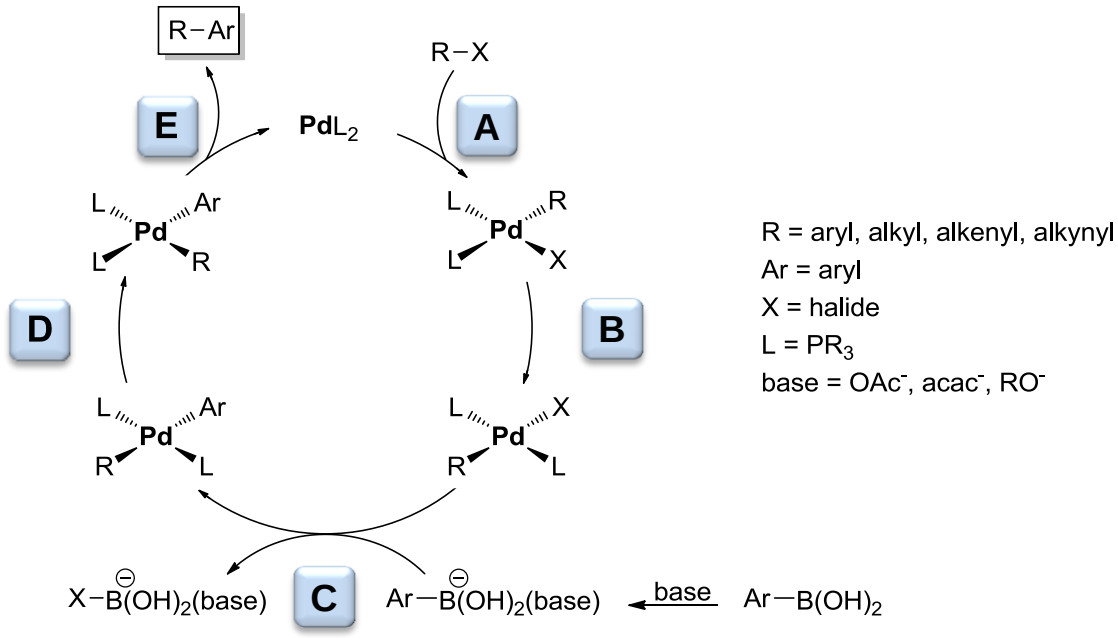

Scheme B15. Mechanism of the Suzuki-Miyaura reaction. [B2e]

The catalytic active species is a coordinatively unsaturated palladium(0) complex which is typically generated either by ligand dissociation/exchange of a palladium(0) complex, for example, $[Pd(PPh_3)_4]$ or $[Pd_2(dba)_3]$ / *n* PPh_3 ($n \geq 2$), or formed *in situ* from a palladium(II) complex, *e. g.* $[PdCl_2(PPh_3)_2]$ or $[Pd(OAc)_2]$ / *n* PPh_3 ($n \geq 2$), *via* reduction. [B1a,B2a,B3a,B26e] Thereby, the reduction can be accomplished by *i*) the phosphine [B26a,b], *ii*) a transmetalation/reductive elimination sequence with, for example, *n*-BuLi [26c] or *iii*) *via* aqueous alkali induced disproportionation to the phosphine oxide and the palladium(0) species[26d].

The first step of the catalytic cycle is the oxidative addition of R-X (**A**) which results after *cis*, *trans*-isomerization (**B**) in a square planar *trans*-palladium(II) complex. [B1a,B2a,B3a,B27]

Mechanistic and theoretical studies showed that the oxidative addition on [PdL_2] follows an oxidative insertion pathway with formation of a *cis*-complex, which undergoes slow isomerization to the appropriate *trans*-complex by means of concurrent auto-catalytic or solvent assisted pathways. [B28] However, the mechanism of the oxidative addition is highly sensitive toward the bulkiness of the applied phosphine. In the presence of bulky electron-rich phosphines, *e. g.* P(*t*-Bu)$_3$, the active species is expected to be a mono-ligated [PdL] system which upon oxidative addition with Ar-X (X = Br, Cl) forms a tri-coordinated T-shaped palladium(II) complex following a dissociative mechanism. [B29] However, an increased phosphine concentration inhibits the oxidative addition. [B29] In contrast, for less sterically demanding phosphines (*e. g.* PCy_3) the active species is typically a [PdL_2] complex and the rate of the reaction is independent of the phosphine concentration. [B29]

The secend step of the catalytic cycle is the transmetalation of [Pd(Ar)(X)L_2] with the organoboronic acid (**C**). [B1a,B2a,B3a,B27,B30] In contrast to oxidative addition and reductive elimination, less is known about the transmetalation, thus several different processes are possible. However, the transmetalation does not occur in absence of a base, due to the low nucleophilicity of the boronic acid. [B1a,B2a,B3a,B26b,B27,B30] So far, three different pathways were proposed in literature to account for the role of the base: *i*) the base reacts with the organoboron compound to form a boronate species, *ii*) the base replaces the halide on the palladium(II) complex and *iii*) an (oxo)palladium(II) complex is formed, which undergoes transmetalation with organoboron compounds without addition of a base. [B1a,B31] Theoretical and experimental studies showed that the most feasible mechanism is the quaternization of the boron atom, due to its high oxophilicity, which enhances the nucleophilicity of the organic group on the boron atom. [B31b] As base typically sodium or potassium carbonates, phosphates, hydroxides, fluorides or alkoxides are applied, either in aqueous solution or suspended in DMF, 1,4-dioxane or toluene. [B1a] The second pathway in which the halide on the palladium(II) is directly substituted by a hydroxide is unlikely. [B31b] Matos and Soderquist could show that upon addition of NaOH to *trans*-[PdBr(Ph)(PPh_3)$_2$] the amount of triphenylphosphine oxide increases significantly suggesting a reaction of the base first with the phosphine followed by slow migration of the OH^- group to the palladium. [B32] This pathway is most likely suitable for reactions, where the organoboron compound cannot form the boronate species, however, leading easily to ligand oxidation and decomposition of the catalyst. [B32] (Oxo)palladium complexes, formed *via* oxidative addition, easily undergo transmetalation with organoboronic acids without the aid of an additional base. [B31b] Hence, its high reactivity can be attributed to its high basicity and the high oxophilicity of the boron

atom. Nevertheless, the results indicate that these processes are highly dependent on the applied organoboron reagent, the base and also the organic electrophile. [B31b]

The final step in the catalytic cycle is the reductive elimination of the product and regeneration of the catalytically active species (**E**). [B1a,B2a,B3a,B27] The requirement for this reaction is a *cis*-configuration at palladium(II) leading to a second isomerization step (**D**). [B31b] In addition, the rate of the reductive elimination is accelerated by electron-withdrawing and sterically demanding ligands at the palladium atom, however, for very bulky ligands the steric properties dominate the electronic ones. [B24e,B33] In general, two different mechanisms of the reductive elimination are possible: *i*) reductive elimination on a tri-coordinated palladium(II) complex and *ii*) reductive elimination on a *cis*-$[Pd(Ar)_2L_2]$ complex at which pathway *i*) is preferred which is based on computantional and experimental studies. [B1c,B24e,B33]

During the last 20 years considerable attention has been focused on the development of catalysts suitable for the coupling of aryl chlorides which are very attractive substrates as they are readily available and inexpensive. However, their poor reactivity based on the strength of the C-Cl bond (bond dissociation energies for Ph-X: Cl = 96 kcal·mol^{-1}, Br = 81 kcal·mol^{-1}, I = 65 kcal·mol^{-1}) [B24b,d,B34] leads to a hindered oxidative addition, the rate determining step. In this regard, once more the phosphapalladacycles of Herrmann must be mentioned (Scheme B16). [B35a] However, also other highly active palladacyclic catalysts have been successfully applied (Scheme B16). [B1a,B2a,B24c,B34a,B35,B36] The thermally stable phosphapalladacycle by Herrmann *et al.* is able to activate aryl bromides and chlorides using palladium loadings of 0.001 and 0.01 mol%, respectively, achieving TON values of 2100 – 74000. [B35a] Another highly active catalyst was reported by Bedford *et al*. who coupled aryl bromides with phenyl boronic acid achieving TONs of 1000000 and TOF values of 900000 h^{-1} at 110 °C (Scheme B16). [B35c] In addition, the phosphite containing palladacycle shows in combination with PCy_3 excellent TON values of 34000 in the coupling of desactivated 4-chloro anisole with phenylboronic acid at 100 °C. [B35c]

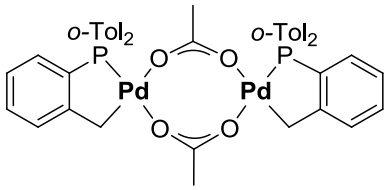

Herrmann *et al*.

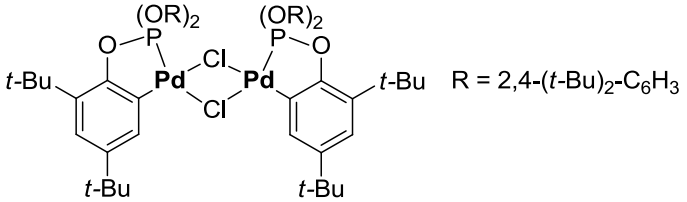

Bedford *et al*.

Scheme B16. Palladacycles. [B35]

In 1997, Shen *et al.* reported on the coupling of various activated aryl chlorides applying $[PdCl_2(PCy_3)_2]$ as catalyst. [B24b,c,B34a,B36,B37] However, the catalyst failed, when using *non*-activated or desactivated as well as *meta*-substituted aryl chlorides. Furthermore, a high catalyst loading of 5 mol% was required leading to extremely low TON values of only 20. [B24c,B37] In contrast, Littke and Fu reported that the catalyst formed *in situ* by $[Pd_2(dba)_3]/PCy_3$ can be used in the coupling of *non*-activated aryl chlorides, but a even better activity is observed, when applying the more bulky and electron-rich, yet air-sensitive P(*t*-Bu)$_3$. [B34a] The optimum palladium/phosphine ratio is found to be between 1 and 1.5 indicating that the active species is $[PdP(t\text{-}Bu)_3]$. [B2a,B24c,B34a] With this versatile catalytic system, electronically and sterically diverse aryl chlorides can be efficiently coupled with arylboronic acids using Cs_2CO_3 as base. [B24b,c,g,B36b,B38] In addition, cross-couplings of aryl chlorides with TONs up to 400 at ambient temperature, the synthesis of sterically hindered di- and tri-*ortho*-substituted biaryls, the coupling of typically unreactive vinyl chlorides at ambient temperature, cross-couplings of vinyl bromides, iodides, and triflates are possible. [B24b,c,g,B36b] An alternative to the highly air-sensitive trialkylphosphines represents air and moisture stable ferrocene-based triarylphosphines (Scheme B17). [B2a,B36b,B39] Fu *et al.* reported that the silyl-functionalized bulky diphenylphosphino ferrocene is suitable for the coupling of desactivated and sterically hindered aryl chlorides with versatile boronic acids at 70 °C. [B39a] Furthermore, this system is able to quantitatively couple activated aryl chlorides at ambient temperature, however, high palladium loadings (5 mol%) are necessary. [B39a] Another ferrocenyl-based system suitable for the reaction of aryl chlorides was reported by Richards and co-workers. [B39b] With the bulky triferrocenyl phosphine, conversions of up to 90 % could be obtained after 5 h at 60 °C. [B39b]

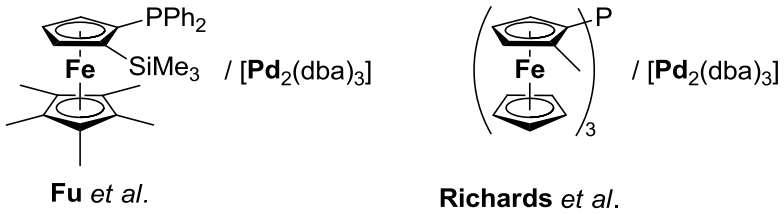

Scheme B17. Ferrocenylphosphine systems. [B39]

A further excellent catalyst obtained from an electron-rich and bulky phosphine and a palladium source was reported by Beller *et al*. (Scheme B18). [B1a,B2a,B24b,B40a] They applied a mixture of PAd$_2$(*n*-Bu) (Ad = adamantyl) and $[Pd(OAc)_2]$ in the reaction of desactivated aryl chlorides achieving TON values of 10000 – 20000. [B24b,B36b,B40a] Furthermore, studies by Hartwig *et al*. showed that the air-stable dimer $[Pd(\mu\text{-}Br)(PAd(t\text{-}Bu_3)_2)]_2$ is able to catalyze

almost quantitatively reactions between sterically hindered aryl bromides and phenylboronic acid at ambient temperature using 0.5 mol% of the catalyst (Scheme B18). [B2a,B24b,c,B34a,B36b,B40b]

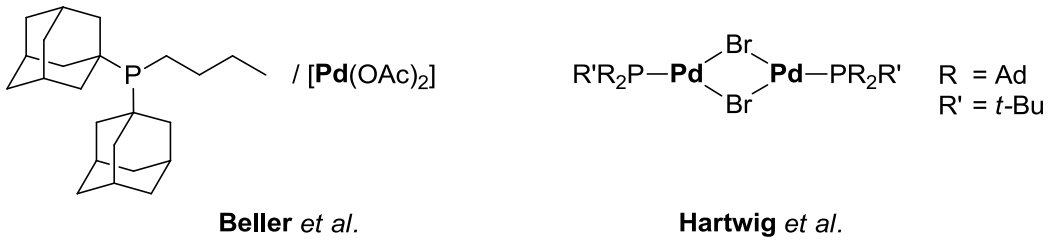

Scheme B18. Alkylphosphines by Beller and Hartwig. [B40]

Another important class of efficient ligands based on dialkylphosphino-substituted biphenyls, was reported by Buchwald *et al*. (Scheme B19). [B1a,B2a,B24b,c,B34a,B36a,b,B41] This system proved to be remarkably active in the coupling of electron-rich as well as electron-defficient aryl and heteroaryl chlorides at ambient temperature using 1.0 – 1.5 mol% [$Pd(OAc)_2$]. [B24c,B41b] In addition, these systems are highly active in the synthesis of biphenyls with up to three *ortho*-substituents and in the coupling of electron-rich aryl chlorides with the highly sterically hindered 2,4,6-tri-*i*-propylboronic acid at 100 °C. [B24b,B41d] The efficiency of these types of ligands can be attributed to the high basicity of the phosphino group and the second phenyl ring which may coordinate and hence stabilize the palladium center. [B41d]

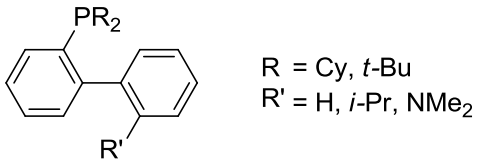

Scheme B19. Buchwald phosphines. [B41]

An alternative to the widely used phosphine ligands represent *N*-heterocyclic carbenes due to their high thermal stability, bulkiness and strong σ donor character (Scheme B20). [B1a, B2a,B24b,B42] The first successful examples were reported by Herrmann and co-workers. [B24b,B42a-c] They coupled aryl bromides and activated chlorides in the presence of a methylene-bridged NHC palladium complex at 120 °C obtaining good to excellent results. [B24b,B42a] Later, Herrmann reported on the synthesis of a bis(adamantyl)-NHC complex being highly active in the coupling of aryl chlorides at ambient temperature using 3 mol% of the catalyst. [B24b,e,B42c] However, a major drawback of *N*-heterocyclic carbenes is their air and moisture sensitivity, meanwhile avoidable by the use of easier-to-handle and commercially available

imidazolium chloride salts thus, forming the active catalyst *in situ*. [B24b,B34a,B36b,B42d,e] In this way, Nolan obtained excellent conversions in the reaction of functionalized aryl chlorides and arylboronic acids with the catalytically active species generated *in situ* by mixing the bis(mesitylene)-imidazolium salt (3 mol%) with $[Pd_2(dba)_3]$ (1.5 mol%). [B42e]

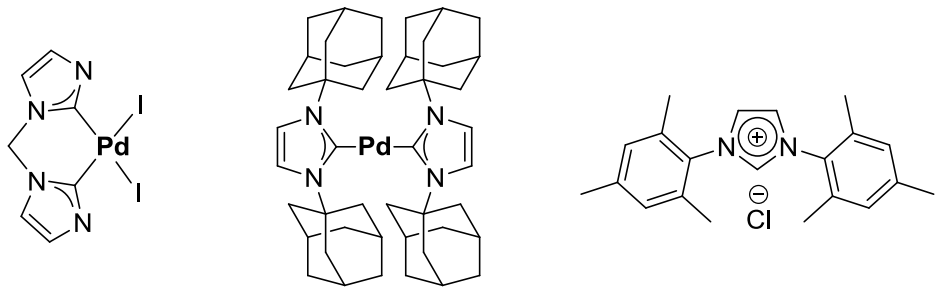

Herrmann *et al.* **Herrmann** *et al.* **Nolan** *et al.*

Scheme B20. *N*-heterocyclic carbene complexes and imidazolium salt. [B42]

Beside the presented catalytic systems other highly active catalysts including ligandless palladium nanoparticles, palladium catalysts supported on polymers or inorganic supports and phase-transfer catalysts have been developed. [B1a,B2a,B3a]

4 *β*-Oxopropyl Ester Synthesis

The selective transformation of alkynes allows an access to a variety of polyfunctional reagents acting as building blocks for organic synthesis. [B43] *β*-Oxoalkyl esters easily form *α*-hydroxy ketones which are of interest in the synthesis of natural products, [B43e,44] antibacterial compounds. [B45] They also allow the synthesis of heterocyclic furanones and imidazoles. [B43a,B45] In addition, they serve as active esters in peptide synthesis [B45] and can be used as photolabile protecting groups for carboxylic acids. [B44c,B46] Several synthetic methodologies for the preparation of *β*-oxoalkyl esters are known including, for example, carboxylation of *α*-halo ketones, [B44c,B47] hydration/esterification of propargylic alcohols, [B43e,B44] or oxidation of ketones *via* metal acetate complexes. [B43e] An atom-economic alternative to classical synthesis methodologies represents the ruthenium-promoted addition of carboxylic acids to terminal alkynes, first described by Dixneuf and co-workers (Scheme B21). [B43a]

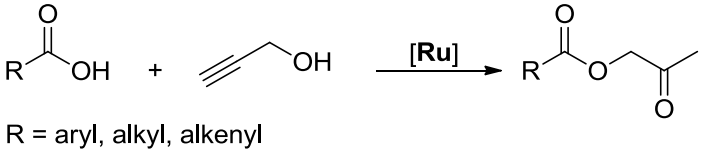

Scheme B21. Ruthenium-catalyzed synthesis of *β*-oxo alkyl esters. [B43c]

The proposed mechanism of the reaction is depicted in Scheme B22. [B43c,e,B44c]

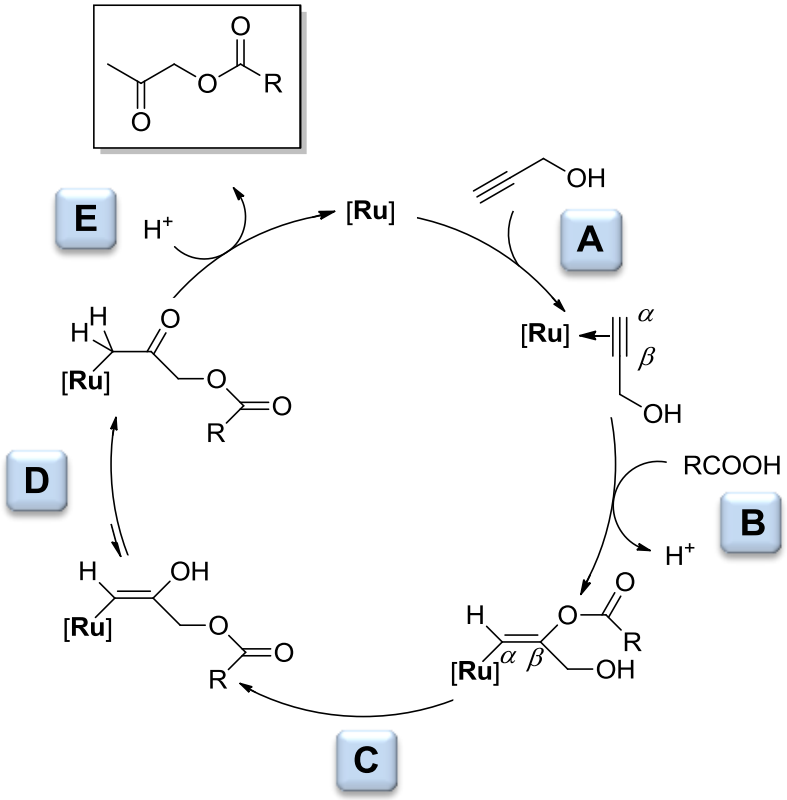

Scheme B22. Proposed mechanism of the ruthenium-catalyzed *β*-oxoalkyl ester synthesis. [B43c,e,B44c]

The first step of the catalytic cycle is the η^2-coordination of the alkyne to the ruthenium(II) complex resulting in an activation of the alkyne (**A**). Afterward, the nucleophilic addition reaction of the carboxylic acid to the *β*-carbon atom of the alkyne takes place resulting in an enol ester complex (**B**). Intramolecular transesterification leads to the enol ester complex (**C**), which upon tautomerization forms the keto ester complex (**D**). Final protonation liberates the *β*-oxoalkyl ester and the catalytically active ruthenium species is regenerated (**E**). However, it is not completely clarified if the tautomerization occurs while the enol is bound to the complex or after the release of the product. In addition, when the internal transesterification cannot take place, functional hydroxy dienyl esters are formed. [B43c,e,B44c]

The catalytic reaction tolerates a variety of bulky and functionalized carboxylic acids such as unsaturated acids, diacids and hydroxy acids or protected amino acids. [B43c] Furthermore, functionalized alkynes, for example enynes, ethoxyacetylenes, propargylic ethers, esters and carbonates can be applied. [B43c] In general, the reaction proceeds under mild reaction conditions (60 °C, 6 h) but, as expected, the obtained results are strongly dependent on the

used ruthenium catalyst. [B43a] Till today, only a few catalysts are known to promote the synthesis of *β*-oxoalkyl esters. Initial works on this reaction involved $[Ru_3(CO)_{12}]$ [B43a,B48] and commercially available ruthenium(III) complexes (*e. g.* $[RuCl_3(H_2O)_3]$, $[RuCl_3(PPh_3)_3]$), [B43a,B47b] however, these compounds showed poor catalytic activity. Yet, the best results concerning activity and productivity were obtained using mono-nuclear half-sandwich ruthenium(II) complexes of type $[RuCl_2(\eta^6\text{-arene})PR_3]$ (arene = *p*-cymene, C_6R_6; R = Me, Ph). [B43a] Dixneuf and co-workers observed that the influence of the arene is negligible and the catalytic activity is only influenced by the phosphino group. [B43a] When exchanging the phosphino group by a phosphite (R = OPh), a significant loss of activity and a yield comparable to $[RuCl_3(H_2O)_3]$ was observed. [B43a] However, these complexes failed in the reaction of *α*-hydroxy acids and propargylic alcohols. Therefore, Dixneuf *et al*. developed a more effective dinuclear ruthenium complex of type $[Ru(\mu\text{-}O_2CH)(CO)_2(PPh_3)]_2$ (Scheme B23). [B43h] This carboxylate-bridged complex allows the addition of functionalized acids under mild conditions and provides a one-step synthesis of optically pure esters from chiral acids. [B43c,h]

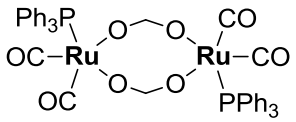

Scheme B23. Dinuclear ruthenium complex by Dixneuf. [B43h]

In contrast, Goosen *et al*. reported that in the related synthesis of enol esters a better catalytic performance can be achieved when electron-defficient phosphines (*e. g*. $P(Fur)_3$) and $[RuCl_2(\eta^6\text{-}p\text{-cymene})]$ are applied. [B47b] Weak *σ*-donating and strongly *π*-accepting phosphines are preferred, due to their ability to increase the rate of the nucleophilic attack of the carboxylate. [B47b] Excellent results were obtained with both, electron-rich and electron-defficient alkyl, aryl and heteroaryl carboxylic acids. [B47b] Even sterically hindered carboxylic acids can be converted and various functionalities including esters, ethers, aldehydes, carbamates and even hydroxy groups are tolerated. [B47b]

Recently, Bauer *et al*. reported on the successful application of phosphoramidite ruthenium complexes in the addition of aromatic and aliphatic, primary, secondary and tertiary propargylic alcohols with aromatic and aliphatic carboxylic acids (Scheme B24). [B44c] The ruthenium complexes are insensitive toward air and moisture. Especially the *N*-benzyl-substituted catalyst shows very good conversions. [B44c]

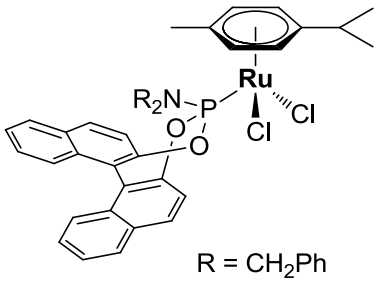

Scheme B24. Phosphoramidite ruthenium complex. [B44c]

Gimeno and co-workers reported on the application of water-soluble ruthenium complexes in the addition of carboxylic acids with functionalized propargylic alcohols in aqueous medium showing very good results (Scheme B25). [B43e] In addition, catalyst recycling was explored but the catalyst can only be re-used twice, due to partial decomposition. [B43e]

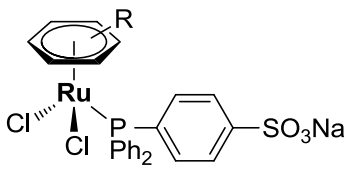

Scheme B25. Water-soluble ruthenium complexes. [B43e]

Another attempt to establish recyclable ruthenium complexes in the formation of *β*-oxoalkyl esters was reported by Štěpnička and co-workers (Scheme B26). [B49] They applied a ferrocenylphosphino-based catalyst on the mesoporous molecular sieve MCM-41 in the addition of benzoic acid with propargylic alcohol. [B49] The obtained results showed that the supported catalyst is less active when compared to the homogeneous catalyst which can most probably be attributed to polymeric side products formed from propargylic alcohol. [B49]

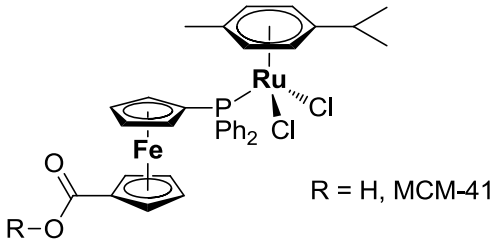

Scheme B26. MCM-41 supported ferrocenyl-based ruthenium complex. [B49]

5 Ferrocenyl Phosphines in *C,C* Cross-Coupling Reactions

Since its discovery in 1951, ferrocene has lost none of its attraction and has become a versatile building block in many areas of research (*e. g.* catalysis, material science or biomedicinal chemistry), due to its distinctive chemical and physical properties. [B50] Especially, the functionalization of ferrocene by phosphanyl groups led to a large family of stable, easy to handle ligands for the application in homogeneous catalysis. [B36b,B50,B51] Furthermore, ferrocenyl phosphino molecules can easily be modified leading to numerous derivatives featuring the same structure motif, however, exhibiting different electronic and steric properties. [B50-B52] Ferrocenyl phosphines are able to form complexes with transition metals in a variety of coordination geometries and oxidation states, thus leading to efficient catalyst precursors for many chemical transformations. [B50a,B53] The most studied ferrocenyl phosphine is 1,1'-bis(diphenyl-phosphino)ferrocene (dppf) which was first described in 1965 by Mertwoy (Scheme B27). [B50,B54] In the late 1970s, the dppf ligand was first employed by Kumada *et al.* in the coupling of Grignard substrates with organic halides leading to an increased interest in this research area. [B50a,B55] Therefore, it is not surprising that it proved useful in numerous metal-catalyzed organic transformations including Kumada-Hayashi, Suzuki-Miyaura and Mizoroki-Heck cross-couplings as well as Buchwald-Hartwig aminations, hydroformylations, hydrogenations and hydrosilylations. [B50,B51a,B54a]

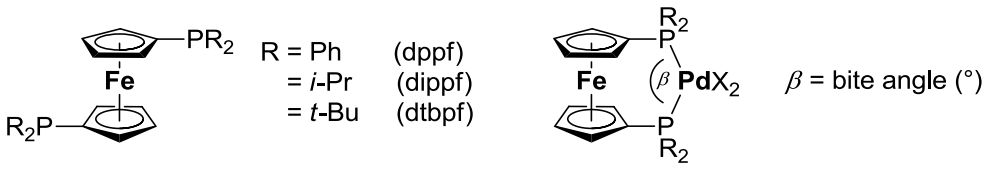

Scheme B27. Bidentate ferrocenyl phosphines and palladium complexes. [B50b,B52b]

The catalytic activity of diphosphine palladium complexes is strongly dependent on the bite angle β because a large bite angle enhances the rate of the oxidative addition and the transmetalation. [B50,B51b] One excellent example is 1,1'-bis(di-*t*-butylphosphino)ferrocene (dtbpf) which is electron-rich, bulky and offers a relatively large bite angle (Scheme B27). [B50b,B51a,B52b] Colacot *et al*. reported on the high activity of [$PdCl_2$(dtbpf)] in the Suzuki-Miyaura reaction of 2-chloro-5-fluoro anisole with phenylboronic acid applying 1.0 mol% palladium at 80 °C. [B52b] The applied catalyst was even superior compared to the air-sensitive [Pd(P(*t*-Bu_3))$_2$] and [Pd(μ-Br)(P(*t*-Bu_3))]$_2$ complexes reported by Fu and Hartwig. [B52b] In comparison to other ferrocenyl diphosphines they observed a decrease of activity in the order: [$PdCl_2$(dtbpf)] > [$PdCl_2$(dippf)] > [$PdCl_2$(dppf)] (dippf = 1,1'-bis(di-*i*-propylphosphino)-ferrocene). [B52b]

In contrast to bidentate ferrocenyl phosphines, the monofunctional ones are less investigated, *i. e.* based on their isolation which is often not an easy exercise due to the lack of suitable synthetic routes and difficulties in their separation from disubstituted analogues. [B50b] However, monodentate ferrocenyl phosphines of type Fc-PR_2 (R = Ph, Me, Et, *i*-Pr, *t*-Bu, Cy) (Scheme B28) have been synthesized and applied in homogeneous catalysis including Baylis-Hillman reactions and diverse C-E coupling reactions (E = C, O, N). [B50b,B51e] Especially, electron-rich and bulky Fc-P(*t*-Bu)$_2$ has attracted much attention because Hartwig *et al*. discovered that in the coupling of phenoxides with unactivated aryl chlorides [$PdCl_2$(dtbpf)] can be cleaved at 110 °C into two monophosphines: Fc-P(*t*-Bu)$_2$ and PPh(*t*-Bu)$_2$. [B51e,B56] Furthermore, they could show that a perarylation of the unsubstituted C_5H_5 ring of Fc-P(*t*-Bu)$_2$ occurred prior to the etherification process leading to a stable, sterically demanding and electron-rich ferrocenyl phosphine known as Q-phos (Scheme B28). [B56a] The catalyst formed from the bulky phosphine and [Pd_2(dba)$_3$] is not only active in etheration processes at ambient temperature but also in the Suzuki-Miyaura cross-coupling of deactivated and sterically hindered aryl chlorides and in the room-temperature Mizoroki-Heck reactions of activated and deactivated aryl bromides achieving conversions > 90 %. [B51e]

Fu *et al*. investigated the structurally related but less electron-donating trimethylsilyl-substituted ferrocenyl phosphine (Scheme B28). [B39] The respective palladium complex is found to be an active catalyst in the reaction of deactivated 4-chloro anisole with *ortho*-tolylboronic acid at 70 °C. [B36b] Richards and co-workers applied the tri-ferrocenyl phosphine (Scheme B28) in the coupling of activated and *non*-activated aryl chlorides and observed that the activity is comparable to P(*t*-Bu)$_3$/[Pd_2(dba)$_3$] although the tri-ferrocenyl phosphine is less Lewis-basic. [B39b,B57] These results draw the conclusion that high σ donor ability is not necessarily required, but the size of the ligand is important as well.

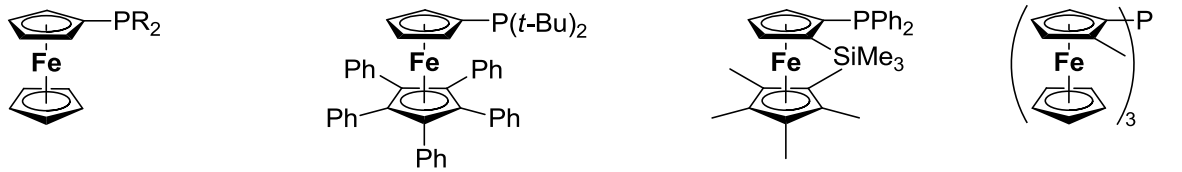

R = Ph, Me, Et, *i*-Pr, *t*-Bu

Hartwig *et al.* "Q-Phos"

Fu *et al.*

Richards *et al.*

Scheme B28. Ferrocenyl phosphines. [B36b,B50b,B51e,B56,B57]

6 Phosphino Imidazoles and their Application in *C,C* Cross-Coupling Reactions

Imidazoles represent an important class of five-membered heterocycles as they are present in a wide range of natural products (*e. g*. histidine or histamine). [B58] Furthermore, their biological importance made them an ubiquitous substructure in numerous synthetic compounds, such as herbicides, fungicides and therapeutical agents. [B58] The discovery of the first stable carbene by Arduengo *et al*. [B59] and the resultant application of *N*-heterocyclic carbenes (NHC) in homogeneous catalysis [B1a,B2a,B3a] aroused the interest in imidazole chemistry. During the last years, especially phosphorus containing imidazoles and imidazolium salts have attracted much interest due to their unique ligand properties. They can act as ambivalent *P, N* donors allowing the coordination of either hard or soft transition metals [B60] and they can be used as easily tuneable ligands in homogeneous catalysis. [B60a,d,B61] In addition, imidazolium salts contain structural elements of ionic liquids, which make them applicable as ligands in two-phasic catalysis, preventing metal-leaching and allowing facile recycling and easy separation of the catalyst. [B60b,d,e,B61a,c,B61]

The application of neutral imidazoles, featuring phosphino groups in 2-position, in homogeneous catalytic reactions is only little described in literature so far. However, these compounds were first successfully introduced by Beller and co-workers in 2004 (Scheme B29). [B61b] They applied a set of functionalized electron-rich and bulky imidazoles and benzimidazoles in the hydroxylation of aryl halides, Buchwald-Hartwig aminations and Suzuki-Miyaura reactions of aryl chlorides. [B61b,B63] Excellent results were obtained especially with the benzimidazole/[$Pd(OAc)_2$] system in the Suzuki-Miyaura reaction of different aryl and heteroaryl chlorides with TON values of up to 8500. [B61b] In addition, *meta*- and *para*-substituted aryl chlorides can be quantitatively coupled regardless of their electronic nature. [B61b] In the coupling of sterically hindered 2,6-dimethyl benzene only moderate yields were observed. [B61b]

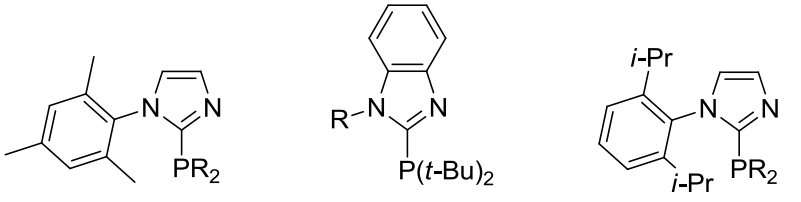

R = Cy, *t*-Bu R = Ph, 1-naphthyl R = Cy, Ad, *t*-Bu

Scheme B29. Phosphino imidazoles synthesized by Beller. [B61b,B63]

In contrast to the neutral phosphino imidazoles, their cationic counterparts are catalytically much better investigated, due to their structural similarities with ionic liquids. This concept was first utilized by Wasserscheidt and co-workers who applied phosphino-functionalized [BMIM]PF_6 (BMIM = 1-*n*-butyl-3-methyl imidazolium) and [DMIM]BF_4 (DMIM = 1,3-dimethyl imidazolium) in the biphasic rhodium catalyzed hydroformylation of 1-octene (Scheme B30). [B60e] They achieved enhanced catalytic activity and recyclability without significant rhodium leaching. [B60e] Once again, it was Beller in 2010 who introduced phosphino imidazolium salts in *C,E* cross-coupling reactions (E = C, N, O). [B61a] However, they applied sterically demanding imidazolium salts preferentially in hydroxylation reactions of various aryl bromides and in the copper-free Sonogashira reaction of 2-bromo thiophene. [B61a] Nevertheless, they also used the sterically demanding cyclohexyl-substituted phosphino imidazolium salt in the synthesis of 2,4,6-trimethyl biphenyl and 4-methoxy biphenyl (Scheme B30). [B61a] Starting from the aryl bromide and applying common 1,4-dioxane as solvent, they obtained 60 – 99 % yields of the respective biphenyl at 100 °C. [B61a] Recently, the group of Wu described the application of the diphenylphosphino-functionalized [BMIM]PF_6 as ligand in the Mizoroki-Heck reaction of sterically hindered, electron-rich aryl iodides and aryl bromides dissolved in [BMIM]PF_6 (Scheme B30). [B64] They found high activity, stability and recyclability of the catalyst. [B64] Furthermore, they observed enhanced stability of the ligand toward oxidation and a synergistic effect between the ligand and the solvent which is responsible for the improved activity. [B64]

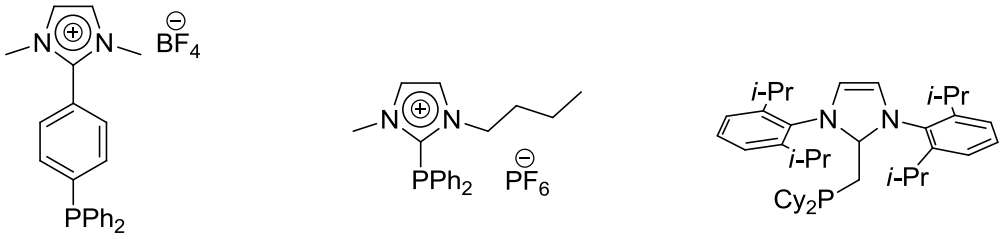

Wasserscheidt *et al.* **Wasserscheidt** *et al.*, **Wu** *et al.* **Beller** *et al.*

Scheme B30. Phosphino imidazolium salts. [B60e,B61a,B64]

7 Motivation

The development of new ligand structures and active catalysts for homogeneous catalysis accelerated rapidly in recent years, particularly with regard to activation of aryl halides under mild reaction conditions, low catalyst loadings and high conversions. Especially, phosphines

are of interest due to their versatility and mutable electronic and steric properties. However, it is still a challenge to predict their performance in homogeneous catalysis since small changes of these properties may affect the activity of the appropriate catalyst.

The main focus within this doctoral thesis laid on the synthesis and characterization of novel phosphines and their application in palladium-promoted *C,C* cross-couplings (Mizoroki-Heck, Suzuki-Miyaura reaction) and the ruthenium-catalyzed *β*-oxopropyl ester synthesis. The applied phosphines should feature various electronic and steric properties and can be divided into two main categories: *(i*) (ethynyl)ferrocenyl-based phosphines and *(ii*) (phosphino)imidazoles or (phosphino)imidazolium salts.

By applying a series of ferrocenyl- and (ferrocenylethynyl)phosphino palladium complexes, the influence of steric and electronic properties on the catalytic activity of the Mizoroki-Heck and Suzuki-Miyaura reaction will be investigated. Furthermore, based on controverse statements concerning the electronic character of the applied phosphines in the formation of *β*-oxopropyl esters, a systematic investigation on the influence of the phosphine on the catalytic performance will be carried out. The synthetic diversity of aryl-substituted imidazoles will be demonstrated by preparation of various organic- and organometallic-functionalized aryl phosphino imidazoles and imidazolium salts. Furthermore, the appropriate phosphines will be applied as ligands in the palladium-promoted Suzuki-Miyaura reaction both in organic solvents and ionic liquids.

8 References

[B1] For example: a) F. Diederich, P. J. Stang *Metal-Catalyzed Cross-Coupling Reactions, Wiley-VCH,* Weinheim, **1998**; b) U. Lehmann, S. Awasthi, T. Minehan *Org. Lett*. **2003**, *5*, 2405; c) P. W. N. M. van Leeuwen, J. C. Chadwick *Homogeneous Catalysts: Activity-Stability-Deactivation*, *Wiley-VCH*, Weinheim, **2011**.

[B2] For example: a) M. Beller, C. Bolm *Transition Metals for Organic Synthesis 2nd Edition, Wiley-VCH,* Weinheim **2004**; b) L. Xue, Z. Lin *Chem. Soc. Rev*. **2010**, *39,* 1692; c) M. Beller *Chemie Ingenieur Technik* **2006**, *78,* 1061; d) H.-U. Blaser, A. Indolese, A. Schnyder *Current Science* **2000**, *78,* 1336; e) B. Cornils, W. A.

Herrmann *Applied Homogenous Catalysis with Organometallic Compounds, Wiley-VCH*, Weinheim, **2002**.

[B3] For example: a) D. Steinborn *Grundlagen der metallorganischen Komplexchemie, Teubner*, Wiesbaden, **2007**; b) A. Behr *Angewandte Homogene Katalyse, Wiley-VCH*, Weinheim, **2008**; c) S. M. Roberts, J. Xiao, J. Whittall, T. E. Pickett *Metal Catalysed Carbon-Carbon Bond-Forming Reactions* in *Catalysts for Fine Chemical Synthesis*, Ed. S. M. Roberts, I. V. Kozhevnikov, E. Derouane, *John Wiley & Sons, Ltd.*, Chichester, **2004**; d) M. Baerns *Basic Principles in Applied Catalysis*, *Springer-Verlag*, Berlin, Heidelberg, New York, **2004**; e) K. C. Nicolaou, P. G. Bulger, D. Sarlah *Angew. Chem. Int. Ed*. **2005**, *44*, 4442.

[B4] a) X-F. Wu, P. Anbarasan, H. Neumann, M. Beller *Angew. Chem. Int. Ed*. **2010**, *49*, 9047; b) W. Shi, C. Liu, A. Lei *Chem. Soc. Rev*. **2011**, *40*, 2761.

[B5] D. Astruc *Anal Bioanal Chem* **2011**, *399*, 1811.

[B6] A. Suzuki, Y. Yamamoto *Chem. Lett*. **2011**, *40*, 894.

[B7] Booklet on *Palladium-Catalysed Coupling Chemistry*, Thermo Fisher Scientific Inc., **2010**.

[B8] J. E. Bäckvall *Scientific Background on the Nobel Prize in Chemistry 2010*, URL: http://www.nobelprize.org/nobel_prizes/chemistry/laureates/2010/advanced-chemistryprize2010.pdf (09.03.2012).

[B9] For example: a) M. Weck, C. W. Jones *Inorg. Chem*. **2007**, *46*, 1865; b) M. Shibasaki, E. M. Vogl *J. Organomet. Chem*. **1999**, *576*, 1; c) M. Ohff, A. Ohff, M. E. van der Boom, D Milstein *J. Am. Chem. Soc*. **1997**, *119*, 11687.

[B10] M. Oestreich *The Mizoroki-Heck Reaction, John Wiley & Sons, Ltd.*, Chichester, **2009**.

[B11] a) T. Mizoroki, K. Mori, A. Ozaki *Bull. Chem. Soc. Jpn*. **1971**, *44*, 581; b) J. P. Nolley, R. F. Heck *J. Org. Chem*. **1972**, *37*, 2320.

[B12] L. Ackermann *Modern Arylation Methods, Wiley-VCH*, Weinheim, **2009**.

[B13] T. Jeffery *J. Chem. Soc. Chem. Commun*. **1984**, 1287.

[B14] I. P. Beletskaya, A. V. Cheprakov *Chem. Rev.* **2000**, *100*, 3009.

[B15] M. T. Reetz, J. G. de Vries *Chem. Commun*. **2004**, 1559.

[B16] a) W. A. Herrmann, V. P. W. Böhm, C.-P. Reisinger *J. Organomet. Chem*. **1999**, *576*, 23; b) G. D. Frey, J. Schütz, E. Herdtweck, W. A. Herrmann *Organometallics* **2005**, *24*, 4416; c) W. A. Herrmann, C. Brossmer, K. Öfele, C.-P. Reisinger, T. Priermeier, M. Beller, H. Fischer *Angew. Chem. Int. Ed. Engl*. **1995**, *34*, 1844.

[B17] W. A. Herrmann, M. Elison, J. Fischer, C. Kocher, G. R. J. Artus *Angew. Chem. Int. Ed. Engl*. **1995**, *34*, 2371.

[B18] a) M. Portnoy, Y. Ben-David, D. Milstein *Organometallics* **1993**, *12*, 4734; b) Y. Ben-David, M. Portnoy, M. Gozin, D. Milstein *Organometallics* **1992**, *11*, 1995.

[B19] K. H. Shaughnessy, P. Kim, J. F. Hartwig *J. Am. Chem. Soc*. **1999**, *121*, 2123.

[B20] a) A. F. Littke, G. C. Fu *J. Am. Chem. Soc*. **2001**, *123*, 6989; b) A. F. Littke, G. C. Fu *J. Org. Chem*. **1999**, *64*, 10; c) M. R. Netherton, G. C. Fu *Org. Lett*. **2001**, *3*, 4295.

[B21] T. Iwasawa, T. Komano, A. Tajima, M. Tokunaga, Y. Obora, T. Fujihara, Y. Tsuji *Organometallics* **2006**, *25*, 4665.

[B22] B. Gümgüm, N. Biricik, F. Durap, I. Özdemir, N. Gürbüz, W. H. Ang, P. J. Dyson *Appl. Organometal. Chem*. **2007**, *21*, 711.

[B23] B. L. Shaw, S. D. Perera *Chem. Commun*. **1998**, 1863.

[B24] For example: a) A. Suzuki *J. Organomet. Chem*. **1999**, *576*, 147; b) F. Bellina, A. Carpita, R. Rossi *Synthesis* **2004**, *15*, 2419; c) S. Kotha, K. Lahiri, D. Kashinath *Tetrahedron* **2002**, *58*, 9633; d) A. F. Littke, G. C. Fu *Angew. Chem. Int. Ed*. **2002**, *41*, 4176; e) U. Christmann, R. Vilar *Angew. Chem. Int. Ed*. **2005**, *44*, 366; f) N. Miyaura *J. Organomet. Chem*. **2002**, *653*, 54; g) A. F. Littke, C. Dai, G. C. Fu *J. Am. Chem. Soc*. **2000**, *122*, 4020.

[B25] For example: a) A. C. Frisch, M. Beller *Angew. Chem. Int. Ed*. **2005**, *44*, 674; b) N. Miyaura, A. Suzuk *Chem. Rev*. **1995**, *95*, 2457.

[B26] a) C. Amatore, A. Jutand, M. A. M'Barki *Organometallics* **1992**, *11*, 3009; b) G. B. Smith, G. C. Dezeny, D. L. Hughes, A. O. King, T. R. Verhoeven *J. Org. Chem*. **1994**, *59*, 8151; c) E. Negishi, T. Takahashi, K. Akiyoshi *J. Chem. Soc., Chem. Commun*. **1986**, 1338; d) V. V. Grushin, H. Alper *Organometallics* **1993**, *12*, 1890; e) C. Amatore, A. Jutand *J. Organomet. Chem*. **1999**, *576*, 254.

[B27] A. A. C. Braga, G. Ujaque, F. Maseras *Organometallics* **2006**, *25*, 3647.

[B28] a) A. L. Casado, P. Espinet *Organometallics* **1998**, *17*, 954; b) F. M. Bickelhaupt, T. Ziegler, P. von Rague Schleyer *Organometallics* **1995**, *14*, 2288.

[B29] a) E. Galardon, S. Ramdeehul, J. M. Brown, A. Cowley, K. K. M. Hii, A. Jutand, *Angew. Chem. Int. Ed*. **2002**, *41*, 1760; b) Z. Li, Y. Fu, Q.-X. Guo, L Liu *Organometallics* **2008**, *27*, 4043.

[B30] Y.-L. Huang, C.-M. Weng, F.-E. Hong *Chem. Eur. J*. **2008**, *14*, 4426.

[B31] a) B. P. Carrow, J. F. Hartwig *J. Am. Chem. Soc*. **2011**, *133*, 2116; b) A. A. C. Braga, N. H. Morgon, G. Ujaque, F. Maseras *J. Am. Chem. Soc*. **2005**, *127*, 9298; c) N. Miyaura *J. Organomet. Chem*. **2002**, *653*, 54.

[B32] K. Matos, J. A. Soderquist *J. Org. Chem*. **1998**, *63*, 461.

[B33] a) A. H. Roy, John F. Hartwig *Organometallics* **2004**, *23*, 1533; b) D. A. Culkin, J. F. Hartwig *Organometallics* **2004**, 23, 3398; c) M. K. Loar, J. K. Stile *J. Am. Chem. Soc*. **1981**, 103, 4174; d) A. Moravskiy, J. K. Stille *J. Am. Chem. Soc*. **1981**, *103*, 4182.

[B34] a) C. Barnard Platinum Metals Rev. **2008**, 52, 38; b) V. V. Grushin, H. Alper *Chem. Rev*. **1994**, *94*, 1047.

[B35] a) M. Beller, H. Fischer, W. A. Herrmann, K. Öfele, C. Brossmer *Angew. Chem. Int. Ed. Engl*. **1995**, *34*, 1848; b) R. B. Bedford, S. L. Welch *Chem. Commun*. **2001**, 129; c) R. B. Bedford, S. L. Hazelwood, M. E. Limmert, D. A. Albisson, S. M. Draper, P. N. Scully, S. J. Coles, M. B. Hursthouse *Chem. Eur. J*. **2003**, *9*, 3216; d) D. A. Albisson, R. B. Bedford, S. E. Lawrence, P. N. Scully *Chem. Commun*. **1998**, 2095.

[B36] a) J. Hassan, M. Sevignon, C. Gozzi, E. Schulz, M. Lemaire *Chem. Rev*. **2002**, *102*, 1359; b) R. B. Bedford, C. S. J. Cazin, D. Holder *Coord. Chem. Rev*. **2004**, *248*, 2283.

[B37] W. Shen *Tetrahedron Lett*. **1997**, *38*, 5575.

[B38] A: F. Littke, G. C. Fu *Angew. Chem. Int. Ed*. **1998**, *37*, 3387.

[B39] a) S.-Y. Liu, M. J. Choi, G. C. Fu *Chem. Commun*. **2001**, 2408; b) T. E. Pickett, C. J. Richards *Tetrahedron Lett*. **2001**, *42*, 3767.

[B40] a) A. Zapf, A. Ehrentraut, M. Beller, *Angew. Chem. Int. Ed*. **2000**, *39*, 4153; b) J. P. Stambuli, R. Kuwano, J. F. Hartwig *Angew. Chem. Int. Ed*. **2002**, *41*, 4746.

[B41] a) J. P. Wolfe, S. L. Buchwald *Angew. Chem. Int. Ed*. **1999**, *38*, 2413; b) J. P. Wolfe, R. A. Singer, B. H. Yang, S. L. Buchwald *J. Am. Chem. Soc*. **1999**, *121*, 9550; c) D. W. Old, J. P. Wolfe, S. L. Buchwald *J. Am. Chem. Soc*. **1998**, *120*, 9722; d) S. D. Walker, T. E. Barder, J. R. Martinelli, S. L. Buchwald *Angew. Chem. Int. Ed*. **2004**, *43*, 1871.

[B42] a) W. A. Herrmann, C.-P. Reisinger, M. Spiegler *J. Organomet. Chem*. **1998**, *557*, 93; b) T. Weskamp, V. P. W. Böhm, W. A. Herrmann *J. Organomet. Chem*. **1999**, *585*, 348; c) C. W. K. Gstöttmayr, V. P. W. Böhm, E. Herdtweck, M. Grosche, W. A. Herrmann *Angew. Chem. Int. Ed*. **2002**, *41*, 1363; d) A. C. Hillier, G. A. Grasa, M. S. Viciu, H. M. Lee, C. Yang, S. P. Nolan *J. Organomet. Chem*. **2002**, *653*, 69; e) C. Zhang, J. Huang, M. L. Trudell, S. P. Nolan *J. Org. Chem*. **1999**, *64*, 3804.

[B43] a) D. Devanne, C. Ruppin, P. H. Dixneuf *J. Org. Chem*. **1988**, *53*, 925; b) C. Bruneau, P. H. Dixneuf *Angew. Chem. Int. Ed*. **2006**, *45*, 2176; c) C. Bruneau, Z. Kabouche, M. Neveux, B. Seiller, P. H. Dixneuf *Inorg. Chim. Acta* **1994**, *222*, 155; d) M. Neveux, B. Seiller, F. Hagedorn, C. Bruneau, P. H. Dixneuf *J. Organomet. Chem*. **1993**, *451*, 133; e) V. Cadierno, J. Francos, J. Gimeno *Green Chem*. **2010**, *12*, 135; f) C. Bruneau, M. Neveux, Z. Kabouche, C. Ruppin, P. H. Dixneuf *Synlett* **1991**, 755; g) T. Mitsudo, Y. Hori, Y. Yamakawa, Y. Watanabe *J. Org. Chem*. **1987**, *52*, 2230; h) M. Neveux, B. Seiller, F. Hagedorn, C. Bruneau, P. H. Dixneuf *J. Organomet. Chem*. **1993**, *451*, 133.

[B44] a) D. W. Hansen, Jr., R. Pappo, R. B. Garland *J. Org. Chem*. **1988**, *53*, 4244; b)) P. Yates, R. S. Grewal, P. C. Hayes, J. F. Sawyer *Can. J. Chem*. **1988**, *66*, 2805; c) S. Costin, N. P. Rath, E. B. Bauer *Adv. Synth. Catal*. **2008**, *350*, 2414.

[B45] M. M. Salunkhe, A. R. Sande, A. S. Kanade, P. P. Wadgaonkarb *Synth. Commun*. **1997**, *27*, 2885.

[B46] a) M. Arfan Ashraf, A. G. Russell, C. W. Wharton, J. S. Snaith *Tetrahedron* **2007**, *63*, 586; b) M. A. Ashraf, M. A. Jones, N. E. Kelly, A. Mullaney, J. S. Snaith, I. Williams *Tetrahedron Lett*. **2003**, *44*, 3151.

[B47] a) A. J. Fry, D. Herr *Tetrahedron Lett*. **1978**, *19*, 1721; b) L. J. Goossen, J. Paetzold, D. Koley *Chem. Comm*. **2003**, 706; c) A. D. Cort *J. Org. Chem*. **1991**, *56*, 6708; d) R. C. Cambie, R. C. Hayward, J. L. Jurlina, P. S. Rutledge, P. D. Woodgate *J. Chem. Soc. Perkin Trans*. **1978**, *1*, 126; e) S. Torii, T. Inokuchi, S. Misima, T. Kobayashi *J.*

Org. Chem. **1980**, *45*, 2731; f) S. Stavber, B. Sket, B. Zajc, M. Zupan *Tetrahedron* **1989**, *45*, 6003.

[B48] M. Rotem, Y. Shvo *Organometallics* **1983**, *2*, 1689.

[B49] P. Štěpnička, J. Demel, J. Cejka *J. Molec. Catal. A: Chem*. **2004**, *224*, 161.

[B50] a) A. Togni, T. Hayashi *Ferrocenes – Homogeneous Catalysis, Organic Synthesis, Materials Science, VCH*, Weinheim, **1995**; b) P.Štěpnička *Ferrocenes: Ligands, Materials and Biomolecules, John Wiley & Sons, Ltd*., Chichester, **2008**.

[B51] a) T. J. Colacot *Platinum Metals Rev*. **2001**, *45*, 22; b) P. W. N. M. van Leeuwen, P. C. J. Kamer, J. N. H. Reek, P. Dierkes *Chem. Rev*. **2000**, *100*, 2741; c) R. C. J. Atkinson, V. C. Gibson, N. J. Long *Chem. Soc. Rev*., **2004**, *33*, 313; d) P. Barbaro, C. Bianchini, G. Giambastiani, S. L. Parisel *Coord. Chem. Rev*. **2004**, *248*, 2131; e) N. Kataoka, Q. Shelby, J. P. Stambuli, J. F. Hartwig *J. Org. Chem*. **2002**, *67*, 5553.

[B52] a) L. E. Hagopian, A. N. Campbell, J. A. Golen, A. L. Rheingold, C. Nataro *J. Organomet. Chem*. **2006**, *691*, 4890; b) T. J. Colacot, H. A. Shea *Org. Lett*. **2004**, *6*, 3731.

[B53] G. Bandoli, A. Dolmella *Coord. Chem. Rev*. **2000**, *209*, 161.

[B54] a) U. Siemeling, T.-C. Auch *Chem. Soc. Rev*. **2005**, *34*, 584, b) G. P. Sollot, J. L. Snead, S. Portnoy, W. R. Peterson, Jr., H. E. Mertwoy, *Chem. Abstr*. **1965**, *63*, 18147b.

[B55] T. Hayashi, M. Konishi, M. Kumada, *Tetrahedron Lett*. **1979**, *20*, 1871.

[B56] a) Q. Shelby, N. Kataoka, G. Mann, J. F. Hartwig *J. Am. Chem. Soc*. **2000**, *122*, 10718; b) G. Mann, C. Incarvito, A. L. Rheingold, J. F. Hartwig *J. Am. Chem. Soc*. **1999**, *121*, 3224.

[B57] T. E. Pickett, F. X. Roca, C. J. Richards *J. Org. Chem*. **2003**, *68*, 2592.

[B58] a) T. L. Gilchrist *Heterocyclenchemie, Wiley-VCH*, Weinheim, **1995**; b) T. Eicher, S. Hauptmann *Chemie der Heterocyclen, Georg Thieme Verlag*, Stuttgart, **1994**; c) R. R. Gupta, M. Kumar, V. Gupta *Heterocyclic Chemistry II, Springer*, Berlin, Heidelberg, **1999**.

[B59] A. J. Arduengo, III, R. L. Harlow, M. Kline *J. Am. Chem. Soc* **1991**, *113*, 361.

[B60] a) H. Willms, W. Frank, C. Ganter *Organometallics*, **2009**, *28*, 3049; b) J. Li, J. Peng, Y. Bai, G. Zhang, G. Lai, X. Li *J. Organomet. Chem*. **2010**, *695*, 431; c) S.

Sauerbrey, P. K. Majhi, J. Daniels, G. Schnakenburg, G. M. Brändle, K. Scherer, R. Streubel *Inorg. Chem*. **2011**, *50*, 793; d) Q.-X. Wan, Y. Liu, Y.-Q. Cai *Catal. Lett*. **2009**, *127*, 386; e) D. J. Brauer, K. W. Kottsieper, C. Liek, O. Stelzer, H. Waffenschmidt, P. Wasserscheid *J. Organomet. Chem*. **2001**, *630*, 177; f) S. S. Moore, G. M. Whitesides *J. Org. Chem*. **1982**, *47*, 1489; g) V. Diez, G. Espino, F. A. Jalon, B. R. Manzano, M. Perez-Manrique *J. Organomet. Chem*. **2007**, *692*, 1482; h) M. A. Jalil, S. Fujinami, T. Honjo, H. Nishikawa *Polyhedron* **2001**, *20*, 1071.

[B61] For example: a) A. Dumrath, X.-F. Wu, H. Neumann, A. Spannenberg, R. Jackstell, M. Beller *Angew. Chem. Int. Ed*. **2010**, *49*, 8988; b) S. Harkal, F. Rataboul, A. Zapf, C. Fuhrmann, T. Riermeier, A. Monsees, M. Beller *Adv. Synth. Catal*. **2004**, *346*, 1742; c) J. Sirieix, M. Oßberger, B. Betzemeier, P. Knochel *Synlett* **2000**, *11*, 1613; d) N. Debono, Y. Canac, C. Duhayon, R. Chauvin *Eur. J. Inorg. Chem*. **2008**, 2991; e) C. Torborg, J. Huang, T. Schulz, B. Schäffner, A. Zapf, A. Spannenberg, A. Börner, M. Beller *Chem. Eur. J*. **2009**, *15*, 1329;

[B62] a) S. Saleh, E. Fayad, M. Azouri, J.-C. Hierso, J. Andrieu, M. Picquet *Adv. Synth. Catal*. **2009**, *351*, 1621; b) C. S. Consorti, G. L. P. Aydos, G. Ebeling, J. Dupont *Org. Lett*. **2008**, *10*, 237; c) J. Andrieu, M. Azouri *Inorg. Chim. Acta* **2007**, *360*, 131; d) P. J. Dyson, T. J. Geldbach in *Catalysis by Metal Complexes-Metal Catalyzed Reactions in Ionic Liquids*, ed. B. James, P. W. N. M. van Leeuwen, *Springer*, Dordrecht, **2005**, vol. 29; e) P. Wasserscheid, T. Welton *Ionic Liquids in Synthesis*, *Wiley- VCH*, Weinheim, 2nd edn, **2008**, vol. 1; f) J. Zhang, M. Dakovic, Z. Popovic, H. Wu, Y. Liu *Catal. Commun*. **2012**, *17*, 160.

[B63] T. Schulz, C. Torborg, B. Schäffner, J. Huang, A. Zapf, R. Kadyrov, A. Börner, M. Beller *Angew. Chem. Int. Ed*. **2009**, *48*, 918.

[B64] Q.-X. Wan, Y. Liu, Y. Lu, M. Li, H.-H. Wu *Catal. Lett*. **2008**, *121*, 331.

C Metallocenyl Phosphine Palladium Dichlorides: Synthesis, Electrochemistry and their Application in *C,C* Coupling Reactions

Bianca Milde, Manja Lohan, Claus Schreiner, Tobias Rüffer, and Heinrich Lang

Published in *Eur. J. Inorg. Chem*. **2011**, 5437 – 5449.

*The ruthenocenyl phosphines **6a** – **d**, the seleno phosphines **7a** – **d** and the palladium complexes **10a** – **d** were prepared and characterized by Dr. Manja Lohan (Dissertation, TU Chemnitz, 2011). She also performed and analyzed the results of the catalytic test reactions of the respective ruthenocenyl phosphine palladium complexes. Dr. Claus Schreiner (Dissertation, TU Chemnitz, 2009) prepared and fully characterized the ferrocenyl-based seleno phosphine **4a**. The preparation, characterization and catalytic test reactions of the remaining novel ferrocenyl compounds were accomplished by the author.*

1 Introduction

The development of novel ligands for palladium-catalyzed *C,C* coupling reactions have accelerated during recent years because new ligand structures may effect activation of aryl-chloro bonds under mild reaction conditions, high conversions, and low catalyst loadings. [C1] Hitherto, mostly mono- and bi-dentate alkyl-, aryl-, and ferrocenyl-functionalized phosphines, *N*-heterocyclic carbenes and palladacycles were successfully used in the synthesis of effective palladium catalysts. [C1-4] Especially electron rich and/or bulky mono- and bidentate phosphines are of particular interest, [C4c,C5] although it is still a challenge to predict their performance in homogeneous catalysis since small changes in their electronic and/or spatial structure may affect the activity of the appropriate catalyst. [C4c] This prompted us to synthesize metallocenyl-based phosphines of type PR_2Fc (Fc = $Fe(\eta^5\text{-}C_5H_4)(\eta^5\text{-}C_5H_5)$) and PR_2Rc (Rc = $Ru(\eta^5\text{-}C_5H_4)(\eta^5\text{-}C_5H_5)$) because the metallocenyl entity achieves a significant increase in stability of the respective phosphine toward air and moisture, while the organic ligands R are responsible to control the electronic and steric properties.

To quantify the σ donor ability of a phosphino group it is likely to measure the magnitude of the ^{31}P-^{77}Se coupling constant of the corresponding seleno phosphine. Allen and Taylor have reported that an increase in $^{1}J(^{31}P$-$^{77}Se)$ indicates an increase in the s character of the phosphorus lone-pair orbital and as result thereof, the basicity of the phosphine decreases. [C6]

We herein enrich the family of metallocenyl-functionalized phosphines featuring electron donating or electron withdrawing organic groups by applying straightforward synthesis methodologies. The use of these phosphines in palladium-catalyzed Mizoroki-Heck and Suzuki-Miyaura reactions is discussed. A quantification of the electronic properties of the phosphines toward the catalytic activities will be performed as well.

2 Results and Discussion

2.1 Ligand Synthesis and Properties

Metallocenyl phosphines **3a** – **e** and **6a** – **d**, the corresponding seleno phosphines **4a** – **e** and **7a** – **d** as well as their palladium complexes **9a** – **e** and **10a** – **d** were prepared according to synthesis methodologies reported earlier (Scheme C1, Reaction C1, Tables C1 and C2). [C4b,C6f,C8]

The synthesis of the metallocenyl phosphines PR_2Mc (Mc = Fc = Fe(η^5-C_5H_4)(η^5-C_5H_5): **3a**, R = Ph; [C7] **3b**, R = *o*-Tol; **3c**, R = Fur; **3d**, R = *t*-Bu; [C7] **3e**, R = Cy [C7]. Mc = Rc = Ru(η^5-C_5H_4)(η^5-C_5H_5): **6a**, R = Ph; **6b**, R = *o*-Tol; **6c**, R = Fur; **6d**, R = Cy) and the appropriate seleno phosphines $Se{=}PR_2Mc$ (Mc = Fc: **4a** – **e**; Mc = Rc: **7a** – **d**) was carried out in a consecutive reaction sequence as depicted in Scheme C1. Lithiation of M(η^5-C_5H_4I)(η^5-C_5H_5) (M = Fe, **1**; M = Ru, **5**) and subsequent treatment with R_2PCl (**2a**, R = Ph; **2b**, R = *o*-Tol; **2c**, R = Fur; **2d**, R = *t*-Bu; **2e**, R = Cy) gave metallocenyl phosphines **3** and **6**, which on further reaction with selenium in its elemental form produced the seleno phosphines **4** and **7**, respectively (Scheme C1, Table C1).

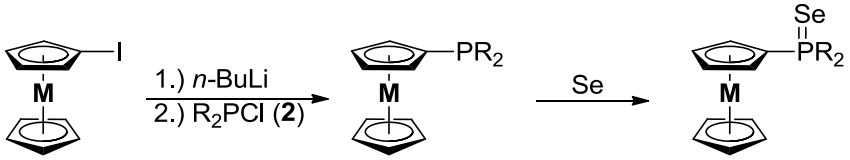

1, M = Fe
5, M = Ru

3, M = Fe
6, M = Ru

4, M = Fe
7, M = Ru

Scheme C1. Synthesis of **3**, **4**, **6** and **7** from **1** or **5**.

Table C1. Synthesis of **3a** – **e**, **4a** – **e**, **6a** – **d**, and **7a** – **d**.

Compd.	M	R	Yield [a]/ %	Compd.	M	R	Yield [a]/ %
3a	Fe	Ph	57	**6a**	Ru	Ph	35
3b	Fe	*o*-Tol	69	**6b**	Ru	*o*-Tol	36
3c	Fe	Fur	63	**6c**	Ru	Fur	46
3d	Fe	*t*-Bu	48	**6d**	Ru	Cy	42
3e	Fe	Cy	31				
4a	Fe	Ph	100	**7a**	Ru	Ph	89
4b	Fe	*o*-Tol	100	**7b**	Ru	*o*-Tol	94
4c	Fe	Fur	100	**7c**	Ru	Fur	84
4d	Fe	*t*-Bu	100	**7d**	Ru	Cy	92
4e	Fe	Cy	100				

[a] Based on **1** and **5** or **3** and **6**.

Complexation of **3** and **6** was possible by addition of these phosphines to $[PdCl_2(cod)]$ (**8**) (cod = cyclo-1,5-octadiene) at ambient temperature (Reaction C1). After appropriate work-up, the orange to red colored ferrocenyl or pale yellow ruthenocenyl phosphine complexes **9** (M = Fe) and **10** (M = Ru) could be isolated in 70 – 90 % yield (Table C2, Experimental Section).

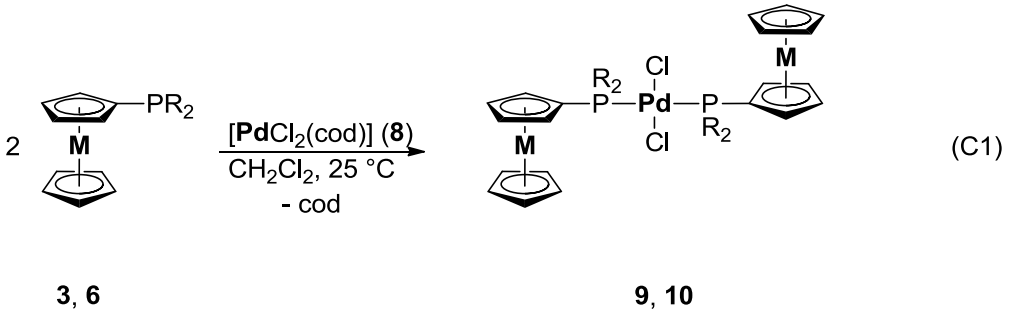

(C1)

3, **6** **9**, **10**

Table C2. Synthesis of **9a** – **9e** and **10a** – **10d**.

Compd.	M	R	Yield [a]/ %	Compd.	M	R	Yield [a]/ %
9a	Fe	Ph	90	**10a**	Ru	Ph	83
9b	Fe	*o*-Tol	84	**10b**	Ru	*o*-Tol	84
9c	Fe	Fur	77	**10c**	Ru	Fur	86
9d	Fe	*t*-Bu	74	**10d**	Ru	Cy	70
9e	Fe	Cy	81				

[a] Based on **8**.

Solid phosphines **3** (yellow) and **6** (pale yellow) are stable in air, no oxidation of the phosphorus(III) center is observed. However, it appeared that solutions containing these molecules slowly oxidize to give the corresponding phosphine oxides. As expected, molecules **4**, **7**, **9** and **10** are stable both in air and moisture. Yet, compound **7d** shows sensitivity toward light and slowly turns pale yellow.

All compounds have been identified by elemental analysis, IR and NMR (^{1}H, ^{13}C{^{1}H}, ^{31}P{^{1}H}) spectroscopy and ESI TOF mass-spectrometry (Experimental Section). The electrochemical behavior of **3**, **4** and **9** was determined.

2.2 Electrochemistry

The redox properties of phosphines **3** and **4** and the corresponding palladium complexes **9** were studied by Cyclic Voltammetry (= CV), Linear Sweep Voltammetry (= LSV, **9**), and Square Wave Voltammetry (= SWV, **9**), and also by spectro-electrochemistry (UV-Vis/NIR spectroscopy, **9b**) in dry dichloromethane utilizing 0.1 mol·L^{-1} [(*n*-Bu)$_4$N][B(C$_6$F$_5$)$_4$] as supporting electrolyte. The latter combination was chosen because it could recently be shown by Geiger *et al.* [C9] that it provides close-to-optimal conditions for electrochemical experiments, since it minimizes electrolyte-analyte interactions and hence, follow-up reactions. The CV studies were carried out at scan rates of 100 mV·s^{-1} and the data are summarized in Table C3. All potentials are referenced to the FcH/FcH^{+} redox couple as internal standard as recommended by IUPAC. [C10]

Table C3. Cyclovoltammetric data (potentials *vs.* FcH/FcH^{+}), scan rate 100 mV·s^{-1} at a glassy-carbon electrode of 1.0 mmol·L^{-1} solutions of **3** and **4** in dry dichloromethane containing 0.1 mol·L^{-1} of [(*n*-Bu)$_4$N][B(C$_6$F$_5$)$_4$] as supporting electrolyte at 25 °C.

Compd.	E^0 (ΔE_p) / V	$E_{ox\text{-}irrev}$ / V	$E_{red\text{-}irrev}$ / V	Compd.	$E_{ox\text{-}irrev}$ / V	$E_{red\text{-}irrev}$ / V
3a	0.064 (0.082)		0.703	**4a**	0.288 0.934 1.058	-0.290 0.021 0.674 0.838
3b	0.013 (0.090)			**4b**	0.241 0.895	-0.449 0.713
3c	0.091 (0.108)			**4c**	0.326 1.122	-0.454 0.238 0.510 0.802

	0.022	-0.046			0.108
3d	0.188	0.158	**4d**	0.216	0.360
	0.806	0.702		0.858	0.712
	0.023	-0.029			-0.290
3e	0.207	0.175	**4e**	0.270	0.176
	0.815	0.713		0.706	0.586

E^0 = redox potential, ΔE_p = difference between oxidation and reduction potential, $E_{ox\text{-}irrev}$ = irreversible oxidation potential, $E_{red\text{-}irrev}$ = irreversible reduction potential.

The electrochemically most studied member of the series of phosphines reported in this work is ferrocenyl diphenyl phosphine. Kotz and Nivert reported that a reversible one-electron oxidation at E^0 = 0.48 V (*vs.* SCE) is observed, when measured to a maximum potential of 0.8 V, whereupon irreversible oxidations occur at higher potentials (1.5 V). [C11a,b] The 1st oxidation process confirms the ferrocenyl oxidation and the resulting ferrocenium ion participates in an intra-molecular electron transfer from the PPh_2 group to iron. [C11] Under our conditions we observed a similar behavior for all other ferrocenyl phosphines (Table C3). Exemplary, the CVs of **3b** and **3e** are shown in Figure C1. As consequence of the nature of the alkyl or aryl substituents at phosphorus a different electronic and hence, electrochemical behavior is expected. The more electron-rich the molecules are the easier is their oxidation. This meets the expected trend furyl < phenyl < *o*-tolyl for the aromatic phosphines, whereupon aliphatic phosphines **3d** and **3e** show a similar electronic character and a completely irreversible behavior (Table C3).

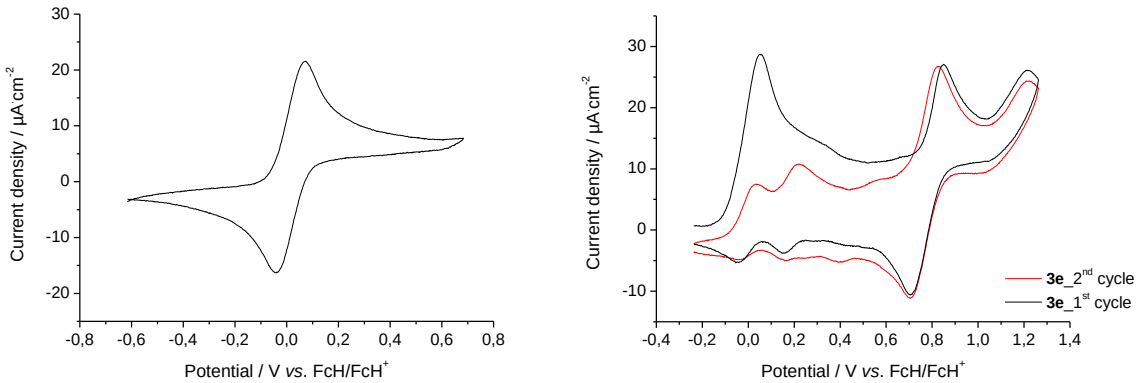

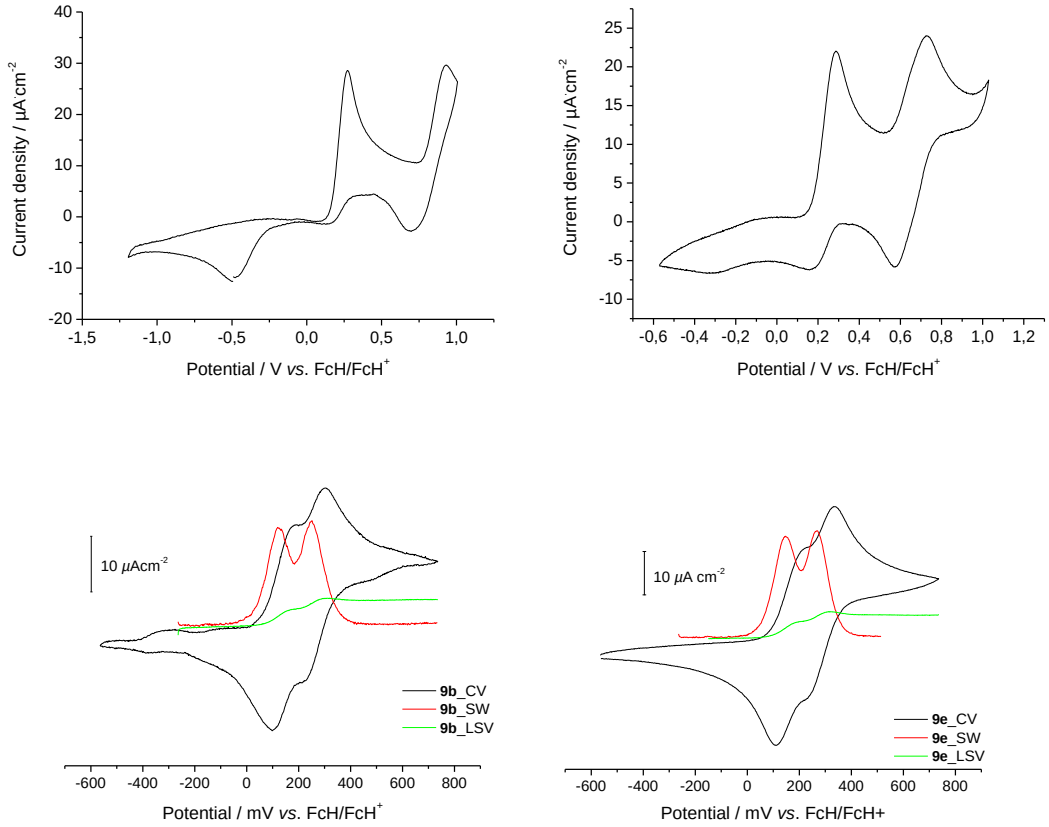

Figure C1. Electrochemical data of dichloromethane solutions containing 1.0 mmol·L^{-1} of **3b** (top, left), **4b** (middle, left), and **9b** (bottom, left) and **3e** (top, right), **4e** (middle, right), and **9e** (bottom, right) at 25 °C, supporting electrolyte [(*n*-Bu)$_4$N][B(C$_6$F$_5$)$_4$] with a scan rate of 100 mV·s^{-1}.

As mentioned earlier, all free phosphines were converted into the appropriate seleno phosphines to investigate their electronic properties (*vide infra*). Ferrocenyl phosphine chalcogenides are electrochemically less investigated than free phosphines, at which phosphine sulfides and oxides showing a reversible behavior are best studied. [C9,C12a,b] While electrochemically induced follow-up reactions are not expected due to the oxidation state of V at phosphorus, however, seleno phosphines show a different behavior. We examined the electrochemistry of **4a** – **e** under the same measurement conditions as described above (Figure C1). As expected, the seleno phosphines are more difficult to oxidize than the appropriate P(III) containing molecules **3a** – **e** (Table C3). In all CVs almost irreversible oxidation events between 0.16 – 0.33 V are observed which give a cathodic response between -0.67 – -0.29 V, most probably attributed to follow-up reactions. Besides, it is apparent that the more reversible the oxidation processes are, the lower the intensity of the cathodic response is. A similar behavior was recently described for diseleno 1,1'-bis(diphenylphosphino) ferrocene

[C12b] and seleno bi- and tri-ferrocenyl phenyl phosphines. [C9] The corresponding follow-up products are presumably resulting from an intra-molecular electron transfer from the selenium-centered radical. Therefore, contributions from either the iron, phosphorus or selenium radicals are expected in the monocations of this series.

However, intra-molecular oxidations are inhibited, when the phosphorus atom in **3a** – **e** is datively-bonded to palladium as given in **9a** – **e** (Figure C1, Table C4). Surprisingly, for these ferrocenyl phosphine palladium complexes two reversible oxidation processes between E^0 = 0.11 and E^0 = 0.27 V with ΔE^0 values between 0.058 - 0.126 V are observed. This indicates that the two metallocenyls can separately be oxidized. The electrochemical data of these transition metal compounds are summarized in Table C4. No further redox events indicating follow-up reactions are observed. Compared to the *non*-coordinated metallocenyl phosphines, the respective palladium complexes are more difficult to oxidize which can be explained by the electron withdrawing character upon coordination of the phosphines to palladium (Figure C1, Table C4). In addition to CV measurements, LSV and SWV studies were carried out (Figure C1) confirming one-electron processes.

Table C4. Cyclovoltammetric data (potentials *vs.* FcH/FcH^+), scan rate 100 $mV \cdot s^{-1}$ at a glassy-carbon electrode of **9a** – **e** in dry dichloromethane solution (1.0 $mmol \cdot L^{-1}$) containing 0.1 $mol \cdot L^{-1}$ of $[(n\text{-}Bu)_4N][B(C_6F_5)_4]$ as supporting electrolyte at 25 °C.

Compd.	$\boldsymbol{E_1^0}$ (ΔE_p) / V	$\boldsymbol{E_2^0}$ (ΔE_p) / V	ΔE^0 / V
9a	0.145 (0.097)	0.263 (0.099)	0.116
9b	0.118 (0.072)	0.244 (0.072)	0.126
9c	0.212 (0.082)	0.270 (0.080)	0.058
9d	0.118 (0.094)	0.203 (0.092)	0.085
9e	0.169 (0.090)	0.276 (0.088)	0.107

E_1^0 = potential of the 1st redox process, E_2^0 = potential of the 2nd redox process, ΔE_p = difference between oxidation and reduction potential, ΔE^0 = potential difference between two redox processes.

To investigate electrochemically generated electronic absorptions in the visible and near infrared regions, a spectro-electrochemical investigation was exemplarily performed with **9b**, since this molecule shows the largest peak separation (ΔE^0 = 0.126 V) between the 1st and 2nd oxidation. Absence of NIR charge transfer bands would point to electron-localized mixed-valent complexes, while their presence would argue in favor of electron delocalization. The spectro-electrochemical studies were conducted by the stepwise increase of the potential from -0.2 to 1.2 V *vs.* Ag/AgCl in an OTTLE [12f,g] cell (OTTLE = Optically Transparent Thin-

Layer Electrode) containing dichloromethane solutions of **9b** (1.0 mmol·L^{-1}) and [(*n*-Bu)$_4$N][B(C$_6$F$_5$)$_4$] (0.1 mol·L^{-1}) as supporting electrolyte. This procedure allowed the generation of **9b**$^+$ from neutral **9b**. From Figure C2 it can be seen that transition metal complex **9b**$^+$ does not exhibit any absorption in the NIR range which confirms that positive charges were very much localized on the Fc$^+$ groups in mixed-valent partially oxidized intermediates (Figure C2). Nevertheless, during oxidation an absorption in the UV/Vis part of the spectrum at 524 nm occurs which can most probably be assigned to a ligand-to-metal charge transfer transition from the ligand to the ferrocenium moiety. [C12c-e] The ΔE^0 value of 0.126 V indicates some electrostatic interaction among the two terminal ferrocenyl groups as oxidation progresses.

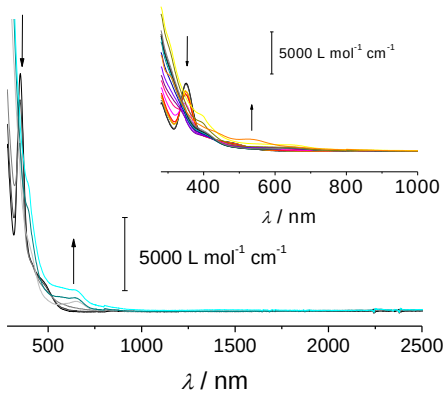

Figure C2. UV-Vis/NIR spectra of **9b** at rising potentials (-0.2 to 1.2 V *vs*. Ag/AgCl) at 25 °C, in dichloromethane, supporting electrolyte [(*n*-Bu)$_4$N][B(C$_6$F$_5$)$_4$]. Arrows indicate increasing or decreasing of absorptions.

2.3 Single Crystal X-ray Structure Determination

The molecular structure of **4b** in the solid state was solved by single X-ray structure analysis. Suitable crystals were obtained from a saturated dichloromethane solution containing **4b** at ambient temperature. The ORTEP diagram, selected bond distances (Å), angles (°) and torsion angles (°) are shown in Figure C3. The crystal and structure refinement data are presented in the Experimental Section.

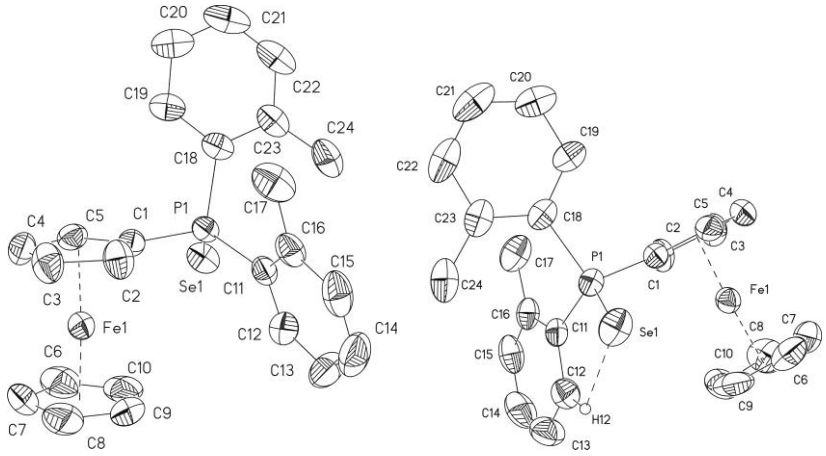

Figure C3. Left: ORTEP diagram (50 % probability level) of the molecular structure of **4b** with the atom numbering scheme. (Hydrogen atoms are omitted for clarity.) Standard uncertainties of the last significant digit(s) are shown in parenthesis (D1 = denotes the centroid of C_5H_4; D2 = denotes the centroid of C_5H_5). Selected bond distances (Å), angles (°) and torsion angles (°): Fe-D1 = 1.673, Fe-D2 = 1.645, C1–P1 = 1.795(3), C11-P1 = 1.829(3), C18–P1 = 1.818(3), P1-Se1 = 2.1198(7); C1–P1–Se1 = 112.30(9), C11–P1–Se1 = 114.04(8), C18–P1–Se1 = 109.92(8), C1-P1-C11 = 103.74(12), C1-P1-C18 = 105.78(12), C18-P1-C11 = 110.63(12), D1–Fe–D2 = 176.8; C16–C11–P1–Se1 = 163.3(2), C12–C11–P1–Se1 = -20.2(2), C23-C18-P1-Se1 = -69.1(2), C5-C1-P1-Se1 = -36.9(2), P1-C18-C23-C24 = -6.3(4), P1-C11-C16-C17 = -4.8(4). Right: Visualization of the short intramolecular Se1-H12 contact (d(Se1···H12) = 2.830 Å).

Molecule **4b** crystallizes in the monoclinic space group *P*2(1)/*n*. The crystal structure of **4b** is set-up by one ferrocenyl unit of which the two cyclopentadienyl rings are with 3° almost parallel oriented to each other. Two *ortho*-tolyl groups, the (η^5-C_5H_4)Fe(η^5-C_5H_5) unit and one selenium atom are bound to the phosphorus atom resulting in a tetrahedrally distorted geometry (Figure C3). The P-C bond separations with 1.795(3) and 1.829(3) Å are representative for P-C_{aryl} entities. [C4b,C6d,C13,C14] Very characteristic is the P1-Se1 bond with 2.1198(7) Å, which is identical to that of other seleno phosphines, *i. e.*, *tri-ortho*-tolyl seleno phosphine [C13,C14] containing electron-donating methyl substituents. As result thereof, the s character of the P orbital involved in bonding to Se is decreased (*vide infra*). The C-P-C angles at P1 (Figure C3) are with 103.74(12) - 110.63(12) in the typical range for tertiary seleno phosphines. [C4b,C6d,C13,C14] Worth mentioning is the Se1-H12 distance of 2.830 Å which is less than the sum of the van-der-Waals radii (3.10 [C15a] – 3.35 [C15b] Å) and might also be a reason for the broadened signals in the NMR spectra (*vide infra*). All other structural

parameters are unexceptional and correspond to those of related compounds. [C4b,C6d,C13,C14] However, the ^{1}H and $^{13}C\{^{1}H\}$ NMR spectra of **4b** and **6b** show very broad resonances for both the C_5H_4 and *ortho*-tolyl protons which indicates a dynamic behavior (Figure C4). Nevertheless, for both compounds it is typical that the $^{31}P\{^{1}H\}$ NMR signal of phosphorus(V) displays a sharp singlet at ambient temperature. The free rotation of the phosphino group could be reduced by cooling NMR samples of **4b** to -90 °C resulting in the appearance of four individual signals for the protons of the C_5H_4 moieties and eight aromatic signals for both *ortho*-tolyl units of equal intensities, respectively (Figure C4). This observation indicates that the *ortho*-tolyl units are not symmetry equivalent and hence, a fast inversion of the configuration of phosphorus must occur at ambient temperature, which is frozen at -90 °C on the NMR time scale. Furthermore, the values of the $^{1}J(^{31}P\text{-}^{13}C)$ coupling constants of both *ortho*-tolyl moieties are almost equal which indicates no significant influence of the spatial orientation of the *ortho*-tolyl groups on the P-C configuration. Additionally, HSQC and *H,H*-COSY measurements were performed as well to completely assign all peaks to the respective hydrogen and carbon atoms (Supporting Information, Figure C7). The splitting pattern of the NMR signals reveal a C_2 symmetry of **4b** at low temperature in solution which is in accordance with the result of the X-ray diffraction analysis. Moreover, the ^{1}H NMR signals assigned to the *ortho*-protons of the tolyl moiety shift significantly upon cooling, which might be explained by the close proximity of those hydrogen atoms toward selenium (*vide supra*).

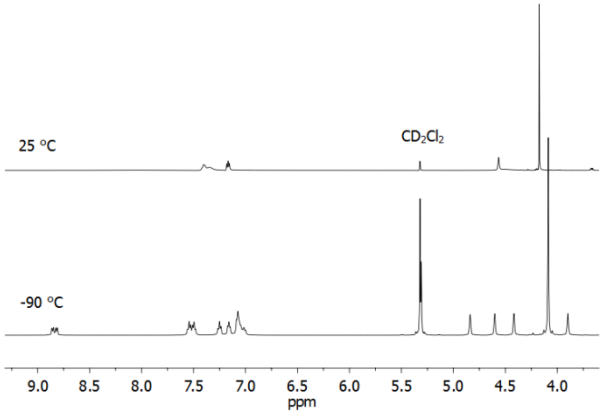

Figure C4. ^{1}H NMR spectra of **4b** in the range between 3.5 and 9.5 ppm in CD_2Cl_2 at 25 °C (top) and at -90 °C (bottom).

The donor properties of PR_3 (R = alkyl, aryl, alkoxyl) toward selenium acceptors can be quantified by $^{1}J(^{31}P\text{–}^{77}Se)$ as indicated by $^{31}P\{^{1}H\}$ NMR spectroscopy. [C6] An electron-withdrawing group at phosphorus increases $^{1}J(^{31}P\text{–}^{77}Se)$ explainable by the increased s character of the phosphorus orbital involved in the P–Se bonding. Consequently, shorter bond

distances between the phosphorus and the acceptor carbon atoms are observed. This electronic impact has direct influence on the phosphorus donor ability and hence, on the electron density at the appropriate transition metal complex. The absolute value of $^{1}J(^{31}P\text{-}^{77}Se)$ is a decisive parameter for the specific design of compounds used as catalytic active species in homogeneous catalysis (*vide infra*). The $^{31}P\{^{1}H\}$ NMR data together with the $^{1}J(^{31}P\text{-}^{77}Se)$ coupling constant for **4a** – **e** and **7a** – **d** are summarized in Table C5.

Table C5. Chemical shifts and $^{1}J(^{31}P\text{-}^{77}Se)$ values of **4a** – **e** and **7a** – **d**, and $Ph_3P{=}Se$ [C6a] for comparison.

Compd.	δ / ppm	$^{1}J(^{31}P\text{-}^{77}Se)$ / Hz	Compd.	δ / ppm	$^{1}J(^{31}P\text{-}^{77}Se)$ / Hz
4a	31.8	733	**7a**	31.2	735
4b	29.4	716	**7b**	29.0	718
4c	-5.3	769	**7c**	-6.8	772
4d	74.7	702	**7d**	49.2	704
4e	49.8	700	**$Ph_3P{=}Se$**[C6a]	35.9	732

From Table C5 it can be seen that **4c** and **7c** carrying the furyl ligands are, as expected, the most electron-poor phosphines as indicated by the absolute value of $J(^{31}P\text{-}^{77}Se)$. The most electron-donating systems are aliphatic *t*-butyl (**4d**) and cyclohexyl (**4e**, **7d**) seleno phosphines with $^{1}J(^{31}P\text{-}^{77}Se)$ of ca. 700 Hz (Table C5). Apparently, the ruthenocenyl phosphines show slightly higher coupling constants than the *iso*-structural ferrocenyl derivatives emphasizing that the ferrocenyl phosphines are somewhat better σ donors. The data summarized in Table C5 are indicative to classify the suitability of the metallocenyl phosphines as ligands in, for example, the Mizoroki-Heck and Suzuki-Miyaura reaction. Furthermore, it is possible to compare the $J(^{31}P\text{-}^{77}Se)$ values of **4a** – **e** with the redox potentials E_1^0 (= potential of the 1st redox process) of the ferrocenyl phosphine palladium complexes **9a** – **e** which results in a linear correlation as it can be seen from Figure C5. It is obvious that only molecules featuring aromatic groups on the phosphorus atom fit this correlation, whereas the aliphatic phosphines are aside. This is most likely attributed to the different hybridization and hence geometry of the groups at the phosphorus atom. Therefore, it is necessary to exclusively compare structurally related molecules.

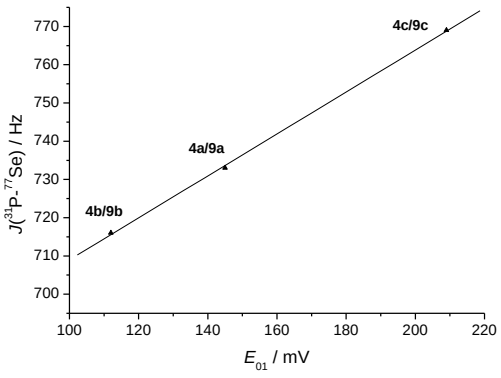

Figure C5. Correlation of redox potentials E_1^0 and $^1J(^{31}P-^{77}Se)$ of **4a**/**9a**, **4b**/**9b** and **4c**/**9c**.

2.4 Catalytic Investigations

2.4.1 Mizoroki-Heck Catalysis

The reaction of iodo benzene with *tert*-butyl acrylate to give *E*-*tert*-butyl cinnamate (Reaction C2) was used as standard reaction to compare the catalytic activity of the newly synthesized metallocenyl phosphine palladium dichloride complexes **9** and **10** with literature known catalysts such as $[PdCl_2(P(i\text{-}Pr)_2Fc)_2]$ and $[PdCl_2(dippf)]$ (dippf = 1,1'-bis(di-*iso*-propylphosphino) ferrocene)). [C4d] The reactions were performed in a mixture of toluene and acetonitrile (ratio 1:1, *v:v*) with a catalyst loading of 0.2 mol% at 80 °C for 10 and 25 h, Et*N*(*i*-Pr)$_2$ was added as base and acetyl ferrocene as internal standard (Table C6; reaction profiles are given in the Supporting Information, Figure C8). The conversions were determined by ^{1}H NMR spectroscopy (Experimental Section).

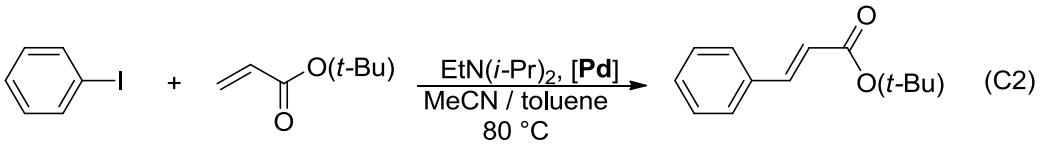

Table C6. Mizoroki-Heck reaction of iodo benzene with *t*-butyl acrylate with a catalyst loading of 0.2 mol% of **9** and **10**, for comparison, yields for $[PdCl_2(P(i\text{-}Pr)_2Fc)_2]$ and $[PdCl_2(dippf)]$ [d)] are given. [C4d]

Entry	Compd.	Conversion / % [a)]	Conversion / % [b)]
1	**9a**	44.9	69.9
2	**9b**	76.4	94.7
3	**9c**	65.2	89.5
4	**9d**	100	100
5	**9e**	59.8	90.0
6	**$[PdCl_2(P(i\text{-}Pr)_2Fc)_2]$**	-	96[c)]

7	**[PdCl$_2$(dippf)]**[d)]	-	100 [c)]
8	**10a**	57.1	81.0
9	**10b**	67.0	77.1
10	**10c**	57.7	76.4
11	**10d**	72.6	84.3

a) Conversion after 10 h. b) Conversion after 25 h. c) GLC yields after 24 h refluxing and a catalyst loading of 1.0 mol%. [C4d] d) dippf = 1,1'-bis(di-*i*-propylphosphino)ferrocene.

It was found that **9d** with its *tert*-butyl phosphino ligands is the most active catalyst (entry 4, Table C6, Supporting Information, Figure C8) within this series of compounds described. Complexes **9b**, **9c** and **9e** (entries 2, 3 and 5; Table C6) are somewhat less active, which can be explained by the more electron-rich phosphine **3d** providing a greater electronic stabilization to the active catalyst **9d**. The ruthenocenyl-based catalysts **10a** – **d** are less active than *iso*-structural ferrocenyl phosphine palladium complexes with conversions of 76 – 84 % after 25 h showing no clear electronic dependency. However, catalysts **9** and **10** show some benefits in homogeneous catalysis, when compared with previously reported ferrocenyl mono- and di-phosphines [C4d] (entries 6 and 7, Table C6). These are by far, *i*) lower catalyst loadings, *ii*) no addition of a reductant (CuI) is necessary and *iii*) the high regio-selectivity (only the *E* isomer was formed). The difference to the systems used by Butler and Boyes [C4d] can be ascribed by electronic and steric reasons of which the bis(*tert*-butyl) ferrocenyl phosphine just associates both criteria optimally. That only one isomer was produced can be explained by the steric congestion of the *tert*-butyl groups (*vide supra*) which is in accordance with the observations made by Butler and Boyes using palladium(II) complexes of (di-*i*-propylphosphino) ferrocenes associated to the less flexibility and chelate effect of the latter sandwich compound. Nevertheless, the ferrocenyl and ruthenocenyl phosphines **3** and **6** are quite less active in the palladium-promoted Mizoroki-Heck reaction than up-to-date used catalytic systems. [C2f,i,m-o]

2.4.2 Suzuki-Miyaura Catalysis

Complexes **9** and **10** were also applied in the Suzuki-Miyaura reaction of 2-bromo toluene or 4-chloro acetophenone with phenylboronic acid in presence of potassium carbonate as base in a solvent mixture of 1,4-dioxane and water (ratio 2:1, *v*:*v*) at 100 °C (Reaction C3). As internal standard for ^{1}H NMR spectroscopic conversion determinations acetyl ferrocene was added.

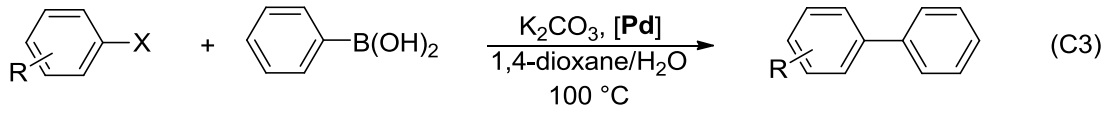

R = 2-CH_3 , X = Br
R = 4-$C(O)CH_3$, X = Cl

As it can be seen from Table C7 and the reaction profiles (Figure C6 and Supporting Information, Figure C9) all complexes are active in Pd-catalyzed Suzuki-Miyaura cross-couplings (*vide supra*) reflecting the electronic dependency of **3** and **6** showing exclusively 2-methyl biphenyl and 4-acetyl biphenyl being the only formed products (Supporting Information, Figure C10). The most active catalysts for C-Br activation are the electron-rich ferrocenyl systems **9a**, **9b**, **9d**, and **9e**, and the ruthenocenyls **10b** and **10d**, reaching complete conversion between 2 – 20 min (Supporting Information, Figure C9). The reaction of activated 4-chloro acetophenone with phenyl boronic acid requires, as expected, longer conversion times and higher catalyst loadings (0.5 mol%) of which only aliphatic **9d** and **9e** reach completion within 10 min and **10d** after 20 min. All other species are by far less active and show conversions below 60 % during 2 h (entries 6 – 8 and 19 – 21, Table C7, Figure C6). Furthermore, it was found that the ruthenocenyl phosphine palladium systems are somewhat less active then the *iso*-structural ferrocenyls, which can be explained by the higher electron-richness of the ferrocenyl species. This also is reflected by the slightly higher $^{1}J(^{31}P\text{-}^{77}Se)$ coupling constants (*vide supra*, Table C5). These results are in accordance with the general statement that electron-rich and bulky phosphines are suitable ligands in Suzuki-Miyaura *C,C* coupling reactions. [C4c,C5a,b] However, compared to presently used catalytic systems complexes **9** and **10** are somewhat less active. [C2e-h,C2j-l,C4e,C7e]

Due to the fact that the Suzuki-Miyaura reaction strongly depends on the electronic nature of the phosphines we could show that a relation between phosphine-basicity and catalyst-activity exists. The lower the $^{1}J(^{31}P\text{-}^{77}Se)$ coupling constant and hence, the higher the basicity of the phosphine, the higher the catalyst activity is.

Table C7. Reaction of 2-bromo toluene and 4-chloro acetophenone with phenylboronic acid after 1 h with different catalyst loadings.

Entry	Compd.	Aryl halide	Catalyst loading / mol%	Conversion / %
1	**9a**		0.1	100
2	**9b**			100
3	**9c**			100

4	**9d**			100
5	**9e**			100
6	**9a**	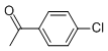	0.5	30.4
7	**9b**			60.0
8	**9c**			0
9	**9d**			100
10	**9e**			100
11	**10a**		0.25	85.8
12			0.1	26.7
13	**10b**		0.25	100
14			0.1	100
15	**10c**		0.25	100
16			0.1	4.0
17	**10d**		0.25	100
18			0.1	100
19	**10a**	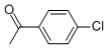	0.5	10.0
20	**10b**			50.2
21	**10c**			2.0
22	**10d**			100

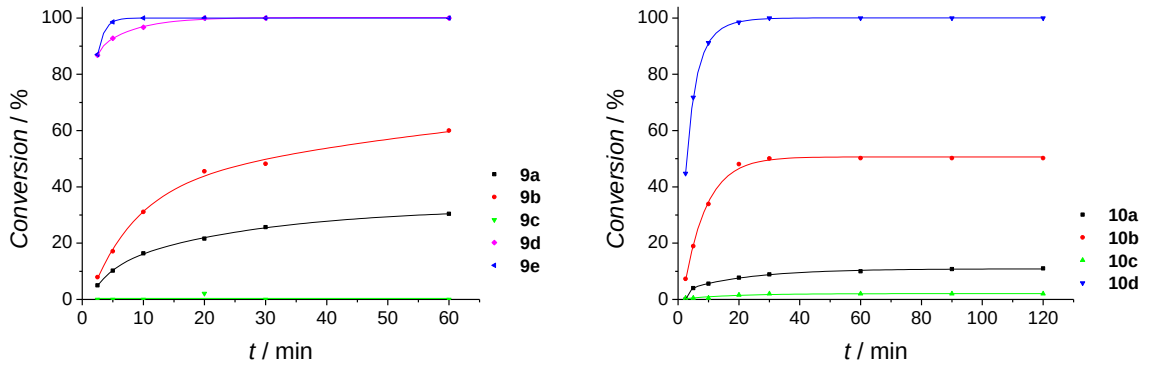

Figure C6. Reaction profiles for catalysts **9a** – **e** (left) and **10a** – **d** (right) for the reaction of 4-chloro acetophenone with phenylboronic acid and a catalyst loading of 0.5 mol%.

3 Conclusions

Within this study the synthesis of a series of metallocenyl phosphine palladium dichloride complexes of type $[PdCl_2(PR_2Mc)_2]$ (Mc = Fc, Rc; Fc = Fe(η^5-C_5H_4)(η^5-C_5H_5), Rc = Ru(η^5-C_5H_4)(η^5-C_5H_5); R = Ph, *o*-Tol, Fur, *t*-Bu, Cy) is reported. They were prepared by treatment of phosphines R_2PMc with $[PdCl_2(cod)]$ (cod = cyclo-1,5-octadiene). Cyclovoltammetric measurements showed that the metallocenyl-functionalized aromatic phosphines are first reversibly oxidized at the metallocenyl fragment, when measuring to 0.8 V. The resulting

ferrocenium ion participates in intra-molecular electron transfer processes from the PR_2 groups to the transition metal ion. Irreversible oxidations occur when going to higher potentials (1.5 V). As expected, electron-rich phosphines are easier to oxidize. This is verified in the series R = furyl < phenyl < *o*-tolyl, however, aliphatic phosphines show a similar electronic character and completely irreversible behavior. Additionally, we investigated the electrochemical behavior of the seleno phosphines **4a** – **e** and the bis(phosphino) palladium(II) complexes **9a** – **e** in which the lone-pair of electrons at phosphorus is part of a phosphorus-selenium or phosphine palladium bond. Nevertheless, as described earlier, [C9,C12b] the seleno phosphines also show follow-up products, presumably resulting from an intra-molecular electron transfer from the selenium-centered radical. Therefore, contributions from either the iron, phosphorus or selenium radicals are expected in the monocations. Such oxidations are inhibited, when the phosphorus atom is datively-bonded to palladium as given in **9a** – **e** (*vide supra*). As expected, the bis(phosphino) palladium complexes are more difficult to oxidize which can be explained by the electron withdrawing character upon coordination of the phosphines to Pd. UV-Vis/NIR spectroscopy revealed the absence of any NIR charge transfer bands indicating electrostatic interactions. For classification of the σ donor ability of the phosphines, the respective seleno phosphines $Se{=}PR_2Mc$ have been prepared by addition of elemental selenium. [C6] High $J(^{31}P\text{-}^{77}Se)$ values indicate electron-poor phosphines and hence, a less donor capability. Furthermore, it is possible to correlate $J(^{31}P\text{-}^{77}Se)$ values with the redox potential E_1^0 of the ferrocenyl phosphine palladium complexes, resulting in a linear correlation for the aromatic phosphines. For the aliphatic *tert*-butyl and cyclohexyl derivatives a different behavior is observed, which is most probably based on the different hybridization. The bis(metallocenylphosphine) palladium(II) complexes were applied as catalysts in *C,C* cross-coupling reactions. In the Mizoroki-Heck reaction, iodo benzene was exemplarily treated with *tert*-butyl acrylate. All complexes are active, although the most efficient catalyst was the one featuring phosphine $(t\text{-Bu})_2PFc$, which is explicable with the bulkiness and electron-richness of this ligand. Also, all of the palladium(II) complexes have been active in Suzuki-Miyaura couplings of aryl-bromide and activated aryl-chloride. It was found that a correlation between the basicity of the phosphines and the activity of the corresponding complexes exist. The lower the $^1J(^{31}P\text{-}^{77}Se)$ coupling constant and hence, the higher the basicity of the phosphine, the higher the catalyst activity is. In summary, the catalysts reported within this work are compared with up-to-date catalytic systems [C2,C4f,C7e] less active but, when compared with other metallocenyl mono- and di-phosphine palladium catalysts, show higher activity under similar reaction conditions. [C4b,c]

Moreover, they are active at lower catalyst loadings (Mizoroki-Heck and Suzuki-Miyaura catalysis), no addition of a reductant ([CuI]) is required and, in addition, show high regio-selectivity (Mizoroki-Heck catalysis).

4 Experimental Section

4.1 General Data

All reactions were carried out under an atmosphere of nitrogen or argon using standard Schlenk techniques. Toluene and tetrahydrofuran were purified by distillation from sodium and sodium/benzophenone, respectively; dichloromethane was purified by distillation from calcium hydride. Celite (purified and annealed, Erg. B.6, Riedel de Haen) was used for filtrations. For column chromatography alumina with a particle size of 90 μm (standard, Merck KGaA) or silica with a particle size of 40 – 60 μm (230 – 400 mesh (ASTM), Becker) was used.

4.2 Instruments

NMR spectra were recorded on a Bruker Avance III 500 spectrometer (500.3 MHz for ^{1}H, 125.7 MHz for ^{13}C{^{1}H}, and 202.5 MHz for ^{31}P{^{1}H} NMR spectra, respectively). Chemical shifts are reported in δ (parts per million) downfield from tetramethylsilane with the solvent as reference signal (^{1}H NMR δ 7.26 for $CDCl_3$ and δ 5.30 for CD_2Cl_2; ^{13}C{^{1}H} NMR δ 77.16 for $CDCl_3$ and δ 53.52 for CD_2Cl_2). HRMS (= High Resolution Mass Spectrometry) were recorded on a Bruker Daltonik micrOTOF-QII spectrometer (ESI-TOF). Elemental analyses were measured with a Thermo FlashAE 1112 series instrument and melting points of analytical pure samples were determined using a Gallenkamp MFB 595 010 M melting point apparatus. FT IR spectra were recorded on a Thermo Nicolet IR 200 spectrometer using either KBr pellets or NaCl plates.

4.3 Electrochemistry

Measurements on 1.0 mmol·L^{-1} solutions of **3**, **4** and **9** in dry degassed dichloromethane containing 0.1 mol·L^{-1} of [(*n*-Bu)$_4$N][B(C$_6$F$_5$)$_4$] as supporting electrolyte were carried out under argon at 25 ˚C utilizing a Radiometer Voltalab PGZ 100 electrochemical workstation interfaced with a personal computer. A three electrode cell, which a Pt auxiliary electrode, a glassy carbon working electrode (surface area 0.031 cm^2) and an Ag/Ag$^+$ (0.01 mmol·L^{-1}

[$AgNO_3$]) reference electrode fixed on a Luggin capillary was used. The working electrode was pre-treated by polishing on a Buehler microcloth first with 1 micron and then ¼ micron diamond paste. The reference electrode was constructed from a silver wire inserted into a solution of 0.01 mmol·L^{-1} [$AgNO_3$] and 0.1 mol·L^{-1} [(*n*-Bu)$_4$N][$B(C_6F_5)_4$] in acetonitrile, in a luggin capillary with a vycor tip. This luggin capillary was inserted into a second luggin capillary with vicor tip filled with a 0.1 mmol·L^{-1} [(*n*-Bu)$_4$N][$B(C_6F_5)_4$] solution in dichloromethane. Experiments under the same experimental conditions showed that all reduction and oxidation potentials were reproducible within 15 mV. Experimental potentials were referenced against an Ag/Ag^+ reference electrode but the presented results are referenced against ferrocene as an internal standard as required by IUPAC. [C10] Data were then processed on a Microsoft Excel worksheet to set the formal reduction potentials of the FcH/FcH^+ couple to 0.0 V. Under our conditions the FcH/FcH^+ couple was at 260 mV *vs*. Ag/Ag^+, ΔE_p = 92 mV.

4.4 Spectro-electrochemistry

Spectro-electrochemical UV-Vis/NIR measurements of a 1.0 mmol·L^{-1} solution of **9b** in dry degassed dichloromethane containing 0.1 mol·L^{-1} of [(*n*-Bu)$_4$N][$B(C_6F_5)_4$] as supporting electrolyte were carried in an OTTLE cell [C12f,g] using a Varian Cary 5000 spectrophotometer.

4.5 Materials

All starting materials were obtained from commercial suppliers and used without further purification. Iodoferrocene [C16] (**1**), iodoruthenocene [C16,C17] (**5**), ferrocenyldiphenyl phosphine [C18] (**3a**), ferrocenyldi-*t*-butyl phosphine [C19] (**3d**), ferrocenyldicyclohexyl phosphine [C20] (**3e**), [$PdCl_2(PPh_2Fc)_2$] [C4e] (**9a**) and [$PdCl_2(P(t\text{-}Bu)_2Fc)_2$] [C21] (**9d**) were prepared according to published procedures. Chlorophosphines **2b** – **e** [C22-C25] and [$PdCl_2$(cod)] [C26] (**8**) were synthesized as described in literature.

4.6 General Procedure for the Synthesis of Phosphines 3 and 6

To compounds **1** or **5** dissolved in dry tetrahydrofuran (50 mL) one equivalent of a 2.5 M solution of *n*-BuLi was added dropwise at -60 °C. After stirring the solution for 30 min at ambient temperature it was again cooled to -30 °C and one equivalent of the appropriate chlorophosphine (**2a** – **e**) was added dropwise. The reaction mixture was stirred for 1 h at

ambient temperature and then concentrated in vacuum. The resulting residue was purified by column chromatography and dried in vacuum.

4.6.1 Synthesis of P(*o*-Tol)$_2$Fc (3b)

Using the general procedure described above, **1** (1.0 g, 3.21 mmol) was reacted with *n*-BuLi (1.30 mL, 3.21 mmol) and chlorodi-*o*-tolylphosphine (**2b**, 0.80 g, 3.21 mmol). The resulting residue was purified by column chromatography (column size: 3.5 x 15 cm on silica gel) using *n*-hexane as eluent. Product **3b** was obtained as an orange solid. Yield: 0.88 g (2.21 mmol, 69 % based on **1**). Anal. Calcd. for $C_{24}H_{23}FeP$ (398.26 g/mol): C, 72.38; H, 5.82. Found: C, 72.40; H, 5.94. Mp.: 168 °C. IR (KBr, $\tilde{\upsilon}$/cm^{-1}): 752 (s, =C-H, *o*-disubst. benzene), 1465 (m, P-C), 1585/1623 (w, C=C), 2845/2908/2965 (w, C-H), 3003/3041 (w, =C-H). ^{1}H NMR (500.30 MHz, $CDCl_3$, δ): 2.56 (s, 6 H, CH_3), 4.10 (s, 5 H, C_5H_5), 4.19 (dpt, $^3J_{HP}$ = 1.8 Hz, $^3J_{HH}$ = 1.8 Hz, 2 H, H$^{\alpha}$/C_5H_4), 4.44 (pt, $^3J_{HH}$ = 1.8 Hz, 2 H, H$^{\beta}$/C_5H_4), 7.10 (m, 4 H, H^{o}/C_6H_4), 7.18 – 7.25 (m, 6 H, H^{m,p}/C_6H_4). ^{13}C{^{1}H} NMR (125.81 MHz, $CDCl_3$, δ): 21.4 (d, $^3J_{CP}$ = 21.8 Hz, CH$_3$), 69.1 (s, C_5H$_5$), 70.9 (d, $^3J_{CP}$ = 4.2 Hz, C$^{\beta}$/C_5H$_4$), 73.4 (d, $^2J_{CP}$ = 15.3 Hz, C$^{\alpha}$/C_5H$_4$), 75.8 (d, $^1J_{CP}$ = 6.0 Hz, C^{i}/C_5H$_4$), 125.7 (s, C^{p}/C_6H$_4$), 128.5 (s, C^{m}/C_6H$_4$), 129.9 (d, $^3J_{CP}$ = 5.2 Hz, C^{m}/C_6H$_4$), 133.5 (s, C^{o}/C_6H$_4$), 137.9 (d, $^1J_{CP}$ = 10.8 Hz, C^{i}/C_6H$_4$), 141.7 (d, $^2J_{CP}$ = 26.3 Hz, C^{o}/C_6H$_4$). ^{31}P{^{1}H} NMR (202.53 MHz, $CDCl_3$, δ): -36.4 (s). HRMS (ESI-TOF) $C_{24}H_{23}FeP$ [M]$^+$ *m/z*: calcd.: 398.0882, found: 398.0836.

4.6.2 Synthesis of PFur$_2$Fc (3c)

Using the general procedure described above, **1** (1.0 g, 3.21 mmol) was reacted with *n*-BuLi (1.30 mL, 3.21 mmol) and chlorodi-2-furylphosphine (**2c**, 0.64 g, 3.21 mmol). The resulting residue was purified by column chromatography on silica gel (column size: 3.5 x 15 cm) using *n*-hexane as eluent. Product **3c** was obtained as an orange solid. Yield: 0.71 g (2.02 mmol, 63 % based on **1**). Anal. Calcd. for $C_{18}H_{15}FeO_2P$ (350.13 g/mol): C, 61.75; H, 4.32. Found: C, 61.37; H, 4.32. Mp.: 115 °C. IR (KBr, $\tilde{\upsilon}$/cm^{-1}): 1009 (s, C-O), 1459 (m, P-C), 1550/1560/1638/1654 (w, C=C), 3078/3125/3147 (w, =C-H). ^{1}H NMR (500.30 MHz, $CDCl_3$, δ): 4.04 (s, 5 H, C_5H_5), 4.35 (pt, $^3J_{HH}$ = 1.5 Hz, H$^{\beta}$/C_5H_4), 4.44 (dpt, $^3J_{HP}$ = 1.9 Hz, $^3J_{HH}$ = 1.8 Hz, H$^{\alpha}$/C_5H_4), 6.40 (dt, $^4J_{HP}$ = 1.6 Hz, $^3J_{HH}$ = 3.2 Hz, $^3J_{HH}$ = 1.6 Hz, 2 H, H^{4}/C_4H_3O), 6.69 (m, 2 H, H^{3}/C_4H_3O), 7.64 (m, 2 H, H^{5}/C_4H_3O). ^{13}C{^{1}H} NMR (125.81 MHz, $CDCl_3$, δ): 69.2 (s, C_5H$_5$), 70.9 (d, $^3J_{CP}$ = 5.4 Hz, C$^{\beta}$/C_5H$_4$), 72.5 (d, $^1J_{CP}$ = 5.1 Hz, C^{i}/C_5H$_4$), 73.7 (d, $^2J_{CP}$ = 18.3 Hz, C$^{\alpha}$/C_5H$_4$), 110.6 (d, $^3J_{CP}$ = 6.2 Hz, C^{4}/C_4H$_3$O), 119.8 (d, $^2J_{CP}$ = 23.6 Hz, C^{3}/C_4H$_3$O), 146.7

(d, $^{3}J_{CP}$ = 2.4 Hz, C^{5}/C_4H_3O), 152.6 (d, $^{1}J_{CP}$ = 8.3 Hz, C^{2}/C_4H_3O). $^{31}P\{^{1}H\}$ NMR (202.53 MHz, $CDCl_3$, δ): -64.4 (s). HRMS (ESI-TOF) $C_{18}H_{15}FeO_2P$ $[M]^+$ *m/z*: calcd.: 350.0154, found: 350.0116.

4.6.3 Synthesis of PPh_2Rc (6a)

Using the general procedure described above, **5** (2.0 g, 5.5 mmol) was reacted with *n*-BuLi (2.20 mL, 3.21 mmol) and chlorodiphenylphosphine (**2a**, 1.21 g, 5.5 mmol). The resulting residue was purified by column chromatography on alumina (column size: 2.5 x 30 cm) using a mixture of *n*-hexane-diethyl ether (ratio 5:1, *v*:*v*) as eluent. Phosphine **6a** was obtained as a pale yellow solid. Yield: 0.80 g (1.92 mmol, 35 % based on **5**). Anal. Calcd. for $C_{22}H_{19}PRu$ (415.43 g/mol): C, 63.61; H, 4.61. Found: C, 63.55; H, 4.62. Mp.: 128 °C. IR (KBr, $\tilde{\upsilon}$/cm^{-1}): 1432 (m, P-C); 1477/1652 (w, C=C), 3047/3067 (w, =C-H). ^{1}H NMR (500.30 MHz, $CDCl_3$, δ): 4.45 (s, 5 H, C_5H_5), 4.49 (dpt, $^{3}J_{HP}$ = 1.7 Hz, $^{3}J_{HH}$ = 1.6 Hz, 2 H, H$^{\alpha}$/C_5H_4), 4.71 (pt, $^{3}J_{HH}$ = 1.6 Hz, 2 H, H$^{\beta}$/C_5H_4), 7.30 - 7.33 (m, 6 H, H^{m,p}/C_6H_5), 7.36 -7.39 (m, 4 H, H^{o}/C_6H_5). $^{13}C\{^{1}H\}$ NMR (125.81 MHz $CDCl_3$, δ): 71.5 (s, C_5H_5), 72.7 (d, $^{3}J_{CP}$ = 3.8 Hz, C$^{\beta}$/C_5H_4), 75.3 (d, $^{2}J_{CP}$ = 16.4 Hz, C$^{\alpha}$/C_5H_4), 79.9 (d, $^{1}J_{CP}$ = 8.8 Hz, C^{i}/C_5H_4), 128.1 (d, $^{3}J_{CP}$ = 6.3 Hz, C^{m}/C_6H_5), 128.4 (s, C^{p}/C_6H_5), 133.4 (d, $^{2}J_{CP}$ = 18.9 Hz, C^{o}/C_6H_5), 139.4 (d, $^{1}J_{CP}$ = 8.8 Hz, C^{i}/C_6H_5). $^{31}P\{^{1}H\}$-NMR (202.53 MHz, $CDCl_3$, δ): -16.0 (s).

4.6.4 Synthesis of $P(o\text{-Tol})_2Rc$ (6b)

Using the general procedure described above, **5** (2.0 g, 5.5 mmol) was reacted with *n*-BuLi (2.2 mL, 3.21 mmol) and chlorodi-*o*-tolylphosphine (**2b**, 1.36 g, 5.5 mmol). The resulting residue was purified by column chromatography on alumina (column size: 2.5 x 30 cm) using a solvent mixture of *n*-hexane-diethyl ether (ratio 5:1, *v*:*v*) as eluent. The title compound **6a** was obtained as a pale yellow solid. Yield: 0.90 g (2.02 mmol, 36 % based on **5**). Anal. Calcd. for $C_{24}H_{23}PRu$ (443.48 g/mol): C, 65.00; H, 5.27. Found: C, 64.71; H, 5.32. Mp.: 127 °C. IR (KBr, $\tilde{\upsilon}$/cm^{-1}): 1432 (m, P-C); 1477 (w, C=C). ^{1}H NMR (500.30 MHz, $CDCl_3$, δ): 2.43 (s, 6 H, CH_3), 4.44 (s, 5 H, C_5H_5), 4.53 (dpt, $^{3}J_{HP}$ = 1.6 Hz, $^{3}J_{HH}$ = 1.6 Hz, 2 H, H$^{\alpha}$/C_5H_4), 4.74 (pt, $^{3}J_{HH}$ = 1.6 Hz, 2 H, H$^{\beta}$/C_5H_4), 7.06 - 7.2 (m, 8 H, C_6H_4). $^{13}C\{^{1}H\}$ NMR (125.81 MHz, $CDCl_3$, δ): 21.4 (d, $^{2}J_{CP}$ = 21.9 Hz, CH_3), 71.4 (s, C_5H_5), 72.7 (d, $^{3}J_{CP}$ = 3.6 Hz, C$^{\beta}$/C_5H_4), 75.7 (d, $^{2}J_{CP}$ = 16.9 Hz, C$^{\alpha}$/C_5H_4), 125.7 (s, C^{p}/C_6H_4), 128.5 (s, C^{m}/C_6H_4), 129.9 (d, $^{3}J_{CP}$ = 4.8 Hz, C^{m}/C_6H_4), 133.3 (s, C^{o}/C_6H_4), 138.0 (d, $^{1}J_{CP}$ = 10.8 Hz, C^{i}/C_6H_4), 141.8 (d, $^{2}J_{CP}$ = 26.4 Hz, C^{o}/C_6H_4). $^{31}P\{^{1}H\}$ NMR (202.53 MHz, $CDCl_3$, δ): -36.1 (s).

4.6.5 Synthesis of $PFur_2Rc$ (6c)

5 (2.0 g, 5.5 mmol) was reacted with *n*-BuLi (2.2 mL, 3.21 mmol) and chlorodi-2-furylphosphine (**2c**, 1.10 g, 5.5 mmol) as reported earlier. The resulting residue was purified by column chromatography on alumina (column size: 2.5 x 30 cm) using a mixture of *n*-hexane-diethyl ether (ratio 5:1, *v*:*v*) as eluent. Phosphine **6a** was obtained as a pale yellow solid. Yield: 1.0 g (2.53 mmol, 46 % based on **5**). Anal. Calcd. for $C_{18}H_{15}O_2PRu$ (395.35 g/mol): C, 54.68; H, 3.82. Found: C, 54.33; H, 3.84. Mp.: 116 °C (dec.). IR (KBr, $\tilde{\upsilon}$/cm^{-1}): 1008 (m, C-O); 1458 (w, P-C); 3100 (m, =C-H). ^{1}H NMR (500.30 MHz, $CDCl_3$, δ): 4.41 (s, 5 H, C_5H_5), 4.69 (pt, $^3J_{HH}$ = 1.6 Hz, 2 H, H^{β}/C_5H_4), 4.85 (dpt, $^3J_{HP}$ = 1.7 Hz, $^3J_{HH}$ = 1.6 Hz, 2 H, H^{α}/C_5H_4), 6.38 (dt, $^4J_{HP}$ = 1.6 Hz, $^3J_{HH}$ = 3.2 Hz, $^3J_{HH}$ = 1.6 Hz, 2 H, H^4/C_4H_3O), 6.67 (m, 2 H, H^3/C_4H_3O), 7.61 (m, 2 H, H^5/C_4H_3O). ^{13}C{^{1}H} NMR (125.81 MHz, $CDCl_3$, δ): 71.5 (s, C_5H_5), 72.8 (d, $^3J_{CP}$ = 5.0 Hz, C^{β}/C_5H_4), 76.0 (d, $^2J_{CP}$ = 19.9 Hz, C^{α}/C_5H_4), 110.6 (d, $^3J_{CP}$ = 6.2 Hz, C^4/C_4H_3O), 119.5 (d, $^2J_{CP}$ = 23.9 Hz, C^3/C_4H_3O), 146.5 (d, $^4J_{CP}$ = 1.9 Hz, C^5/C_4H_3O), 153.0 (d, $^1J_{CP}$ = 8.1 Hz, C^2/C_4H_3O). ^{31}P{^{1}H} NMR (202.53 MHz, $CDCl_3$, δ): - 65.2 (s).

4.6.6 Synthesis of PCy_2Rc (6d)

2.0 g (5.5 mmol) of **5** were reacted with 2.2 mL (3.21 mmol) of *n*-BuLi and 1.28 g (5.5 mmol) of chlorodicyclohexylphosphine (**2d**) as reported earlier. The resulting residue was purified by column chromatography on alumina (column size: 2.5 x 30 cm) using a mixture of *n*-hexane-diethyl ether (ratio 5:1, *v:v*) as eluent. Please, notice that phosphine **6a** could not completely be separated from free ruthenocene and hence was used without additional purification for further reactions. Anal. Calcd. for $C_{22}H_{31}PRu$ (427.53 g/mol): C, 61.81; H, 7.31. ^{1}H NMR (500.30 MHz, $CDCl_3$, δ): 1.18 - 1.27 (m, 10 H, C_6H_{11}), 1.62 - 1.88 (m, 10 H, C_6H_{11}), 1.81 - 1.84 (m, 2 H, C_6H_{11}), 4.45 (s, 5 H, C_5H_5), 4.48 (m, 2 H, C_5H_4), 4.56 (pt, $^3J_{HH}$ = 1.5 Hz, 2 H, C_5H_4). ^{13}C{^{1}H} NMR (125.81 MHz, $CDCl_3$, δ): 26.6 (s, C_6H_{11}), 27.4 (d, J_{CP} = 8.3 Hz, C_6H_{11}), 27.5 (d, J_{CP} = 11.2 Hz, C_6H_{11}), 30.3 (d, J_{CP} = 2.5 Hz, C_6H_{11}), 30.4 (d, J_{CP} = 7.5 Hz, C_6H_{11}), 33.8 (d, $^1J_{CP}$ = 11.2 Hz, C^1/C_6H_{11}), 70.2 (s, Ru(η^5-C_5H_5)$_2$), 71.4 (d, $^3J_{CP}$ = 2.6 Hz, C^{β}/C_5H_4), 71.6 (s, C_5H_5), 74.4 (d, $^2J_{CP}$ = 12.7 Hz, C^{α}/C_5H_4), 77.3 (C^i/C_5H_4*)). ^{31}P{^{1}H} NMR (202.53 MHz, $CDCl_3$, δ): -7.1 (s). HRMS (ESI-TOF) $C_{22}H_{21}PRu$ $[M+H]^+$ *m/z*: calcd.: 429.1278, found: 429.1286; $C_{10}H_{10}Ru$ $[M+H]^+$ *m/z*: calcd.: 232.9897, found: 232.9901. *) signal concealed by $CDCl_3$.

4.7 General Procedure for the Synthesis of the Seleno Phosphines 4 and 7

To a toluene solution (20 mL) containing phosphines **3** or **6** (100 mg), 1.2 equivalents of selenium in its elemental form were added in a single portion and the reaction mixture was stirred for 1 h at 100 °C. After cooling to ambient temperature, the reaction mixture was filtrated through a pad of Celite. The eluate was then dried in membrane pump vacuum.

4.7.1 Synthesis of Se=PPh$_2$Fc (4a)

The reaction of **3a** (100 mg, 0.27 mmol) with elemental selenium (26 mg, 0.33 mmol) gave, after appropriate work-up, **4a** as an orange solid. Yield: 120 mg (0.27 mmol, 100 % based on **3a**). Anal. Calcd. for $C_{22}H_{19}FePSe$ (449.17 g/mol): C, 58.83; H, 4.26. Found: C, 58.90; H, 4.28. IR (KBr, $\tilde{\upsilon}$/cm^{-1}): 572 (s, P=Se), 1434 (m, P-C), 1638 (m, C=C), 3071 (w, =C-H). ^{1}H NMR (500.30 MHz, $CDCl_3$, δ): 4.16 (s, 5 H, C_5H_5), 4.45 (dpt, $^3J_{HP}$ = 2.1 Hz, $^3J_{HH}$ = 1.9 Hz, 2 H, H$^{\alpha}$/C_5H_4), 4.52 (dpt, $^4J_{HP}$ = 1.7 Hz, $^3J_{HH}$ = 1.8 Hz, 2 H, H$^{\beta}$/C_5H_4), 7.38 – 7.42 (m, 4 H, H^{m}/C_6H_5), 7.44 – 7.46 (m, 2 H, H^{p}/C_6H_5), 7.70 – 7.74 (m, 4 H, H^{o}/C_6H_5). ^{13}C{^{1}H} NMR (125.81 MHz, $CDCl_3$, δ): 70.2 (s, C_5H_5), 72.0 (d, $^3J_{CP}$ = 10.0 Hz, C$^{\beta}$/C_5H_4), 73.4 (d, $^2J_{CP}$ = 12.6 Hz, C$^{\alpha}$/C_5H_4), 74.0 (d, $^1J_{CP}$ = 89.2 Hz, C^{i}/C_5H_4), 128.2 (d, $^2J_{CP}$ = 12.6 Hz, C^{o}/C_6H_5), 131.3 (d, ^4JCP = 2.9 Hz, C^{p}/C_6H_5), 132.1 (d, $^3J_{CP}$ = 10.9 Hz, C^{m}/C_6H_5), 133.6 (d, $^1J_{CP}$ = 78.4 Hz, C^{i}/C_6H_5). ^{31}P{^{1}H} NMR (202.53 MHz, $CDCl_3$, δ): 31.8 ($^1J_{31P77Se}$ = 733.2 Hz). HRMS (ESI-TOF) $C_{22}H_{19}FePSe$ [M+H]$^+$ *m/z*: calcd.: 450.9814, found: 450.9757; [M-H+MeCN]$^+$ *m/z*: calcd.: 489.9923, found: 489.9812.

4.7.2 Synthesis of Se=P(*o*-Tol)$_2$Fc (4b)

Using the general procedure described above, **3b** (100 mg, 0.25 mmol) was reacted with elemental selenium (24 mg, 0.30 mmol). After appropriate work-up, **4b** was obtained as an orange solid. Yield: 119 mg (0.25 mmol, 100 % based on **3b**). Anal. Calcd. for $C_{24}H_{23}FePSe$ (477.22 g/mol): C, 60.40; H, 4.86. Found: C, 60.49; H, 5.34. IR (KBr, $\tilde{\upsilon}$/cm^{-1}): 560/575 (s, P=Se), 761 (s, =C-H, *o*-disubst. benzene), 1449 (m, P-C), 1635 (m, C=C), 2857/2917/2965 (w, C-H), 3002/3034/3088 (w, =C-H). ^{1}H NMR (500.30 MHz, CD_2Cl_2, -90 °C, δ): 1.70 (s, 3 H, CH_3), 1.99 (s, 3 H, CH_3), 3.88 (m, 1 H, H$^{\beta}$/C_5H_4), 4.07 (s, 5 H, C_5H_5), 4.40 (m, 1 H, H$^{\alpha}$/C_5H_4), 4.58 (m, 1 H, H$^{\beta}$/C_5H_4), 4.82 (m, 1 H, H$^{\alpha}$/C_5H_4), 7.00 (t, $^3J_{HH}$ = 7.6 Hz, 1 H, H^{o}/C_6H_4), 7.03 (t, $^3J_{HH}$ = 6.9 Hz, 2 H, H^{m}/C_6H_4), 7.06 (t, $^3J_{HH}$ = 6.9 Hz, 1 H, H^{m}/C_6H_4), 7.14 (t, $^3J_{HH}$ = 6.1 Hz, 1 H, H^{m}/C_6H_4), 7.23 (t, $^3J_{HH}$ = 7.2 Hz, 1, H, H^{p}/C_6H_4), 7.47 (t $^3J_{HH}$ = 7.2 Hz, 1 H, H^{p}/C_6H_4), 7.52 (t, $^3J_{HH}$ = 7.4 Hz, 1 H, H^{m}/C_6H_4), 8.82 (dd, $^3J_{HP}$ = 18.2 Hz, $^3J_{HH}$ = 7.5 Hz, 1H, H^{o}/C_6H_4). ^{13}C{^{1}H} NMR (125.81 MHz, CD_2Cl_2, -90 °C, δ): 19.9 (d, $^3J_{CP}$ = 6.1 Hz, CH_3),

22.0 (d, $^{3}J_{CP}$ = 3.5 Hz, *C*H$_3$), 69.6 (s, *C*$_5$H$_5$), 71.2 (d, $^{2}J_{CP}$ = 9.1 Hz, C$^{\alpha}$/*C*$_5$H$_4$), 71.5 (d, $^{3}J_{CP}$ = 5.5 Hz, C$^{\beta}$/*C*$_5$H$_4$), 71.6 (d, $^{3}J_{CP}$ = 5.4 Hz, C$^{\beta}$/*C*$_5$H$_4$), 72.2 (d, $^{1}J_{CP}$ = 90.1 Hz, C^{i}/*C*$_5$H$_4$), 74.5 (d, $^{2}J_{CP}$ = 14.0 Hz, C$^{\alpha}$/*C*$_5$H$_4$), 125.4 (d, $^{3}J_{CP}$ = 12.2 Hz, C^{m}/*C*$_6$H$_4$), 125.6 (d, $^{1}J_{CP}$ = 72.2 Hz, C^{i}/*C*$_6$H$_4$), 126.0 (d, $^{3}J_{CP}$ = 14.1 Hz, C^{m}/*C*$_6$H$_4$), 128.8 (d, $^{2}J_{CP}$ = 10.5 Hz, C^{o}/*C*$_6$H$_4$), 130.2 (d, $^{4}J_{CP}$ = 2.0 Hz, C^{p}/*C*$_6$H$_4$), 130.6 (d, $^{3}J_{CP}$ = 9.9 Hz, C^{m}/*C*$_6$H$_4$), 130.9 (d, $^{3}J_{CP}$ = 10.5 Hz, C^{m}/*C*$_6$H$_4$), 131.3 (d, $^{4}J_{CP}$ = 2.7 Hz, C^{p}/*C*$_6$H$_4$), 133.6 (d, $^{1}J_{CP}$ = 77.8 Hz, C^{i}/*C*$_6$H$_4$), 135.1 (d, $^{2}J_{CP}$ = 17.0 Hz, C^{o}/*C*$_6$H$_4$), 138.6 (d, $^{2}J_{CP}$ = 6.4 Hz, C^{o}/*C*$_6$H$_4$), 138.9 (d, $^{2}J_{CP}$ = 10.4 Hz, C^{o}/*C*$_6$H$_4$). ^{31}P{^{1}H} NMR (202.53 MHz, $CDCl_3$, δ): 29.4 ($^{1}J_{31P77Se}$ = 715.5 Hz). HRMS (ESI-TOF) $C_{24}H_{23}FePSe$ $[M]^+$ *m/z*: calcd.: 478.0049, found: 478.0004; $[M+K]^+$ *m/z*: calcd.: 516.9685, found: 516.9624.

4.7.3 Synthesis of Se=PFur$_2$Fc (4c)

3c (100 mg, 0.29 mmol) was reacted with selenium (26 mg, 0.34 mmol) according to the synthesis methodology reported earlier. After appropriate work-up, phosphine **4c** was obtained as an orange solid. Yield: 124 g (0.29 mmol, 100 % based on **3c**). Anal. Calcd. for $C_{18}H_{15}FeO_2PSe$ (429.09 g/mol): C, 50.38; H, 3.52. Found: C, 50.53; H, 3.48. Mp.: 80 °C. IR (KBr, $\tilde{\upsilon}$/cm^{-1}): 577 (m, P=Se), 1005 (m, C-O), 1458 (w, P-C), 3080/3105/3119 (w, =C-H). ^{1}H NMR (500.30 MHz, $CDCl_3$, δ): 4.17 (s, 5 H, C$_5$*H*$_5$), 4.51 (dpt, $^{4}J_{HP}$ = 1.8 Hz, $^{3}J_{HH}$ = 1.8 Hz, 2 H, H$^{\beta}$/C$_5$*H*$_4$), 4.60 (pt, $^{3}J_{HP}$ = 2.3 Hz, $^{3}J_{HH}$ = 2.1 Hz, 2 H, H$^{\alpha}$/C$_5$*H*$_4$), 6.49 (dpt, $^{4}J_{HP}$ = 1.7 Hz, $^{3}J_{HH}$ = 3.4 Hz, $^{3}J_{HH}$ = 1.6 Hz, 2 H, H^{4}/C$_4$*H*$_3$O), 7.11 (m, 2 H, H^{3}/C$_4$*H*$_3$O), 7.71 (m, 2 H, H^{5}/C$_3$*H*$_4$O). ^{13}C{^{1}H} NMR (125.81 MHz, $CDCl_3$, δ): 70.4 (s, *C*$_5$H$_5$), 72.1 (d, $^{3}J_{CP}$ = 11.1 Hz, C$^{\beta}$/*C*$_5$H$_4$), 73.1 (d, $^{2}J_{CP}$ = 14.5 Hz, C$^{\alpha}$/*C*$_5$H$_4$), 111.2 (d, $^{3}J_{CP}$ = 9.1 Hz, C^{4}/*C*$_4$H$_3$O), 122.2 (d, $^{2}J_{CP}$ = 21.8 Hz, C^{3}/*C*$_4$H$_3$O), 147.4 (d, $^{1}J_{CP}$ = 114.3 Hz, C^{2}/*C*$_4$H$_3$O), 148.3 (d, $^{4}J_{CP}$ = 7.1 Hz, C^{5}/*C*$_4$H$_3$O). ^{31}P{^{1}H} NMR (202.53 MHz, $CDCl_3$, δ): -5.3 ($^{1}J_{31P77Se}$ = 769.3 Hz). HRMS (ESI-TOF) $C_{18}H_{15}FeO_2PSe$ $[M+H]^+$ *m/z*: calcd.: 430.9388, found: 430.9399.

4.7.4 Synthesis of Se=P(*t*-Bu)$_2$Fc (4d)

3d (100 mg, 0.30 mmol) was reacted with selenium (28 mg, 0.36 mmol) as described earlier. After appropriate work-up, compound **4d** was obtained as an orange solid. Yield: 122 g (0.30 mmol, 100 % based on **3d**). Anal. Calcd. for $C_{18}H_{27}FePSe$ (409.19 g/mol): C, 52.83; H, 6.65. Found: C, 52.81; H, 6.81. Mp.: 145 °C. IR (KBr, $\tilde{\upsilon}$/cm^{-1}): 565 (m, P=Se), 1456 (P-C), 2867/2899/2968/2951/2988 (m, C-H), 3085 (w, =C-H). ^{1}H NMR (500.30 MHz, $CDCl_3$, δ): 1.39 (d, $^{3}J_{HP}$ = 15.4 Hz, 18 H, C(C*H*$_3$)$_3$), 4.32 (s, 5 H, C$_5$*H*$_5$), 4.47 (dpt, $^{4}J_{HP}$ = 1.6 Hz, $^{3}J_{HH}$ = 1.5 Hz, 2 H, H$^{\beta}$/C$_5$*H*$_4$), 4.59 (dpt, $^{3}J_{HP}$ = 1.7 Hz, $^{3}J_{HH}$ = 1.5 Hz, 2 H, H$^{\alpha}$/C$_5$*H*$_4$). ^{13}C{^{1}H} NMR

(125.81 MHz, $CDCl_3$, δ): 28.9 (d, $^2J_{CP}$ = 2.0 Hz, C(CH_3)$_3$), 38.3 (d, $^1J_{CP}$ = 36.2 Hz, C(CH$_3$)$_3$), 70.3 (d, $^3J_{CP}$ = 8.2 Hz, C$^{\beta}$/C_5H_4), 70.7 (s, C_5H_5), 73.8 (d, $^2J_{CP}$ = 9.1 Hz, C$^{\alpha}$/C_5H_4), 74.6 (d, $^1J_{CP}$ = 64.1 Hz, C^{i}/C_5H_4). $^{31}P\{^1H\}$ NMR (202.53 MHz, $CDCl_3$, δ): 74.7 ($^1J_{31P77Se}$ = 701.7 Hz). HRMS (ESI-TOF) $C_{18}H_{27}FePSe$ $[M]^+$ *m/z*: calcd.: 410.0361, found: 410.0312.

4.7.5 Synthesis of Se=PCy$_2$Fc (4e)

According to the procedure described earlier, **3e** (100 mg, 0.26 mmol) was reacted with selenium (24 mg, 0.31 mmol). After appropriate work-up, **4e** was obtained as an orange solid. Yield: 119 mg (0.26 mmol, 100 % based on **3e**). Anal. Calcd. for $C_{22}H_{31}FePSe$ (461.26 g/mol): C, 57.29; H, 6.77. Found: C, 57.40; H, 6.99. Mp.: 116 °C. IR (NaCl, $\tilde{\upsilon}$/cm^{-1}): 531/551 (m, P=Se), 1453 (m, P-C), 2853/2930 (s, C-H), 3076/3097 (w, =C-H). ^1H NMR (500.30 MHz, $CDCl_3$, δ): 1.14 – 1.21 (m, 2 H, C_6H_{11}), 1.23 – 1.31 (m, 6 H, C_6H_{11}), 1.33 – 1.40 (m, 2 H, C_6H_{11}), 1.66 – 1.69 (m, 2 H, C_6H_{11}), 1.81 – 1.86 (m, 4 H, C_6H_{11}), 1.97 – 2.03 (m, 6 H, C_6H_{11}), 4.32 (s, 5 H, C_5H_5), 4.41 (dpt, $^3J_{HP}$ = 1.8 Hz, $^3J_{HH}$ = 1.6 Hz, H$^{\alpha}$/C_5H_4), 4.43 (dpt, $^4J_{HP}$ = 1.7 Hz, $^3J_{HH}$ = 1.6 Hz, H$^{\beta}$/C_5H_4). $^{13}C\{^1H\}$ NMR (125.81 MHz, $CDCl_3$, δ): 26.0 (d, J_{CP} = 1.4 Hz, C_6H_{11}), 26.4 (d, J_{CP} = 1.6 Hz, C_6H_{11}), 26.6 (d, J_{CP} = 2.8 Hz, C_6H_{11}), 26.7 (d, J_{CP} = 1.8 Hz, C_6H_{11}), 27.4 (d, J_{CP} = 3.2 Hz, C_6H_{11}), 37.4 (d, $^1J_{CP}$ = 44.9 Hz, C_6H_{11}), 70.5 (d, $^3J_{CP}$ = 8.9 Hz, C$^{\beta}$/C_5H_4), 70.5 (s, C_5H_5), 72.2 (d, $^2J_{CP}$ = 10.0 Hz, C$^{\alpha}$/C_5H_4), 72.6 (d, $^1J_{CP}$ = 71.0 Hz, C^{i}/C_5H_4). $^{31}P\{^1H\}$ NMR (202.53 MHz, $CDCl_3$, δ): 49.8 ($^1J_{31P77Se}$ = 699.9 Hz). HRMS (ESI-TOF) $C_{22}H_{31}FePSe$ $[M+H]^+$ *m/z*: calcd.: 463.0743, found: 463.0753; $C_{22}H_{31}FePSeCH_3CN$ $[M-H]^+$ m/z: calcd. 502.0843, found: 502.0862.

4.7.6 Synthesis of Se=PPh$_2$Rc (7a)

Using the general procedure described above, the reaction of **5a** (100 mg, 0.22 mmol) with selenium (22 mg, 0.28 mmol) gave **7a** as a pale red solid. Yield: 105 mg (0.21 mmol, 89 % based on **5a**). Anal. Calcd. for $C_{22}H_{19}PRuSe \cdot 0.25\ Et_2O$ (494.39 g/mol): C, 53.85; H, 4.22. Found: C, 53.87; H, 4.15. Mp.: 179 °C. IR (KBr, $\tilde{\upsilon}$/cm^{-1}): 534/545 (m, P=Se); 1449 (m, P-C); 1476 (m, C=C). ^1H NMR (500.30 MHz, $CDCl_3$, δ): 1.21 (t, $^3J_{HH}$ = 7.0 Hz, (CH_3CH_2)$_2$O), 3.43 (q, $^3J_{HH}$ = 7.0 Hz, (CH$_3$CH_2)$_2$O), 4.45 (s, 5 H, C_5H_5), 4.68 (dpt, $^3J_{HP}$ = 1.9 Hz, $^3J_{HH}$ = 1.7 Hz, 2 H, H$^{\alpha}$/C_5H_4), 4.74 (dpt, $^4J_{HP}$ = 1.6 Hz, $^3J_{HH}$ = 1.7 Hz, 2 H, H$^{\beta}$/C_5H_4), 7.32 - 7.4 (m, 6 H, H^{m,p}/C_6H_5), 7.64 - 7.69 (m, 4 H, H^{o}/C_6H_5). $^{13}C\{^1H\}$ NMR (125.81 MHz, $CDCl_3$, δ): 15.2 (s, (CH$_3$CH$_2$)$_2$O), 65.9 ((CH$_3$$CH_2$)$_2$O), 73.0 (s, C_5H_5), 73.7 (d, $^3J_{CP}$ = 9.2 Hz , C$^{\beta}$/C_5H_4), 75.4 (d, $^2J_{CP}$ = 13.3 Hz, C$^{\alpha}$/C_5H_4), 79.2 (d, $^1J_{CP}$ = 86.1 Hz, C^{i}/C_5H_4), 128.2 (d, $^2J_{CP}$ = 12.5 Hz, C^{o}/C_6H_5), 131.4 (d, $^4J_{CP}$ = 2.8 Hz, C^{p}/C_6H_5), 132.3 (d, $^3J_{CP}$ = 10.9 Hz, C^{m}/C_6H_5), 133.7 (d,

$^{1}J_{CP}$ = 78.8 Hz, C^{i}/C_6H_5). $^{31}P\{^{1}H\}$ NMR (202.53 MHz, $CDCl_3$, δ): 31.2 ppm ($^{1}J_{31P77Se}$ = 735.2 Hz).

4.7.7 Synthesis of Se=P(*o*-Tol)$_2$Rc (7b)

According to the general procedure described earlier, **5b** (100 mg, 0.23 mmol) was reacted with selenium (21 mg, 0.27 mmol) to give **7b** as a colorless solid. Yield: 110 mg (0.21 mmol, 94 % based on **5b**). Anal. Calcd. for $C_{24}H_{23}PRuSe \cdot 0.5\ Et_2O$ (522.44 g/mol): C, 55.81; H, 5.04. Found: C, 55.91; H, 4.94. Mp.: 200 °C (dec.). IR (KBr, $\tilde{\upsilon}$/cm^{-1}): 571 (m, P=Se); 1453 (m, P-C); 1559 (m, C=C). ^{1}H NMR (500.30 MHz, $CDCl_3$, δ): 1.21 (t, $^{3}J_{HH}$ = 7.0 Hz, (CH_3CH_2)$_2$O), 2.05 (s, 6 H, CH_3), 3.43 (q, $^{3}J_{HH}$ = 7.0 Hz, (CH_3CH_2)$_2$O), 4.52 (s, 5 H, C_5H_5), 4.84 (m, 4 H, H$^{\alpha,\beta}$/C_5H_4), 7.10 - 7.13 (m, 2 H, C_6H_4), 7.35 - 7.37 (m, 4 H, C_6H_4), 7.9 - 8.4 (m, 2 H, C_6H_4). $^{13}C\{^{1}H\}$ NMR (125.81 MHz, $CDCl_3$, δ): 15.2 (s, (CH_3CH_2)$_2$O), 22.0 (d, $^{3}J_{CP}$ = 3.9 Hz, CH_3), 65.9 (s, (CH_3CH_2)$_2$O), 73.2 (s, C_5H_5), 73.6 (d, $^{2}J_{CP}$ = 9.1 Hz, C$^{\alpha}$/C_5H_4), 74.7 (m, C$^{\beta}$/C_5H_4), 80.3 (d, $^{1}J_{CP}$ = 85.4 Hz, C^{i}/C_5H_4), 126.4 (d, $^{2}J_{CP}$ = 13.4 Hz, C^{o}/C_6H_4), 131.5 (d, $^{4}J_{CP}$ = 2.4 Hz, C^{p}/C_6H_4), 131.7 (d, $^{3}J_{CP}$ = 10.3 Hz, C^{m}/C_6H_4), 140.1 (d, $^{1}J_{CP}$ = 9.2 Hz, C^{i}/C_6H_4). $^{31}P\{^{1}H\}$ NMR (202.53 MHz, $CDCl_3$, δ): 29.0 ($^{1}J_{31P77Se}$ = 717.5 Hz).

4.7.8 Synthesis of Se=PFur$_2$Rc (7c)

The reaction of **5c** (100 mg, 0.25 mmol) with selenium (24 mg, 0.30 mmol) gave **7c** as a pale red solid. Yield: 100 mg (0.21 mmol, 84 % based on **5c**). Anal. Calcd. for $C_{18}H_{15}O_2PRuSe$ (474.30 g/mol): C, 45.58; H, 3.19. Found: C, 45.45; H, 3.20. Mp.: 242 °C. IR (KBr, $\tilde{\upsilon}$/cm^{-1}): 549/570 (m, P=Se); 1013 (m, C-O); 1457 (w, P-C), 1556 (m, C=C), 3097 (m, =C-H). ^{1}H NMR (500.30 MHz, $CDCl_3$, δ): 4.51 (s, 5 H, C_5H_5), 4.81 (dpt, $^{3}J_{HP}$ = 1.6 Hz, $^{3}J_{HH}$ = 1.5 Hz, 2 H, H$^{\beta}$/C_5H_4), 5.06 (dpt, $^{3}J_{HP}$ = 2.0 Hz, $^{3}J_{HH}$ = 1.8 Hz, 2 H, H$^{\alpha}$/C_4H_5), 6.48 (dpt, $^{4}J_{HP}$ = 1.7 Hz, $^{3}J_{HH}$ = 3.4 Hz, $^{3}J_{HH}$ = 1.7 Hz, 2 H, H^{4}/C_4H_3O), 7.12 (m, 2 H, H^{3}/C_4H_3O), 7.68 (m, 2 H, H^{5}/C_3H_4O). $^{13}C\{^{1}H\}$ NMR (125.81 MHz, $CDCl_3$, δ): 72.9 (s, C_5H_5), 73.7 (d, $^{3}J_{CP}$ = 10.7 Hz, C$^{\beta}$/C_5H_4), 74.8 (d, $^{2}J_{CP}$ = 15.5 Hz, C$^{\alpha}$/C_5H_4), 75.9 (d, $^{1}J_{CP}$ = 98.0 Hz, C^{i}/C_5H_4), 111.1 (d, $^{3}J_{CP}$ = 9.2 Hz, C^{4}/C_4H_3O), 122.0 (d, $^{2}J_{CP}$ = 21.9 Hz, C^{3}/C_4H_3O), 147.3 (d, $^{1}J_{CP}$ = 114.7 Hz, C^{2}/C_4H_3O), 148.2 (d, $^{4}J_{CP}$ = 7.1 Hz, C^{5}/C_4H_3O). $^{31}P\{^{1}H\}$ NMR (202.53 MHz, $CDCl_3$, δ): -6.8 ($^{1}J_{31P77Se}$ = 772 Hz).

4.7.9 Synthesis of Se=PCy$_2$Rc (7d)

According to the general procedure described above, **5d** (100 mg, 0.26 mmol) was reacted with selenium (22 mg, 0.28 mmol). After appropriate work-up, compound **7d** could be

isolated as a colorless solid. Anal. Calcd. for $C_{22}H_{31}PRuSe$ (506.49 g/mol): C, 52.17; H, 6.17. Found: C, 53.33; H, 6.29. *) IR (KBr, $\tilde{\nu}$/cm^{-1}): 549 (m, P=Se); 1453 (w, P-C), 1556 (m, C=C), 3097 (m, =C-H). ^{1}H NMR (500.30 MHz, $CDCl_3$, δ): 1.15 - 1.41 (m, 10 H, C_6H_{11}), 1.66 - 1.69 (m, 2 H, C_6H_{11}), 1.79 - 1.86 (m, 4 H, C_6H_{11}), 1.96 – 2.02 (m, 6 H, C_6H_{11}), 4.63 (s, 5 H, C_5H_5), 4.74 (m, 2 H, C_5H_4), 4.76 (dpt, J_{HP} = 1.6 Hz, J_{HH} = 1.5 Hz, 2 H, C_5H_4). ^{13}C{^{1}H} NMR (125.81 MHz, $CDCl_3$, δ): 26.0 (d, J_{CP} = 1.4 Hz, C_6H_{11}), 26.4 (d, J_{CP} = 1.6 Hz, C_6H_{11}), 26.6 (d, J_{CP} = 4.5 Hz, C_6H_{11}), 26.7 (d, J_{CP} = 3.7 Hz, C_6H_{11}), 27.6 (d, J_{CP} = 3.3 Hz, C_6H_{11}), 37.3 (d, $^1J_{CP}$ = 44.7 Hz, C^1/C_6H_{11}), 72.4 (d, $^3J_{CP}$ = 8.0 Hz, C^β/C_5H_4), 73.1 (s, C_5H_5), 74.3 (d, $^2J_{CP}$ = 10.8 Hz, C^α/C_5H_4), 76.7 (d, $^1J_{CP}$ = 68.0 Hz, C^i/C_5H_4). ^{31}P{^{1}H} NMR (202.53 MHz, $CDCl_3$, δ): 49.2 ($^1J_{31P77Se}$ = 704 Hz). HRMS (ESI-TOF) $C_{22}H_{31}PRuSe$ $[M+H]^+$ *m/z*: calcd.: 509.0455, found: 509.0378. *) Please, notice that the results of the elemental analysis deviate from the calculated values due to the light sensitivity and therefore, decomposition of this compound.

4.8 General Procedure for the Synthesis of the Palladium Complexes 9a – e and 10a – d

Phosphine **3** or **6** (0.5 g) and $[PdCl_2(cod)]$ (**8**, 0.5 eq.) were dissolved in dry dichloromethane (40 mL). This solution was stirred for 2 h at ambient temperature. Then all volatile materials were removed in membrane pump vacuum and the residue was washed five times with diethyl ether (5 mL portions). After drying the residue in membrane pump vacuum, the respective complexes were obtained as yellow or red solids.

4.8.1 Synthesis of $[PdCl_2(P(o\text{-}Tol)_2Fc)_2]$ (9b)

Following the general procedure described above, **3b** (0.5 g, 1.26 mmol) was reacted with **8** (0.18 g, 0.63 mmol). After appropriate work-up, complex **9b** could be isolated as an air stable red solid. Yield: 0.52 g (0.53 mmol, 84 % based on **8**). Anal. Calcd. for $C_{48}H_{46}Cl_2Fe_2P_2Pd \cdot 2/3\ CH_2Cl_2$ (1030.46 g/mol): C, 56.72; H, 4.63. Found: C, 56.23; H, 4.64. Mp.: 210 °C (dec.). IR (KBr, $\tilde{\nu}$/cm^{-1}): 754 (s, =C-H, *o*-disubst. benzene), 1449 (m, P-C), 1561/1638/1655 (m, C=C), 2928/2969 (w, C-H), 3053 (w, =C-H). ^{1}H NMR (500.30 MHz, CD_2Cl_2, δ): 2.39 (s, 12 H, CH_3), 4.23 (s, 10 H, C_5H_5), 4.51 (pt, $^3J_{HH}$ = 1.7 Hz, 4 H, C_5H_4), 4.68 (m, 4 H, C_5H_4), 5.29 (s, CH_2Cl_2), 7.16 – 7.19 (m, 8 H, C_6H_4), 7.32 – 7.35 (m, 4 H, C_6H_4), 7.85 – 7.89 (m, 4 H, C_6H_4). ^{13}C{^{1}H} NMR (125.81 MHz, CD_2Cl_2, δ): 23.9 (pt, $^3J_{CP}$ = 3.4 Hz, CH_3), 53.5 (s, CH_2Cl_2), 70.9 (s, C_5H_5), 71.1 (pt, $^3J_{CP}$ = 4.0 Hz, C^β/C_5H_4), 77.4 (pt, $^2J_{CP}$ = 6.4 Hz, C^α/C_5H_4), 125.0 (pt, J_{CP} = 5.0 Hz, C_6H_4), 130.4 (s, C^p/C_6H_4), 131.1 (pt, J_{CP} = 4.2 Hz, C_6H_4), 134.9 (pt, J_{CP} = 5.7 Hz, C_6H_4), 142.7 (pt, J_{CP} = 5.3 Hz, C_6H_4). ^{31}P{^{1}H} NMR (202.53

MHz, CD_2Cl_2, δ): 13.9 (s). HRMS (ESI-TOF) $C_{48}H_{46}Fe_2P_2PdCl_2$ $[M\text{-}Cl]^+$ *m/z*: calcd.: 937.0510, found: 937.0464; $[M\text{-}H\text{-}2Cl]^+$ *m/z*: calcd.: 901.0746, found: 901.0699.

4.8.2 Synthesis of $[PdCl_2(PFur_2Fc)_2]$ (9c)

Following the general procedure described above, **3c** (0.5 g, 1.43 mmol) was reacted with 8 (0.20 g, 0.70 mmol). Appropriate work-up, gave **9c** as an air stable red solid. Yield: 0.47 g (0.54 mmol, 77 % based on **8**). Anal. Calcd. for $C_{36}H_{30}Cl_2Fe_2O_4P_2Pd \cdot 1/3\ CH_2Cl_2$ (905.90 g/mol): C, 48.17; H, 3.41. Found: C, 48.65; H, 3.45. Mp.: 242 °C (dec.). IR (KBr, $\tilde{\upsilon}/cm^{-1}$): 1005/1010 (s, C-O); 1457 (w, P-C), 1654 (w, C=C), 3047/31273152 (w, =C-H). ^1H NMR (500.30 MHz, CD_2Cl_2, δ): 4.43 (s, 10 H, C_5H_5), 4.50 (pt, $^3J_{HH}$ = 1.8 Hz, 4 H, C_5H_4), 4.74 (m, 4 H, C_5H_4), 5.30 (s, CH_2Cl_2), 6.50 (m, 4 H, H^4/C_4H_3O), 7.00 (m, 4 H, H^3/C_4H_3O), 7.75 (m, 4 H, $/H^5C_4H_3O$). $^{13}C\{^1H\}$ NMR (125.81 MHz, CD_2Cl_2, δ): 53.5 (s, CH_2Cl_2), 70.5 (s, C_5H_5), 71.9 (pt, $^3J_{CP}$ = 4.5 Hz, C^{β}/C_5H_4), 74.7 (pt, $^2J_{CP}$ = 7.4 Hz, C^{α}/C_5H_4), 110.9 (pt, $^3J_{CP}$ = 3.4 Hz, C^4/C_4H_3O), 123.3 (m, C^3/C_4H_3O), 147.8 (pt, $^4J_{CP}$ = 3.1 Hz, C^5/C_4H_3O). $^{31}P\{^1H\}$ NMR (202.53 MHz, CD_2Cl_2, δ): -14.0 (s). HRMS (ESI-TOF) $C_{36}H_{30}Cl_2Fe_2O_4P_2Pd$ $[M\text{-}Cl]^+$ *m/z*: calcd.: 840.9051, found: 840.9041; $[M\text{-}(C_{18}H_{15}FeO_2P)\text{-}Cl]^+$ *m/z*: calcd.: 492.8880, found: 492.8847.

4.8.3 Synthesis of $[PdCl_2(PCy_2Fc)_2]$ (9e)

According to the general procedure described earlier, **3e** (0.5 g, 1.31 mmol) was reacted with 8 (0.18 g, 0.63 mmol). Appropriate work-up, gave **9e** as an air stable red solid. Yield: 0.48 g (0.51 mmol, 81 % based on **8**). Anal. Calcd. for $C_{44}H_{62}Cl_2Fe_2P_2Pd \cdot 1/2\ Et_2O$ (978.68 g/mol): C, 56.44; H, 6.90. Found: C, 56.70; H, 6.78. Mp.: 253 °C (dec.). IR (KBr, $\tilde{\upsilon}/cm^{-1}$): 1433/1436 (m, P-C), 2857/2926/2979 (w, C-H), 3038/3050/3088 (w, =C-H). ^1H NMR (500.30 MHz, CD_2Cl_2, δ): 1.27 – 1.31 (m, 12 H, C_6H_{11} + $(CH_3CH_2)_2O$), 1.69 – 1.78 (m, 20 H, C_6H_{11}), 2.08 – 2.10 (m, 4 H, C_6H_{11}), 2.33 – 2.55 (m, 4 H, C_6H_{11}), 2.56 – 2.61 (m, 4 H, H^1/C_6H_{11}), 3.48 (q, $^3J_{HH}$ = 7.0 Hz, $(CH_3CH_2)_2O$), 4.36 (s, 10 H, C_5H_5), 4.41 (m, 4 H, C_5H_4), 4.71 (m, 4 H, C_5H_4). $^{13}C\{^1H\}$ NMR (125.81 MHz, CD_2Cl_2, δ): 15.4 (s, $(CH_3CH_2)_2O$), 26.5 (s, C^6/C_6H_{11}), 27.6 (pt, $^2J_{CP}$ = 5.5 Hz, $C^{2/3}/C_6H_{11}$), 27.8 (pt, $^2J_{CP}$ = 6.3 Hz, $C^{2/3}/C_6H_{11}$), 28.9 (s, $C^{4/5}/C_6H_{11}$), 30.2 (s, $C^{4/5}/C_6H_{11}$), 36.9 (pt, $^1J_{CP}$ = 11.7 Hz, C^1/C_6H_{11}), 65.9 (s, $(CH_3CH_2)_2O$), 70.1 (pt, $^3J_{CP}$ = 3.4 Hz, C^{β}/C_5H_4), 70.2 (s, C_5H_5), 72.1 (pt, $^1J_{CP}$ = 20.0 Hz, C^i/C_5H_4), 75.0 (pt, $^2J_{CP}$ = 5.3 Hz, C^{α}/C_5H_4). $^{31}P\{^1H\}$ NMR (202.53 MHz, $CDCl_3$, δ): 18.0 (s). HRMS (ESI-TOF) $C_{44}H_{62}Cl_2Fe_2P_2Pd$ $[M\text{-}H\text{-}C_{22}H_{31}FePCl_2]^+$ *m/z*: calcd.: 487.0475, gef.: 487.0413.

4.8.4 Synthesis of [$PdCl_2(PPh_2Rc)_2$] (10a)

Following the synthesis methodology described above, **6a** (0.5 g, 1.20 mmol) was reacted with **8** (0.17 g, 0.60 mmol). After appropriate work-up, **10a** was isolated as an air stable yellow solid. Yield: 0.50 g (0.50 mmol, 83 % based on **8**). Anal. Calcd. for $C_{44}H_{38}Cl_2P_2PdRu_2 \cdot 1/3\ CH_2Cl_2$ (1008.19 g/mol): C, 51.37; H, 3.76. Found: C, 51.41; H, 3.83. Mp.: 164 °C (dec.). IR (KBr, $\tilde{\upsilon}$/cm^{-1}): 1437 (w, P-C), 1481 (m, C=C). ^{1}H NMR (500.30 MHz, $CDCl_3$, δ): 4.81 (m, 4 H, C_5H_4), 4.84 (m, 10 H, C_5H_5), 4.95 (m, 4 H, C_5H_4), 5.30 (s, CH_2Cl_2), 7.36 - 7.47 (m, 12 H, $H^{m,p}/C_6H_5$), 7.63 - 7.67 (m, 8 H, H^o/C_6H_5). ^{13}C{^{1}H} NMR (125.81 MHz, $CDCl_3$, δ): 53.5 (s, CH_2Cl_2), 72.9 (s, C_5H_5), 73.3 (m, C_5H_4), 77.5 (m, C_5H_4), 127.7 (pt $^3J_{CP}$ = 4.9 Hz, C^m/C_6H_5), 130.4 (s, $C^p/(C_6H_5)$, 131.5 (pt, $^1J_{CP}$ = 25.3 Hz, C^i/C_6H_5), 134.3 (pt, $^2J_{CP}$ = 5.9 Hz, C^o/C_6H_5). ^{31}P{^{1}H} NMR (202.53 MHz, $CDCl_3$, δ): 14.8 ppm (s). HRMS (ESI-TOF) $C_{44}H_{38}ClP_2PdRu_2$ $[M]^+$ *m/z*: calcd.: 972.9278, gef.: 972.9249; $C_{22}H_{19}ClPRu$ $[M]^+$ *m/z*: calcd.: 450.9954, found: 450.9926.

4.8.5 Synthesis of [$PdCl_2(P(o\text{-}Tol)_2Rc)_2$] (10b)

Following the synthesis procedure described above, **6b** (0.5 g, 1.13 mmol) was reacted with **8** (0.16 g, 0.56 mmol). Appropriate work-up, gave **10b** as an air stable yellow solid. Yield: 0.50 mg (0.47 mmol, 84 % based on **8**). Anal. Calcd. for $C_{48}H_{46}Cl_2P_2PdRu_2 \cdot 1/2\ CH_2Cl_2$ (1064.29 g/mol): C, 52.58; H, 4.36. Found: C, 52.36; H, 4.39. Mp.: 250 °C (dec.). IR (KBr, $\tilde{\upsilon}$/cm^{-1}): 1448 (w, P-C), 1559 (m, C=C). ^{1}H NMR (500.30 MHz, $CDCl_3$, δ): 2.69 (s, 12 H, CH_3), 4.66 (s, 10 H, C_5H_5), 4.79 (m, 4 H, C_5H_4), 5.00 (pt, $^3J_{HH}$ = 1.6 Hz, 4 H, C_5H_4), 5.30 (s, CH_2Cl_2), 7.12 - 7.15 (m, 4 H, C_6H_4), 7.21 - 7.23 (m, 4 H, C_6H_4), 7.34 - 7.37 (m, 4 H, C_6H_4), 7.57 – 7.61 (m, 4 H, C_6H_4). ^{13}C{^{1}H} NMR (125.81 MHz, $CDCl_3$, δ): 24.3 (pt, $^3J_{CP}$ = 3.3 Hz, CH_3), 53.5 (CH_2Cl_2), 72.9 (pt, $^3J_{CP}$ = 3.6 Hz, C^β/C_5H_4), 73.5 (s, C_5H_5), 77.8 (pt, $^1J_{CP}$ = 25.5 Hz, C^i/C_5H_4), 79.3 (pt, $^2J_{CP}$ = 6.8 Hz, C^α/C_5H_4), 125.0 (pt, J_{CP} = 5.2 Hz, C_6H_4), 130.4 (s, C_6H_4), 130.6 (pt, $^1J_{CP}$ = 24.0 Hz, C^i/C_6H_4), 131.1 (pt, J_{CP} = 3.8 Hz, C_6H_4), 135.2 (pt, J_{CP} = 5.7 Hz, C_6H_4), 142.6 (pt, J_{CP} = 5.3 Hz, C_6H_4). ^{31}P{^{1}H} NMR (202.53 MHz, $CDCl_3$, δ): 16.2 ppm (s). HRMS (ESI-TOF) $C_{48}H_{46}ClP_2PdRu_2$ $[M]^+$ *m/z*: calcd.: 1028.9906, found: 1028.9891 (36.71 %); $C_{48}H_{46}P_2PdRu_2$ $[M]^+$ *m/z*: calcd.: 994.02, found: 994.0216; $C_{24}H_{23}PPdClRu$ $[M]^+$ *m/z*: calcd.: 584.9309, found: 584.9286; $C_{24}H_{23}PPdRu$ $[M\text{-}H]^+$ *m/z*: calcd.: 548.9547, found: 548.9517.

4.8.6 Synthesis of [$PdCl_2(PFur_2Rc)_2$] (10c)

Reaction of **6c** (0.5 g, 1.26 mmol) with **8** (0.18 g, 0.63 mmol) gave **10c** as an air stable yellow solid (reaction procedure see earlier). Yield: 0.52 g (0.54 mmol, 86 % based on **8**). Anal. Calcd. for $C_{36}H_{30}Cl_2O_4P_2PdRu_2$ (968.03 g/mol): C, 44.67; H, 3.12. Found: C, 44.63; H, 3.13. Mp.: 242 °C. IR (KBr, $\tilde{\upsilon}$/cm^{-1}): 1024 (w, C-O), 1454 (w, P-C), 1536 (m, C=C). ^{1}H NMR (500.30 MHz, $CDCl_3$, δ): 4.75 (s, 10 H, C_5H_5), 4.79 (pt, $^3J_{HH}$ = 1.7 Hz, 4 H, C_5H_4), 5.13 (m, 4 H, C_5H_4), 6.45 (m, 4 H, H^4/C_4H_3O), 7.08 (m, 4 H, H^3/C_4H_3O), 7.67 (m, 4 H, H^5/C_4H_3O). ^{13}C{^{1}H} NMR (125.81 MHz, $CDCl_3$, δ): 73.0 (s, C_5H_5), 73.5 (pt, $^3J_{CP}$ = 4.2 Hz, C^{β}/C_5H_4), 76.5 (pt, $^2J_{CP}$ = 7.5 Hz, C^{α}/C_5H_4), 110.9 (pt, $^3J_{CP}$ = 3.5 Hz, C^4/C_4H_3O), 123.4 (pt, $^2J_{CP}$ = 9.2 Hz, C^3/C_4H_3O), 144.59 (pt, $^1J_{CP}$ = 39.2 Hz, C^2/C_4H_3O), 147.6 (pt, $^4J_{CP}$ = 2.8 Hz, C^5/C_4H_3O). ^{31}P{^{1}H} NMR (202.53 MHz, $CDCl_3$, δ): -15.0 ppm (s).

4.8.7 Synthesis of [$PdCl_2(PCy_2Rc)_2$] (10d)

Following the synthesis procedure described earlier, **6d** (0.5 g, 1.17 mmol) was reacted with **8** (0.16 g, 0.56 mmol). After appropriate work-up, complex **10d** was obtained as an air stable red solid. Yield: 0.40 g (0.39 mmol, 70 % based on **8**). Anal. Calcd. for $C_{44}H_{62}Cl_2P_2PdRu_2$ (1032.38 g/mol): C, 51.19; H, 6.05. Found: C, 51.19; H, 5.92. Mp.: 180 °C (dec.). IR (KBr, $\tilde{\upsilon}$/cm^{-1}): 1448 (m, P-C), 1655 (w, C=C), 2847/2927 (s, C-H), 3108 (w, =C-H). ^{1}H NMR (500.30 MHz, $CDCl_3$, δ): 1.23 - 1.27 (m, 12 H, C_6H_{11}), 1.70 - 1.79 (m, 20 H, C_6H_{11}), 2.09 - 2.11 (m, 4 H, C_6H_{11}), 2.25 - 2.27 (m. 4 H, C_6H_{11}), 2.49 - 2.54 (m, 4 H, H^1/C_6H_{11}), 4.68 (s, 10 H, C_5H_5), 4.70 (m, 4 H, C_5H_4), 5.00 (m, 4 H, C_5H_4). ^{13}C{^{1}H} NMR (125.81 MHz, $CDCl_3$, δ): 26.5 (s, C^6/C_6H_{11}), 27.7 (pt, $^2J_{CP}$ = 5.7 Hz, $C^{2/3}/C_6H_{11}$), 27.8 (pt, $^2J_{CP}$ = 6.3 Hz, $C^{2/3}/C_6H_{11}$), 28.9 (s, $C^{4/5}/C_6H_{11}$), 30.3 (s, $C^{4/5}/C_6H_{11}$), 37.1 (pt, $^1J_{CP}$ = 11.8 Hz, C^1/C_6H_{11}), 72.0 (pt, $^3J_{CP}$ = 3.0 Hz, C^{β}/C_5H_4), 72.6 (s, C_5H_5), 75.2 (pt, $^1J_{CP}$ = 19.0 Hz, C^i/C_5H_4), 77.0 (pt, $^2J_{CP}$ = 5.6 Hz, C^{α}/C_5H_4). ^{31}P{^{1}H} NMR (202.53 MHz, $CDCl_3$, δ): 16.4 (s). HRMS (ESI-TOF) $C_{44}H_{62}ClP_2PdRu_2$ $[M]^+$ *m/z*: calcd.: 977.1156, found: 997.1156.

4.9 General Procedure for the Mizoroki-Heck Reaction

612 mg (3.0 mmol) of iodo benzene, 397 mg (3.1 mmol) of *t*-butyl acrylate, 452 mg (3.5 mmol) of $EtN(i\text{-}Pr)_2$, and 114 mg (0.5 mmol) of acetyl ferrocene were dissolved in 15 mL of a mixture of toluene-acetonitrile (ratio 1:1, *v*:*v*) and 0.2 mol% of the respective catalyst (**9a** – **e** or **10a** – **d**). The reaction mixture was stirred at 80 °C and samples (1 mL) were taken in periods of 1 h. The samples were chomatographed on silica gel with diethyl ether as eluent. All volatiles were evaporated and the conversions were determined by ^{1}H NMR spectroscopy.

4.10 General Procedure for the Suzuki-Miyaura Reaction

2-bromo toluene (500 mg, 2.92 mmol) or 4-chloro acetophenone (464 mg, 3.00 mmol), phenylboronic acid (470 mg, 3.85 mmol), potassium carbonate (1.21 g, 8.76 mmol), and acetyl ferrocene (114 mg, 0.50 mmol) were dissolved in a 1,4-dioxane-water mixture (12 mL, ratio 2:1, *v*:*v*). After addition of 0.1 mol%, 0.25 mol% (reaction of 2-bromo toluene) or 0.5 mol% (reaction of 4-chloro acetophenone) of the appropriate catalyst (**9a** – **e** or **10a** – **d**), the reaction mixture was stirred for 1 h at 100 °C. Samples of 1 mL were taken after 2.5, 5, 10, 20, 30, and 60 min and chromatographed on silica gel with diethyl ether as eluent. All volatiles were evaporated under reduced pressure and the conversions were determined by ^{1}H NMR spectroscopy.

4.11 Crystal Data for 4b

$C_{24}H_{23}FePSe$, M_r = 477.20 g·mol^{-1}, monoclinic, P2(1)/n, λ = 0.71073 Å, a = 15.7844(4) Å, b = 7.4393(2) Å, c = 17.6781(5) Å, β = 90.127(2) °, V = 2075.84(10) Å^3, Z = 4, ρ_{calcd} = 1.527 mg·m^{-3}, μ = 2.563 mm^{-1}, T = 298(2) K, Θ range = 3.03 – 26.00 °, reflections collected: 10904, independent: 4054 (R_{int} = 0.0321), R_1 = 0.0297, wR_2 = 0.0647 [$I > 2\sigma(I)$]. Single crystals of **4b** were obtained from a saturated dichloromethane solution containing **4b** at 298 K. Data were collected with an Oxford Gemini S diffractometer, with graphite monochromatized Mo K_α radiation (λ = 0.71073 Å). The structure was solved by direct methods and refined by full-matrix least square procedures on F². [C27]

5 Supporting Information

NMR spectra and reaction profiles are given. Crystallographic data of **4b** as CIF file is available free of charge *via* the Cambridge Crystallographic Database as file no. CCDC 834561.

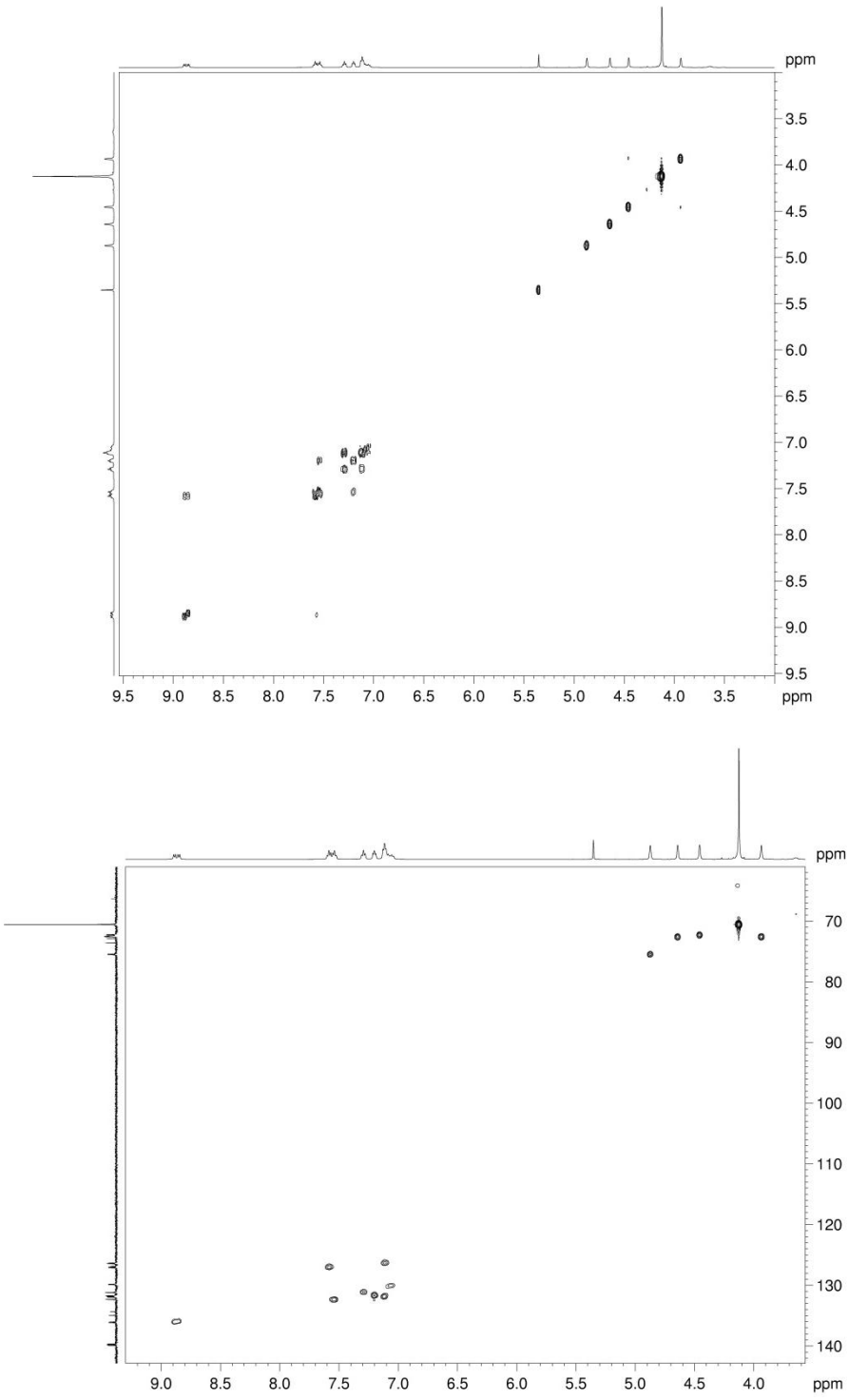

Figure C7. Top: *H*, *H* COSY NMR spectrum of **4b** in CD_2Cl_2 at -90 °C; Bottom: HSQC NMR spectrum of **4b** in CD_2Cl_2 at -90 °C.

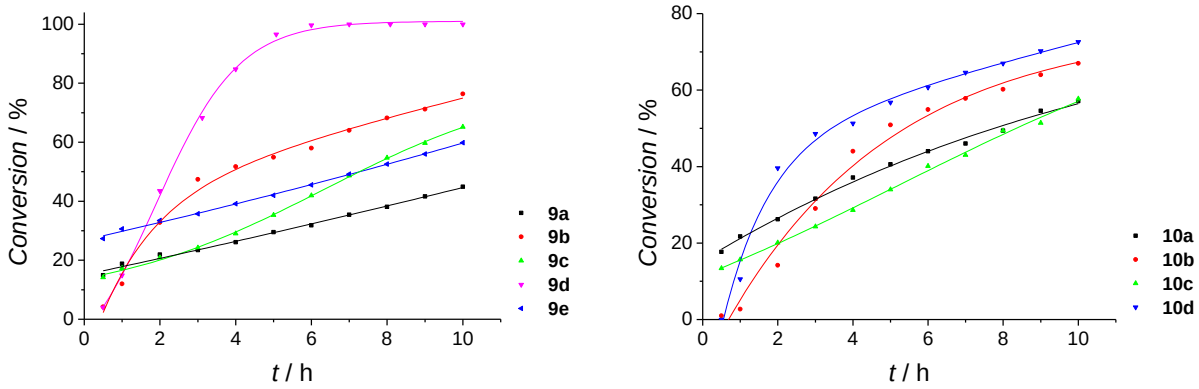

Figure C8. Reaction profiles for catalysts **9** (left) and **10** (right) for the reaction of iodo benzene with *t*-butyl acrylate and a catalyst loading of 0.2 mol%.

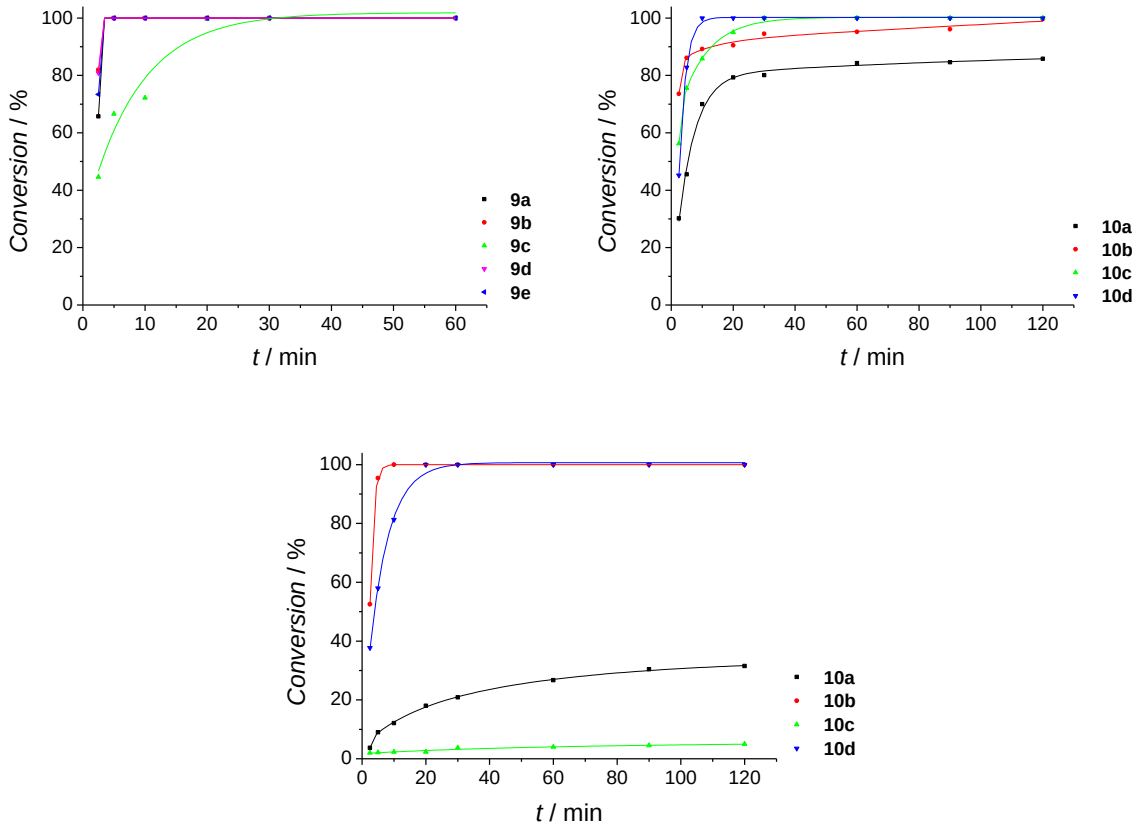

Figure C9. Reaction profiles for catalysts **9** (0.1 mol%: top left) and **10** (0.25 mol%: top right, 0.1 mol%: bottom) for the reaction of 2-bromo toluene with phenyl boronic acid at 100 °C.

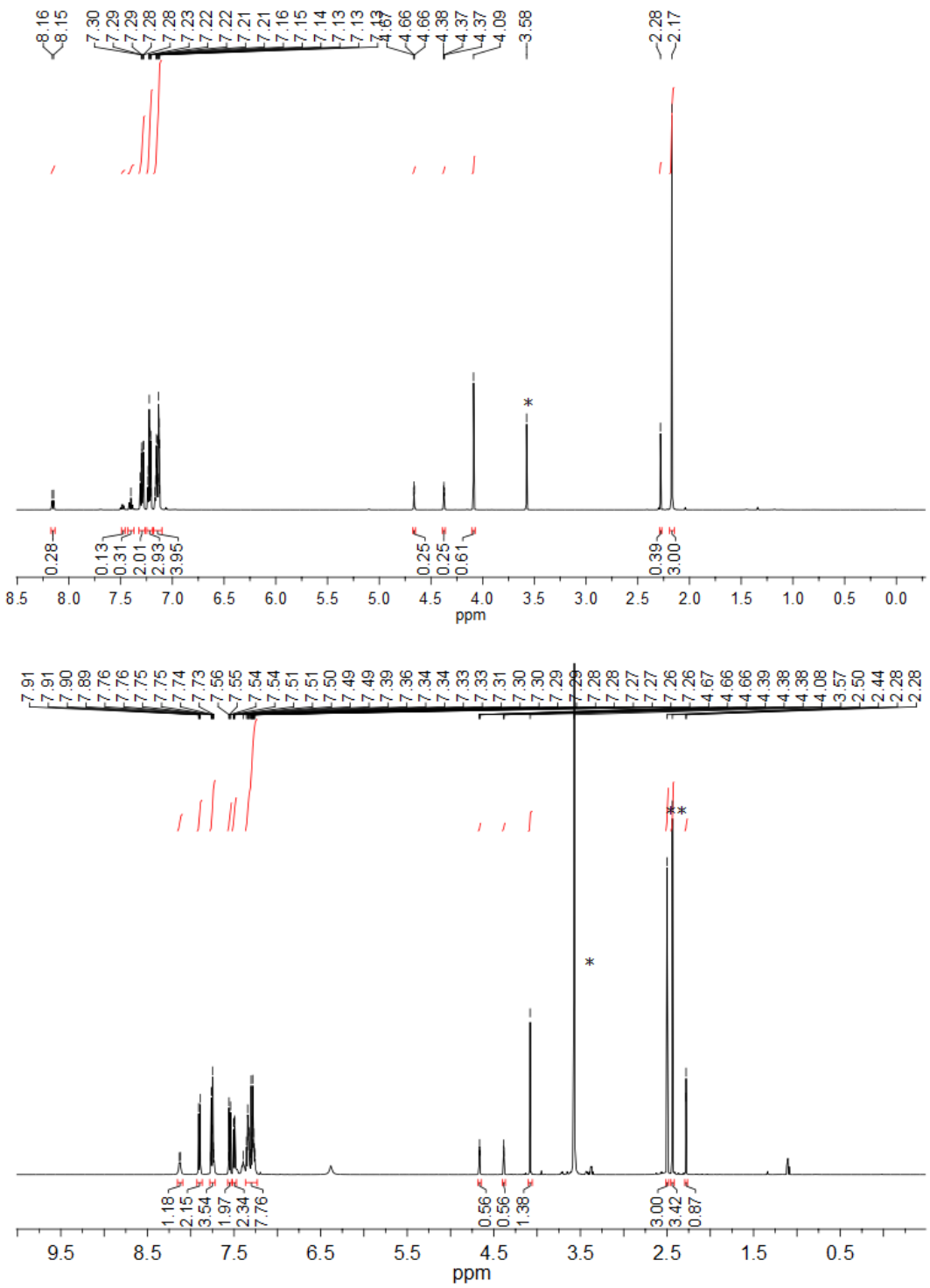

Figure C10. ^{1}H NMR spectra of samples taken from the reaction of 2-bromo toluene (top, after 20 min, conversion: 100 %) and 4-chloroacetophenone (bottom, after 60 min, conversion: 60 %.) with phenyl boronic acid using catalyst **9b** and acetyl ferrocene as internal standard; *) 1,4-dioxane; **) 4-chloroacetophenone.

6 Acknowledgement

We are grateful to the Deutsche Forschungsgemeinschaft and the Fonds der Chemischen Industrie for generous financial support.

7 References

[C1] For example: a) X. Chen, K. M. Engle, D.-H. Wang, J.-Q. Yu *Angew. Chem. Int. Ed.* **2009**, *48*, 5094; b) N. Marion, S. P. Nolan *Acc. Chem. Res*. **2008**, *41*, 1440; c) V. Polshettiwara, C. Len, A. Fihri *Coord. Chem. Rev*. **2009**, *253*, 2599; d) M.-N. Birkholz, Z. Freixa, P. W. N. M. van Leeuwen *Chem. Soc. Rev*. **2009**, *38*, 1099; e) X.-F. Wu, P. Anbarasan, H. Neumann, M. Beller *Angew. Chem. Int. Ed*. **2010**, *49*, 9047; f) D. Astruc *Anal. Bioanal. Chem.* **2011**, *399*, 1811; g) I. J. S. Fairlamb, R. J. K. Taylor, J. L. Serrano, G. Sanchez *New J. Chem*. **2006**, *30*, 1695; h) R. Martin, S. L. Buchwald *Acc. Chem. Res*. **2008**, *41*, 1461; i) E. A. B. Kantchev, C. J. O'Brien, M. G. Organ *Angew. Chem. Int. Ed*. **2007**, *46*, 2768.

[C2] For example: a) D. Steinborn *Grundlagen der metallorganischen Komplexkatalyse*, *Teubner*, Wiesbaden **2007**; b) M. Beller, C. Bolm *Transition Metals for Organic Synthesis 2nd Edition*, *Wiley-VCH*, Weinheim **2004**; c) B. Cornils, W. A. Herrmann *Applied Homogeneous Catalysis with Organometallic Compounds*, *VCH*, Weinheim **1996**; d) F. Diederich, P. J. Stang *Metal-catalyzed-Cross-coupling-Reactions 2nd Edition*, *Wiley-VCH*, Weinheim **2004**; e) S. Kumar, M. M. Shaikh, P. Ghosh *J. Organomet. Chem*. **2009**, *694*, 4162; f) M. Albrecht, G. van Koten *Angew. Chem. Int. Ed*. **2001**, *40*, 3750; g) N. Debono, A. Labande, E. Manoury, J.-C. Daran, R. Poli *Organometallics* **2010**, *29*, 1879; h) N. Kataoka, Q. Shelby, J. P. Stambuli, J. F. Hartwig *J. Org. Chem*. **2002**, *67*, 5553; i) A. F. Littke, G. C. Fu *J. Org. Chem.* **1999**, *64*, 10; j) C. Zhang, M. L. Trudell *Tetrahedron Lett.* **2000**, *41*, 595; k) J. P. Wolfe, R. A. Singer, B. H. Yang, S. L. Buchwald *J. Am. Chem. Soc.* **1999**, *121*, 9550; l) H. Weissman, D. Milstein *Chem. Comm.* **1999**, 1901; m) B. L. Shaw, S. D. Perera, E. A. Staley *Chem. Commun.* **1998**, 1361; n) M. T. Reetz, G. Lohmer, R. Schwickardi, *Angew. Chem., Int. Ed. Engl*. **1998**, *37*, 481; o) W. A. Herrmann, C. Brossmer, C.-P. Reisinger, T. H. Riermeier, K. Öfele, M. Beller *Chem. Eur. J.* **1997**, *3*, 1357.

[C3] P. Štěpnička *Ferrocenes: Ligands, Materials and Biomolecules*, *John Wiley & Sons Ltd*, Chichester, **2008**.

[C4] For example: a) T. J. Colacot, *Chem. Rev.* **2003**, *103*, 3101; b) A. Jakob, B. Milde, P. Ecorchard, C. Schreiner, H. Lang *J. Organomet. Chem*. **2008**, *693*, 3821; c) O. V. Gusev, T. A. Peganova, A. M. Kalsin, N. V. Vologdin, P. V. Petrovskii, K. A. Layssenko, A. V. Tsvetkov, I. P. Beletskaya *Organometallics* **2006**, *25*, 2750; d) A. L. Boyes, I. R. Butler, S. C. Quayle *Tetrahedron Lett.* **1998**, *39*, 7763; e) S. Teo, Z. Weng, T. S. A. Hor *Organometallics* **2006**, *25*, 1199; f) D. Schaarschmidt, H. Lang *Eur. J. Inorg. Chem.* **2010**, *30*, 4811; g) D. Schaarschmidt, H. Lang *Cat. Commun*. **2010**, *11*, 581; h) J.-C. Hierso, M. Beauperin, P. Meunier *Eur. J. Inorg. Chem*. **2007**, 3767.

[C5] a) S.-Y. Liu, M. J Choi, G. C. Fu *Chem. Comm*. **2001**, 2408; b) T. E. Pickett, C. J. Richards *Tetrahedron Lett.* **2001**, *42*, 3767; c) I. P. Beletskaya, A. V. Cheprakov *Chem. Rev*. **2000**, *100*, 3009.

[C6] a) S. Jeulin, S. Duprat de Paule, V. Ratovelomanana-Vidal, J.-P. Genet, N. Champion, P. Dellis *Angew. Chem. Int. Ed*. **2004**, *43*, 320; b) D. W. Allen, B. F. Taylor, *J. Chem. Soc. Dalton Trans*. **1982**, 51; c) R. P. Pinnell, C. A. Megerle, S. L. Manatt, P. A. Kroon *J. Am. Chem. Soc*. **1973**, *95*, 977; d) D. W. Allen, I. W. Nowell *J. Chem. Soc. Dalton Trans*. **1985**, 2505; e) D. J. M. Snelders, C. van der Burg, M. Lutz, A. L. Spek, G. van Koten, R. J. M. Klein Gebbink *Chem. Cat. Chem.* **2010**, *2*, 1425; f) A. Suarez, M. A. Mendez-Rojas, A. Pizzano *Organometallics* **2002**, *21*, 4611.

[C7] a) S.-S. Ng, C.-Y. Ho, T. F. Jamison *J. Am. Chem. Soc*. **2006**, *128*, 11513; b) S. I. Pereira, J. Adrio, A. M. S. Silva, J. C. Carretero *J. Org. Chem.* **2005**, *70*, 10175; c) R. M. Moslin, T. F. Jamison *Org. Lett*. **2006**, *8*, 455; d) M. Juricek, H. Brath, P. Kasak, M. Putala *J. Organomet. Chem*. **2007**, *692*, 5279; e) C. Baillie, L. Zhang, J. Xiao *J. Org. Chem.* **2004**, *69*, 7779; f) A. Ramos, A. J. Lough, D. W. Stephan *Chem. Commun*., **2009**, 1118; g) J. P. Wolkowski, J. F. Hartwig *Angew. Chem. Int. Ed*. **2002**, *41*, 4289; h) O. Oms, T. Jarrosson, L. H. Tong, A. Vaccaro, G. Bernardinelli, A. F. Williams *Chem. Eur. J*. **2009**, *15*, 5012; i) J. P. Stambuli, S. R. Stauffer, K. H. Shaughnessy, J. F. Hartwig *J. Am. Chem. Soc.* **2001**, *123*, 2677; j) C. Schreiner, *Ph. D. Thesis* **2010**, TU Chemnitz/Germany.

[C8] I. R. Butler, R. L. Davies *Synthesis* **1996**, *11*, 1350.

[C9] F. Barriere, R. U. Kirss, W. E. Geiger *Organometallics* **2005**, *24*, 48.

[C10] G. Gritzner, J. Kuta *Pure Appl. Chem*. **1984**, *56*, 461.

[C11] a) J. C. Kotz, C. L. Nivert *J. Organomet. Chem*. **1973**, *52*, 387; b) J. C. Kotz, C. L. Nivert, J. M. Lieber *J. Organomet. Chem*. **1975**, *91*, 87; c) M. A. Bennett, S. K. Bhargava, A. M. Bond, I. M. Burgar, S.-X. Guo, G. Kar, S. H. Priver, J. Wagler, A. C. Willis, A. A. J. Torriero *Dalton Trans*. **2010**, *39*, 9079; d) J. Podlaha, P. Štěpnička, J. Ludvik, I. Cisarova *Organometallics* **1996**, *15*, 543.

[C12] a) C. L. Mandell, S. S. Kleinbach, W. G. Dougherty, S. Kassel, C. Nataro *Inorg. Chem*. **2010**, *49*, 9718; b) B. D. Swartz, C. Nataro *Organometallics* **2005**, *24*, 2447; c) F. Paul, B. G. Ellis, M. I. Bruce, L. Toupet, T. Roisnel, K. Costuas, J.-F. Halet, C. Lapinte, *Organometallics* **2006**, *25*, 649; d) M. Lohan, P. Ecorchard, T. Rüffer, F. Justaud, C. Lapinte, H. Lang, *Organometallics* **2009**, *28*, 1878; e) A. Hildebrandt, D. Schaarschmidt, H. Lang, *Organometallics* **2011**, *30*, 556; f) M. Krejcik, M. Danek, F. Hartl *J. Electroanal. Chem*. **1991**, *317*, 179; g) A. Hildebrandt, T. Rüffer, E. Erasmus, J. C. Swarts, H. Lang *Organometallics* **2010**, *29*, 4900.

[C13] J. A. S. Howell, N. Fey, J. D. Lovatt, P. C. Yates, P. McArdle, D. Cunningham, E. Sadeh, H. E. Gottlieb, Z. Goldschmidt, M. B. Hursthouse, M. E. Light *Dalton Trans*. **1999**, 3015.

[C14] J. Malito, E. C. Alyea *Phosphorus, Sulfur, and Silicon* **1990**, *54*, 95.

[C15] a) A. Bondi *J. Phys. Chem*. **1964**, *68*, 441; b) N. L. Allinger, J. A. Hirsch, M. A. Miller, I. J. Tyminski, F. A. Van-Catledge *J. Am. Chem. Soc.* **1968**, *90*, 1199.

[C16] a) R. Sanders, U. T. Müller-Westerhoff *J. Organomet. Chem*. **1996**, *512*, 219; b) U. T. Müller-Westerhoff, Z. Yang, G. Ingram *J. Organomet. Chem*. **1993**, *463*, 163.

[C17] L. Bednarik, E. Neuse *J. Organomet. Chem*. **1979**, *168*, C8.

[C18] D. Guillaneux, H. B. Kagan *J. Org. Chem*. **1995**, 60, 2502.

[C19] K. Fujita, M. Yamashita, F. Puschmann, M. Martinez Alvarez-Falcon, C. D. Incarvito, J. F. Hartwig *J. Am. Chem. Soc*. **2006**, *128*, 9044.

[C20] K. A. Ahrendt, R. G. Bergman, J. A. Ellman *Org. Lett*. **2003**, *5*, 1301.

[C21] G. Mann, Q. Shelby, A. H. Roy, J. F. Hartwig *Organometallics* **2003**, *22*, 2775.

[C22] P. W. Clark, B. W. Mulraney *J. Organomet. Chem*. **1981**, *217*, 51.

[C23] P. W. Dyer, J. Fawcett, M. J. Hanton *Organometallics* **2008**, *27*, 5082.

[C24] N. G. Andersen, R. McDonald, B. A. Keay *Tetrahedron: Asymmetry* **2001**, *12*, 263.

[C25] H. Tomori, J. M. Fox, S. L. Buchwald *J. Org. Chem.* **2000**, *65*, 5334.

[C26] D. Drew, J. R. Doyle *Inorg. Synth*. **1990**, *28*, 346.

[C27] a) G. M. Sheldrick *Acta Cryst., Sect. A* **1990**, *46*, 467; (b) G. M. Sheldrick, SHELXL-97, *Program for Crystal Structure Refinement*, University of Göttingen, **1997**.

D Fundamental Study of (Ferrocenylethynyl)phosphines: Correlation of Steric and Electronic Effects in *C,C* Cross-Coupling Reactions

Bianca Milde, Dieter Schaarschmidt, Petra Ecorchard, and Heinrich Lang

Published in *J. Organomet. Chem*. **2012**, *706-707*, 52 – 65.

1 Introduction

Recently, alkynyl phosphines of general type $P(C{\equiv}CR')_nR_{3-n}$ (n = 1, 2, 3; R, R' = organic or organometallic single-bonded group; R = R'; R ≠ R') have come into focus because they are of interest due to their versatile reaction chemistry toward different organometallic and metal-organic compounds leading into the area of, for example, clusters, [D1]coordination polymers, [D2] polynuclear complexes, [D2c,D3] or metallacycles. [D4] The properties of alkynyl phosphines are unique including their structure, chemical behavior, reactivity, and catalytic activity. The reaction chemistry of these molecules is driven either by the fact that they act as *P* and/or C≡C donors toward metal species or by the cleavage of the $P\text{-}C_{alkynyl}$ bond induced by thermolysis, photolysis or chemical activation resulting in the formation of phosphido and acetylide fragments, respectively. [D2a,D4b,D5] In addition, (ferrocenylethynyl)phosphines have gained attraction in supra- and macro-molecular chemistry allowing the development of new materials with peculiar physical and chemical properties. [D5b,D6] Just as the alkynyl phosphines, (ferrocenylethynyl)phosphines found use as ligands in homogeneous *C,C* cross-coupling reactions (Mizoroki-Heck and Suzuki-Miyaura), [D2c,D7] and as redox-active compounds to study multinuclear redox processes[D5c,D6,D8]. Palladium-promoted Suzuki-Miyaura and Mizoroki-Heck carbon-carbon cross-couplings represent one of the most effective transformations in organometallic and organic synthesis. The Mizoroki-Heck reaction allows to convert (un)saturated halides or triflates into substituted alkenes in a very efficient, convenient and inexpensive way in the presence of a base and a palladium source. [D9] In this respect, most active catalysts are bulky, electron-rich phosphine-, [D10] NHC-, [D11] and biphenyl phosphine-based palladium complexes, [D12] as well as phosphapalladacycles.

[D12b,D13] The Suzuki-Miyaura reaction is the conversion of aryl- or vinyl-boronic acids with an aryl- or vinyl-halide to polyolefins, styrenes, and substituted biphenyls, and has been extended to incorporate alkyl bromides in the presence of palladium. [D9]

In this work we present the synthesis of a series of (ferrocenylethynyl)phosphines and their reaction behavior toward selenium and palladium dichloride. The utilization of the appropriate phosphine palladium dichlorides in Mizoroki-Heck and Suzuki-Miyaura *C,C* couplings is reported as well.

2 Results and Discussion

2.1 Synthesis, Reaction Chemistry and Characterization

(Ferrocenylethynyl)phosphines $P(C{\equiv}CFc)R_2$ (Fc = $Fe(\eta^5\text{-}C_5H_4)(\eta^5\text{-}C_5H_5)$; **3a**, R = Ph; [D6b] **3b**, R = *o*-Tol; **3c**, R = Mes; **3d**, R = Fur; **3e**, R = *t*-Bu; **3f**, R = Cy) were synthesized by reacting FcC≡CH (**1**) with one equivalent of *n*-butyllithium and subsequent treatment with $ClPR_2$ (**2a** – **f**) (Reaction D1).

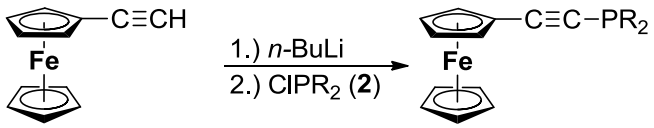

(D1)

1 **3**

3a, R = Ph[6b] **3d**, R = Fur
3b, R = *o*-Tol **3e**, R = *t*-Bu
3c, R = Mes **3f**, R = Cy

To obtain 1st information on the Lewis-basicity of phosphines **3a** – **f** we prepared the respective seleno phosphines $(Se)P(C{\equiv}CFc)R_2$ (**4a** – **f**) by treatment of **3a** – **f** with elemental selenium in toluene at 100 °C (Experimental Section). Seleno phosphines **4a** – **f** could be isolated in virtually quantitative yield as yellow to orange solids.

Addition of $[PdCl_2(cod)]$ (**5**) (cod = cyclo-1,5-octadiene) to dichloromethane solutions containing **3a** – **f** in a molar ratio of 1:2 gave complexes $[Pd(Cl)(\mu\text{-}Cl)(P(C{\equiv}CFc)R_2)]_2$ (**6e**, R = *t*-Bu; **6f**, R = Cy) and *cis/trans*-$[PdCl_2(P(C{\equiv}CFc)R_2)_2]$ (**7a**, R = Ph; **7b**, R = *o*-Tol; **7c**, R = Mes; **7d**, R = Fur), respectively (Scheme 1). While the formation of **7a** – **d** is expected, the building of **6e** and **6f** surprises at first. The latter complexes are also generated, when repeating the reactions in a 1:1 molar ratio. From these reactions it is obvious that the alkyl groups R at phosphorus favor the formation of a palladium dimer with a planar $Pd_2(\mu\text{-}Cl)_2$

four-membered cycle, while aryl substituents solely gave mononuclear **7a** – **d** as it could be proven by single X-ray structure determination (see below). For bulky substituents at phosphorus this reaction behavior is a known phenomenon. [D14] It can be explained by the different solubility of the palladium sources and the formed complexes in dichloromethane [D14a] as well as the size of their coordinated ligands (*e. g.* NCMe, cod). [D14f] Another straightforward synthesis methodology to prepare **7a** – **f** is given by treatment of **3a** – **f** with the palladium source $[PdCl_2(SEt_2)_2]$ (**8**) (Scheme D1). However, by this reaction exclusively **7a** – **f** are formed.

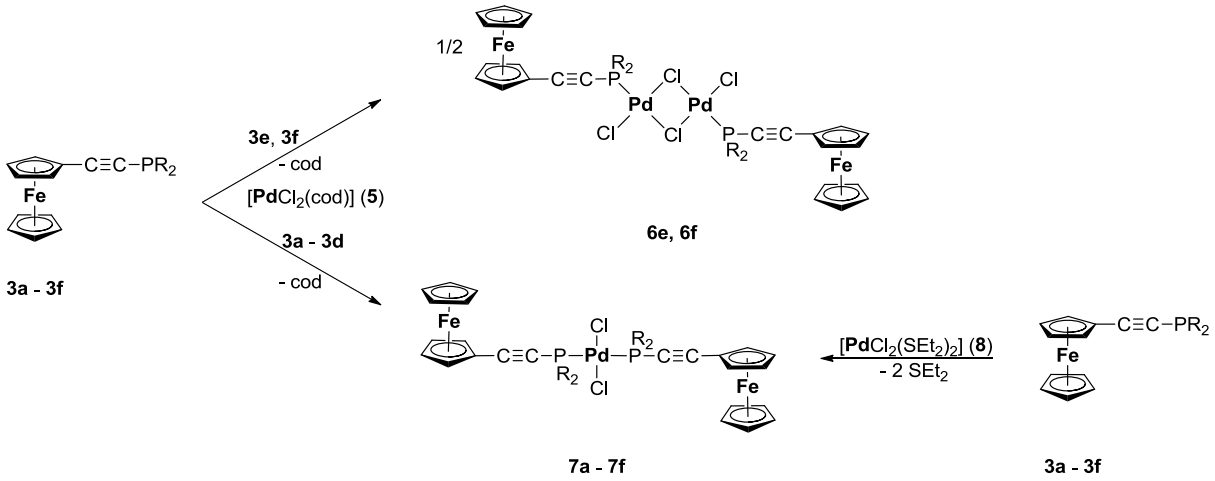

Scheme D1. Synthesis of **6e**, **6f** and **7a** – **7f** from **3**, **5**, and **8**.

Seleno phosphines **4a** – **f** as well as complexes **6e**, **f** and **7a** – **f** are stable in air and moisture both in the solid state and in solution, whereas **3a** – **f** slowly oxidize in solution. All compounds have been identified by elemental analysis as well as by IR and NMR (^{1}H, ^{13}C{^{1}H}, ^{31}P{^{1}H}) spectroscopy. High resolution ESI-TOF mass-spectrometry and single crystal X-ray structure analysis (**6e**, **6f**, **7b** and **7c**) were additionally carried out. The electrochemical behavior of the newly prepared compounds (cyclic voltammetry (CV) (**3**, **4**, **6** and **7**), square wave voltammetry (SWV) (**6**, **7**), linear sweep voltammetry (LSV) (**7**), UV-Vis/NIR spectroscopy (280 – 3000 nm) and *in situ* IR spectroscopy (**7f**)) is discussed as well.

Single crystals of **6e**, **6f**, *cis*-**7b**, and *trans*-**7c** suitable for X-ray diffraction studies could be obtained by diffusion of *n*-hexane or diethyl ether into chloroform solutions containing the appropriate complexes at ambient temperature. The molecular structures of **6e** and **6f** in the solid state are shown in Figure D1, the ones of *cis*-**7b** and *trans*-**7c** in Figure D2. Important bond distances (Å), bond angles (°) and torsion angles (°) are summarized in Table D1. For crystal and structure refinement data see Experimental Section.

Complexes **6e** and **6f** crystallize in the triclinic space group $P\bar{1}$ as red needles. Both species are *iso*-structural possessing $Pd_2P_2Cl_2(\mu\text{-}Cl)_2$ moieties featuring a crystallographically imposed inversion symmetry with the inversion center in the middle between the palladium atoms Pd1 and Pd1A (symmetry transformations used to generate equivalent atoms: -x+1, -y+1, -z+1) (Figure D1). The (ferrocenylethynyl) groups are oppositely oriented with the ferrocenyl units above or below the slightly distorted square-planar $Pd_2P_2Cl_2(\mu\text{-}Cl)_2$ core (**6e**: r. m. s. deviation 0.0120 Å, highest deviation from planarity observed for Pd1 with -0.0240 Å; **6f**: r. m. s. deviation 0.0049 Å, highest deviation from planarity observed for Pd1 with -0.0098 Å) with characteristic parameters for this type of compounds. [D14] The Pd1-Cl2 and Pd1-Cl2A bond distances in **6e** and **6f** are asymmetric with the somewhat longer bonds situated opposite the more strongly *trans* influencing (ferrocenylethynyl)phosphine substituents (Table D1). Obviously, the palladium-chloride distances within the $Pd_2(\mu\text{-}Cl)_2$ cycle (Pd1-Cl2: **6e**, 2.3176(6) Å; **6f**, 2.4479(6) Å) are longer as the terminal Pd1-Cl1 bonds (Pd1-Cl1: **6e**, 2.2755(6) Å; **6f**, 2.2729(6) Å) allegeable due to their different environment (Figure D1, Table D1). The bond lengths and angles of the P-C units are comparable to those observed in similar species, *i. e.* $[PdCl(\mu\text{-}Cl)(PPh_2(n\text{-}Pr))]_2$ [D14d] and $[PdCl(\mu\text{-}Cl)(PFur_3)]_2$, [D14b] respectively. The (ethynyl)phosphine units are essentially linear (Table D1) which is in contrast to other (ferrocenylethynyl) palladium complexes, *e. g.* $[PdCl_2(P(C{\equiv}CFc)Ph_2)_2]$ in which a significant deviation from linearity was found (P-C≡C: 171, 157°) [D6b]. The cyclopentadienyl ligands at the iron centers show an almost staggered conformation (**6e**: 4.6°, **6f**: -2.7°).

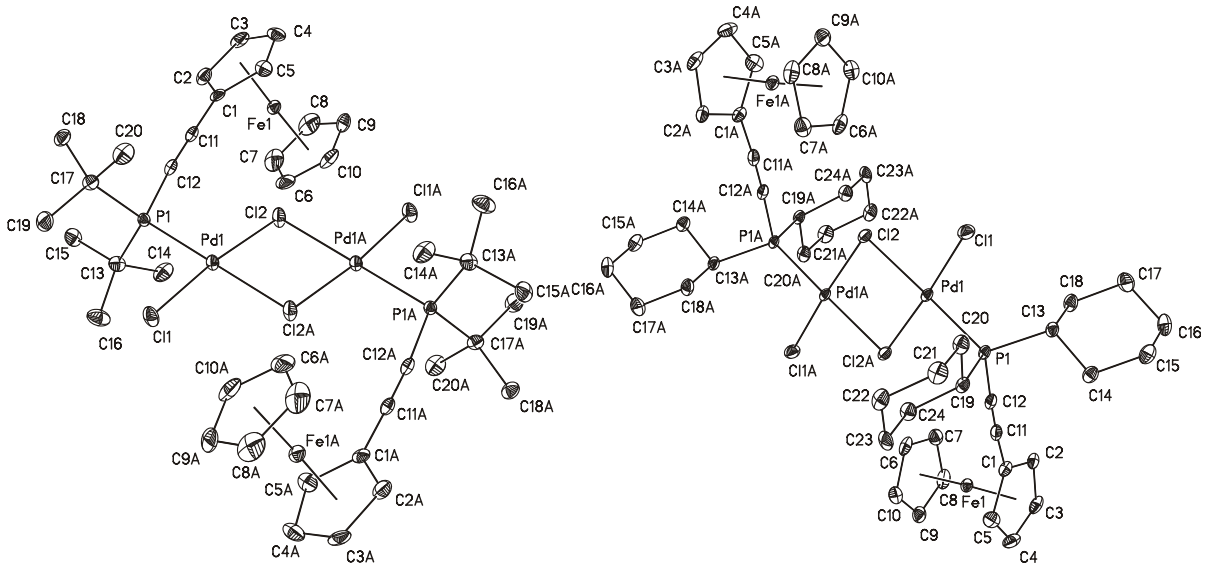

Figure D1. ORTEP diagrams (50 % probability level) of the molecular structures of **6e** (left) and **6f** (right) with the atom-numbering scheme. All hydrogen atoms and two $CHCl_3$ solvent molecules (**6f**) have been omitted for clarity. For selected bond distances (Å), angles (°) and

torsion angles (°) see Table 1. (Symmetry generated atoms are indicated by the suffix A; symmetry code: -x+1, -y+1, -z+1.)

In crystals of **7b** the molecules are packed in the monoclinic space group *C*2/*c*, in **7c** the crystals are packed in the triclinic space group $P\bar{1}$. Complex **7b** exhibits a mirror plane through the palladium center Pd1, while **7c** possesses an inversion center at the central palladium atom Pd1 (Figure D2). The crystal structure analysis showed that **7b** is *cis*-configurated, whereas **7c** owns a *trans* arrangement in the solid state (Figure D2). *cis*-Configuration is generally observed for (alkynyl)phosphine palladium chloride complexes, although corresponding palladium iodide species are *trans* oriented. [D6b] However, in solution only one isomer exists, most likely showing the thermodynamically more stable *trans*-configuration as indicated by IR and NMR studies (*vide infra*). For both species, the complex geometries around palladium are square-planar as expected for a d^8 transition metal ion (**7b**: r. m. s. deviation 0.0728 Å, highest deviation from planarity observed for P1 with -0.0914 Å). Typical for **7b** is that the P-C≡C-C_{Fc} ligands are not coplanar to the PdP_2Cl_2 core, similar to [M(P(C≡CFc)Ph_2)$_2$$Cl_2$] (M = Pd, Pt), with a P-C≡C angle of 175.1(4)° (Table D1). [D5c,D6b,D8] In **7c** a coplanar *s-trans*-like structure for the (ferrocenylethynyl)phosphines is found (Figure D2). The *trans* orientation in **7c**, compared to *cis*-**7b**, is most probably attributed to the larger substituents at phosphorus, which also has an influence on the linearity of the (alkynyl)phosphine units. The P-C≡C and C≡C-C_{Fc} angles in **7c** deviate more from linearity then the ones in **7b** (Table D1). All other structural parameters are similar to other (ferrocenyl) [D6b] and (phenylethynyl) [D2c] phosphine palladium complexes.

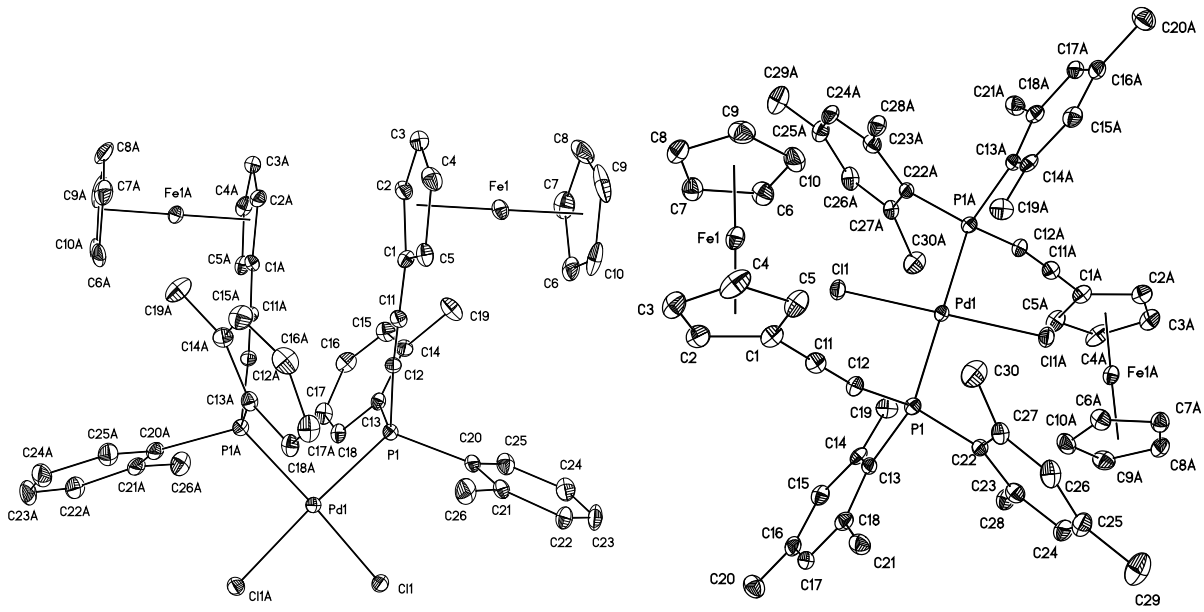

Figure D2. ORTEP diagrams (30 % (**7b**), 50 % (**7c**) probability level) of the molecular structures of *cis*-**7b** (left) and *trans*-**7c** (right) with the atom-numbering scheme. All hydrogen atoms and two molecules of the solvent $CHCl_3$ (**7b**) have been omitted for clarity. For selected bond distances (Å), angles (°) and torsion angles (°) see Table D1. (Symmetry generated atoms are indicated by the suffix A; symmetry code: **7b**: -x, y, -z+1/2; **7c**: -x, -y, -z+2.)

Table D1. Selected Bond Lengths (Å), Bond Angles and Torsion Angles (°) for Complexes **6e**, **6f**, **7b**, and **7c**.[a)]

	6e	**6f**	**7b**	**7c**
Pd1-P1	2.2504(6)	2.2297(6)	2.2644(13)	2.3227(7)
Pd1-Cl1	2.2755(6)	2.2729(6)	2.3422(13)	2.3075(7)
Pd1-Cl2	2.3176(6)	2.4479(6)		
Pd1-Cl2A [c)]	2.4081(5)	2.3341(6)		
P1-C12	1.748(2)	1.747(3)	1.732(5)	1.760(3)
P1-C13	1.874(2)	1.834(2)	1.814(5)	1.843(3)
P1-C17	1.882(2)			
P1-C19		1.839(2)		
P1-C20			1.829(5)	
P1-C22				1.833(3)
C1-C11	1.421(3)	1.426(4)	1.416(7)	1.434(4)
C11-C12	1.199(3)	1.203(4)	1.205(6)	1.201(4)
D1-Fe1[b)]	1.6377(3)	1.6429(5)	1.6465(7)	1.6482(3)
D2-Fe2[b)]	1.6468(3)	1.6503(5)	1.6513(7)	1.6548(3)
P1-Pd1-Cl1	91.89(2)	88.71(2)	88.09(4)	88.49(3)
P1-Pd1-Cl2	94.20(2)	178.81(2)		
P1-Pd1-Cl2A [c)]	178.857(19)	94.37(2)		
P1-Pd1-P1A [c)]			93.57(7)	180.0
P1-Pd1-Cl1A [c)]			175.24(5)	91.51(2)
Pd1-Cl2-Pd1A [c)]	94.992(19)	95.33(2)		
Cl1-Pd1-Cl2	173.64(2)	92.23(2)		
Cl1-Pd1-Cl1A [c)]			90.61(6)	180.0
P1-C12-C11	175.46(19)	177.1(2)	175.1(4)	171.1(3)
C1-C11-C12	176.9(2)	176.2(3)	176.5(5)	173.6(3)
D1-Fe1-D2[b)]	178.43(2)	176.86(4)	179.46(5)	178.94(3)
P1-C12-C11-C1	-66(5)	86(6)	129(7)	-106(3)
Pd1-P1-C12-C11	18(2)	75(5)	90(5)	-8.4(18)
Pd1-P1-C13-C14	-62.81(15)	-177.15(14)	161.0(3)	4.4(3)
Pd1-P1-C17-C18	156.65(13)			
Pd1-P1-C19-C20		-66.84(18)3		

Pd1-P1-C20-C21			-58.9(5)	
Pd1-P1-C22-C27				85.7(2)
Cl1-Pd1-P1-C12	170.44(7)	-155.11(9)	-148.92(18)	-48.97(10)
Cl1-P1-Pd1-C13	-77.47(8)	-36.74(9)	90.94(17)	64.74(11)
Cl1-P1-Pd1-C17	56.83(8)			
Cl1-P1-Pd1-C19		87.92(9)		
Cl1-Pd1-P1-C20			-32.4(2)	
Cl1-Pd1-P1-C22				-165.81(11)

a) Standard uncertainties of the last significant digit(s) are shown in parenthesis. b) D1 denotes the centroid of C_5H_4 at Fe1; D2 denotes the centroid of C_5H_5 at Fe1. c) Symmetry generated atoms (for symmetry code see Figures D1 and D2).

The completeness of the reaction of **1** with *n*-BuLi/**2** to give **3** (Reaction D1) can be confirmed by IR spectroscopy, since the C≡C and ≡C-H vibrations of the HC≡C unit in **1** [D30] at 2102 and 3279 cm^{-1}, respectively, disappear during the course of the reaction and new absorptions between 2140 and 2155 cm^{-1} appear which can be assigned to the $\tilde{\upsilon}_{C\equiv C}$ frequencies of the (ferrocenylethynyl)phosphines **3a** – **f** (Experimental Section). Oxidation of **3a** – **f** with selenium in its elemental form to afford the seleno phosphines **4a** – **f** as well as the coordination of the phosphorus atoms of **3a** – **3f** to palladium(II) to produce the corresponding phosphine palladium complexes **6** and **7** resulted in a shift of the $\tilde{\upsilon}_{C\equiv C}$ bands to higher wavenumbers, which is typical for these reactions (Experimental Section). [D6b] Next to IR also $^{13}C\{^1H\}$ and $^{31}P\{^1H\}$ NMR spectroscopy allows to monitor the reaction progress owing to the C≡C units and the phosphorus atoms present in **1**, **3**, **4**, **6**, and **7** (Experimental Section). In this respect, most indicative is $^{31}P\{^1H\}$ NMR spectroscopy. It was found that upon coordination of the phosphorus atom to palladium a shift to lower field is observed, *i. e.* **3b**: -47.7 ppm, **7b**: -6.8 ppm (Experimental Section). Changing the phosphorus oxidation state of III in **3** to V in **4** also induces, as expected, a significant down-field shift (*i. e.* **3b**: -47.7 ppm; **4b**: 0.9 ppm). In general, the donor capacity of phosphines PRR'R'' (R = R' = R''; R ≠ R' ≠ R''; R, R', R'' = alkyl, aryl, alkoxyl) toward selenium acceptors can be quantified by the coupling constant $^1J(^{31}P–^{77}Se)$. [D7,D15] It was found that electron-withdrawing groups at phosphorus increase $^1J(^{31}P–^{77}Se)$, due to the increased *s* character of the phosphorus orbital involved in the P–Se bonding. Furthermore, the steric demand around phosphorus causes marked changes in the behavior of the respective transition metal complexes. These features are essential parameters for the specific design of transition metal complexes. The $^1J(^{31}P-^{77}Se)$ values for seleno phosphines **4a** – **f** are summarized in Table D2. Since electronic and steric effects are intimately related, [D16] Table D2 also contains the Tolman cone angles of **6e**, **6f**,

and **7a** – **c**. The Tolman cone angle *Θ* is the apex angle of a cylindrical cone centered 2.28 Å from the center of the phosphorus atom which touches the van-der-Waals radii of the outermost atoms. [D16] Increasing the M-P-R angle between P and R decreases the percentage of the *s* character in the phosphorus lone-pair. Within our studies we replaced one substituent R of PR_3 by a (ferrocenylethynyl) ligand to obtain $R_2(FcC{\equiv}C)P$ (**3a** – **f**). Out of this reason, we calculated the Tolman cone angle from the structural data obtained from the single X-ray determination of **6e**, **6f**, **7a**, [D6b] **7b** and **7c** using the program STERIC [D17] (Table D2).

Table D2. Chemical shifts (ppm) of **4a** – **f**, **6e**, **6f**, **7a** – **c**, $^1J(^{31}P\text{-}^{77}Se)$ coupling constants (Hz) of **4a** – **f** and calculated Tolman cone angles *Θ* (°) of **6e**, **6f** and **7a** – **c**; $Ph_3P(=Se)$ and $[(Ph_3P)_2PdCl_2]$ for comparison.

Compd.	*δ* [ppm]	$^1J(^{31}P\text{-}^{77}Se)$ [Hz]	Compd.	*δ* [ppm]	*Θ* [°] a)
4a	4.3	746	**6e**	49.7	183
4b	0.9	729	**6f**	31.0	177
4c	-17.5	710			
4d	-37.9	784	**7a** [6b]	5.0	168
4e	56.3	715	**7b**	-6.8	168
4f	31.0	713	**7c**	-24.0	213
Ph_3P=Se	35.9 [D7]	732 [D7]	**$[(PPh_3)_2PdCl_2]$**	24.5	145 [D16a]

a) *Θ* = Tolman cone angle calculated by STERIC [D17].

From Table D2 it can be seen that substitution of R by a ferrocenylethynyl unit causes a shielding of the phosphorus atom with an increase of $^1J(^{31}P\text{-}^{77}Se)$ confirming that the (ferrocenylethynyl) building block is electron-withdrawing. Furthermore, the replacement of R by FcC≡C directly influences the Tolman cone angle *Θ* (for example, PPh_3 (145 °) [D16a] / **3a** (168 °)) showing that the introduction of a FcC≡C unit increases *Θ*. However, for larger substituents, *i. e*. mesityl, the increase in the Tolman cone angle is less significant ($PMes_3$ (212 °) [D16a] / **3c** (213 °)). The electronic and steric parameters can be used for the specific design of catalytic active palladium transition metal complexes, for example, for *C,C* coupling reactions (*vide supra*) which should have direct influence on the catalytic activity of the appropriate catalyst.

The redox properties of (ferrocenylethynyl)phosphines **3**, **4**, and their corresponding palladium complexes **6** and **7** were studied by cyclic voltammetry (CV), square wave voltammetry (SWV, complexes **6** and **7**), linear sweep voltammetry (LSV, **7**), and spectro-

electrochemistry (*in situ* UV-Vis/NIR and IR spectroscopy, **7f**) in dry dichloromethane utilizing 0.1 mol·L^{-1} solutions containing [(*n*-Bu)$_4$N][B(C$_6$F$_5$)$_4$] as supporting electrolyte. Tetra-*n*-butyl ammonium tetrakis(perfluorophenyl)borate was chosen because it provides close-to-optimal conditions for electrochemical experiments by minimizing nucleophilic attack by the electrolyte anion and improvement of the product solubility[D18]. The cyclovoltammetric studies were carried out at scan rates of 100 mV·s^{-1} and the results are summarized in Table D3. All potentials are referenced to the FcH/FcH$^+$ redox couple (Fc = (η^5-C$_5$H$_4$)Fe(η^5-C$_5$H$_5$)) as recommended by IUPAC. [D19]

Table D3. Cyclovoltammetric data (potentials *vs.* FcH/FcH$^+$), scan rate 100 mV·s^{-1} at a glassy-carbon electrode of 1.0 mmol·L^{-1} solutions of **3**, **4**, **6**, and **7** in dry dichloromethane containing 0.1 mol·L^{-1} of [(*n*-Bu)$_4$N][B(C$_6$F$_5$)$_4$] as supporting electrolyte at 25 °C.

Compd.	E^0 (ΔE_p) / V (V)	$E_{ox\text{-}irrev}$ / V	$E_{red\text{-}irrev}$ / V	Compd.	E_1^0 (ΔE_p) / V (V)	E_2^0 (ΔE_p) / V (V)	E_{irrev} / V	ΔE^0 / V
3a	0.161 (0.068)			**6e**	0.204 (0.144) a)		E_{red} = -0.976	
3b	0.149 (0.094)			**6f**	0.204 (0.120) a)		E_{red} = -0.916	
3c		0.153 0.271 0.483 0.807	0.085 0.287 0.407					
3d	0.165 (0.072)	1.161	0.497	**7a**	0.630 (0.080) b)			
3e		0.152 0.528 1.182	0.078 0.262 0.450	**7b**	0.280 (0.100)	0.374 (0.100)		0.094
3f		0.144 0.380 0.496	0.314 0.444	**7c**	0.162 (0.184) a)			
				7d	0.301 (0.142) a)			
4b		0.293 0.629 0.745	-0.799 -0.413 0.249 0.495	**7e**	0.152 (0.140) a)			

4c		0.234	-0.616	**7f**	0.273	0.438	0.165
		0.578	0.270		(78)	(0.080)	
		0.808	0.476				
4d	0.292	0.529	-0.627				
	(0.082)		0.491				
4e		0.289	-0.355				
		0.753	0.161				
			0.603				
4f		0.286	-0.400				
		0.716	0.192				
			0.592				

a) Two *non*-resolved Fe(II)/Fe(III) processes. b) Redox potential E^0 and ΔE_p from reference [D6b]. E^0 = redox potential, E_1^0 = potential of 1st redox process, E_2^0 = potential of 2nd redox process, $E_{ox\text{-}irrev}$ = irreversible oxidation potential, $E_{red\text{-}irrev}$ = irreversible reduction potential, ΔE_p = difference between oxidation and reduction potential, ΔE^0 = potential difference between two redox processes.

The electrochemically most studied member of the series of (ferrocenylethynyl)phosphines **3a** – **f** is **3a**, [D6b] which undergoes a reversible one electron oxidation at E^0 = 0.161 V (Table D3). As already described in literature for various phosphines, including 1,1'-bis(diphenylphosphine)ferrocene, the resulting ferrocenium ion participates in intra-molecular electron transfer from the PPh_2 group to iron. The formed phosphorus(IV) radical then reacts in different follow-up reactions, *e. g.* dimerization or reaction with traces of oxygen. [D20, D21a] Nevertheless, in consecutive cycles depending on the groups R reversible as well as irreversible oxidations occur as it is typical of ferrocenyl phosphines (Figure D3)[D20, D21a]. Obviously, the phosphines featuring electron-rich organic groups, for example, **3c**, **3e** and **3f** show without exception irreversible behavior and more follow-up processes (Figure D3).

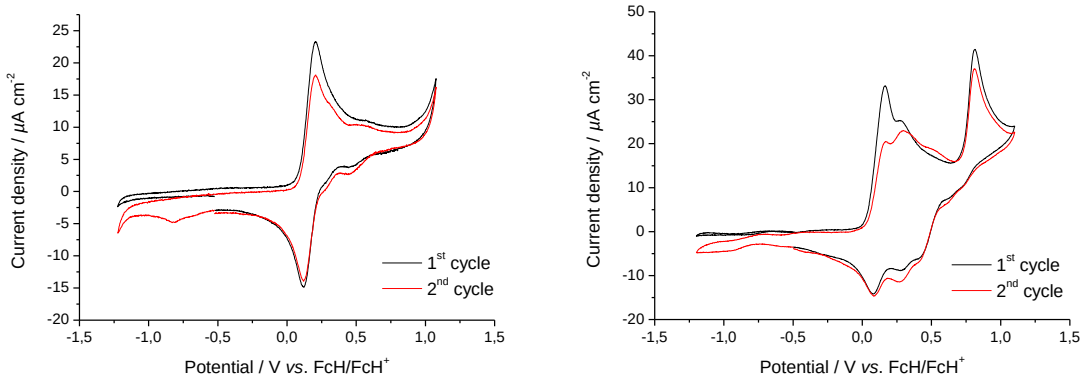

Figure D3. Electrochemical data of dichloromethane solutions containing 1.0 mmol·L^{-1} of **3a** (left) and **3c** (right) at 25 °C, supporting electrolyte $[(n\text{-}Bu)_4N][B(C_6F_5)_4]$ with a scan rate of 100 mV·s^{-1}.

From Table D3 it further can be seen that more electron-rich species can more easily be oxidized. The potential E^0 and $E_{ox\text{-}irrev}$, respectively, decreases, for example, in the series: furyl > phenyl > *o*-tolyl ≈ mesityl. The appropriate alkyl-functionalized ferrocenylethynyl phosphines show the trend *E*(*t*-butyl) > *E*(cyclohexyl) (Table D3). Compared with the corresponding ferrocenyl phosphines $PFcR_2$, [D15g] the ferrocenylethynyl-functionalized derivatives are more difficult to oxidize which complies with the electron-withdrawing character of the ethynyl spacer unit. As recently described for ferrocenyl phosphines, [D15g] we did synthesize the seleno phosphines **4a** – **f** (*vide supra*) which show a similar behavior with irreversible oxidation events and follow-up reactions as ferrocenyl-substituted seleno phosphines (Table D3). [D15g,D18,D21a] Compared to **3a** – **f** with phosphorus III, the seleno phosphines **4a** – **f** with phosphorus in the oxidation state +V are, as expected, more difficult to oxidize (Table D3).

Coordination of the phosphorus lone-pair in **3a** – **f** to palladium (complexes **6** and **7**) inhibits intra-molecular oxidation of the phosphorus (Figure D4).

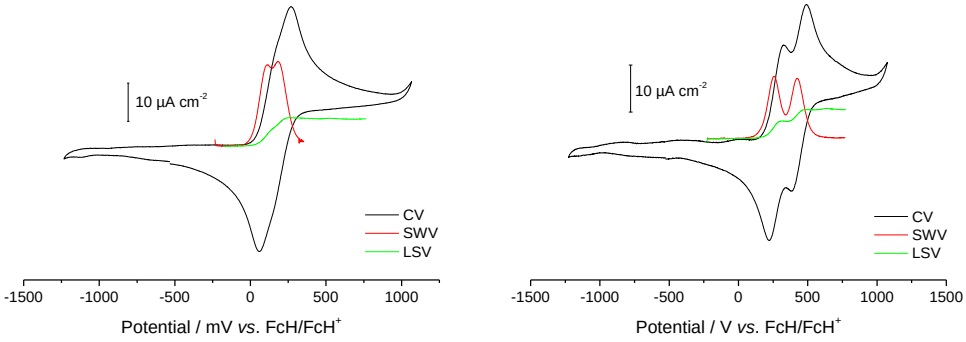

Figure D4. Electrochemical data of dichloromethane solutions containing 1.0 mmol·L^{-1} of **7c** (left) and **7f** (right) at 25 °C, supporting electrolyte [(*n*-Bu)$_4$N][B(C$_6$F$_5$)$_4$] with a scan rate of 100 mV·s^{-1} (CV = Cyclic Voltammetry, SWV = Square Wave Voltammetry, LSV = Linear Sweep Voltammetry).

Typical for both dimeric palladium complexes **6e** and **6f** is that in the cyclic voltammograms beside two *non*-resolved redox events at 0.204 V (ΔE_p = 0.144 V (**6e**) and ΔE_p = 0.120 V (**6f**), respectively) for the oxidation of the ferrocenyl groups an irreversible reduction peak at -0.9 V associated with the reduction of Pd(II) to Pd(0) [D21b,c] is observed (Supporting Information, Figure D9; Table D3). However, mononuclear palladium complexes **7b** – **f** show two reversible redox events between 0.2 – 0.5 V, *i. e.* **7f**: E_1^0 = 0.27 V (ΔE_p = 0.078 V), E_2^0 = 0.44 V (ΔE_p = 0.080 V) (Table D3, Figure D4). The same behavior is found

for all other species, even though they are partially not separable. Conspicuous is the observation that aliphatic **7f** shows a larger peak separation of the 1st and 2nd oxidation than the aromatic systems **7a** – **d** (Figure D4). Square wave (SWV) and linear sweep (LSV) voltammetric studies indicated, as exemplary shown for **7f** (Figure D4, right), two reversible one-electron processes with a peak separation of 0.165 V. This divergent behavior shows that the two ferrocenyl moieties in **7f** can separately be oxidized rather than **7a** – **e**. As already described for **3a** – **f** and **4a** – **f**, respectively, complexes **7** show the same trend, in that the ferrocenyl groups of the more electron-rich aromatic phosphines are, as expected, easier to oxidize. Compared to the *non*-coordinated (ferrocenylethynyl)phosphines, the respective palladium complexes are also more difficult to oxidize which can be explained by electron donation of the phosphines to palladium upon coordination (Table D3). In addition, for **6** and **7** no further redox events indicating follow-up reactions have been observed.

To probe, if the redox splitting in **7f** is due to electronic communication we investigated the electronic absorptions in the visible and near infrared region of the electrochemically generated oxidized species (**7f**$^{+}$, **7f**$^{2+}$) (Figure D5). In general, the absence of any NIR charge transfer bands points to electron-localized mixed-valent species, whereas the presence of such absorptions would argue in favor of electron delocalization. The spectro-electrochemical studies were conducted by stepwise increase of the potential from 0.0 to 1.2 V *vs.* Ag/AgCl in an OTTLE cell (OTTLE = Optically Transparent Thin-Layer Electrode) containing dichloromethane solutions of **7f** (1.0 mmol·L^{-1}) and [(*n*-Bu)$_4$N][B(C$_6$F$_5$)$_4$] (0.1 mol·L^{-1}) as supporting electrolyte allowing the generation of mono-cationic **[7f]**$^{+}$ and di-cationic **[7f]**$^{2+}$ species. Complex **7f** does not display, as expected, any absorption in the NIR range. Surprisingly, the spectrum of the mono-oxidized species **7f[B(C$_6$F$_5$)$_4$]** shows an absorption with relatively high intensity (Figure D5), which is in contrast to other ferrocenyl phosphine palladium complexes, *i. e.* [PdCl$_2$(P(*o*-Tol)$_2$Fc)$_2$]. [D15g] Nevertheless, it must be noted that during the UV-Vis/NIR measurements decomposition of the oxidized species occurred, which resulted in incomplete disappearance of the IVCT band. However, when increasing the speed of the measurement and reducing the amount of data, the IVCT band completely disappeared (Figure 10, Supplementary Information). To investigate this behavior we tried to synthesize the mono-cationic species by treatment of **7f** with one equivalent of [Ag][B(C$_6$F$_5$)$_4$] in tetrahydrofuran at -60 °C. After filtration and precipitation with *n*-hexane a dark purple solid could be obtained. Nevertheless, characterization of this material indicated that solely dicationic **[7f]**$^{2+}$ was formed. UV-Vis/NIR measurements showed no absorption in the NIR range (Supporting Information, Figure 11).

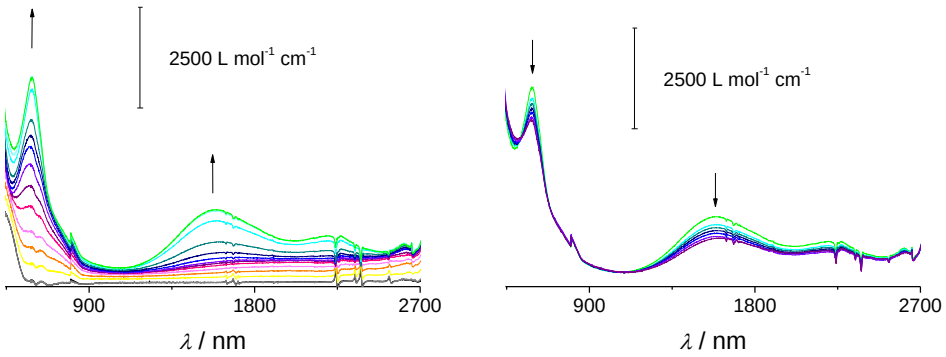

Figure D5. NIR-Spectra of **7f** at rising potentials (left: 0.0 to 0.775 V; right: 0.8 to 1.2 V *vs.* Ag/AgCl) at 25 °C, in dichloromethane, supporting electrolyte $[(n\text{-Bu})_4N][B(C_6F_5)_4]$.

Deconvolution of the NIR absorption of *in situ* generated $\mathbf{[7f]}^+$ was achieved by using three separate overlapping transitions with Gaussian shapes (Figure D6). The fits provide an almost exact overlay of the sum of the Gaussian curves with the experimental spectra. Two bands were found at 6303 and 4444 cm^{-1}, respectively. The absorption possessing the highest intensity (ε_{max} = 1410 $L \cdot mol^{-1} \cdot cm^{-1}$) at 6303 cm^{-1} showed a characteristic peak width-at-half-height for inter-valence charge transfer bands (2089 cm^{-1}). [D22] The band at 4444 cm^{-1} can be assigned to a ligand-to-metal charge transfer absorption. [D23] A 3rd Gaussian curve represents the baseline correction.

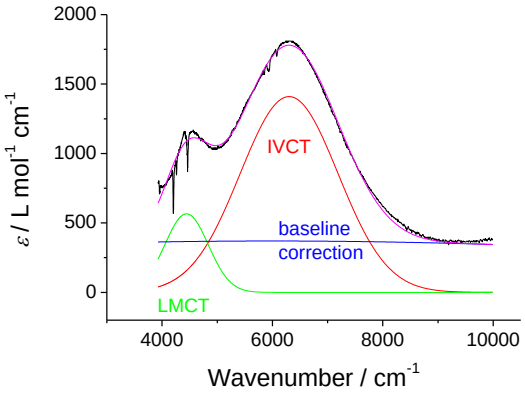

Figure D6. Deconvolution of NIR absorptions of electro generated $\mathbf{[7f]}^+$ using three Gaussian-shaped bands. Black line: experimental data; colored lines: Gaussian-shaped absorptions.

In addition, band shape analysis was performed according to the Hush model for symmetric mixed-valent species (equations (D1) and (D2))[23b,24] and the classification criteria of Brunschwig, Creutz and Sutin[D25].

$$(\Delta\nu_{\frac{1}{2}})_{\mathbf{theo}} = \sqrt{2310 \cdot \nu_{\mathbf{max}}} \quad \text{(D1)}$$

$$\Gamma = 1 - \frac{\left(\Delta\nu_{\frac{1}{2}}\right)}{(\Delta\nu_{\frac{1}{2}})_{\mathbf{theo}}} \quad \text{(D2)}$$

Theoretical band width-at-half-height could be calculated as 3816 cm^{-1} for **[7f]**$^+$ and a Γ value of 0.45 indicates that this radical cation is rather close to a Class II/III borderline system. According to this classification, complex **7f** can be assigned as moderately coupled class II system.

Additionally, spectro-electrochemical IR measurements of **7f** were performed to confirm electronic interactions. These studies were performed by stepwise increase of the potential from -1.0 to +1.2 V in an OTTLE cell containing a dichloromethane solution of **7f** (2.5 $mmol \cdot L^{-1}$) and [(*n*-Bu)$_4$N][B(C$_6$F$_5$)$_4$] (0.1 $mol \cdot L^{-1}$) as supporting electrolyte. The IR spectrum of **7f** displays one strong $\tilde{\upsilon}_{C\equiv C}$ band at 2159 cm^{-1} and one very weak band at 2180 cm^{-1} which most probably can be assigned to the *trans*-complex (Figure D7). Oxidation of **7f** to [**7f**]$^+$ results in a shift to lower wavenumbers (2154 cm^{-1}) and the disappearance of the 2nd weak band. Further oxidation to [**7f**]$^{2+}$ causes an additional shift (2151 cm^{-1}) and a broadening of the respective absorption. Besides, for [**7f**]$^+$ only one absorption is observed which seems like the average of the neutral and di-cationic species. However, these differences are small. [D26]

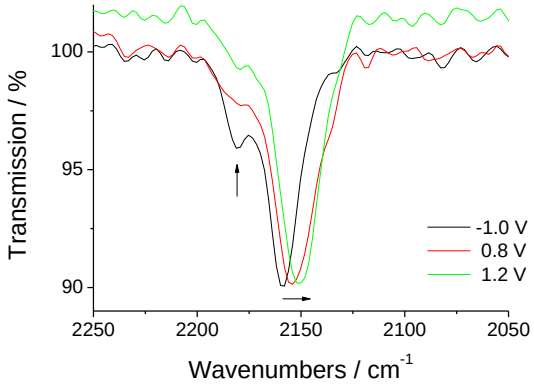

Figure D7. IR spectra of **7f** at rising potentials (-1.0 to +1.2 V *vs.* Ag/AgCl) at 25 °C in dichloromethane, supporting electrolyte [(*n*-Bu)$_4$N][B(C$_6$F$_5$)$_4$].

2.2 *C,C* Cross-Coupling Reactions

Suzuki-Miyaura and Mizoroki-Heck reactions are of great interest because they allow *C,C* coupling of alkyl and aryl halides with aryl boronic acids, or aryl and alkenyl halides with *α*-olefines under mild conditions, providing a convenient access to biaryls and diverse alkenes. [D9] These couplings are one of the most powerful C_{sp^2},C_{sp^2} bond forming reactions in organic and organometallic synthesis. Next to *N*-heterocyclic carbenes [D11] and phosphapalladacycles [D13] *etc*., phosphines remain among the best studied ligands in such reactions. [D10]

2.2.1 Suzuki-Miyaura Reaction

In recent years, manifold and efficient synthetic methodologies were developed to synthesize specifically designed phosphine ligands for the homogeneous palladium-catalyzed Suzuki-Miyaura cross-coupling reaction. [D9] Contrary, transition metal-containing phosphines are only little described of which dppf (= 1,1'-bis(diphenylphosphino)ferrocene) and derivatives thereof have been best investigated. [D10f] With this study we enrich the family of ferrocenyl phosphine palladium dichloride complexes and describe their use as catalysts in the Suzuki-Miyaura reaction. The reactants 2-bromo toluene and 4-chloro acetophenone, respectively, of the catalytic process were treated with phenyl boronic acid in presence of potassium carbonate in a 2:1 (*v*:*v*) mixture of 1,4-dioxane/water (Reaction D2). The reaction mixture was stirred at 100 °C for 1 h, samples were taken after defined periods of time (Experimental Section). Acetyl ferrocene was added as internal standard for ^{1}H NMR analysis to determine the conversions of the catalytic reactions. Palladium complexes **6** and **7** were applied in the catalytic reaction of 2-bromo toluene with phenyl boronic acid (Figure D8, left). From these studies the most promising candidates were additionally used in the coupling of 4-chloro acetophenone with phenyl boronic acid (Figure D8, right).

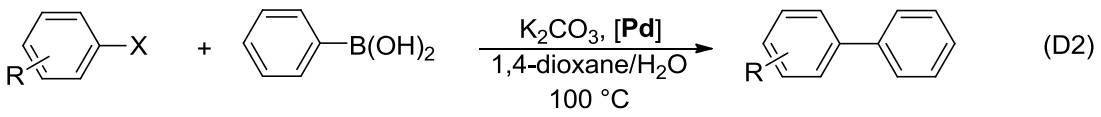

(D2)

R = 2-Me , X = Br
R = 4-C(O)Me , X = Cl

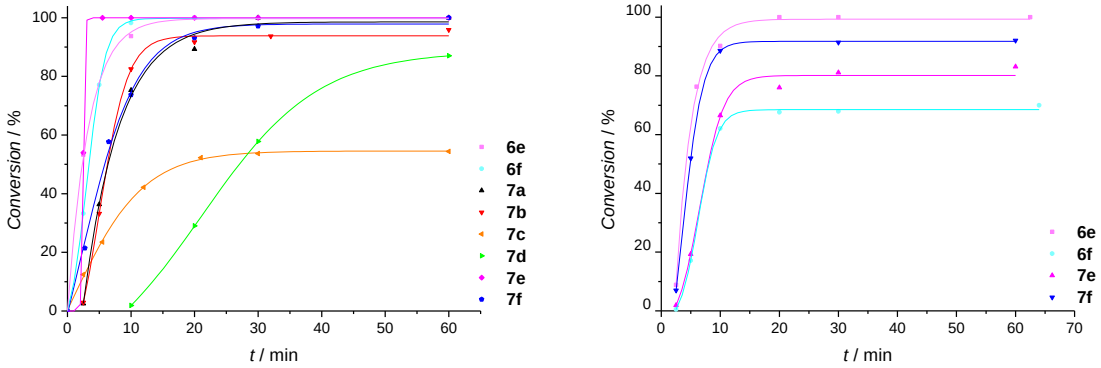

Figure D8. Reaction profiles for the coupling of 2-bromo toluene (left) and 4-chloro acetophenone (right) (2.92 or 3.0 mmol) with phenylboronic acid (3.85 mmol) using **6e**, **f** and **7a** – **f** as catalysts (catalyst loading 0.25 (2-bromo toluene) and 0.5 mol% (4-chloro acetophenone), 100 °C, 1 h, K_2CO_3 (8.76 mmol) in a mixture of 1,4-dioxane/water (ratio 2:1, *v*:*v*) (10 mL)).

In the Suzuki-Miyaura reaction electron-rich phosphine ligands are best suited, [10a,b] which correlates with our results (Figure D8). From Figure D8 it further can be seen that quantitative conversions are obtained for the reaction of 2-bromo toluene with phenyl boronic acid using **6** and **7** as catalyst, except **7c** (54 % conversion) and **7d** (87 % conversion), respectively. At first glance this is surprising but considering the Tolman cone angles (**7c**, 212 °; *vide supra*) in a certain manner it is comprehensible. Complex **7d** features with its furyl groups electron-withdrawing substituents and hence shows the lowest catalytic activity and needs an induction period of ca. 10 min. From these studies we chose complexes **6e**, **6f**, **7e** and **7f** as catalysts for the activation of 4-chloro acetophenone. These results are depicted in Figure D8 (right). The highest catalytic activity is observed for **6e** and **7f**, whereas complete conversion is only observed for **6e**. A clear trend between dimeric **6** and monomeric **7** cannot be seen. Compared to ferrocenyl phosphine palladium dichloride complexes of type $[PdCl_2(PR_2Fc)_2]$ (Fc = Fe(η^5-C_5H_4)(η^5-C_5H_5)) [D15g] and up-to-date used catalyic systems [D9-D13] they show, however, a lower activity and productivity.

2.2.2 Mizoroki-Heck Reaction

The palladium-promoted Mizoroki-Heck *C*,*C* cross-coupling between aryl or vinyl halides and triflates and alkenes in the presence of a base allows the straightforward synthesis of C_{sp2},C_{sp2} single bonds for fine chemical synthesis. [D9] One advantage of the Mizoroki-Heck

reaction is its *trans* selectivity. As catalysts, for example, phosphapalladacycles, [D13] various palladium(II)acetate/phosphine systems, [D9] palladium nanoparticles, [D27] and *N*-heterocyclic carbene palladium complexes [D11] have been applied. Within this work, complexes **6e**, **6f**, and **7a**–**f** were used in the coupling of iodo benzene with *t*-butyl acrylate (Reaction D3) in a mixture of toluene-acetonitrile (ratio 1:1, *v:v*) in presence of NEt(*i*-Pr)$_2$ at 80 °C with a catalyst loading of 0.5 mol-% (Experimental Section, Table D4).

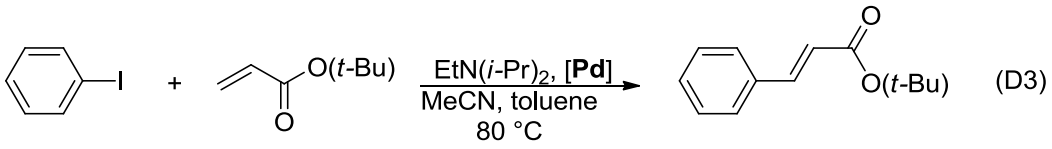

(D3)

From Table D4 it can be seen that the catalyst featuring sterically demanding tolyl (**7b**) and mesityl phosphines (**7c**), or weekly σ donating furyl ligands (**7d**) are best suited for *C,C* couplings under the above mentioned conditions. However, with these species quantitative conversion could not be reached. Complexes **6e**, **6f**, and **7a** with aliphatic (**6e**, **b**) or less bulky and electron-poor phosphines show lesser activity and productivity as compared with **7b**, **7c**, and **7d**. It is obvious that dimeric **6e** and **6f** are only active at the beginning of the reaction but significantly slowed down in activity due to their lower stability, when compared to **7a**–**f** (Supporting Information, Figure D12). Based on these results, we did not consider the reactions of bromo or chloro benzene with *t*-butyl acrylate supported by catalysts **6** and **7** since smaller conversions and longer reaction times are expected. In contrast to now-a-days used catalysts [D11f,D12d,D28] our systems are less active and productive. Compared to ferrocenylphosphine palladium catalysts the appropriate (ferrocenylethynyl) complexes possess lower activity attributed to the electron-withdrawing effect of the ethynyl linker unit.

Table D4. Mizoroki-Heck reaction of iodo benzene with *t*-butyl acrylate with a catalyst loading of 0.5 mol-% of **6** and **7**, 10 h reaction time.

Entry	Compd.	Yield / %	Entry	Compd.	Yield / %
1	**6e**	27.1	5	**7c**	41.9
2	**6f**	41.2	6	**7d**	52.9
3	**7a**	41.9	7	**7e**	3.8
4	**7b**	61.9	8	**7f**	21.4

3 Conclusions

Within this study the synthesis of a series of (ferrocenylethynyl)phosphine palladium dichloride complexes of type [Pd(Cl)(μ-Cl)(P(C≡CFc)R$_2$)]$_2$ (Fc = Fe(η^5-C$_5$H$_4$)(η^5-C$_5$H$_5$); R =

t-Bu, Cy) and $[PdCl_2(P(C{\equiv}CFc)R_2)_2]$ (R = Ph, *o*-Tol, Mes, Fur, *t*-Bu, Cy) by the reaction of $P(C{\equiv}CFc)R_2$ with $[PdCl_2(cod)]$ (cod = cyclo-1,5-octadiene) or $[PdCl_2(SEt_2)_2]$ is discussed. The structures of four complexes could be determined by single crystal X-ray diffraction analysis. $[PdCl_2(P(C{\equiv}CFc)(o\text{-}Tol)_2)_2]$ shows in the solid state a *cis*-configuration, whereas $[PdCl_2(P(C{\equiv}CFc)(Mes)_2)_2]$ prefers the *trans*-form with linear FcC≡CP moieties. In contrast, $[Pd(Cl)(\mu\text{-}Cl)(P(C{\equiv}CFc)(t\text{-}Bu)_2)]_2$ and $[Pd(Cl)(\mu\text{-}Cl)(P(C{\equiv}CFc)(Cy)_2)]_2$ form dimers with a planar $Pd_2P_2Cl_2(\mu\text{-}Cl)_2$ core with the (ferrocenylethynyl) ligands oriented above and below the square-planar unit. For classification of the σ donor ability of the (ferrocenylethynyl)-phosphines the respective seleno derivatives $(Se)P(C{\equiv}CFc)R_2$ have been synthesized upon addition of selenium in its elemental form to the (ferrocenylethynyl)phosphines. High $^1J(^{31}P\text{-}^{77}Se)$ values indicate electron-poor phosphines and hence less donor capability. [D7,D15] Cyclovoltammetric measurements showed that depending on the groups R reversible as well as irreversible oxidations occur. The oxidation at the iron center leads to an intra-molecular electron transfer process from the phosphino group to iron resulting in irreversible oxidations which lead to various follow-up processes. [D20,D21a] We also investigated the electrochemistry of the newly synthesized seleno phosphines and (ferrocenylethynyl)phosphine palladium(II) complexes in which the lone-pair of electrons at phosphorus is part of a phosphorus-selenium or phosphorus-palladium bond. Nevertheless, the seleno phosphines also show follow-up processes, presumably resulting from an intra-molecular electron transfer from the selenium-centered radical. [D15g,D18,D21] Such oxidations are, however, inhibited, when the phosphorus atom is datively-bonded to Pd as implemented in the respective transition metal complexes. As expected, the phosphino palladium species are more difficult to oxidize because of electron donation to Pd(II). Complex $[PdCl_2(P(C{\equiv}CFc)(Cy)_2)_2]$ revealed two reversible one-electron processes with a peak separation of ΔE^0 = 0.165 V in dichloromethane and in the presence of $[(n\text{-}Bu)_4N][B(C_6F_5)_4]$ as supporting electrolyte. *In situ* UV-Vis/NIR spectroscopy confirmed moderate electronic coupling between the (ferrocenylethynyl) units and the complex can be classified as class II system according to Robin and Day [D29] by band shape analysis of the IVCT absorption. Due to the long "through bond" electron transfer distance between the end-grafted ferrocenyl moieties we suppose that communication occurs rather "through space" than "through bond". Additional *in situ* IR measurements showed a small shift in the $\tilde{\upsilon}_{C\equiv C}$ band which underlines the supposition of "through space" electronic coupling.

All (ferrocenylethynyl)phosphine palladium(II) complexes were tested as catalysts in *C,C* coupling reactions. In the palladium-promoted Mizoroki-Heck reaction, iodo benzene was

treated with *t*-butyl acrylate. All complexes are active, although the most efficient catalysts were the ones featuring furyl, mesityl or *o*-tolyl substituted phosphines explainable either by the bulkiness (Tolman cone angle) or the weak σ donor ability ($^{1}J(^{31}P\text{-}^{77}Se)$) of these ligands. Furthermore, it could be shown that all Pd species are active in Suzuki-Miyaura couplings of aryl-bromide and activated aryl chloride with phenyl boronic acid. A relation between the basicity of the phosphines and the activity of the corresponding complexes exists. The lower the $^{1}J(^{31}P\text{-}^{77}Se)$ coupling constant and hence the higher the basicity of the phosphine, the higher the catalyst activity. However, the catalysts reported within this work are compared with up-to-date catalytic systems [D9-D13,D15g,D28] less active.

4 Experimental Section

4.1 General Data and Materials

All reactions were carried out under an atmosphere of nitrogen or argon using standard Schlenk techniques. Toluene and diethyl ether were purified by distillation from sodium/benzophenone, dichloromethane was purified by distillation from calcium hydride. Celite (purified and annealed, Erg. B.6, Riedel de Haen) was used for filtrations. For column chromatography alumina with a particle size of 90 µm (standard, Merck KGaA) or silica with a particle size of 40 – 60 μm (230 – 400 mesh (ASTM), Becker) was used. All starting materials were obtained from commercial suppliers and were used without further purification. Ethynylferrocene [D30] (**1**), (ethynylferrocenyl)diphenyl phosphine [D6b] (**3a**), (ethynylferrocenyl)diphenyl seleno phosphine [D7] (**4a**) and bis((ethynyl-ferrocenyl)diphenylphosphino)palladiumdichloride [D6b] (**7a**) were prepared according to published procedures. Chlorophosphines **2b** – **f** [D31], $[PdCl_2(cod)]$ [D32] (**5**) and $[PdCl_2(SEt_2)_2]$ [D33] (**8**) were synthesized as described in literature.

4.2 Instruments

NMR spectra were recorded on a Bruker Avance III 500 spectrometer (500.3 MHz for ^{1}H, 125.7 MHz for $^{13}C\{^{1}H\}$, and 202.5 MHz for $^{31}P\{^{1}H\}$ NMR spectra). Chemical shifts are reported in δ units (parts per million) downfield from tetramethylsilane with the solvent as reference signal (^{1}H NMR: standard internal $CDCl_3$, δ 7.26 or CD_2Cl_2, δ 5.30; $^{13}C\{^{1}H\}$ NMR: standard internal $CDCl_3$, δ 77.16 or CD_2Cl_2, δ 53.52; $^{31}P\{^{1}H\}$ NMR: standard external rel. 85 % H_3PO_4, δ 0.0 or $P(OMe)_3$, δ 139.0, respectively). HRMS were recorded on a Bruker

Daltonik micrOTOF-QII spectrometer (ESI-TOF). Elemental analyses were measured with a Thermo FlashAE 1112 series instrument. Melting points of analytical pure samples were determined by a Gallenkamp MFB 595 010 M melting point apparatus. FT IR spectra were recorded on a Thermo Nicolet IR 200 spectrometer using either KBr pellets or NaCl plates.

4.3 Electrochemistry

Measurements on 1.0 mmol·L^{-1} solutions of **3**, **4**, **6** and **7** in dry degassed dichloromethane containing 0.1 mol·L^{-1} of [(*n*-Bu)$_4$N][B(C_6F_5)$_4$] as supporting electrolyte were conducted under a blanket of purified argon at 25 ˚C utilizing a Radiometer Voltalab PGZ 100 electrochemical workstation interfaced with a personal computer. A three electrode cell, which utilized a Pt auxiliary electrode, a glassy carbon working electrode (surface area 0.031 cm^2) and an Ag/Ag^+ (0.01 mol·L^{-1} [$AgNO_3$]) reference electrode mounted on a luggin capillary was used. The working electrode was pre-treated by polishing on a Buehler microcloth first with 1 micron and then ¼ micron diamond paste. The reference electrode was constructed from a silver wire inserted into a solution of 0.01 mol·L^{-1} [$AgNO_3$] and 0.1 mol·L^{-1} [(*n*-Bu)$_4$N][B(C_6F_5)$_4$] in acetonitrile, in a luggin capillary with a vycor tip. This luggin capillary was inserted into a second luggin capillary with vycor tip filled with a 0.1 mol·L^{-1} [(*n*-Bu)$_4$N][B(C_6F_5)$_4$] solution in dichloromethane. Successive experiments under the same experimental conditions showed that all formal reduction and oxidation potentials were reproducible within 10 mV. Experimentally potentials were referenced against an Ag/Ag^+ reference electrode but results are presented referenced against ferrocene as an internal standard as required by IUPAC. [D19] Data were manipulated on a Microsoft Excel worksheet to set the formal reduction potentials of the FcH/FcH^+ couple to 0.0 V. Under our conditions the FcH/FcH^+ couple was at 230 mV *vs*. Ag/Ag^+.

4.4 Spectro-electrochemistry

Spectro-electrochemical UV/Vis-NIR measurements of a 1.0 mmol·L^{-1} solution of **7f** in dry degassed dichloromethane containing 0.1 mol·L^{-1} of [(*n*-Bu)$_4$N][B(C_6F_5)$_4$] as supporting electrolyte were carried in an OTTLE cell [D34] using a Varian Cary 5000 spectrometer. *In situ* spectro-electrochemical IR measurements of **7f** (2.5 mmol·L^{-1}) in dichloromethane (0.1 mol·L^{-1} [(*n*-Bu)$_4$N][B(C_6F_5)$_4$]) were also carried in an OTTLE cell [D34] using a Thermo IR 100 spectrometer.

4.5 General Procedure for the Synthesis of Phosphines 3b – f

To a solution of **1** dissolved in 50 mL of dry diethyl ether one equivalent of a 2.5 M solution of *n*-BuLi was added dropwise at -30 °C. After stirring the solution for 30 min at ambient temperature it was again cooled to -30 °C and one equivalent of the appropriate chlorophosphine **2** was added dropwise. The reaction mixture was stirred for 1 h at ambient temperature and then concentrated in vacuum. The resulting residue was purified by column chromatography (column size: 15 × 3.0 cm) and dried in vacuum.

4.5.1 Synthesis of P(C≡CFc)(*o*-Tol)$_2$ (3b)

Using the general procedure described above, 1.0 g (4.76 mmol) of **1** was reacted with 1.90 mL (4.75 mmol) of *n*-BuLi and then 1.18 g (4.75 mmol) of chlorodi-*o*-tolylphosphine (**2b**) was added in a single portion. The resulting residue was purified by column chromatography on alumina using a mixture of *n*-hexane/diethyl ether (ratio 20:1, *v*:*v*) as eluent. Phosphine **3b** was obtained as a yellow solid. Yield: 1.33 g (3.15 mmol, 66 % based on **2b**). Anal. Calcd. for $C_{26}H_{23}FeP$ (422.28 g/mol): C, 73.95; H, 5.49. Found: C, 73.71; H, 5.23. Mp.: 118 °C. IR (KBr, $\tilde{\upsilon}$/cm^{-1}): 745 (s, =C-H, *o*-disubst. benzene), 1449 (m, P-C), 2150 (m, C≡C), 2913/2937/2966 (w, C-H), 3059/3083 (w, =C-H). ^{1}H NMR (500.30 MHz, $CDCl_3$, δ): 2.52 (s, 6 H, 2-CH_3C$_6$H$_4$), 4.22 (s, 5 H, C$_5H_5$), 4.24 (pt, $^3J_{HH}$ = 1.9 Hz, 2 H, C$_5H_4$), 4.52 (pt, $^3J_{HH}$ = 1.9 Hz, 2 H, C$_5H_4$), 7.20 – 7.26 (m, 4 H, 2-CH$_3$C$_6H_4$), 7.28 – 7.34 (m, 2 H, 2-CH$_3$C$_6H_4$), 7.56 – 7.62 (m, 2 H, 2-CH$_3$C$_6H_4$). ^{13}C{^{1}H} NMR (125.81 MHz, $CDCl_3$, δ): 21.3 (d, $^3J_{CP}$ = 20.6 Hz, 2-*C*H$_3$C$_6$H$_4$), 69.2 (m, C$^{\beta}$/*C*$_5$H$_4$), 70.1 (s, *C*$_5$H$_5$), 72.0 (d, $^2J_{CP}$ = 1.6 Hz, C$^{\alpha}$/*C*$_5$H$_4$), 81.1 (d, $^2J_{CP}$ = 3.9 Hz, -*C*≡C-P), 107.7 (d, $^1J_{CP}$ = 5.5 Hz, -C≡*C*-P), 126.3 (d, J_{CP} = 2.2 Hz, 2-CH$_3$*C*$_6$H$_4$), 129.3 (s, 2-CH$_3$*C*$_6$H$_4$), 130.3 (d, J_{CP} = 5.1 Hz, 2-CH$_3$*C*$_6$H$_4$), 133.0 (d, J_{CP} = 3.4 Hz, 2-CH$_3$*C*$_6$H$_4$), 133.7 (d, J_{CP} = 6.4 Hz, 2-CH$_3$*C*$_6$H$_4$), 142.0 (d, J_{CP} = 26.6 Hz, 2-CH$_3$*C*$_6$H$_4$). ^{31}P{^{1}H} NMR (202.53 MHz, $CDCl_3$, δ): -47.7. HRMS (ESI-TOF) $C_{26}H_{23}FeP$ $[M+H]^+$ *m/z*: calcd.: 423.0960, found: 423.0963.

4.5.2 Synthesis of P(C≡CFc)(Mes)$_2$ (3c)

Using the general procedure described above, 1.0 g (4.76 mmol) of **1** was reacted with 1.90 mL (4.75 mmol) of *n*-BuLi and then with 1.45 g (4.75 mmol) of chlorodimesitylphosphine (**2c**). The resulting residue was purified by column chromatography on silica gel using *n*-hexane/diethyl ether (ratio 15:1, *v*:*v*) as eluent. Compound **3c** was obtained as a yellow solid.

Yield: 1.82 g (3.80 mmol, 80 % based on **2c**). Anal. Calcd. for $C_{30}H_{31}FeP$ (478.39 g/mol): C, 75.32; H, 6.53. Found: C, 75.27; H, 6.63. Mp.: 113 °C. IR (KBr, $\tilde{\upsilon}$/cm^{-1}): 820 (s, =C-H, *p*-subst. benzene), 1449/1467 (m, P-C), 1598 (m, C=C), 2140 (m, C≡C), 2919/2954 (m, C-H), 3096 (w, =C-H). ^{1}H NMR (500.30 MHz, $CDCl_3$, δ): 2.28 (s, 6 H, 2,*4*,6-(C*H*$_3$)$_3$C$_6$H$_2$), 2.47 (s, 12 H, *2*,4,*6*-(C*H*$_3$)$_3$C$_6$H$_2$), 4.16 (s, 5 H, C$_5$*H*$_5$), 4.20 (pt, $^{3}J_{HH}$ = 1.8 Hz, 2 H, C$_5$*H*$_4$), 4.41 (pt, $^{3}J_{HH}$ = 1.8 Hz, 2 H, C$_5$*H*$_4$), 6.84 (d, $^{4}J_{HP}$ = 3.1 Hz, 4 H, 2,4,6-(CH$_3$)$_3$C$_6$*H*$_2$). ^{13}C{^{1}H} NMR (125.81 MHz, $CDCl_3$, δ): 21.0 (s, 2,4,*6*-(*C*H$_3$)$_3$C$_6$H$_2$), 23.2 (d, $^{3}J_{CP}$ = 14.3 Hz, *2*,*4*,6-(*C*H$_3$)$_3$C$_6$H$_2$), 65.8 (m, C^{i}/C$_5$H$_4$), 68.9 (s, C$^{\beta}$/*C*$_5$H$_4$), 69.7 (s, *C*$_5$H$_5$), 71.4 (d, $^{4}J_{CP}$ = 1.6 Hz, C$^{\alpha}$/*C*$_5$H$_4$), 83.4 (d, $^{2}J_{CP}$ = 2.9 Hz, *C*≡C-P), 106.2 (d, $^{1}J_{CP}$ = 9.4 Hz, C≡*C*-P), 130.0 (d, $^{3}J_{CP}$ = 3.6 Hz, C^{m}/2,4,6-(CH$_3$)$_3$*C*$_6$H$_2$), 130.4 (d, $^{1}J_{CP}$ = 12.6 Hz, C^{i}/2,4,6-(CH$_3$)$_3$*C*$_6$H$_2$), 138.2 (s, C^{p}/2,4,6-(CH$_3$)$_3$*C*$_6$H$_2$), 142.0 (d, $^{2}J_{CP}$ = 15.8 Hz, C^{o}/2,4,6-(CH$_3$)$_3$*C*$_6$H$_2$). ^{31}P{^{1}H} NMR (202.53 MHz, $CDCl_3$, δ): -55.7. HRMS (ESI-TOF) $C_{30}H_{31}PFe$ $[M]^+$ *m/z*: calcd.: 478.1508, found: 478.1507.

4.5.3 Synthesis of P(C≡CFc)(Fur)$_2$ (3d)

Using the general procedure described above, 1.0 g (4.76 mmol) of **1** was reacted with 1.90 mL (4.75 mmol) of *n*-BuLi and then with 0.95 g (4.74 mmol) of chlorodi-2-furylphosphine (**2d**). The resulting residue was purified by column chromatography on alumina using *n*-hexane as eluent giving **3c** as a yellow solid. Yield: 1.37 g (3.66 mmol, 77 % based on **2d**). Anal. Calcd. for $C_{20}H_{15}FeO_2P$ (374.15 g/mol): C, 64.20; H, 4.04. Found: C, 64.33; H, 4.04. Mp.: 110 °C. IR (KBr, $\tilde{\upsilon}$/cm^{-1}): 1010 (s, C-O), 1458 (m, P-C), 1655 (w, C=C), 2153 (m, C≡C), 3114/3142 (w, =C-H). ^{1}H NMR (500.30 MHz, $CDCl_3$, δ): 4.19 (s, 5 H, C$_5$*H*$_5$), 4.22 (pt, $^{3}J_{HH}$ = 1.9 Hz, C$_5$*H*$_4$), 4.50 (pt, $^{3}J_{HH}$ = 1.9 Hz, C$_5$*H*$_4$), 6.44 (dt, $^{4}J_{HP}$ = 1.8 Hz, $^{3}J_{HH}$ = 3.3 Hz, $^{3}J_{HH}$ = 1.8 Hz, 2 H, H^{4}/C$_4$*H*$_3$O), 6.90 (m, 2 H, H^{3}/C$_4$*H*$_3$O), 7.67 (m, 2 H, H^{5}/C$_4$*H*$_3$O). ^{13}C{^{1}H} NMR (125.81 MHz, $CDCl_3$, δ): 70.4 (m, *C*$_5$H$_4$), 70.6 (s, *C*$_5$H$_5$), 72.6 (m, *C*$_5$H$_4$), 111.9 (pt, $^{3}J_{CP}$ = 4.9 Hz, C^{4}/*C*$_4$H$_3$O), 125.2 (d, $^{2}J_{CP}$ = 24.8 Hz, C^{3}/*C*$_4$H$_3$O), 140.9 (d, $^{1}J_{CP}$ = 99.3 Hz, C^{2}/*C*$_4$H$_3$O), 148.8 (d, $^{4}J_{CP}$ = 2.9 Hz, C^{5}/*C*$_4$H$_3$O). ^{31}P{^{1}H} NMR (202.53 MHz, $CDCl_3$, δ): -83.4. HRMS (ESI-TOF) $C_{20}H_{15}FeO_2P$ $[M]^+$ *m/z*: calcd.: 374.0154, found: 374.0053; $[M+K]^+$ *m/z*: calcd.: 412.9791, found: 412.9884. The ^{13}C signals for the ethynyl functionality could not be observed.

4.5.4 Synthesis of P(C≡CFc)(*t*-Bu)$_2$ (3e)

1.0 g (4.76 mmol) of **1** was reacted according to the general synthesis methodology described earlier with 1.90 mL (4.75 mmol) of *n*-BuLi and 0.86 g (4.75 mmol) of chlorodi-*t*-butylphosphine (**2e**). The resulting residue was purified by column chromatography on silica gel using *n*-hexane as eluent. Compound **3e** was obtained as a yellow solid. Yield: 1.03 g (2.90 mmol, 61 % based on **2e**). Anal. Calcd. for $C_{20}H_{27}FeP$ (354.25 g/mol): C, 67.81; H, 7.68. Found: C, 67.92; H, 7.85. Mp.: 121 °C. IR (KBr, $\tilde{\upsilon}$/cm^{-1}): 1467 (m, P-C), 1653 (w, C=C), 2364 (s, C≡C), 2859/2954 (s, C-H), 3099 (w, =C-H). ^{1}H NMR (500.30 MHz, $CDCl_3$, δ): 1.29 (d, $^3J_{HP}$ = 12.5 Hz, 18 H, C(CH_3)$_3$), 4.20 (pt, $^3J_{HH}$ = 1.9 Hz, C_5H_4), 4.23 (s, 5 H, C_5H_5), 4.46 (pt, $^3J_{HH}$ = 1.9 Hz, C_5H_4). ^{13}C{^{1}H} NMR (125.81 MHz, $CDCl_3$, δ): 29.8 (d, $^2J_{CP}$ = 14.4 Hz. C(CH$_3$)$_3$), 32.7 (d, $^1J_{CP}$ = 16.3 Hz, C(CH$_3$)$_3$), 69.9 (s, C_5H_5), 70.2 (m, C$^{\alpha}$/C_5H_4), 71.8 (d, $^3J_{CP}$ = 0.9 Hz, C$^{\beta}$/C_5H_5), 83.9 (d, $^1J_{CP}$ = 18.0 Hz, -C≡C-P), 104.8 (d, $^2J_{CP}$ = 2.2 Hz, -C≡C-P). ^{31}P{^{1}H} NMR (202.53 MHz, $CDCl_3$, δ): 10.9. HRMS (ESI-TOF) $C_{20}H_{27}FeP$ $[M+H]^+$ *m/z*: calcd.: 354.1194, found: 355.1152.

4.5.5 Synthesis of P(C≡CFc)(Cy)$_2$ (3f)

1.0 g (4.76 mmol) of **1** was reacted (general synthesis procedure see earlier) with 1.90 mL (4.75 mmol) of *n*-BuLi followed by addition of 1.10 g (4.73 mmol) of chlorodicyclohexylphosphine (**2f**). The resulting residue was purified by column chromatography on silica gel using *n*-hexane as eluent. Phosphine **3f** was obtained as a yellow solid. Yield: 1.71 g (4.21 mmol, 89 % based on **2f**). Anal. Calcd. for $C_{24}H_{31}FeP$ (406.32 g/mol): C, 70.94; H, 7.69. Found: C, 70.48; H, 7.77. Mp.: 77 °C. IR (KBr, $\tilde{\upsilon}$/cm^{-1}): 1444 (m, P-C), 1657 (w, C=C), 2146 (m, C≡C), 2847/2923 (s, C-H). 3095 (w, =C-H). ^{1}H NMR (500.30 MHz, $CDCl_3$, δ): 1.25-1.44 (m, 10 H, C_6H_{11}), 1.71-1.84 (m, 10 H, C_6H_{11}), 1.97-2.02 (m, 2 H, H_1/C_6H_{11}), 4.21 (pt, $^3J_{HH}$ = 1.8 Hz, 2 H, C_5H_4), 4.22 (s, 5 H, C_5H_5), 4.47 (pt, $^3J_{HH}$ = 1.8 Hz, 2 H, C_5H_4). ^{13}C{^{1}H} NMR (125.81 MHz, $CDCl_3$, δ): 26.4 (s, C_6H_{11}), 26.8 (d, J_{CP} = 18.2 Hz, C_6H_{11}), 26.9 (d, J_{CP} = 1.9 Hz, C_6H_{11}), 29.2 (d, J_{CP} = 4.5 Hz, C_6H_{11}), 30.0 (d, J_{CP} = 18.1 Hz, C_6H_{11}), 32.9 (d, $^1J_{CP}$ = 8.2 Hz, C^1/C_6H_{11}), 65.2 (s, C^i/C_5H_4), 68.6 (s, C_5H_4), 69.9 (s, C_5H_5), 71.6 (s, C_5H_4), 82.5 (d, $^1J_{CP}$ = 20.1 Hz, -C≡C-P), 104.4 (d, $^2J_{CP}$ = 2.3 Hz, -C≡C-P). ^{31}P{^{1}H} NMR (202.53 MHz, $CDCl_3$, δ): -22.1. HRMS (ESI-TOF) $C_{24}H_{31}FeP$ $[M+H]^+$ *m/z*: calcd.: 407.1586, found: 407.1571.

4.6 General Procedure for the Synthesis of Seleno Phosphines 4b – f

To a toluene solution (20 mL) containing 100 mg of the respective phosphine **3b** – **f**, 1.2 equivalents of elemental selenium were added in a single portion and the reaction mixture was stirred for 1 h at 100 °C. After cooling the reaction mixture to ambient temperature, it was filtered through a pad of Celite. All volatiles were removed in vacuum giving the appropriate compounds.

4.6.1 Synthesis of (Se)P(C≡CFc)(*o*-Tol)$_2$ (4b)

100 mg (0.24 mmol) of **3b** were reacted with 22 mg (0.28 mmol) of elemental selenium. After appropriate work-up, **4b** was obtained as a yellow solid. Yield: 120 mg (0.24 mmol, 100 % based on **3b**). Anal. Calcd. for $C_{26}H_{23}FePSe$ (501.24 g/mol): C, 62.30; H, 4.63. Found: C, 62.12; H, 4.83. Mp.: 64 °C. IR (KBr, $\tilde{\upsilon}$/cm^{-1}): 556 (m, P-Se), 1450 (m, P-C), 2155 (s, C≡C), 2922/2961 (w, C-H), 3055 (w, =C-H). ^{1}H NMR (500.30 MHz, $CDCl_3$, δ): 2.29 (s, 6 H, 2-CH_3C$_6$H$_4$), 4.23 (s, 5 H, C$_5H_5$), 4.32 (pt, $^3J_{HH}$ = 1.8 Hz, 2 H, C$_5H_4$), 4.58 (pt, $^3J_{HH}$ = 1.8 Hz, 2 H, C$_5H_4$), 7.17 – 7.20 (m, 2 H, H^p/2-CH$_3$C$_6H_4$), 7.38 – 7.45 (m, 4 H, H^m/2-CH$_3$C$_6H_4$), 8.38 – 8.43 (m, 4 H, H^o/2-CH$_3$C$_6H_4$). [c] 21.3 (d, $^3J_{CP}$ = 5.7 Hz, 2-*C*H$_3$C$_6$H$_4$), 61.1 (d, $^3J_{CP}$ = 4.1 Hz, C^i/*C*$_5$H$_4$), 70.2 (s, *C*$_5$H$_5$), 70.3 (s, *C*$_5$H$_4$), 72.4 (s, *C*$_5$H$_4$), 76.7 (d, $^1J_{CP}$ = 148.9 Hz, -C≡*C*-P), 108.8 (d, $^2J_{CP}$ = 26.3 Hz, -*C*≡C-P), 126.4 (d, J_{CP} = 14.7 Hz, 2-CH$_3$*C*$_6$H$_4$), 129.4 (d, J_{CP} = 85.5 Hz, 2-CH$_3$*C*$_6$H$_4$), 132.1 (d, J_{CP} = 11.1 Hz, 2-CH$_3$*C*$_6$H$_4$), 132.2 (d, J_{CP} = 3.0 Hz, 2-CH$_3$*C*$_6$H$_4$), 133.8 (d, J_{CP} = 15.2 Hz, 2-CH$_3$*C*$_6$H$_4$), 140.5 (d, J_{CP} = 9.7 Hz, 2-CH$_3$*C*$_6$H$_4$). ^{31}P{^{1}H} NMR (202.53 MHz, $CDCl_3$, δ): 0.9 ($^1J_{PSe}$ = 728.7 Hz). HRMS (ESI-TOF) $C_{26}H_{23}FePSe$ $[M+Na]^+$ *m/z*: calcd.: 524.9946, found: 524.9946; $[M+K]^+$ *m/z*: calcd.: 540.9686, found: 540.9665.

4.6.2 Synthesis of (Se)P(C≡CFc)(Mes)$_2$ (4c)

100 mg (0.21 mmol) of **3c** were reacted with 20 mg (0.25 mmol) of elemental selenium. After appropriate work-up, **4c** was obtained as an orange solid. Yield: 117 mg (0.21 mmol, 100 % based on **3c**). Anal. Calcd. for $C_{30}H_{31}FePSe$ (557.35 g/mol): C, 64.65; H, 5.61. Found: C, 64.91; H, 5.22. Mp.: 165 °C. IR (KBr, $\tilde{\upsilon}$/cm^{-1}): 563 (m, P-Se), 821 (m, =C-H, *p*-subst. benzene), 1448 (m, P-C), 2157 (s, C≡C), 2924/2963 (m, C-H), 3021/3098 (w, =C-H). ^{1}H NMR (500.30 MHz, $CDCl_3$, δ): 2.28 (s, 6 H, 2,*4*,6-(C*H*$_3$)$_3$C$_6$H$_2$), 2.61 (s, 12 H, *2*,4,*6*-(C*H*$_3$)$_3$C$_6$H$_2$), 4.18 (s, 5 H, C$_5H_5$), 4.27 (pt, $^3J_{HH}$ = 1.9 Hz, 2 H, H$^\beta$/C$_5H_4$), 4.49 (pt, $^3J_{HH}$ = 1.9 Hz, 2 H, H$^\alpha$/C$_5H_4$), 6.85 (dd, $^4J_{HP}$ = 5.2 Hz, $^4J_{HH}$ = 0.4 Hz, 4 H, 2,4,6-(CH$_3$)$_3$C$_6H_2$); ^{13}C{^{1}H}

NMR (125.81 MHz, $CDCl_3$, δ): 21.9 (d, $^5J_{CP}$ = 1.5 Hz, 2,*4*,6-(*C*H_3)$_3$$C_6H_2$), 23.2 (d, $^3J_{CP}$ = 6.9 Hz, *2*,4,*6*-(*C*H_3)$_3$$C_6H_2$), 62.2 (d, $^3J_{CP}$ = 4.5 Hz, C^i/C_5H_4), 69.9 (s, C$^\beta$/C_5H_4), 69.9 (s, C_5H_5), 71.9 (d, $^4J_{CP}$ = 1.4 Hz, C$^\alpha$/C_5H_4), 81.0 (d, $^1J_{CP}$ = 143.7 Hz, -C≡*C*-P), 107.3 (d, $^2J_{CP}$ = 26.8 Hz, -*C*≡C-P), 128.4 (d, $^1J_{CP}$ = 86.1 Hz, C/2,4,6-(CH_3)$_3$$C_6H_2$), 131.8 (d, J_{CP} = 11.6 Hz, C/2,4,6-(CH_3)$_3$$C_6H_2$), 140.5 (d, J_{CP} = 10.9 Hz, C/2,4,6-(CH_3)$_3$$C_6H_2$), 140.6 (d, J_{CP} = 2.4 Hz, C/2,4,6-(CH_3)$_3$$C_6H_2$); $^{31}P\{^1H\}$ NMR (202.53 MHz, $CDCl_3$, δ): -17.5 ($^1J_{PSe}$ = 709.5 Hz). HRMS (ESI-TOF) $C_{30}H_{31}FePSe$ $[M]^+$ *m/z*: calcd.: 558.0675, found: 558.0627.

4.6.3 Synthesis of (Se)P(C≡CFc)(Fur)$_2$ (4d)

100 mg (0.27 mmol) of **3d** were reacted with 25 mg (0.32 mmol) of elemental selenium. After appropriate work-up, **4d** was obtained as an orange solid. Yield: 122 mg (0.27 mmol, 100 % based on **3d**). Anal. Calcd. for $C_{20}H_{15}FeO_2PSe$ (453.11 g/mol): C, 53.01; H, 3.34. Found: C, 53.40; H, 3.37. Mp.: 162 °C. IR (NaCl, $\tilde{\upsilon}$/cm^{-1}): 575 (m, P-Se), 1005 (m, C-O), 1456 (w, P-C), 1549 (w, C=C), 2156 (vs, C≡C), 3108 (w, =C-H). ^{1}H NMR (500.30 MHz, $CDCl_3$, δ): 4.26 (s, 5 H, C_5H_5), 4.34 (pt, $^3J_{HH}$ = 1.9 Hz, C_5H_4), 4.60 (pt, $^3J_{HH}$ = 1.9 Hz, C_5H_4), 6.51 (dpt, $^4J_{HP}$ = 1.8 Hz, $^3J_{HH}$ = 3.5 Hz, $^3J_{HH}$ = 1.7 Hz, 2 H, H^4/C_4H_3O), 7.31 (m, 2 H, H^3/ C_4H_3O), 7.74 (m, 2 H, H^5/ C_4H_3O). $^{13}C\{^1H\}$ NMR (125.81 MHz, $CDCl_3$, δ): 60.1 (d, $^3J_{CP}$ = 5.1 Hz, C^i/C_5H_4), 70.6 (s, C$^\beta$/C_5H_4), 70.6 (s, C_5H_5), 72.8 (d, $^4J_{CP}$ = 1.5 Hz, C$^\alpha$/C_5H_4), 74.0 (d, $^1J_{CP}$ = 169.3 Hz, -C≡*C*-P), 108.6 (d, ^2JCP = 32.7 Hz, -*C*≡C-P), 111.6 (d, $^3J_{CP}$ = 10.2 Hz, C^4/C_4H_3O), 122.8 (d, $^2J_{CP}$ = 25.3 Hz, C^3/C_4H_3O), 145.4 (d, $^1J_{CP}$ = 132.1 Hz, C^2/C_4H_3O), 149.0 (d, $^4J_{CP}$ = 8.1 Hz, C^5/C_4H_3O). $^{31}P\{^1H\}$ NMR (202.53 MHz, $CDCl_3$, δ): -37.9 ($^1J_{PSe}$ = 783.9 Hz). HRMS (ESI-TOF) $C_{20}H_{15}FeO_2PSe$ $[M]^+$ *m/z*: calcd.: 453.9320, found: 453.9275.

4.6.4 Synthesis of (Se)P(C≡CFc)(*t*-Bu)$_2$ (4e)

100 mg (0.28 mmol) of **3e** were reacted with 27 mg (0.34 mmol) of selenium in its elemental form. After appropriate work-up, **4e** was obtained as an orange solid. Yield: 113 mg (0.28 mmol, 100 % based on **3e**). Anal. Calcd. for $C_{20}H_{27}FePSe$ (433.21 g/mol): C, 55.45; H, 6.28. Found: C, 55.50; H, 6.19. Mp.: 165 °C. IR (NaCl, $\tilde{\upsilon}$/cm^{-1}): 533 (m, P-Se), 1470 (m, P-C), 2158 (s, C≡C), 2868/2922/2962 (s, C-H), 3092 (w, =C-H). ^{1}H NMR (500.30 MHz, $CDCl_3$, δ): 1.46 (d, $^3J_{HP}$ = 17.3 Hz, 18 H, C(CH_3)$_3$), 4.24 (s, 5 H, C_5H_5), 4.27 (pt, $^3J_{HH}$ = 1.8 Hz, 2 H, C_5H_4), 4.52 (pt, $^3J_{HH}$ = 1.8 Hz, 2 H, C_5H_4). $^{13}C\{^1H\}$ NMR (125.81 MHz, $CDCl_3$, δ): 27.7 (d, $^2J_{CP}$ = 2.8 Hz, C(*C*H_3)$_3$), 38.4 (d, $^1J_{CP}$ = 41.9 Hz, *C*(CH_3)$_3$), 61.5 (d, $^3J_{CP}$ = 3.8 Hz, C^i/C_5H_4), 69.9 (s, C$^\beta$/C_5H_4), 70.1 (s, C_5H_5), 72.2 (d, $^4J_{CP}$ = 1.3 Hz, C$^\alpha$/C_5H_4), 75.0 (d, $^1J_{CP}$ =

114.2 Hz, -C≡*C*-P), 106.7 (d, $^{2}J_{CP}$ = 15.8 Hz, -*C*≡C-P). $^{31}P\{^{1}H\}$ NMR (202.53 MHz, $CDCl_3$, δ): 56.3 ($^{1}J_{PSe}$ = 715.3 Hz). HRMS (ESI-TOF) $C_{20}H_{27}FePSe$ $[M+Na]^+$ *m/z*: calcd.: 457.0259, found: 457.0256.

4.6.5 Synthesis of (Se)P(C≡CFc)(Cy)$_2$ (4f)

100 mg (0.25 mmol) of **3f** were reacted with 24 mg (0.30 mmol) of selenium. After appropriate work-up, **4f** was obtained as an orange solid. Yield: 121 mg (0.25 mmol, 100 % based on **3f**). Anal. Calcd. for $C_{24}H_{31}FePSe$ (485.28 g/mol): C, 59.40; H, 6.44. Found: C, 60.12; H, 6.60. Mp.: 135 °C. IR (NaCl, $\tilde{\upsilon}$/cm^{-1}): 526/536 (m, P-Se), 1448 (m, P-C), 2158 (s, C≡C), 2852/2928 (s, C-H), 3095 (w, =C-H). ^{1}H NMR (500.30 MHz, $CDCl_3$, δ): 1.24 - 1.78 (m, 11 H, C_6H_{11}), 1.91 - 2.09 (m, 11 H, C_6H_{11}), 4.26 (s, 5 H, C_5H_5), 4.30 (pt, $^{3}J_{HH}$ = 1.9 Hz, 2 H, C_5H_4), 4.55 (pt, $^{3}J_{HH}$ = 1.9 Hz, 2 H, C_5H_4). $^{13}C\{^{1}H\}$ NMR (125.81 MHz, $CDCl_3$, δ): 25.9 (d, J_{CP} = 8.0 Hz, C_6H_{11}), 25.9 (d, J_{CP} = 6.5 Hz, C_6H_{11}), 26.2 (d, J_{CP} = 15.5 Hz, C_6H_{11}), 26.4 (d, J_{CP} = 13.8 Hz, C_6H_{11}), 27.1 (d, J_{CP} = 4.4 Hz, C_6H_{11}), 38.3 (d, $^{1}J_{CP}$ = 50.9 Hz, C^{1}/C_6H_{11}), 61.3 (d, $^{3}J_{CP}$ = 3.6 Hz, C^{i}/C_5H_4), 70.0 (s, C^{β}/C_5H_4), 70.3 (s, C_5H_5), 72.5 (m, C^{α}/C_5H_4), 74.5 (d, $^{1}J_{CP}$ = 118.4 Hz, -C≡*C*-P), 106.6 (d, $^{2}J_{CP}$ = 17.6 Hz, -*C*≡C-P). $^{31}P\{^{1}H\}$ NMR (202.53 MHz, $CDCl_3$, δ): 31.0 ($^{1}J_{PSe}$ = 712.5 Hz). HRMS (ESI-TOF) $C_{24}H_{31}FePSe$ $[M]^+$ *m/z*: calcd.: 486.0675, found: 486.0679.

4.7 General Procedure for the Synthesis of Palladium Complexes 6e, 6f and 7a – f

Phosphines **3a** – **3f** were reacted with 0.5 equivalents of $[PdCl_2(cod)]$ (**5**) or $[PdCl_2(SEt_2)_2]$ (**8**) in 40 mL of dry dichloromethane. The appropriate reaction solution was stirred for 2 h at ambient temperature. Afterward, the solvent was removed in vacuum and the residue was washed 5 – 6 times with 5 mL portions of diethyl ether. After drying in vacuum the appropriate complexes were obtained as red or brown solids.

4.7.1 Synthesis of [Pd(Cl)(μ-Cl)(P(C≡CFc)(*t*-Bu)$_2$)]$_2$ (6e)

0.5 g (1.41 mmol) of **3f** were reacted with 0.20 g (0.70 mmol) of **5**. After appropriate work-up, **6e** was isolated as a brown solid. Yield: 700 mg (0.66 mmol, 94 % based on **5**). Anal. Calcd. for $C_{40}H_{54}Cl_4Fe_2P_2Pd_2$ (1063.15 g/mol): C, 45.19; H, 5.12. Found: C, 44.91; H, 5.16. Mp.: 156 °C. IR (KBr, $\tilde{\upsilon}$/cm^{-1}): 1468 (w, P-C), 2155 (vs, C≡C), 2867/2890/2922/2966 (w, C-H), 3097 (w, =C-H). ^{1}H NMR (500.30 MHz, $CDCl_3$, δ): 1.62 (d, $^{3}J_{HP}$ = 16.9 Hz, 36 H,

C(CH_3)$_3$), 4.28 (pt, $^3J_{HH}$ = 1.9 Hz, 4 H, C$_5H_4$), 4.32 (s, 10 H, C$_5H_5$), 4.58 (pt, $^3J_{HH}$ = 1.9 Hz, 4 H, C$_5H_4$). ^{13}C{^{1}H} NMR (125.81 MHz, $CDCl_3$, δ): 30.2 (d, $^2J_{CP}$ = 3.4 Hz, C(CH_3)$_3$), 40.2 (d, $^1J_{CP}$ = 24.5 Hz, C(CH$_3$)$_3$), 62.0 (m, C^i/C_5H_4), 70.0 (s, C_5H_4), 70.7 (s, C_5H_5), 72.7 (s, C_5H_4), 77.3 (C≡C-P[*)]), 116.8 (s, -C≡C-P). ^{31}P{^{1}H} NMR (202.53 MHz, $CDCl_3$, δ): 49.7. HRMS (ESI-TOF) $C_{40}H_{54}Cl_4Fe_2P_2Pd_2$ $[M\text{-}Cl]^+$ *m/z*: calcd.: 1026.9536, found: 1026.9515. [*)] signal concealed by $CDCl_3$

4.7.2 Synthesis of [Pd(Cl)(μ-Cl)(P(C≡CFc)(Cy)$_2$)]$_2$ (6f)

0.5 g (1.23 mmol) of **3f** were reacted with 0.17 g (0.61 mmol) of **5**. After appropriate work-up, **6f** was obtained as a brown solid. Yield: 642 mg (0.55 mmol, 90 % based on **5**). Anal. Calcd. for $C_{48}H_{62}Cl_4Fe_2P_2Pd_2$ (1167.30 g/mol): C, 52.58; H, 5.70. Found: C, 52.71; H, 5.65. Mp.: 200 °C (dec). IR (KBr, $\tilde{\upsilon}$/cm^{-1}): 1446 (w, P-C), 1653 (w, C=C), 2151 (s, C≡C), 2851/2928 (vs, C-H), 3098 (w, =C-H). ^{1}H NMR (500.30 MHz, $CDCl_3$, δ): 1.26 – 1.37 (m, 8 H, C$_6H_{11}$), 1.75 – 2.01 (m, 20 H, C$_6H_{11}$), 2.21 – 2.38 (m, 8 H, C$_6H_{11}$), 2.52 – 2.58 (m, 4 H, C$_6H_{11}$), 2.88 – 2.92 (m, 4 H, C$_6H_{11}$), 4.28 (m, 4 H, C$_5H_4$), 4.29 (s, 10 H, C$_5H_5$), 4.56 (pt, $^3J_{HH}$ = 1.7 Hz, 4 H, C$_5H_4$). ^{13}C{^{1}H} NMR (125.81 MHz, $CDCl_3$, δ): 25.9 (, C^6/C_6H_{11}), 26.6 (m, C$^{2/3}$/C_6H_{11}), 26.8 (m, C$^{2/3}$/C_6H_{11}), 29.0 (m, C$^{4/5}$/C_6H_{11}), 31.2 (s, C$^{4/5}$/C_6H_{11}), 36.4 (d, $^1J_{CP}$ = 35.5 Hz, C^1/C_6H_{11}), 62.6 (s, C^i/C_5H_4), 70.2 (s, C_5H_4), 70.8 (s, C_5H_5), 72.8 (s, C_5H_4), 75.7 (d, $^1J_{CP}$ = 91.5 Hz, C≡C-P), 110.2 (pt, $^{2,3}J_{CP}$ = 5.3 Hz, C≡C-P). ^{31}P{^{1}H} NMR (202.53 MHz, $CDCl_3$, δ): 31.0. HRMS (ESI-TOF) $C_{48}H_{62}Cl_4Fe_2P_2Pd_2$ $[M]^+$ *m/z*: calcd.: 1167.9843, found: 1167.9851.

4.7.3 Synthesis of [PdCl$_2$(P(C≡CFc)(*o*-Tol)$_2$)$_2$] (7b)

0.5 g (1.18 mmol) of **3b** were reacted with 0.17 g (0.59 mmol) of **5**. After appropriate work-up, **7b** was obtained as a red solid. Yield: 560 mg (0.55 mmol, 95 % based on **5**). Anal. Calcd. for $C_{52}H_{46}Cl_2Fe_2P_2Pd \cdot 1/3\ CH_2Cl_2$ (1050.20 g/mol): C, 59.85; H, 4.48. Found: C, 60.14; H, 4.44. Mp.: 214 °C. IR (KBr, $\tilde{\upsilon}$/cm^{-1}): 756 (s, =C-H, *o*-disubst. benzene), 1448 (w, P-C), 1627 (C=C), 2159 (vs, C≡C), 2922/2963 (w, C-H), 3056/3081 (w, =C-H). ^{1}H NMR (500.30 MHz, $CDCl_3$, δ): 2.86 (s, 12 H, 2-CH_3C$_6$H$_4$), 4.24 (pt, $^3J_{HH}$ = 1.9 Hz, 4 H, C$_5H_4$), 4.25 (s, 10 H, C$_5H_5$), 4.55 (pt, $^3J_{HH}$ = 1.9 Hz, 4 H, C$_5H_4$), 5.30 (s, CH_2Cl$_2$), 7.18 - 7.41 (m, 12 H, H^{m,p}/2-CH$_3$C$_6H_4$), 7.77 - 7.86 (m, 4 H, H^o/2-CH$_3$C$_6H_4$). ^{13}C{^{1}H} NMR (125.81 MHz, $CDCl_3$, δ): 23.5 (pt, $^3J_{CP}$ = 4.0 Hz, 2-CH$_3$C$_6$H$_4$), 53.52 (s, CH$_2$Cl$_2$), 62.9 (m, C^i/C_5H_4), 69.7 (s, C$^\beta$/C_5H_4), 70.4 (s, C_5H_5), 72.3 (s, C$^\alpha$/C_5H_4), 74.9 (pt, $^1J_{CP}$ = 51.9 Hz, -C≡C-P), 111.4 (d, $^2J_{CP}$

= 9.2 Hz, -*C*≡C-P), 125.9 (pt, J_{CP} = 6.0 Hz, 2-$CH_3C_6H_4$), 126.8 (pt, $^1J_{CP}$ = 28.7. Hz, C^i/2-$CH_3C_6H_4$), 131.3 (s, C^p/2-$CH_3C_6H_4$), 131.5 (pt, J_{CP} = 4.2 Hz, 2-$CH_3C_6H_4$), 135.1 (pt, J_{CP} = 8.0 Hz, 2-$CH_3C_6H_4$), 142.6 (pt, J_{CP} = 5.5 Hz, 2-$CH_3C_6H_4$). $^{31}P\{^1H\}$ NMR (202.53 MHz, $CDCl_3$, δ): -6.8. HRMS (ESI-TOF) $C_{52}H_{46}Cl_2Fe_2P_2Pd$ $[M]^+$ *m/z*: calcd.: 1022.0186, found: 1022.0145; $[M\text{-}Cl]^+$ *m/z*: calcd.: 985.0511, found: 985.0487; $[M]^{2+}$ *m/z*: calcd.: 511.0090, found: 511.0083; $[M\text{-}Cl]^{2+}$ *m/z*: calcd.: 492.5253, found: 492.5236.

4.7.4 Synthesis of $[PdCl_2(P(C{\equiv}CFc)(Mes)_2)_2]$ (7c)

0.5 g (1.05 mmol) of **3c** were reacted with 0.15 g (0.52 mmol) of **5**. After appropriate work-up, **7c** could be isolated as a brown solid. Yield: 556 mg (0.49 mmol, 94 % based on **5**). Anal. Calcd. for $C_{60}H_{62}Cl_2Fe_2P_2Pd$ (1134.10 g/mol): C, 63.54; H, 5.51. Found: C, 63.67; H, 5.69. Mp.: 172 °C. IR (KBr, $\tilde{\upsilon}$/cm^{-1}): 818 (m, =C-H, *p*-subst. benzene), 1459 (m, P-C), 1603 (m, C=C), 2152 (s, C≡C), 2923/2963 (w, C-H), 3072 (w, =C-H). ^1H NMR (500.30 MHz, $CDCl_3$, δ): 2.24 (s, 6 H, 2,*4*,6-(CH_3)$_3C_6H_2$), 2.70 (s, 12 H, *2*,4,*6*-(CH_3)$_3C_6H_2$), 4.19 (s, 5 H, C_5H_5), 4.20 (pt, $^3J_{HH}$ = 1.8 Hz, 2 H, C_5H_4), 4.49 (pt, $^3J_{HH}$ = 1.8 Hz, 2 H, C_5H_4), 6.84 (m, 4 H, 2,4,6-(CH_3)$_3C_6H_2$). $^{13}C\{^1H\}$ NMR (125.81 MHz, $CDCl_3$, δ): 21.1 (s, 2,*4*,6-(CH_3)$_3C_6H_2$), 25.6 (pt, $^3J_{CP}$ = 4.1 Hz, *2*,4,*6*-(CH_3)$_3C_6H_2$), 64.2 (pt, $^3J_{CP}$ = 1.2 Hz, C^i/C_5H_4), 69.3 (s, C$^\beta$/C_5H_4), 70.1 (s, C_5H_5), 72.0 (s, C$^\alpha$/C_5H_4), 77.4 (pt, $^1J_{CP}$ = 66.7 Hz, C≡*C*-P), 109.1 (pt, $^2J_{CP}$ = 8.9 Hz, *C*≡C-P), 126.0 (pt, $^1J_{CP}$ = 27.6 Hz, C^i/2,4,6-(CH_3)$_3C_6H_2$), 130.7 (pt, $^3J_{CP}$ = 4.5 Hz, C^m/2,4,6-(CH_3)$_3C_6H_2$), 140.1 (s, C^p/2,4,6-(CH_3)$_3C_6H_2$), 142.5 (pt, $^2J_{CP}$ = 5.8 Hz, C^o/2,4,6-(CH_3)$_3C_6H_2$). $^{31}P\{^1H\}$ NMR (202.53 MHz, $CDCl_3$, δ): -24.0. HRMS (ESI-TOF) $C_{60}H_{62}Cl_2Fe_2P_2Pd$ $[M]^+$ *m/z*: calcd.: 1134.1441, found: 1134.1351; $[M\text{-}Cl]^+$ *m/z*: calcd.: 1097.1765, found: 1097.1688; $[M\text{-}H\text{-}2Cl]^+$ *m/z*: calcd.: 1061.2001, found: 1061.1929; $[M\text{-}(C_{30}H_{31}FeP)PdCl_2]^+$ *m/z*: calcd.: 478.1508, found: 478.1480.

4.7.5 Synthesis of $[PdCl_2(P(C{\equiv}CFc)(Fur)_2)_2]$ (7d)

0.5 g (1.34 mmol) of **3d** were reacted with 0.19 g (0.67 mmol) of **5**. After appropriate work-up, **7d** was obtained as a dark red solid. Yield: 596 mg (0.64 mmol, 96 % based on **5**). Anal. Calcd. for $C_{40}H_{30}Cl_2Fe_2O_4P_2Pd \cdot 1/4\ CH_2Cl_2$ (946.86 g/mol): C, 51.06; H, 3.25. Found: C, 51.05; H, 3.32. Mp.: > 250 °C. IR (KBr, $\tilde{\upsilon}$/cm^{-1}): 1010 (m, C-O), 1454 (w, P-C), 1573 (w, C=C), 2155 (s, C≡C), 3107 (w, =C-H). ^1H NMR (500.30 MHz, $CDCl_3$, δ): 4.12 (s, 5 H, C_5H_5), 4.26 (pt, $^3J_{HH}$ = 1.6 Hz, 2 H, C_5H_4), 4.32 (pt, $^3J_{HH}$ = 1.6 Hz, 2 H, C_5H_4), 5.30 (s, CH_2Cl_2), 6.53 (m, 2 H, H^4/C_4H_3O), 7.33 (m, 2 H, H^3/C_4H_3O), 7.70 (m, 2 H, H^2/C_4H_3O).

$^{13}C\{^1H\}$ NMR (125.81 MHz, $CDCl_3$, δ): 53.52 (s, CH_2Cl_2), m60.8 (m, C^i/C_5H_4), 70.4 (s, C_5H_4), 70.6 (s, C_5H_5), 72.6 (s, C_5H_4), 73.7 (d, $^1J_{CP}$ = 60.0 Hz, C≡C-P), 94.6 (pt, $^2J_{CP}$ = 8.1 Hz, C≡C-P), 111.9 (pt, $^3J_{CP}$ = 4.4 Hz, C^4/C_4H_3O), 125.2 (d, $^2J_{CP}$ = 24.8 Hz, C^3/C_4H_3O), 148.8 (d, $^1J_{CP}$ = 99.1 Hz, C^2/C_4H_3O), 148.8 (pt, $^4J_{CP}$ = 3.3 Hz, C^5/C_4H_3O). $^{31}P\{^1H\}$ NMR (202.53 MHz, $CDCl_3$, δ): -32.4. HRMS (ESI-TOF) $C_{40}H_{30}Cl_2Fe_2O_4P_2Pd$ $[M]^+$ *m/z*: calcd.: 925.8727, found: 925.8656.

4.7.6 Synthesis of $[PdCl_2(P(C{\equiv}CFc)(t\text{-}Bu)_2)_2]$ (7e)

0.5 g (1.41 mmol) of **3e** were reacted with 0.25 g (0.70 mmol) of **8**. After appropriate work-up, **7e** was obtained as an orange solid. Yield: 584 mg (0.66 mmol, 94 % based on **8**). Anal. Calcd. for $C_{40}H_{54}Cl_2Fe_2P_2Pd$ (885.82 g/mol): C, 54.24; H, 6.14. Found: C, 53.75; H, 6.17. Mp.: 250 °C. IR (KBr, $\tilde{\upsilon}$/cm^{-1}): 1459 (w, P-C), 1655 (w, C=C), 2162 (s, C≡C), 2863/2917/2955 (m, C-H), 3097 (w, =C-H). ^1H NMR (500.30 MHz, CD_2Cl_2, δ): 1.59 (t, $^3J_{HP}$ = 7.7 Hz Hz, 36 H, $C(CH_3)_3$), 4.25 (pt, $^3J_{HH}$ = 1.8 Hz, 4 H, C_5H_4), 4.28 (s, 10 H, C_5H_5), 4.54 (pt, $^3J_{HH}$ = 1.8 Hz, 4 H, C_5H_4). $^{13}C\{^1H\}$ NMR (125.81 MHz, $CDCl_3$, δ): 30.2 (pt, $^2J_{CP}$ = 3.4 Hz, $C(CH_3)_3$), 40.1 (pt, $^1J_{CP}$ = 24.5 Hz, $C(CH_3)_3$), 62.0 (m, C^i/C_5H_4), 70.0 (s, C_5H_4), 70.7 (s, C_5H_5), 72.7 (s, C_5H_4), 77.4 (C≡C-P[*)]), 116.8 (m, C≡C-P). $^{31}P\{^1H\}$ NMR (202.53 MHz, $CDCl_3$, δ): 49.7. HRMS (ESI-TOF) $C_{40}H_{54}Cl_2Fe_2P_2Pd$ $[M]^+$ *m/z*: calcd.: 886.0808, found: 886.0780; $[M\text{-}Cl]^+$ *m/z*: calcd.: 849.1134, found: 849.1083; $[M+H\text{-}2Cl]^+$ *m/z*: calcd.: 815.1526, found: 815.1471; $[M]^{2+}$ *m/z*: calcd.: 443.0401, found: 443.0332. [*)] signal concealed by $CDCl_3$.

4.7.7 Synthesis of $[PdCl_2(P(C{\equiv}CFc)(Cy)_2)_2]$ (7f)

0.5 g (1.23 mmol) of **3f** were reacted with 0.22 g (0.61 mmol) of **8**. After appropriate work-up, **7f** was obtained as an orange solid. Yield: 481 mg (0.58 mmol, 95 % based on **8**). Anal. Calcd. for $C_{48}H_{62}Cl_2Fe_2P_2Pd$ (829.71 g/mol): C, 58.24; H, 6.31. Found: C, 58.34; H, 6.80. Mp.: 210 °C. IR (KBr, $\tilde{\upsilon}$/cm^{-1}): 1447 (w, P-C), 1655 (w, C=C), 2158 (s, C≡C), 2849/2925 (s, C-H), 3075 (w, =C-H). ^1H NMR (500.30 MHz, CD_2Cl_2, δ): 1.28 (m, 4 H, H^6/C_6H_{11}), 1.39 (m, 8 H, $H^{2/3}/C_6H_{11}$), 1.63 (m, 8 H, $H^{4/5}/C_6H_{11}$), 1.74 (m, 4 H, H^6/C_6H_{11}), 1.86 (m, 8 H, $H^{2/3}/C_6H_{11}$), 2.13 (m, 4 H, $H^{4/5}/C_6H_{11}$), 2.45 (m, 4 H, $H^{4/5}/C_6H_{11}$), 2.76 (m, 4 H, H^1/C_6H_{11}), 4.21 (s, 10 H, C_5H_5), 4.26 (pt, $^3J_{HH}$ = 1.5 Hz, 4 H, C_5H_4), 4.36 (pt, $^3J_{HH}$ = 1.5 Hz, 4 H, C_5H_4). $^{13}C\{^1H\}$ NMR (125.81 MHz, $CDCl_3$, δ): 25.2 (s, C^6/C_6H_{11}), 25.8 (pt, $^2J_{CP}$ = 5.7 Hz, $C^{2/3}/C_6H_{11}$), 26.0 (pt, $^2J_{CP}$ = 8.0 Hz, $C^{2/3}/C_6H_{11}$), 28.7 (m, $C^{4/5}/C_6H_{11}$), 29.3 (s, $C^{4/5}/C_6H_{11}$),

37.5 (dpt, $^{1}J_{CP}$ = 32.3 Hz, C^{1}/C_6H_{11}), 61.4 (m, C^{i}/C_5H_4), 68.9 (s, C_5H_4), 69.0 (s, C_5H_5), 71.0 (s, C_5H_4), 74.4 (d, $^{1}J_{CP}$ = 92.7 Hz, C≡*C*-P), 109.4 (pt, $^{2}J_{CP}$ = 5.1 Hz, *C*≡C-P). $^{31}P\{^{1}H\}$ NMR (202.53 MHz, $CDCl_3$, δ): 28.4. HRMS (ESI-TOF) $C_{48}H_{62}Cl_2Fe_2P_2Pd$ $[M]^+$ *m/z*: calcd.: 990.1437, found: 990.1377; $[M\text{-}Cl]^+$ *m/z*: calcd.: 953.1762, found: 953.1705; $[M]^{2+}$ *m/z*: calcd.: 495.0716, found: 495.0667; $[M\text{-}Cl]^{2+}$ *m/z*: calcd.: 477.5872, found: 477.5838.

4.8 Synthesis of $[PdCl_2(P(C{\equiv}CFc)(Cy)_2)_2][B(C_6F_5)_4]_2$ ([7f][$(B(C_6F_5)_4)]_2$)

80 mg (0.096 mmol) of **7f** were dissolved in 20 mL of dry tetrahydrofuran, cooled to -60 °C and 83 mg (0.096 mmol) of $[AgB(C_6F_5)_4]\cdot Et_2O$ dissolved in 20 mL of dry tetrahydrofuran were added dropwise. The resulting yellow solution was slowly warmed to ambient temperature and stirred overnight. After concentration in vacuum to 5 mL, 20 mL of *n*-hexane were added forming a dark precipitate. The supernatant layer was decanted and the precipitate was washed 3 times with 10 mL portions of *n*-hexane. The product was obtained as a dark purple solid after drying it in vacuum. Yield: 95 mg (0.040 mmol, 42 % based on **7f**). Anal. Calcd. for $C_{96}H_{62}B_2Cl_2F_{40}Fe_2P_2Pd$ (2348.04 g/mol): C, 49.11; H, 2.66. Found: C, 50.66; H, 3.89. Mp: 196 °C (dec.). IR (KBr, $\tilde{\upsilon}$/cm^{-1}): 1465 (s, P-C), 1642 (w, C=C), 2146 (s, C≡C), 2856/2934 (s, C-H). HRMS (ESI-TOF) $C_{96}H_{62}B_2Cl_2F_{40}Fe_2P_2Pd$ $[M\text{-}2B(C_6F_5)_4]^{2+}$ *m/z*: calcd.: 953.1762, found: 953.1568.

4.9 General Procedure for the Suzuki-Miyaura Reaction

2-Bromo toluene (500 mg, 2.92 mmol) or 4-chloro acetophenone (464 mg, 3.00 mmol), phenylboronic acid (470 mg, 3.85 mmol), potassium carbonate (1.21 g, 8.76 mmol) and acetyl ferrocene (114 mg, 0.50 mmol) were dissolved in a 1,4-dioxane-water mixture (12 mL, ratio 2:1, *v*:*v*). After addition of 0.1 mol% (reaction of 2-bromo toluene) or 0.5 mol% (reaction of 4-chloro acetophenone) of the appropriate catalyst (**6e**, **6f**, **7a** – **f**), the reaction mixture was stirred for 1 h at 100 °C. Samples of 1 mL were taken after 2.5, 5, 10, 20, 30, and 60 min and chromatographed on silica gel with diethyl ether as eluent. All volatiles were evaporated under reduced pressure and the conversions were determined by ^{1}H NMR spectroscopy.

4.10 General Procedure for the Mizoroki-Heck Reaction

Iodo benzene (612 mg, 3.0 mmol), *t*-butyl acrylate (397 mg, 3.1 mmol), $EtN(i\text{-}Pr)_2$ (452 mg, 3.5 mmol) and acetylferrocene (114 mg, 0.5 mmol) were dissolved in a toluene-

acetonitrile mixture (15 mL, 1:1, *v*:*v*) and loaded with 0.5 mol% of the respective catalyst (**6e**, **6f**, **7a** – **7f**). The reaction mixture was stirred at 80 °C and samples (1 mL) were taken in periods of 1 h. The samples were chomatographed on silica gel with diethyl ether as eluent. All volatiles were evaporated and the conversions were determined by ^{1}H NMR spectroscopy.

4.11 Crystal Structure Determination

The crystal and intensity collection data for **6e**, **6f**, **7b**, and **7c** are summarized in Table 5. All data were collected on an Oxford Gemini S diffractometer with graphite monochromatized Mo K_α radiation (λ = 0.71073 Å) at 100 K (**6e**, **7b**, **7c**) and graphite monochromatized Cu K_α radiation (λ = 1.54 Å) at 110 K (**6f**). The structures were solved by direct methods using *SHELXS-97* [D35] (**6e**, **6f**) or *SIR-92* [D36] (**7b**, **7c**) and refined by full-matrix least-square procedures on F^2 using *SHELXL-97* [D37]. All *non*-hydrogen atoms were refined anisotropically and a riding model was employed in the refinement of the hydrogen atom positions.

Table D5. Crystal and intensity collection data for **6e**, **6f**, **7b**, and **7c**.

	6e	**6f**	**7b**	**7c**
Formula weight	1063.07	1405.95	1260.56	1134.04
Chemical formula	$C_{40}H_{54}Cl_4Fe_2P_2Pd_2$	$C_{50}H_{64}Cl_{10}Fe_2P_2Pd_2$	$C_{54}H_{48}Cl_8Fe_2P_2Pd$	$C_{60}H_{62}Cl_2Fe_2P_2Pd$
Crystal system	Triclinic	Triclinic	Monoclinic	Triclinic
Space group	P -1	P-1	C2/c	P-1
a (Å)	7.8922(3)	11.1687(5)	16.5847(4)	10.7065(3)
b (Å)	11.3363(6)	12.0851(5)	15.3081(18)	11.1859(3)
c (Å)	12.7408(6)	12.3642(5)	21.4121(14)	11.7479(3)
α (°)	107.024(4)	108.658	90.02	70.779(2)
β (°)	92.317(3)	104.146	95.826(7)	78.395(2)
γ (°)	101.085(3)	110.544	90.0010(10)	74.904(2)
V (Å³)	1063.92(9)	1355.68(10)	5408.0(7)	1272.35(6)
ρ_{calc} (g cm^{-3})	1.659	1.722	1.548	1.480
F(000)	536	708	2544	584
Crystal dimensions (mm)	0.2 × 0.2 × 0.1	0.1 × 0.1 × 0.05	0.05 × 0.05 × 0.05	0.2 × 0.1 × 0.08
Z	1	1	4	1
Max. and min. transmission	1.00000, 0.92315	1.00000, 0.30942	1.00000, 0.74777	1.00000, 0.95654

Absorption coefficient (λ, mm^{-1})	1.854	14.834	1.349	1.120
Scan range (°)	2.92 - 26.06	4.37 - 61.99	2.97 - 26.07	2.88 - 26.00
Index ranges	$-9 \le h \le 9$, $-14 \le k \le 14$, $-15 \le l \le 15$	$-12 \le h \le 12$, $-11 \le k \le 13$, $-14 \le l \le 14$	$-20 \le h \le 20$, $-18 \le k \le 18$, $-26 \le l \le 26$	$-13 \le h \le 13$, $-11 \le k \le 13$, $-14 \le l \le 13$
Total reflections	9450	10537	15697	12216
Unique reflections	4174	4247	5113	4963
R_{int}	0.0205	0.0199	0.0844	0.0242
Data/restraints/ parameters	4174 / 0 / 226	4247 / 0 / 298	5113 / 0 / 303	4963 / 0 / 304
Goodness-of-fit on F^2	0.971	1.073	0.951	1.117
R_1[a], wR_2[a] [I 2ρ(I)]	0.0212 , 0.0451	0.0233, 0.0636	0.0439, 0.0843	0.0315, 0.0877
R_1[a], wR_2[a] (all data)	0.0306 , 0.0467	0.0262, 0.0653	0.0955, 0.1024	0.0432, 0.0939
Largest differences in peak and hole peak in final Fourier map (e $Å^{-3}$)	0.550, -0.431	0.542, -0.575	0.766, -0.692	0.708, -0.670

[a] $R_1 = [\Sigma(||F_o| - |F_c||)/\Sigma|F_o|]$; $wR_2 = [\Sigma(w(F_o^2 - F_c^2)^2)/\Sigma(wF_o^4)]^{1/2}$; $S = [\Sigma w(F_o^2 - F_c^2)^2]/(n - p)^{1/2}$. n = number of reflections, p = parameters used.

5 Supporting Information

Cyclic voltammograms of dinuclear complexes **6e** and **6f** and UV/Vis-NIR spectra of **[7f][B(C$_6$F$_5$)$_4$]$_2$** are presented. The reaction profiles for the Mizoroki-Heck coupling in presence of catalysts **6e**, **6f** and **7a** – **f** are given and are available free of charge *via* the Internet at http://www.elsevier.com. Crystallographic data of **6e** (CCDC 838741), **6f** (CCDC 838740), **7b** (CCDC 838738) and **7c** (CCDC 838739) are available as *CIF* files free of charge from the Cambridge Crystallographic Database *via* www.ccdc.cam.ac.uk/products/csd/request/.

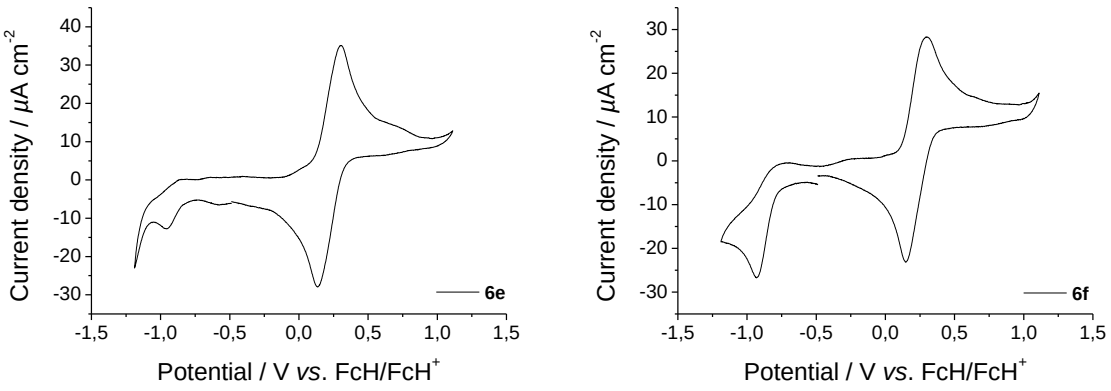

Figure D9. Electrochemical data of dichloromethane solutions containing 1.0 mmol·L^{-1} of **6e** (left) and **6f** (right) at 25 °C supporting electrolyte [(*n*-Bu$_4$)N][B(C$_6$F$_5$)$_4$] with a scan rate of 100 mV·s^{-1}.

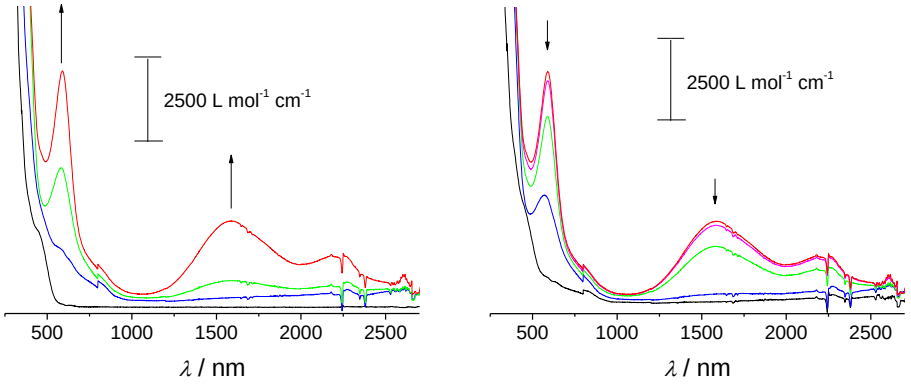

Figure D10. NIR-Spectra of **7f** at rising potentials (left: 0.0 to 0.775 V; right: 0.8 to 1.2 V *vs.* Ag/AgCl) at 25 °C, in dichloromethane, supporting electrolyte [(*n*-Bu$_4$)N][B(C$_6$F$_5$)$_4$].

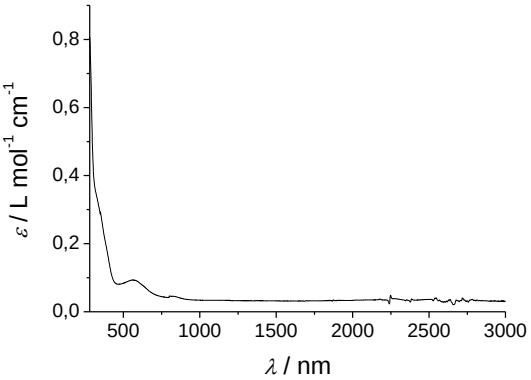

Figure D11. UV/Vis-NIR-Spectrum of **[7f][B(C$_6$F$_5$)$_4$]$_2$** at 25 °C, in dichloromethane, supporting electrolyte [(*n*-Bu$_4$)N][B(C$_6$F$_5$)$_4$].

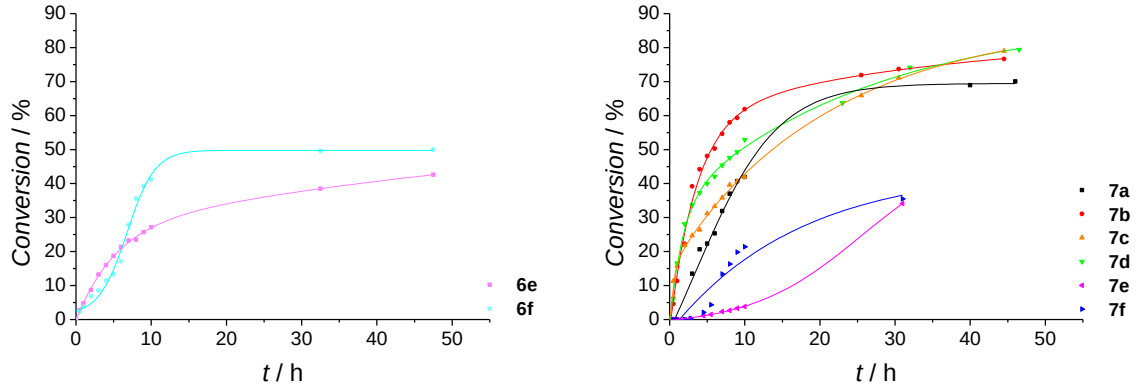

Figure D12. Reaction profile for the coupling of iodo benzene (3.0 mmol) with *t*-butyl acrylate (3.1 mmol) using **6** (left) and **7** (right) as catalysts (catalyst loading 0.5 mol%), 80 °C, EtN(*i*-Pr)$_2$ (3.5 mmol) in a mixture of toluene-acetonitrile (ratio 1:1, *v*:*v*) (15 mL)).

6 Acknowledgement

We are grateful to the Deutsche Forschungsgemeinschaft and the Fonds der Chemischen Industrie for financial support.

7 References

[D1] For example: P. J. Low, T. M. Hayes, K. A. Udachin, A. E. Goeta, J. A. K. Howard, G. D. Enright, A. J. Carty *J. Chem. Soc. Dalton Trans*. **2002** 1455 and references cited therein.

[D2] For example: a) J. Fornies, E. Lalinde, A. Martin, M. T. Moreno, A. J. Welch *J. Chem. Soc. Dalton Trans*. **1995**, *1*, 1333; b) M. Bardaji, A. Laguna *Organometallics* **2001**, *20*, 3906; c) T. Baumgartner, K. Huynth, S. Schleidt, A. J. Lough, I. Manners *Chem. Eur. J*. **2002**, *8*, 4622; d) T. De Simone, R. S. Dickson, B. W. Skelton, A. W. White *Inorg. Chim. Acta* **1995**, *240*, 323; e) I. Moldes, J. Ros *Inorg. Chim. Acta* **1995**, *232*, 75.

[D3] For example: a) H. Lang, L. Zsolnai *Chem. Ber*. **1991**, 259; b) J. Fornies, M. A. Gomez-Saso, E. Lalinde, F. Martinez, M. T. Moreno *Organometallics* **1992**, *11*, 2873; c) J. R. Berenguer, L. R. Falvello, J. Fornies, E. Lalinde, M. Tomas *Organometallics* **1993**, *12*, 6; d) M. Bardaji, A. Laguna, P. G. Jones *Organometallics*

2001, *20*, 3906; e) J. Diez, M. P. Gamasa, J. Gimeno, E. Lastra, A. Villar *Eur. J. Inorg. Chem*. **2006**, *1*, 78; f) F. Hong, Y. Ho, Y. Chang, Y. Lai *Tetrahedron* **2004**, *60*, 2639; g) H. Lang, M. Leise, A. Schmitzer *J. Organomet. Chem*. **1995**, *489*, 77.

[D4] For example: a) E. Louattini, I. Moldes, J. Suades, J. F. M. Piniella, A. Alvarez-Larena *Organometallics* **1998**, *17*, 3394; b) J. P. H. Charmant, J. Fornies, J. Gomez, E. Lalinde, M. T. Moreno, A. G. Orpen, S. Solano *Angew. Chem. Int. Ed.* **1999**, *38*, 3058; c) E. Louattani, I. Moldes, J. Suades, J. F. Piniella, A. Alvarez-Larena *Organometallics* **1998**, *17*, 3394; d) Y. Miquel, A. Igau, B. Donnadieu, J. P. Mayoral, N. Pirio, P. Meunier *J. Am. Chem. Soc*. **1998**, *120*, 3504.

[D5] For example: a) B. Li, S. Xu, H. Song, B. Wang *Eur. J. Inorg. Chem*. **2008**, 5494; b) C. Ledesma, A. Alvarez-Larena, J. Suades *J. Organomet. Chem*. **2008**, *693*, 2775; c) A. Diez, E. Lalinde, M. T. Moreno, S. Sanchez *Dalton Trans*. **2009**, 3434.

[D6] a) B. Di Credico, F. Fabrizi de Biani, L. Gonsalvi, A. Guerri, A. Ienco, F. Laschi, M. Peruzzini, G. Reginato, A. Rossin, P. Zanello *Chem. Eur. J.* **2009**, *15*, 11985; b) T. Baumgartner, M. Fiege, F. Pontzen, R. Arteaga-Müller *Organometallics* **2006**, *25*, 5657 and references cited therein.

[D7] A. Jakob, B. Milde, P. Ecorchard, C. Schreiner, H. Lang *J. Organomet. Chem*. **2008**, *693*, 3821.

[D8] A. Jakob, P. Ecorchard, M. Linseis, R. F. Winter, H. Lang *J. Organomet. Chem*. **2009**, *694*, 655.

[D9] For example: a) D. Astruc *Anal Bioanal Chem*. **2011**, *399*, 1811; b) X.-F. Wu, P. Anbarasan, H. Neumann, M. Beller *Angew. Chem. Int. Ed*. **2010**, *49*, 9047; c) R. Jana, T. P. Pathak, M. S. Sigman *Chem. Rev*. **2011**, *111*, 1417; d) D. Steinborn; *Grundlagen der metallorganischen Komplexkatalyse*, *Teubner*, Wiesbaden, **2007**; e) M. Beller, C. Bolm; *Transition Metals for Organic Synthesis* 2nd Edition, *Wiley-VCH*, Weinheim **2004**; f) B. Cornils, W. A. Herrmann; *Applied Homogeneous Catalysis with Organometallic Compounds*, *VCH*, Weinheim, **1996**; g) F. Diederich, P. J. Stang; *Metal-catalyzed Cross Coupling Reactions* 2nd Edition, *Wiley-VCH*, Weinheim, **2004**.

[D10] a) S.-Y. Liu, M. J Choi, G. C. Fu *Chem. Comm*. **2001**, 2408; b) T. E. Pickett, C. J. Richards *Tetrahedron* **2001**, *42*, 3767; c) D. Schaarschmidt, H. Lang *Cat. Commun*.

2010, *11*, 581; d) D. Schaarschmidt, H. Lang *Eur. J. Inorg. Chem*. **2010**, *30*, 4811; e) A. L. Boyes, I. R. Butler, S. C. Quayle *Tetrahedron Lett*. **1998**, *39*, 7763; f) O. V. Gusev, T. A. Peganova, A. M. Kalsin, N. V. Vologdin, P. V. Petrovskii, K. A. Layssenko, A. V. Tsvetkov, I. P. Beletskaya *Organometallics* **2006**, *25*, 2750; g) J.-C. Hierso, M. Beauperin, P. Meunier *Eur. J. Inorg. Chem*. **2007**, 3767; h) T. J. Colacot, H. A. Shea *Org. Lett*. **2004**, *6*, 3731.

[D11] For example: a) A. T. Normand, K. J. Cavell *Eur. J. Inorg. Chem*. **2008**, 2781; b) J. A. Loch, M. Albrecht, E. Peris, J. Mata, J. W. Faller, R. H. Crabtree *Organometallics* **2002**, *21*, 700; c) X. Xu, B. Xu, Y. Li, S. H. Hong *Organometallics* **2010**, *29*, 6343; d) N. Debono, A. Labande, E. Manoury, J.-C. Daran, R. Poli *Organometallics* **2010**, *29*, 1879; e) J.-Y. Lee, P.-Y. Cheng, Y.-H. Tsai, G.-R. Lin, S.-P. Liu, M.-H. Sie, H. M. Lee *Organometallics* **2010**, *29*, 3901; f) C. Zhang, M. L. Trudell *Tetrahedron Lett*. **2000**, *41*, 595.

[D12] For example: a) C. Baillie, L. Zhang, J. Xiao *J. Org. Chem*. **2004**, *69*, 7779; b) S. Nadri, M. Joshaghani, E. Rafiee *Organometallics* **2009**, *28*, 6281; c) W. A. Herrmann, M. Elison, J. Fischer, C. Köcher, G. R. J. Artus *Angew. Chem. Int. Ed. Engl*. **1995**, *34*, 2371; d) J. P. Wolfe, S. L. Buchwald *Angew. Chem. Int. Ed. Engl*. **1999**, *38*, 2413.

[D13] For example: a) W. A. Herrmann, V. P. W. Böhm *J. Organomet. Chem*. **1999**, *572*, 141; b) A. Zapf, M. Beller *Chem. Eur. J*. **2001**, *7*, 2908.

[D14] a) S. Vuoti, M. Haukka, J. Pursiainen *J. Organomet. Chem*. **2007**, *692*, 5044; b) P. Zoufala, R. Gyepes, P. Štěpnička *J. Organomet. Chem*. **2004**, *689*, 3556; c) S. Vuoti, J. Autio, M. Laitila, M. Haukka, J. Pursiainen *Eur. J. Inorg. Chem*. **2008**, 397; d) S. J. Coles, P. Faulds, M. B. Hursthouse, D. G. Kelly, G. C. Ranger, A. J. Toner, N. M. Walker *J. Organomet. Chem*. **1999**, *586*, 234; e) J. O. Yu, E. Lam, J. L. Sereda, N. C. Rampersad, A. J. Lough, C. S. Browning, D. H. Farrar *Organometallics* **2005**, *24*, 37; f) J. J. Stone, R. A. Stockland, Jr., N. P. Rath *Inorg Chim. Acta* **2003**, *342*, 236; g) R. A. Baber, A. G. Orpen, P. G. Pringle, M. J. Wilkinson, R. L. Wingad *Dalton Trans*. **2005**, 659.

[D15] a) R. P. Pinnell, C. A. Megerle, S. L. Manatt, P. A. Kroon *J. Am. Chem. Soc*. **1973**, *95*, 977; b) D. W. Allen, B. F. Taylor *J. Chem. Soc. Dalton Trans*. **1982**, *37*, 51; c) D. W. Allen, I. W. Nowell *J. Chem. Soc. Dalton Trans*. **1985**, 2505; d) A. Suarez, M. A.

Mendez-Rojas, A. Pizzano *Organometallics* **2002**, *21*, 4611; e) D. J. M. Snelders, C. van der Burg, M. Lutz, A. L. Spek, G. van Koten, R. J. M. Klein Gebbink *Chem. Cat. Chem* **2010**, *2*, 1425; f) S. Jeulin, S. Duprat de Paule, V. Ratovelomanana-Vidal, J.-P. Genet, N. Champion, P. Dellis *Angew. Chem. Int. Ed*. **2004**, *43*, 320; g) B. Milde, M. Lohan, C. Schreiner, T.; Rüffer, H. Lang *Eur. J. Inorg. Chem*. **2011**, 5437 – 5449.

[D16] a) C. A. Tolman *Chem. Rev*. **1977**, *77*, 313; b) C. A. Tolman, W. C. Seidel, L. W. Gosser *J. Am. Chem. Soc*. **1974**, *96*, 53.

[D17] a) J. M. Smith, B. C. Taverner, N. J. Coville *J. Organomet. Chem*. **1997**, *530*, 131; b) B. C. Taverner, *STERIC, Program for Calculation of Cone Angles*, University of the Witwatersrand/South Africa, **1996**.

[D18] F. Barriere, R. U. Kirss, W. E. Geiger *Organometallics* **2005**, *24*, 48.

[D19] G. Gritzner, J. Kuta *Pure Appl. Chem*. **1984**, *56*, 461.

[D20] a) J. C. Kotz, C. L. Nivert *J. Organomet. Chem*. **1973**, *52*, 387; b) J. C. Kotz, C. L. Nivert, J. M. Lieber *J. Organomet. Chem*. **1975**, *91*, 87; c) J. Podlaha, P. Štěpnička, J. Ludvik, I. Cisarova *Organometallics* **1996**, *15*, 543; d) M. A. Bennett, S. K. Bhargava, A. M. Bond, I. M. Burgar, S.-X. Guo, G. Kar, S. H. Priver, J. Wagler, A. C. Willis, A. A. J. Torriero *Dalton Trans*. **2010**, *39*, 9079.

[D21] a) B. D. Swartz, C. Nataro *Organometallics* **2005**, *24*, 2447; b) C. Amatore, M. Azzabi, A. Jutand *J. Am. Chem. Soc*. **1991**, *113*, 8375; c) C. Amatore, M. Azzabi, A. Jutand *J. Am. Chem. Soc*. **1991**, *113*, 1670.

[D22] a) F. Paul, C. Lapinte *Coord. Chem. Rev*. **1998**, *178 – 180*, 431; b) D. M. D'Alessandro, F. R. Keene *Chem. Soc. Rev*. **2006**, *35*, 424; c) W. Kaim, B. Sarkar *Coord. Chem. Rev*. **2007**, *251*, 584.

[D23] a) M. Lohan, P. Ecorchard, T. Rüffer, F. Justaud, C. Lapinte, H. Lang *Organometallics* **2009**, *28*, 1878; b) A. Hildebrandt, D. Schaarschmidt, H. Lang *Organometallics* **2011**, *30*, 556.

[D24] a) N. S. Hush *Electrochim. Acta* **1968**, *13*, 1005; b) C. Lapinte *J. Organomet. Chem*. **2008**, *693*, 793; c) D. Astruc; *Electron Transfer and Radical Processes in Transition-Metal Chemistry*; *VCH*: New York, **1995**.

[D25] B. S. Brunschwig, C. Creutz, N. Sutin *Chem. Soc. Rev*. **2002**, *31*, 168.

[D26] a) M. Sato, Y. Hayashi *Organometallics* **1996**, *15*, 721; b) M. I. Bruce, P. J. Low, F. Hartl, P. A. Humphrey, F. de Montigny, M. Jevric, C. Lapinte, G. J. Perkins, R. L. Roberts, B. W. Skelton, A. H. White *Organometallics* **2005**, *24*, 5241.

[D27] For example: a) S. Dietrich, A. Nicolai, H. Lang *J. Organomet. Chem*. **2011**, *696*, 739; b) I. P. Beletskaya, A. V. Cheprakov *Chem. Rev.* **2000**, *100*, 3009.

[D28] For example: a) W. A. Herrmann, C. Brossmer, C.-P. Reisinger, T. H. Riermeier, K. Öfele, M. Beller *Chem. Eur. J*. **1997**, *3*, 1357; b) A. F. Littke, G. C. Fu *J. Org. Chem*. **1999**, *64*, 10; c) J. P. Wolfe, R. A. Singer, B. H. Yang, S. L. Buchwald *J. Am. Chem. Soc.* **1999**, *121*, 9550; d) H. Weissman, D. Milstein *Chem. Commun*. **1999**, 1901; e) N. Kataoka, Q. Shelby, J. P. Stambuli, J. F. Hartwig *J. Org. Chem*. **2002**, *67*, 5553.

[D29] M. B. Robin, P. Day *Adv. Inorg. Chem. Radiochem*. **1967**, *10*, 247.

[D30] J. Polin, H. Schottenberger *Org. Synth*. **1996**, *73*, 262.

[D31] a) P. W. Clark, B. W. Mulraney *J. Organomet. Chem*. **1981**, *217*, 51; b) P. W. Dyer, J. Fawcett, M. J. Hanton *Organometallics* **2008**, *27*, 5082; c) N. G. Andersen, R. McDonald, B. A. Keaya *Tetrahedron: Asymmetry* **2001**, *12*, 263; d) H. Tomori, J. M. Fox, S. L. Buchwald *J. Org. Chem*. **2000**, *65*, 5334.

[D32] D. Drew, J. R. Doyle *Inorg. Synth*. **1990**, *28*, 348.

[D33] D. Zim, A. L. Monteiro, J. Dupont *Tetrahedron Lett*. **2000**, *41*, 8199.

[D34] a) M. Krejcik, M. Danek, F. Hartl *J. Electroanal. Chem*. **1991**, *317*, 179; b) A. Hildebrandt, T. Rüffer, E. Erasmus, J. C. Swarts, H. Lang *Organometallics* **2010**, *29*, 4900.

[D35] G. M. Sheldrick *Acta Cryst., Sect. A* **1990**, *46*, 467.

[D36] A. Altomare, G. Cascarano, C. Giacovazzo, A. Gualardi *J. Appl. Cryst*. **1993**, *26*, 343.

[D37] G. M. Sheldrick, SHELXL-97, *Program for Crystal Structure Refinement*, University of Göttingen, **1997**.

E (Ethynylferrocenyl)phosphine Ruthenium Complexes in Catalytic *β*-Oxopropyl Benzoate Formation

Bianca Milde, Tobias Rüffer, and Heinrich Lang*

Published in *Inorg. Chim. Acta* **2012**, *387*, 338 – 345.

1 Introduction

Since the pioneering work of P. Dixneuf, [E1a] the ruthenium-promoted synthesis of *β*-oxo esters developed rapidly and is now-a-days an integral part in homogeneous catalysis, applicable on bulky or functionalized carboxylic acids. [E2] This reaction is atom-economic, which provides an elegant alternative to classical synthesis methodologies of *β*-oxo esters. Established standard methods for the preparation of *β*-oxo esters include, for example, the preparation from propargylic alcohols by hydration-esterification steps [E3-E6] or the carboxylation of *α*-halo ketones. [E6-E13] In general, *β*-oxo esters are of versatile interest in organic synthesis and industry, because they easily form *α*-hydroxy ketones which are structural building blocks in, for example, the synthesis of natural products, [E3-E6] antibacterial compounds [E14] and intermediates for furanones and imidazoles, respectively. [E1a,E14] In addition, *β*-oxo esters can be used as photolabile protecting groups for carboxylic acids [E6,E15] or even as activated esters for peptide synthesis. [E14] Early works on the catalytic addition of terminal alkynes to carboxylic acids include the application of $[Ru_3(CO)_{12}]$ [E1,E16] or $[RuCl_3 \times 3H_2O]$ [E1a] as catalyst precursors. In recent years, several phosphine-carrying catalysts have been developed, for example, $[RuCl_2(\eta^6\text{-}p\text{-cymene})(PR_3)]$ (R = Ph, Me, OPh)[E1,E17] or $[Ru(O_2CH)(CO)_2(PPh_3)]_2$, [E1b,E2] which show high conversions and regioselectivity under mild reaction conditions using basic phosphines. In contrast, Goosen *et al.* reported that even better yields are obtained using phosphines with strong *π* acceptor ability, *e. g.* $P(Fur)_3$. [E9] In addition, also water-soluble [E3] or on MCM-41-immobilized ruthenium(II) [E19] catalysts have been developed.

We here report on the synthesis of diverse (ethynylferrocenyl)phosphino ruthenium(II) complexes and their application in the catalytic formation of *β*-oxopropyl benzoate to clarify

the question whether strong or weak electron donating groups at the phosphorus atom are responsible for the activity. Given the fact that PR_3 groups are known to be highly sensitive toward oxygen we introduced a ferrocenyl group for more stability and an additional alkynyl functionality due to its electron-withdrawing nature. Also, the preparation of a molecule featuring three ruthenium dichloro *p*-cymene units is discussed to evaluate possible synergistic and cooperative effects in the catalytic performance.

2 Experimental Section

2.1 General Procedure and Materials

All reactions were performed under an atmosphere of nitrogen using standard Schlenk techniques. Diethyl ether and dichloromethane were dried over sodium/benzophenone and calcium hydride, respectively, and purified by distillation. For filtrations Celite (purified and annealed, Erg. B.6, Riedel de Haen) was used. Column chromatographies were performed using silica with a particle size of 40 – 60 μm (230 – 400 mesh (ASTM), Becker). Compounds Fc-C≡C-PR_2 (**1a** – **1e**), [E20,E21] HC≡C-PPh_2 (**4**), [E22] $P(NEt_2)Cl_2$ (**5**) [E23] and $[RuCl_2(\eta^6\text{-}p\text{-cymene})]_2$ (**7**) [E24] were synthesized according to published procedures. All other chemicals were obtained from commercial suppliers and used without further purification.

The ^1H NMR spectra were recorded on a Bruker Avance III 500 spectrometer working at 500.3 MHz. The $^{13}C\{^1H\}$ and $^{31}P\{^1H\}$ NMR spectra were recorded at 125.7 MHz and 202.5 MHz, respectively. Chemical shifts are reported in δ units (parts per million) downfield from tetramethylsilane with the solvent as reference signal (^1H NMR: standard internal $CDCl_3$, δ 7.26; $^{13}C\{^1H\}$ NMR: standard internal $CDCl_3$, δ 77.16; $^{31}P\{^1H\}$ NMR: standard external rel. 85 % H_3PO_4, δ 0.0 and $P(OMe)_3$, δ 139.0). High resolution mass spectra were recorded on a Bruker Daltonik micrOTOF-QII spectrometer (ESI-TOF). Elemental analyses were carried out on a Thermo FlashAE 1112 series instrument. Melting points of analytical pure samples were determined by a Gallenkamp MFB 595 010 M melting point apparatus. FT IR spectra were recorded on a Thermo Nicolet IR 200 spectrometer using either KBr pellets or NaCl plates.

2.2 General Procedure for the Synthesis of Ruthenium Complexes 3a – 3e and 10

0.5 g of **1** or **9** and 0.5 or 1.5 equivalents of $[RuCl_2(\eta^6\text{-}p\text{-cymene})]_2$ (**2**) were dissolved in 40 mL of dry dichloromethane. The solution was stirred for 2 h at ambient temperature. Afterwards, the solvent was removed in vacuum and the residue was washed 5 - 6 times with 5 mL portions of diethyl ether. After drying in vacuum the appropriate complexes were obtained as orange solids.

2.2.1 Synthesis of (FcC≡C)Ph_2P($RuCl_2(\eta^6\text{-}p\text{-cymene})$) (3a)

Following the synthesis methodology described above, 0.5 g (1.27 mmol) of **1a** were reacted with 0.39 g (0.63 mmol) of **2**. After appropriate work-up, **3a** was isolated as an air stable orange solid. Yield: 0.88 g (1.22 mmol, 97 % based on **2**). Anal. Calcd. for $C_{34}H_{33}Cl_2FePRu \cdot 1/4\ CH_2Cl_2$ (721.65 g/mol): C, 57.00; H, 4.68. Found: C, 56.96; H, 4.66. Mp.: 200 °C (dec.). IR (KBr, $\tilde{\upsilon}$/cm^{-1}): 1436 (m, P-C), 2153 (m, C≡C). ^{1}H NMR (500.30 MHz, $CDCl_3$, δ): 1.23 (d, $^3J_{HH}$ = 6.9 Hz, 6 H, CH(CH_3)$_2$), 2.00 (s, 3 H, CH_3), 2.95 (sept, $^3J_{HH}$ = 7.0 Hz, 1 H, CH(CH$_3$)$_2$), 4.30 (s, 5 H, C_5H_5), 4.37 (pt, $^3J_{HH}$ = 1.9 Hz, 2 H, C_5H_4), 4.62 (pt, $^3J_{HH}$ = 1.9 Hz, 2 H, C_5H_4), 5.23 – 5.26 (m, 2 H, C_6H_4), 5.30 (s, CH_2Cl_2), 5.31 – 5.33 (m, 2 H, C_6H_4), 7.33 – 7.39 (m, 6 H, H^{m,p}/C_6H_5), 8.01 – 8.09 (m, 4 H, H^o/ C_6H_5). ^{13}C{^{1}H} NMR (125.81 MHz, $CDCl_3$, δ): 17.7 (s, *C*H$_3$), 22.2 (s, CH(*C*H$_3$)$_2$), 30.5 (s, *C*H(CH$_3$)$_2$), 53.57 (s, *C*H$_2$Cl$_2$), 62.1 (d, $^3J_{CP}$ = 3.0 Hz, C^i/*C*$_5$H$_4$), 70.1 (s, C$^\beta$/*C*$_5$H$_4$), 70.4 (s, *C*$_5$H$_5$), 72.4 (d, $^4J_{CP}$ = 1.0 Hz, C$^\alpha$/*C*$_5$H$_4$), 78.3 (d, $^1J_{CP}$ = 53.3 Hz, C≡*C*-P), 86.8 (d, $^2J_{CP}$ = 6.2 Hz, *C*$_6$H$_4$), 90.6 (d, $^2J_{CP}$ = 4.3 Hz, *C*$_6$H$_4$), 96.0 (s, C^i/*C*$_6$H$_4$), 109.6 (s, C^i/*C*$_6$H$_4$), 110.4 (d, $^2J_{CP}$ = 13.4 Hz, *C*≡C-P), 128.1 (d, $^3J_{CP}$ = 10.8 Hz, C^m/*C*$_6$H$_5$), 130.4 (d, $^4J_{CP}$ = 2.7 Hz, C^p/*C*$_6$H$_5$), 132.7 (d, $^1J_{CP}$ = 54.2 Hz, C^i/*C*$_6$H$_5$), 133.3 (d, $^2J_{CP}$ = 10.3 Hz, C^o/*C*$_6$H$_5$). ^{31}P{^{1}H} NMR (202.53 MHz, $CDCl_3$, δ): -3.3. HRMS (ESI-TOF) $C_{34}H_{33}Cl_2FePRu$ $[M+K]^+$ *m/z*: calcd.: 740.9717, found: 740.9639; $[M\text{-}Cl]^+$ *m/z*: calcd.: 665.0404, found: 665.0448.

2.2.2 Synthesis of (FcC≡C)(*o*-Tol)$_2$P($RuCl_2(\eta^6\text{-}p\text{-cymene})$) (3b)

0.5 g (1.18 mmol) of **1b** were reacted with 0.36 g (0.59 mmol) of **2**. After appropriate work-up, complex **3b** was isolated as orange solid. Yield: 0.71 g (0.97 mmol, 82 % based on **2**). Anal. Calcd. for $C_{36}H_{37}Cl_2FePRu$ (728.47 g/mol): C, 59.35; H, 5.12. Found: C, 59.42; H, 5.13. Mp.: 195 °C. IR (KBr, $\tilde{\upsilon}$/cm^{-1}): 1468 (m, P-C), 2150 (s, C≡C). ^{1}H NMR (500.30 MHz, $CDCl_3$, δ): 1.08 (d, $^3J_{HH}$ = 7.0 Hz, 6 H, CH(CH_3)$_2$), 2.10 (s, 3 H, CH_3), 2.16 (s, 6 H, 2-CH_3C$_6$H$_4$), 2.86 (sept, $^3J_{HH}$ = 7.0 Hz, 1 H, CH(CH$_3$)$_2$), 4.18 (s, 5 H, C_5H_5), 4.30 (pt, $^3J_{HH}$ = 1.9

Hz, 2 H, C_5H_4), 4.52 (pt, $^3J_{HH}$ =1.9 Hz, 2 H, C_5H_4), 5.04 – 5.07 (m, 2 H, C_6H_4), 5.31 – 5.34 (m, 2 H, C_6H_4), 7.09 – 7.14 (m, 2 H, H^p/2-$CH_3C_6H_4$), 7.29 – 7.35 (m, 4 H, H^m/2-$CH_3C_6H_4$), 8.43 – 8.52 (m, 2 H, H^o/2-$CH_3C_6H_4$). $^{13}C\{^1H\}$ NMR (125.81 MHz, $CDCl_3$, δ): 17.5 (s, CH_3), 21.8 (s, $CH(CH_3)_2$), 22.5 (d, $^3J_{CP}$ = 4.9 Hz, 2-$CH_3C_6H_4$), 30.0 (s, $CH(CH_3)_2$), 62.7 (d, $^3J_{CP}$ = 3.4 Hz, C^i/C_5H_4), 69.9 (s, C^β/C_5H_4), 70.3 (s, C_5H_5), 72.1 (d, $^4J_{CP}$ = 0.6 Hz, C^α/C_5H_4), 79.6 (C≡C-P[*)]), 86.6 (d, $^2J_{CP}$ = 5.3 Hz, C_6H_4), 91.5 (d, $^2J_{CP}$ = 5.1 Hz, C_6H_4), 95.2 (s, C^i/C_6H_4), 109.5 (d, $^2J_{CP}$ = 13.5 Hz, C≡C-P), 109.6 (s, C^i/C_6H_4), 125.7 (d, J_{CP} = 12.5 Hz, 2-$CH_3C_6H_4$), 130.4 (d, J_{CP} = 16.7 Hz, 2-$CH_3C_6H_4$), 130.9 (d, J_{CP} = 2.4 Hz, 2-$CH_3C_6H_4$), 131.8 (d, J_{CP} = 7.9 Hz, 2-$CH_3C_6H_4$), 135.4 (m, 2-$CH_3C_6H_4$), 141.9 (d, J_{CP} = 5.9 Hz, 2-$CH_3C_6H_4$). $^{31}P\{^1H\}$ NMR (202.53 MHz, $CDCl_3$, δ): -9.1. HRMS (ESI-TOF) $C_{36}H_{37}Cl_2FePRu$ $[M]^+$ *m/z*: calcd.: 728.0403, found: 728.0413; $[M\text{-}Cl]^+$ *m/z*: calcd.: 693.0717, found: 693.0709. [*)] signal concealed by $CDCl_3$.

2.2.3 Synthesis of (FcC≡C)(Fur)$_2$P(RuCl$_2$(η^6-*p*-cymene)) (3c)

0.5 g (1.34 mmol) of **1c** were reacted with 0.41 g (0.67 mmol) of **2**. After appropriate work-up, **3c** was isolated as an orange solid. Yield: 0.88 g (1.26 mmol, 94 % based on **2**). Anal. Calcd. for $C_{30}H_{29}Cl_2FeO_2PRu \cdot 1/5\ CH_2Cl_2$ (697.33 g/mol): C, 52.02; H, 4.25. Found: C, 52.03; H, 4.49. Mp.: 175 °C. IR (KBr, $\tilde{\upsilon}$/cm^{-1}): 1007 (s, C-O), 1458 (w, P-C), 2159 (s, C≡C). ^1H NMR (500.30 MHz, $CDCl_3$, δ): 1.18 (d, $^3J_{HH}$ = 6.9 Hz, 6 H, $CH(CH_3)_2$), 2.06 (s, 3 H, CH_3), 2.91 (sept, $^3J_{HH}$ = 6.9 Hz, 1 H, $CH(CH_3)_2$), 4.27 (s, 5 H, C_5H_5), 4.31 (pt, $^3J_{HH}$ = 1.9 Hz, 2 H, C_5H_4), 4.58 (pt, $^3J_{HH}$ = 1.9 Hz, 2 H, C_5H_4), 5.30 (s, CH_2Cl_2), 5.49 – 5.51 (m, 2 H, C_6H_4), 5.54 – 5.57 (m, 2 H, C_6H_4), 6.48 (dt, $^4J_{HP}$ = 1.6 Hz, $^3J_{HH}$ = 3.4 Hz, $^3J_{HH}$ = 1.6 Hz, 2 H, H^4/C_4H_3O), 7.21 (m, 2 H, H^3/C_4H_3O), 7.68 (m, 2 H, H^5/C_4H_3O). $^{13}C\{^1H\}$ NMR (125.81 MHz, $CDCl_3$, δ): 17.8 (s, CH_3), 22.0 (s, $CH(CH_3)_2$), 30.4 (s, $CH(CH_3)_2$), 53.53 (s, CH_2Cl_2), 61.7 (d, $^3J_{CP}$ = 3.7 Hz, C^i/C_5H_4), 70.1 (s, C^β/C_5H_4), 70.7 (s, C_5H_5), 72.5 (d, $^4J_{CP}$ = 0.8 Hz, C_α/C_5H_4), 74.0 (d, $^1J_{CP}$ = 112.6 Hz, C≡C-P), 86.9 (d, $^2J_{CP}$ = 6.7 Hz, C_6H_4), 90.9 (d, $^2J_{CP}$ = 5.4 Hz, C_6H_4), 96.7 (s, C^i/C_6H_4), 109.0 (d, $^2J_{CP}$ = 18.1 Hz, C≡C-P), 109.5 (s, C^i/C_6H_4), 111.6 (d, $^3J_{CP}$ = 7.6 Hz, C^4/C_4H_3O), 123.0 (d, $^2J_{CP}$ = 17.7 Hz, C^3/C_4H_3O), 144.5 (d, $^1J_{CP}$ = 81.0 Hz, C^2/C_4H_3O), 147.4 (d, $^4J_{CP}$ = 5.6 Hz, C^5/C_4H_3O). $^{31}P\{^1H\}$ NMR (202.53 MHz, $CDCl_3$, δ): -26.0. HRMS (ESI-TOF) $C_{30}H_{29}Cl_2FeO_2PRu$ $[M]^+$ *m/z*: calcd.: 679.9674, found: 679.9673.

2.2.4 Synthesis of (FcC≡C)(*t*-Bu)$_2$P(RuCl$_2$(η^6-*p*-cymene)) (3d)

Reaction of 0.5 g (1.41 mmol) of **1d** with 0.42 g (0.69 mmol) of **2** gave, after appropriate work-up, complex **3d** which was isolated as an air stable orange solid. Yield: 0.87 g (1.28 mmol, 93 % based on **2**). Anal. Calcd. for $C_{30}H_{41}Cl_2FePRu \cdot 1/4\ CH_2Cl_2$ (681.68 g/mol): C, 53.30; H, 6.14. Found: C, 53.26; H, 6.22. Mp.: 151 °C (dec.). IR (KBr, $\tilde{\upsilon}$/cm^{-1}): 1467 (w, P-C), 2158 (s, C≡C), 2959 (s, C-H). ^{1}H NMR (500.30 MHz, $CDCl_3$, δ): 1.30 (d, $^3J_{HH}$ = 6.9 Hz, 6 H, CH(CH_3)$_2$), 1.51 (d, $^3J_{HP}$ = 14.8 Hz, 18 H, C(CH_3)$_3$), 2.15 (s, 3 H, CH_3), 3.12 (sept, $^3J_{HH}$ = 6.5 Hz, 1 H, CH(CH$_3$)$_2$), 4.31 (s, 5 H, C$_5H_5$), 4.37 (m, 2 H, C$_5H_4$), 4.57 (m, 2 H, C$_5H_4$), 5.30 (s, CH_2Cl$_2$), 5.40 – 5.48 (m, 4 H, C$_6H_4$). ^{13}C{^{1}H} NMR (125.81 MHz, $CDCl_3$, δ): 17.7 (s, *C*H$_3$), 22.2 (s, CH(*C*H$_3$)$_2$), 29.5 (s, *C*H(CH$_3$)$_2$), 30.6 (d, $^2J_{CP}$ = 3.5 Hz, C(*C*H$_3$)$_3$), 39.3 (d, $^1J_{CP}$ = 14.8 Hz, *C*(CH$_3$)$_3$), 53.52 (s, *C*H$_2$Cl$_2$), 62.8 (d, $^3J_{CP}$ = 2.3 Hz, C^i/*C*$_5$H$_4$), 69.9 (s, *C*$_5$H$_4$), 70.0 (s, *C*$_5$H$_5$), 72.0 (s, *C*$_5$H$_4$), 80.8 (d, $^1J_{CP}$ = 33.0 Hz, C≡*C*-P), 89.2 (d, $^2J_{CP}$ = 5.0 Hz, *C*$_6$H$_4$), 89.3 (d, $^2J_{CP}$ = 4.6 Hz, *C*$_6$H$_4$), 97.2 (s, *C*$_6$H$_4$), 106.5 (s, *C*$_6$H$_4$), 108.1 (d, $^2J_{CP}$ = 2.2 Hz, *C*≡C-P). ^{31}P{^{1}H} NMR (202.53 MHz, $CDCl_3$, δ): 26.7. HRMS (ESI-TOF) $C_{30}H_{41}Cl_2FePRu$ [M-Cl]$^+$ *m/z*: calcd.: 625.1029, found: 625.0936; [M-(η^6-*p*-cymen)RuCl$_2$]$^+$ *m/z*: calcd.: 354.1194, found: 354.1188.

2.2.5 Synthesis of (FcC≡C)(Cy)$_2$P(RuCl$_2$(η^6-*p*-cymene)) (3e)

Reaction of 0.5 g (1.23 mmol) of **1e** with 0.38 g (0.62 mmol) of **2** gave, after appropriate work-up, **3e** which was isolated as an orange solid. Yield: 0.86 g (1.17 mmol, 94 % based on **2**). Anal. Calcd. for $C_{34}H_{45}Cl_2FePRu \cdot 1/4\ CH_2Cl_2$ (733.75 g/mol): C, 56.06; H, 6.25. Found: C, 56.37; H, 6.49. Mp.: 201 °C. IR (KBr, $\tilde{\upsilon}$/cm^{-1}): 1447 (m, P-C), 2154 (m, C≡C), 2924 (vs, C-H). ^{1}H NMR (500.30 MHz, $CDCl_3$, δ): 1.25 (d, $^3J_{HH}$ = 6.9 Hz, 6 H, CH(CH_3)$_2$), 1.22 – 1.35 (m, 6 H, C$_6H_{11}$), 1.54 –1.69 (m, 6 H, C$_6H_{11}$), 1.76 – 1.81 (m, 4 H, C$_6H_{11}$), 1.90 – 1.94 (m, 2 H, C$_6H_{11}$), 2.01 – 2.03 (m, 2 H, C$_6H_{11}$), 2.11 (s, 3 H, CH_3), 2.47 – 2.53 (m, 2 H, H^1/C$_6H_{11}$), 3.02 (sept, $^3J_{HH}$ = 6.9 Hz, CH(CH$_3$)$_2$), 4.28 (s, 5 H, C$_5H_5$), 4.36 (pt, $^3J_{HH}$ = 1.8 Hz, 2 H, C$_5H_4$), 4.57 (pt, $^3J_{HH}$ = 1.8 Hz, 2 H, C$_5H_4$), 5.29 (s, CH_2Cl$_2$), 5.39 – 5.42 (m, 4 H, C$_6H_4$). ^{13}C{^{1}H} NMR (125.81 MHz, $CDCl_3$, δ): 17.7 (s, *C*H$_3$), 22.2 (s, CH(*C*H$_3$)$_2$), 26.2 (s, *C*$_6$H$_{11}$), 26.9 (d, J_{CP} = 11.0 Hz, *C*$_6$H$_{11}$), 27.3 (d, J_{CP} = 13.3 Hz, *C*$_6$H$_{11}$), 27.9 (d, J_{CP} = 4.0 Hz, *C*$_6$H$_{11}$), 28.7 (m, *C*$_6$H$_{11}$), 29.9 (s, *C*H(CH$_3$)$_2$), 34.3 (d, $^1J_{CP}$ = 26.4 Hz, C$_1$/*C*$_6$H$_{11}$), 53.55 (s, *C*H$_2$Cl$_2$), 62.8 (d, $^3J_{CP}$ = 2.7 Hz, C^i/*C*$_5$H$_4$), 69.9 (s, *C*$_5$H$_4$), 70.3 (s, *C*$_5$H$_5$), 72.3 (s, *C*$_5$H$_4$), 79.0 (d, $^1J_{CP}$ = 65.1 Hz, C≡*C*-P), 88.5 (d, $^2J_{CP}$ = 4.8 Hz, *C*$_6$H$_4$), 90.0 (d, $^2J_{CP}$ = 4.5 Hz, *C*$_6$H$_4$), 97.3 (s, *C*$_6$H$_4$), 105.1 (s,

C_6H_4), 108.1 (d, $^2J_{CP}$ = 4.5 Hz, *C*≡C-P). $^{31}P\{^1H\}$ NMR (202.53 MHz, $CDCl_3$, δ): 14.4. HRMS (ESI-TOF) $C_{34}H_{45}Cl_2FePRu$ $[M\text{-}Cl]^+$ *m/z*: calcd.: 677.1343, found: 677.1249.

2.3 Synthesis of $(Et_2N)P(C{\equiv}C\text{-}PPh_2)_2$ (6)

Phosphine **6** was synthesized by a modified literature procedure. [E22] To 2.0 g (9.52 mmol) of **4** dissolved in 50 mL of dry diethyl ether, 3.8 mL (9.5 mmol) of *n*-BuLi were added dropwise at -50 °C. After stirring the solution for 30 min at ambient temperature it was again cooled to -30 °C and 0.69 mL (826 mg, 4.75 mmol) of Cl_2PNEt_2 (**5**) were added dropwise. The reaction mixture was stirred at ambient temperature for 1 h and then filtered through a pad of Celite. The resulting solution was evaporated to dryness and the product was obtained as brown viscous oil in high purity. Phosphine **6** was used without further purification steps. Yield: 2.4 g (4.68 mmol, 97 % based on **5**). $C_{32}H_{30}NP_3$ (521.51 g/mol). $^{31}P\{^1H\}$ NMR (101.249 MHz, $CDCl_3$, δ): -34.0 (d, $^3J_{PP}$ = 2.7 Hz, Ph_2P), -0.9 (t, $^3J_{PP}$ = 3.2 Hz, Et_2NP).

2.4 Synthesis of $P(C{\equiv}CFc)(C{\equiv}CPPh_2)_2$ (9)

To a solution of 2.4 g (4.68 mmol) of **6** in 50 mL of dry diethyl ether, 10 mL of a 1.0 M solution of HCl (2 eq) in diethyl ether were added slowly at ambient temperature. The resulting mixture was stirred for 1 h and then added dropwise to a cooled solution (-50 °C) of **8** in dry diethyl ether. Compound **8** was prepared by dropwise addition of 1.7 mL (4.25 mmol) of *n*-BuLi to a solution of 0.89 g (4.26 mmol) of ethynyl ferrocene in 30 mL of dry diethyl ether. The resulting mixture was stirred for 1 h at ambient temperature and was then concentrated in vacuum. The residue was purified by column chromatography on silica gel (column size: 4 × 20 cm) using *n*-hexane as eluent. Phosphine **9** was obtained as a red solid. Yield: 1.63 g (2.48 mmol, 58 % based on *n*-BuLi). Anal. Calcd. for $C_{40}H_{29}FeP_3$ (658.42 g/mol): C, 72.97; H, 4.44. Found: C, 73.33; H, 4.62. IR (NaCl, $\tilde{\upsilon}$/cm^{-1}): 1434 (m, P-C), 2151 (s, C≡C), 2175 (m, C≡C). ^1H NMR (250.130 MHz, $CDCl_3$, δ): 4.26 (s, 5 H, C_5H_5), 4.30 (pt, $^3J_{HH}$ = 1.9 Hz, 2 H, C_5H_4), 4.57 (pt, $^3J_{HH}$ = 1.9 Hz, C_5H_4), 7.32 – 7.40 (m, 12 H, $H^{m,p}/C_6H_5$), 7.63 – 7.71 (m, 8 H, H^o/C_6H_5). $^{13}C\{^1H\}$ NMR (62.895 MHz, $CDCl_3$, δ): 62.8 (d, $^3J_{CP}$ = 0.5 Hz, C^i/C_5H_4), 69.8 (s, C^β/C_5H_4), 70.4 (s, C_5H_5), 72.4 (d, $^4J_{CP}$ = 1.8 Hz, C^α/C_5H_4), 74.1 (dpt, $^1J_{CP}$ = 13.4 Hz, $^4J_{CP}$ = 2.3 Hz, FcC≡*C*P), 99.7 (dpt, $^1J_{CP}$ = 3.8 Hz, $^2J_{CP}$ = 2.3 Hz, $Ph_2PC{\equiv}C$), 105.6 (dd, $^1J_{CP}$ = 19.1 Hz, $^2J_{CP}$ = 4.2 Hz, $Ph_2PC{\equiv}C$), 107.5 (d, $^2J_{CP}$ = 13.7 Hz, Fc*C*≡CP), 128.9 (d, $^3J_{CP}$ = 7.8 Hz, C^m/C_6H_5), 129.4 (s, C^p/C_6H_5), 132.9 (d, $^2J_{CP}$ = 20.6 Hz, C^o/C_6H_5), 135.1 (d, $^1J_{CP}$ = 6.2 Hz, $^4J_{CP}$ = 1.0 Hz, C^i/C_6H_5). $^{31}P\{^1H\}$ NMR (101.249 MHz, $CDCl_3$, δ): -

88.2 (t, $^{3}J_{PP}$ = 4.8 Hz, FcC≡C*P*), -32.7 (d, $^{3}J_{PP}$ = 4.8 Hz, Ph_2*P*C≡C). HRMS (ESI-TOF) $C_{40}H_{29}FeP_3$ $[M]^+$ *m/z*: calcd.: 658.0827, found: 658.0778.

2.5 Synthesis of (RuCl$_2$(η^6-*p*-cymene))(FcC≡C)P(C≡CPPh$_2$(RuCl$_2$(η^6-*p*-cymene)))$_2$ (10)

0.5 g (0.76 mmol) of **9** were reacted with 0.70 g (1.14 mmol) of **2**. After appropriate work-up (Chapter E2.2), **10** was isolated as an orange solid. Yield: 1.18 g (0.75 mmol, 99 % based on **9**). Anal. Calcd. for $C_{70}H_{71}Cl_6FeP_3Ru_3$ (1577.01 g/mol): C, 53.31; H, 4.54. Found: C, 53.05; H, 4.45. Mp.: 150 °C. IR (NaCl, $\tilde{\upsilon}$/cm^{-1}): 1435 (m, P-C), 2155 (m, C≡C), 2179 (m, C≡C). ^{1}H NMR (250.130 MHz, $CDCl_3$, δ): 0.98 (d, $^{3}J_{HH}$ = 4.5 Hz, 6 H, CH(C*H*$_3$)$_2$), 1.00 (d, $^{3}J_{HH}$ = 4.5 Hz, 6 H, CH(C*H*$_3$)$_2$), 1.23 (d, $^{3}J_{HH}$ = 6.0 Hz, 6 H, CH(C*H*$_3$)$_2$), 1.81 (s, 6 H, C*H*$_3$), 2.00 (s, 3 H, C*H*$_3$), 2.55 (sept, $^{3}J_{HH}$ = 6.9 Hz, 2 H, C*H*(CH$_3$)$_2$), 2.88 (sept, $^{3}J_{HH}$ = 6.9 Hz, 1 H, C*H*(CH$_3$)$_2$), 4.23 (s, 5 H, C$_5$*H*$_5$), 4.36 (pt, $^{3}J_{HH}$ = 1.9 Hz, C$_5$*H*$_4$), 4.58 (pt, $^{3}J_{HH}$ = 1.9 Hz, C$_5$*H*$_4$), 5.22 – 5.25 (m, 2 H, C$_6$*H*$_4$), 5.39 – 5.49 (m, 6 H, C$_6$*H*$_4$), 5.56 – 5.58 (m, 2 H, C$_6$*H*$_4$), 5.64 – 5.67 (m, 2 H, C$_6$*H*$_4$), 7.27 – 7.31 (m, 6 H, H^{m,p}/C$_6$*H*$_5$), 7.35 – 7.38 (m, 6 H, H^{m,p}/C$_6$*H*$_5$), 8.01 – 8.09 (m, 8 H, H^{o}/ C$_6$*H*$_5$). ^{13}C{^{1}H} NMR (125.81 MHz, $CDCl_3$, *δ*): 17.6 (s, *C*H$_3$), 18.1 (s, *C*H$_3$), 21.7 (s, CH(*C*H$_3$)$_2$), 22.2 (s, CH(*C*H$_3$)$_2$), 22.3 (s, CH(*C*H$_3$)$_2$), 30.4 (s, *C*H(CH$_3$)$_2$), 30.8 (s, *C*H(CH$_3$)$_2$), 60.1 (d, $^{3}J_{CP}$ = 3.6 Hz, C^{i}/*C*$_5$H$_4$), 70.8 (s, C$^{\beta}$/*C*$_5$H$_4$), 70.9 (s, *C*$_5$H$_5$), 72.7 (m, C$^{\alpha}$/*C*$_5$H$_4$), 73.5 (d, $^{1}J_{CP}$ = 127.4 Hz, FcC≡*C*P), 86.4 (d, $^{2}J_{CP}$ = 5.4 Hz, *C*$_6$H$_4$), 87.3 (d, $^{2}J_{CP}$ = 6.0 Hz, *C*$_6$H$_4$), 88.0 (d, $^{2}J_{CP}$ = 6.2 Hz, *C*$_6$H$_4$), 89.9 (d, $^{2}J_{CP}$ = 7.0 Hz, *C*$_6$H$_4$), 90.0 (d, $^{2}J_{CP}$ = 4.3 Hz, *C*$_6$H$_4$), 91.4 (d, $^{2}J_{CP}$ = 5.0 Hz, *C*$_6$H$_4$), 97.1 (s, C^{i}/*C*$_6$H$_4$), 97.6 (s, C^{i}/*C*$_6$H$_4$), 97.9 (s, C^{i}/*C*$_6$H$_4$), 102.0 (d, $^{1}J_{CP}$ = 9.1 Hz, Ph_2PC≡*C*), 102.5 (d, $^{1}J_{CP}$ = 8.7 Hz, Ph_2P*C*≡C), 109.0 (s, C^{i}/*C*$_6$H$_4$), 110.5 (d, $^{2}J_{CP}$ = 23.4 Hz, Fc*C*≡CP), 110.9 (s, C^{i}/*C*$_6$H$_4$), 128.3 (d, $^{3}J_{CP}$ = 10.9 Hz, C^{m}/*C*$_6$H$_5$), 128.8 (d, $^{3}J_{CP}$ = 10.9 Hz, C^{m}/*C*$_6$H$_5$), 130.1 (d, $^{1}J_{CP}$ = 53.4 Hz, C^{i}/*C*$_6$H$_5$), 130.8 (d, $^{4}J_{CP}$ = 2.3 Hz, C^{p}/*C*$_6$H$_5$), 130.9 (d, $^{4}J_{CP}$ = 2.2 Hz, C^{p}/*C*$_6$H$_5$), 132.3 (d, $^{1}J_{CP}$ = 52.5 Hz, C^{i}/*C*$_6$H$_5$), 133.0 (d, $^{2}J_{CP}$ = 10.8 Hz, C^{o}/*C*$_6$H$_5$), 134.4 (d, $^{2}J_{CP}$ = 10.5 Hz, C^{o}/*C*$_6$H$_5$). ^{31}P{^{1}H} NMR (101.249 MHz, $CDCl_3$, *δ*): -44.8 (s, FcC≡C*P*), -0.8 (s, Ph_2*P*C≡C). HRMS (ESI-TOF) $C_{70}H_{71}FeP_3Ru_3Cl_6$ $[M]^+$ *m/z*: calcd.: 1578.9370, found: 1578.9253; [M-RuCl$_2$(η^6-*p*-cymene)]$^+$ *m/z*: calcd.: 1270.9866, found: 1270.9751.

2.6 General Procedure for the Catalytic Reactions

122 mg (1.0 mmol) of benzoic acid, 77 mg (0.5 mmol) of acenaphthene (internal standard) and 1.0 mol% (based in Ru) of the respective catalyst (**3a** – **3e** or **10**) were dissolved in 15 mL of chloro benzene. After addition of 0.87 mL (84 mg, 1.5 mmol) of propargyl alcohol the

reaction mixture was stirred at 80 °C and samples (0.5 mL) were taken in periods of 1 h. The samples were dried in vacuum and the conversions were determined by ^{1}H NMR spectroscopy.

2.7 Crystal Structure Determination

The crystal and intensity collection data for **3b**, **3c**, and **10** are summarized in Table E1. The data were collected on an Oxford Gemini S diffractometer with graphite monochromatized Mo K_α radiation (λ = 0.71073 Å) at 100 K. The structures were solved by direct methods using *SHELXS-97* [E25] and refined by full-matrix least-square procedures on F^2 using *SHELXL-97*. [E26] All *non*-hydrogen atoms were refined anisotropically and a riding model was employed in the refinement of the hydrogen atom positions.

Table E1. Crystal and intensity collection data for **3b**, **3c** and **10**.

	3b	**3c**	**10**
Formula weight	847.81	680.32	3681.84
Chemical formula	$C_{37}H_{38}Cl_5FePRu$	$C_{30}H_{29}Cl_2FeO_2PRu$	$C_{145}H_{149}Cl_{25}Fe_2P_6Ru_6$
Crystal system	triclinic	triclinic	triclinic
Space group	*P*-1	*P*-1	*P*-1
a (Å)	10.1745(3)	9.7028(12)	12.1915(5)
b (Å)	12.3193(4)	10.8658(6)	14.3215(5)
c (Å)	15.2195(4)	13.8545(7)	25.1595(10)
α (°)	81.358	74.085	96.926
β (°)	87.010	78.058	103.679
γ (°)	69.003	85.551	96.136
V (Å^3)	1760.76(9)	1373.9(2)	4195.2(3)
ρ_{calc} (g cm^{-3})	1.599	1.644	1.457
F(000)	860	688	1850
Crystal dimensions (mm)	0.3 × 0.3 × 0.3	0.2 × 0.2 × 0.1	0.2 × 0.2 × 0.1
Z	2	2	1
Max. and min. transmission	1.00000, 0.95682	1.00000, 0.94896	1.00000, 0.93550
Absorption coefficient (λ, mm^{-1})	1.293	1.357	1.192
Scan range (°)	3.03 - 25.00	2.78 - 25.00	3.27 - 25.00
Index ranges	$-8 \le h \le 12$ $-14 \le k \le 14$	$-11 \le h \le 11$ $-12 \le k \le 12$	$-14 \le h \le 14$ $-17 \le k \le 16$

	$-18 \le l \le 18$	$-16 \le l \le 16$	$-29 \le l \le 29$
Total reflections	14838	12978	33943
Unique reflections	6158	4798	14712
R_{int}	0.0234	0.0234	0.0234
Data / restraints / parameters	6158 / 0 / 406	4798 / 0 / 334	14712 / 66 / 868
Goodness-of-fit on F^2	1.043	1.107	1.059
R_1[a], wR_2[a] [I $2\sigma(I)$]	0.0508, 0.1249	0.0200, 0.0508	0.0527, 0.1430
R_1[a], wR_2[a] (all data)	0.0622, 0.1298	0.0252, 0.0526	0.0616, 0.1494
Largest differences in peak and hole peak in final Fourier map (e Å^{-3})	1.821, -1.155	0.450, -0.391	2.737, -1.691

[a] $R_1 = [\Sigma(||F_o| - |F_c||)/\Sigma|F_o|]$; $wR_2 = [\Sigma(w(F_o^2 - F_c^2)^2)/\Sigma(wF_o^4)]^{1/2}$; $S = [\Sigma w(F_o^2 - F_c^2)^2]/(n - p)^{1/2}$. n = number of reflections, p = parameters used.

3 Results and Discussion

The (ethynylferrocenyl)phosphino ruthenium(II) complexes (FcC≡C)R_2P(RuCl_2(η^6-*p*-cymene)) (**3a**, R = Ph; **3b**, R = *o*-Tol; **3c**, R = Fur; **3d**, R = *t*-Bu; **3e**, R = Cy; *p*-cymene = 1-*i*-Pr-4-Me-C_6H_4; Fc = Fe(η^5-C_5H_4)(η^5-C_5H_5)) were synthesized by treatment of P(C≡CFc)R_2 (**1a** – **1e**) [E20] with 0.5 equiv. of dimeric [RuCl_2(η^6-*p*-cymene)]$_2$ (**2**) in dichloromethane at ambient temperature (Reaction E1). After appropriate work-up, compounds **3a** – **3e** could be isolated as orange solid materials which are stable toward air and moisture for months. They dissolve in common organic solvents including dichloromethane, chloroform and tetrahydrofuran, while in diethyl ether, *n*-hexane and toluene they are not soluble.

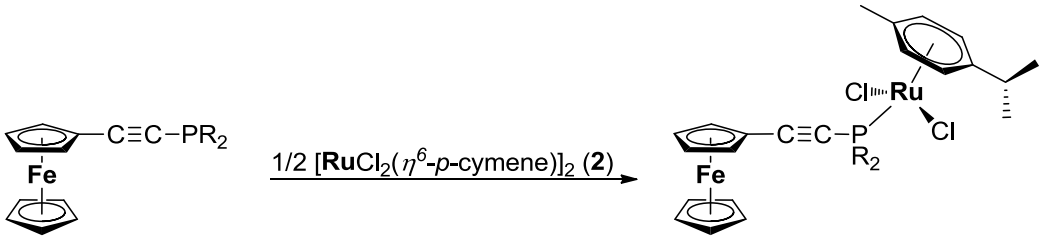

(E1)

1 **3a - e**

Tetrametallic **10** was prepared applying the consecutive synthesis sequence shown in Scheme 1 of which the first three steps could be carried out in a one-pot procedure. Attempts to isolate chlorophosphine **7** failed due to its high reactivity and hence it was used in the

synthesis of **9** without additional purification (Experimental Section). Addition of **7** to LiC≡CFc (**8**) in diethyl ether at low temperature gave by concomitant precipitation of LiCl red P(C≡CFc)(C≡CPPh$_2$)$_2$ (**9**) in moderate yield. Treatment of **9** with **2** produced (RuCl$_2$(η^6-*p*-cymene))(FcC≡C)P(C≡CPPh$_2$(RuCl$_2$(η^6-*p*-cymene))$_2$ (**10**). In heterometallic Ru$_3$Fe **10** the building blocks FcC≡C, C≡CPPh$_2$(RuCl$_2$(η^6-*p*-cymene) and RuCl$_2$(η^6-*p*-cymene) give rise to coordination number 4 at phosphorus.

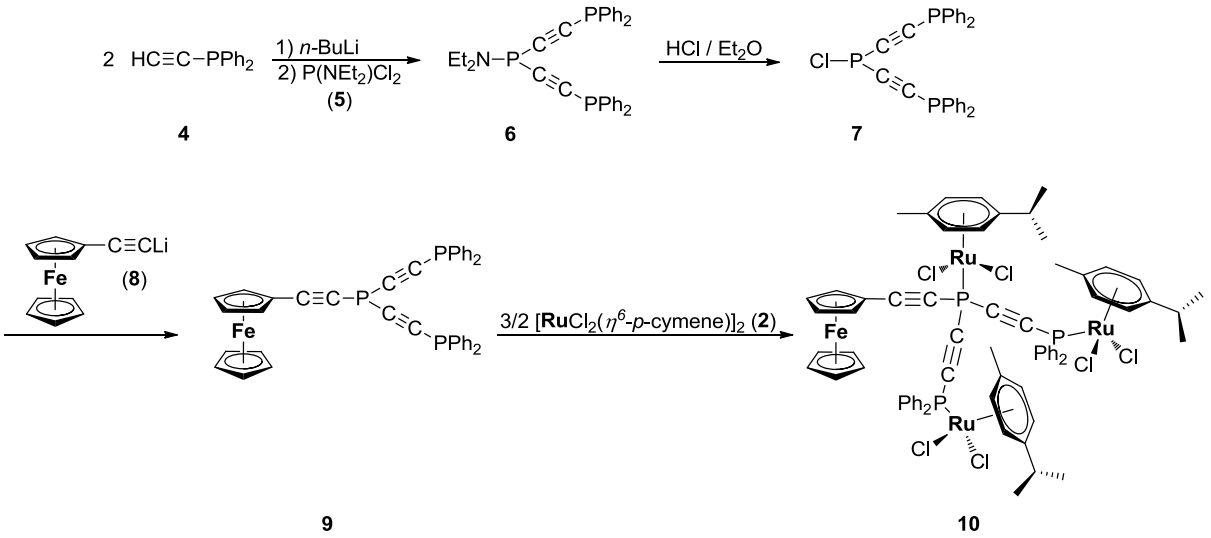

Scheme E1. Consecutive synthesis of tetrametallic **10**.

Newly synthesized organometallic compounds **3**, **9** and **10** have been identified by elemental analysis, IR and NMR (^{1}H, ^{13}C{^{1}H}, ^{31}P{^{1}H}) spectroscopy. ESI TOF mass-spectrometry and single crystal X-ray structure analysis of **3b**, **3c** and **10** were additionally carried out. However, all complexes show the tendency to enclose solvent molecules which, even after 2 – 3 days in vacuum, could not be completely removed. These solvents include chloroform, dichloromethane and diethyl ether, whereas dichloromethane is able to displace the other solvents.

The IR spectra of **3**, **9** and **10** show very characteristic absorptions for the FcC≡C and Ph$_2$PC≡C alkynyl units in the expected region, *i. e.* at 2151 cm^{-1} ($\tilde{\upsilon}_{C\equiv CPPh2}$) and 2175 ($\tilde{\upsilon}_{C\equiv CFc}$) for **9** as well as 2155 cm^{-1} ($\tilde{\upsilon}_{C\equiv CPPh2}$) and 2179 ($\tilde{\upsilon}_{C\equiv CFc}$) for **10**. Upon coordination of the phosphorus atom in **1** and **9** to the 16-valence electron complex fragment RuCl$_2$(η^6-*p*-cymene) (formation of **3** and **10**) a small shift of the ferrocenyl acetylide and the phosphine alkynyl stretching frequencies to higher wavenumbers is induced, whereby the ferrocenyl-bonded C≡C triple bond is more affected (*i. e.* **1c**, $\tilde{\upsilon}_{C\equiv C}$ = 2153; [E20] **3c**, $\tilde{\upsilon}_{C\equiv C}$ = 2159 cm^{-1};

Experimental Section). As consequence thereof, IR spectroscopy is suited to monitor the progress of the reactions.

In the $^{13}C\{^1H\}$ NMR spectra the alkynyl groups create two (**3**) or four (**9** and **10**) exceptional resonance signals of which the phosphorus- (73 – 80 ppm, $^1J_{PC}$ = 13 – 127 Hz) and the ferrocenyl-bonded acetylide carbon atoms (107 – 110 ppm, $^2J_{PC}$ = 4 – 23 Hz) in **3a** – **3e** and **10** appear as doublets (Experimental Section). Complexation of the phosphorus atom in **1** and **9** to a $RuCl_2(\eta^6$-*p*-cymene)-fragment induces a shift of the phosphorus atom signal to lower field, which is characteristic in phosphorus transition metal chemistry. [E18] While the coupling patterns in **1**, **3** and **10** are as expected (Experimental Section), compound **9** possesses a more complex signal splitting which is attributed to the increased number of phosphorus atoms present. Through the formation of a dative phosphorus-ruthenium bond in **10** the $^2J_{PC}$ coupling constant diminishes and hence is not anymore detectable in the spectrum. Also a shift of the *p*-cymene carbon atoms is observed when going from *non*-complexed to the coordinated species (Experimental Section). In **10** a set of two cymene units in the ratio of 2:1 is visible due to their different chemical environments of which the signal of the inner phosphorus-bonded ruthenium dichloro cymene moiety is found at lower magnetic field. Notable in the spectrum of **10** is the observation of three signal sets for the *iso*-propyl groups which can be explained by hindered rotation. The same behavior is found for the diphenylphosphino building blocks (Experimental Section).

As might have been expected, the ^1H NMR spectra of **3**, **9** and **10** consist of distinctive signal patterns as typical for the ferrocenyl and *p*-cymene units, respectively (Experimental Section).

A more expressive method than IR spectroscopy to verify the progress of the reaction is $^{31}P\{^1H\}$ NMR spectroscopy. A significant shift to lower field is observed upon coordination of the phosphines **3** and **9** to ruthenium (*i.e.* **1c**, -83.4; [E20] **3c**, -26.0 ppm, Experimental Section). Peculiar for **9** is the detection of a triplet at -88.2 (FcC≡CP) and a doublet at -32.7 ($C{\equiv}CPPh_2$) with $^3J_{PP}$ = 4.8 Hz, while in **10** this coupling diminishes.

The structures of **3b**, **3c**, and **10** in the solid state were determined by single X-ray diffraction studies confirming the half-sandwich configuration about the ruthenium(II) center and the tetrahedral environment at phosphorus. Single crystals of **3b** and **3c** could be grown from a saturated chloroform solution at ambient temperature, while crystals of **10** were accessible by slow diffusion of *n*-hexane into a saturated dichloromethane-chloroform

solution (1:1, *v*:*v*) containing **10** at 25 °C. It was found that all molecules crystallize in the triclinic space group $P\bar{1}$. The molecular structures of **3b** and **3c** are shown in Figure E1, Figure E2 displays tetrametallic **10**. Geometric details of **3b** and **3c** are listed in Table E2, while the ones of **10** are summarized in the caption of Figure E2. The crystallographic and refinement data of all compounds can be found in Table E2 (Experimental Section). Bond distances (Å), angles (°) and torsion angles (°) of the ethynylferrocenyl and *p*-cymene units are as expected and similar to those reported for closely related organometallic compounds. [E19-E21,E27]

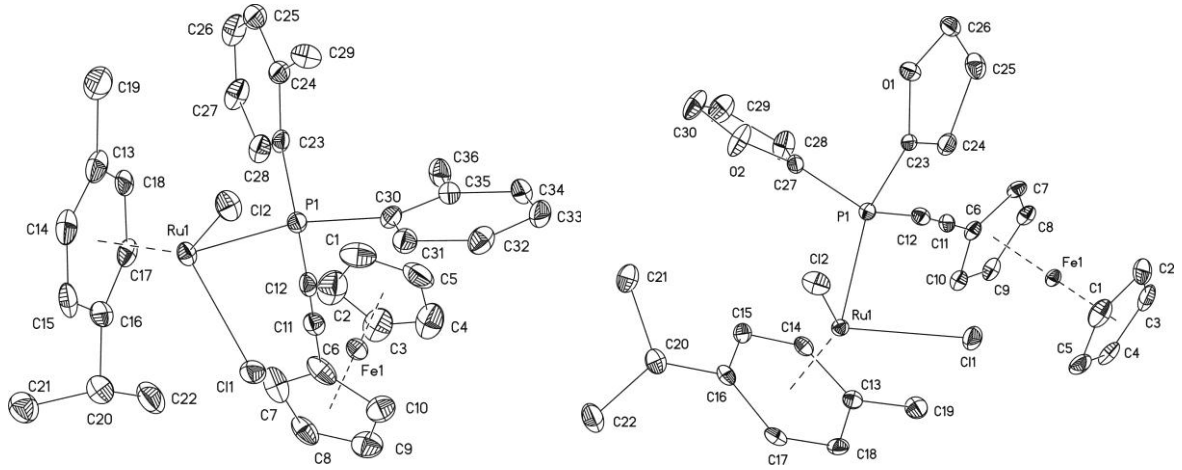

Figure E1. ORTEP diagram (50 % probability level) of the molecular structures of **3b** (left) and **3c** (right) with the atom numbering scheme. (Hydrogen atoms and chloroform as packing solvent of **3b** are omitted for clarity.)

Table E2. Selected bond lengths (Å), bond angles and torsion angles (°) for **3b** and **3c**.[a)]

	3b	**3c**
Ru1–P1	2.3799(13)	2.3035(5)
Ru1–Cl1	2.4118(13)	2.4137(5)
Ru1–Cl2	2.4069(13)	2.4121(6)
P1–C12	1.764(6)	1.754(2)
P1–C23	1.831(5)	1.790(2)
P1–C27		1.804(2)
P1–C30	1.839(5)	
C11–C12	1.198(8)	1.204(3)
O1–C23		1.383(2)
O1–C26		1.362(2)
O2–C27		1.368(2)
O2–C30		1.371(3)
D1–Fe1 [b)]	1.634	1.640

D2–Fe1 [b)]	1.675	1.646
D3–Ru1 [b)]	1.706	1.696
Cl1–Ru1–Cl2	87.93(5)	88.29(2)
Cl1–Ru1–P1	84.06(5)	85.891(18)
Cl2–Ru1–P1	95.62(4)	91.442(19)
Ru1–P1–C12	108.98(17)	111.60(6)
Ru1–P1–C23	109.27(16)	119.87(6)
Ru1–P1–C27		116.38(6)
Ru1–P1–C30	123.96(18)	
P1–C12–C11	178.8(5)	170.91(18)
C12–C11–C6	178.1(6)	177.5(2)
C26–O1–C23		105.78(15)
C27–O2–C30		106.50(16)
D1–Fe1–D2 [b)]	178.1	179.6
P1–C12–C11–C6	-115(24)	21(6)
P1–C23–C24–C29	12.4(7)	
P1–C30–C35–C36	-1.1(8)	
Ru1–P1–C12–C11		69.7(11)
Ru1–P1–C23–O1		-167.51(11)
Ru1–P1–C27–O2		68.11(16)

a) Standard uncertainties of the last significant digit(s) are shown in parenthesis. b) D1 denotes the centroid of C_5H_5 at Fe1; D2 denotes the centroid of C_5H_4 at Fe1; D3 denotes the centroid of C_6H_4 at Ru1.

Compounds **3b** and **3c** are set-up by the ferrocenylethynyl unit, the two organic groups R and the ruthenium dichloro *p*-cymene moiety at phosphorus (Figure E1). For **3b** and **3c**, respectively, the bond angles around phosphorus P1 range from 108 – 123° and those around Ru1 from 84 – 95° (Table E2) indicating a characteristic "piano-stool" geometry (Figure E1). The carbon-carbon triple bond distances C11–C12 are 1.198(8) (**3b**) and 1.204(3) (**3c**) Å, which is typical for this type of bonding. [E20,E21,E27] The P1–C11–C12 and C11–C12–C6 units are with 178.8(5) and 178.1(6)° (**3b**) as well as 170.91(18) and 177.5(2)° (**3c**) essentially linear. The two ferrocenyl cyclopentadienyl rings in molecule **3c** are in a nearly eclipsed conformation (3.1°), whereas in complex **3b** both cyclopentadienyl rings are with 22.5° about in the middle between the fully eclipsed (0°) and the fully staggered (36°) conformation. The D1–Fe1 and D2–Fe1 separations are between 1.634 – 1.675 Å (D1 = centroid of C_5H_5, D2 = centroid of C_5H_4) and are similar to those of related compounds. [20,21,27]

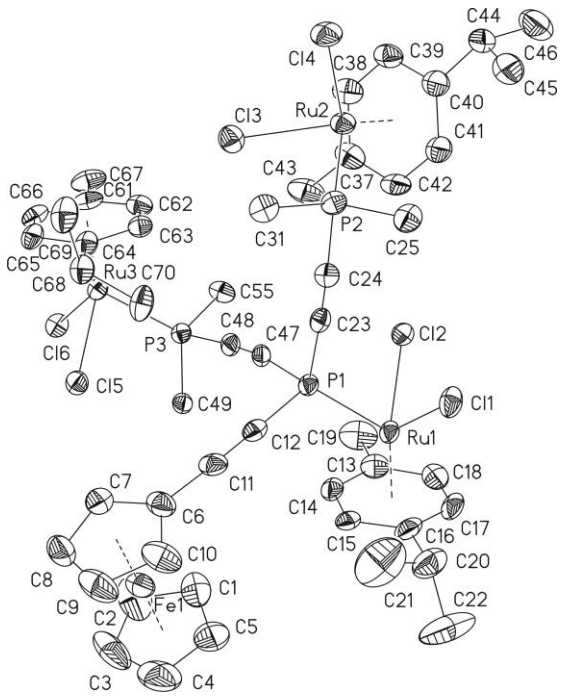

Figure E2. ORTEP diagram (50 % probability level) of the molecular structure of **10** with the atom numbering scheme. (Hydrogen atoms, packing solvent molecules and the phenyl groups (except the *ipso*-carbon atoms) are omitted for clarity.) Selected bond distances (Å), angles (°) and torsion angles (°): Fe1–D1 = 1.661, Fe1–D2 = 1.630, Ru1–D3 = 1.699, Ru2–D4 = 1.703, Ru3–D5 = 1.702, C11–C12 = 1.205(7), C23–C24 = 1.196(7), C47–C48 = 1.205(7), Ru1–Cl1 = 2.3995(12), Ru1–Cl2 = 2.4095(13), Ru1–P1 = 2.2772(12), Ru2–Cl3 = 2.4072(13), Ru2–Cl4 = 2.4171(13), Ru2–P2 = 2.3309(13), Ru3–Cl5 = 2.4077(12), Ru3–Cl6 = 2.4068(12), Ru3–P3 = 2.3185(12), P1–C12 = 1.742(5), P1–C23 = 1.764(5), P1–C47 = 1.758(5), P2–C24 = 1.770(5), P2–C25 = 1.831(5), P2–C31 = 1.822(5), P3–C48 = 1.763(5), P3–C49 = 1.829(5), P3–C55 = 1.826(5); D1–Fe1–D2 = 179.6, P1–C12–C11 = 170.1(5), P1–C23–C24 = 177.7(5), P1–C47–C48 = 170.3(4), C6–C11–C12 = 177.8(6), P2–C24–C23 = 175.9(4), P3–C48–C47 = 173.8(4); P1–C12–C11–C6 = -71(16), P1–C23–C24–P2 = -96(13), P1–C47–C48–P3 = 73(5). Standard uncertainties of the last significant digit(s) are shown in parenthesis. D1 = denotes the centroid of C_5H_5; D2 = denotes the centroid of C_5H_4, D3 – D5 = denotes the centroids of C_6H_4.

The key structural data of **10** (Figure E2) confirm the half-sandwich structure about Ru1, Ru2 and Ru3. The coordination number around P1 – P3 is four and along with the appropriate bond lengths and angles a “piano-stool” geometry is setup (Figure E2). Mentionable are the distances Ru1–P1 (2.2772(12) Å, Ru2–P2 (2.3309(13) Å) and Ru3–P3 (2.3185(12) Å) proving, as expected, the stronger binding of the $RuCl_2(\eta^6$-cymene) unit by P1 explainable by the lower σ donor capability compared with the respective alkynyl phosphine moieties. [E20,E27]

All other bond distances and angles agree well with those building blocks reported for similar compounds. [E19-E21,E27]

The application of **3a** – **3e** and **10** in the homogeneous ruthenium-catalyzed addition of benzoic acid to propargyl alcohol for the synthesis of *β*-oxo propyl benzoate was studied as model system (Reaction E2).

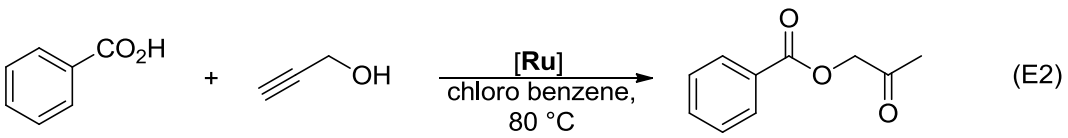

[Ru] = 3a - 3e, 10

Various ruthenium complexes featuring different electron-rich or electron-poor (ferrocenylethynyl)phosphino entities were screened in order to identify factors that may influence the catalytic activity and productivity. The donor capacity of the phosphines can be quantified by measuring the $^{1}J(^{31}P\text{-}^{77}Se)$ coupling constant of the appropriate seleno phosphines. Results thereof were previously published [E20] indicating that phosphine **3c** possesses the weakest *σ* donor ability whereat the aliphatic phosphines **3d**, **e** show the best *σ* donor ability. [E20]

After screening different solvents, temperatures and catalyst concentrations we chose as best suited reaction conditions a temperature of 80 °C, a concentration of 1.0 mol% and chloro benzene as solvent. However, in contrast to well-established systems, [E1a,E9] below 80 °C no catalytic activity was observed. As best solvent chloro benzene was found which benefits from the high polarity and hence better solubility when compared to the commonly used solvent toluene. [E28] The results of the catalytic investigations are summarized in Figure E3.

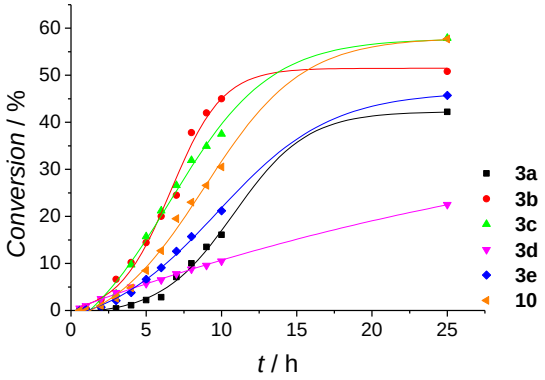

Figure E3. Reaction profiles for catalysts **3a** – **3e** and **10** for the reaction of benzoic acid with propargyl alcohol to give *β*-oxopropyl benzoate (Reaction E2, catalyst loading 1.0 mol% based on Ru, 80 °C, chloro benzene). Conversions equal ^{1}H NMR spectroscopic yields and are based on benzoic acid.

From Figure E3 it can be seen that under the reaction conditions mentioned above all complexes are catalytically active in the formation of *β*-oxo propyl benzoate in moderate to good yields. The most active catalyst is **3b** which shows a conversion of 45 % within 10 hours. Somewhat less active is furyl-substituted **3c** but shows the highest productivity (conversion 58 %) after 25 hours of all complexes **3a** – **3e**. Nevertheless, the lowest conversion (42 %) within the series of aromatic/heteroaromatic phosphines is observed for the phenyl derivative **3a**. In addition, this phosphine needs a longer induction period of ca. five hours to form the catalytically active species which might be responsible for the poor performance and low yield. Comparing the aromatic with the aliphatic phosphine substituents it is obvious that more electron-rich systems **3d** and **3e** are less active and only show productivities of 46 (**3e**) or 23 % (**3d**) after 25 hours (Figure E3). However, due to the long reaction times necessary, all catalysts suffer from a loss of activity, which can be attributed to gradually decomposition of the catalyst during the course of the reaction. Nevertheless, no formation of "ruthenium black" which indicates the formation of ruthenium particles could be observed.

Also from Figure E3 it can be seen that tetrametallic **10** with its three ruthenium(II) centers shows a significantly higher productivity than **3a** featuring only one ruthenium dichloro *p*-cymene building block. Furthermore, no induction period is observable. This phenomenon can most probably be ascribed to synergistic and cooperative effects between the appropriate transition metals which improves the catalytic activity with increasing number of active centers present in one molecule, *i. e.* dendritic carbene-palladium complexes, [E29] phosphino palladium-functionalized PAMAM dendrimers [E30,E31] and carbosilane dendrimers with end-grafted NCN pincer-nickel(II) groups. [E32] Further examples include metallo-enzymes [E33] and metal oxide supported catalysts. [E34]

Compared to $[RuCl_2(\eta^6\text{-}p\text{-cymene})(PR_3)]$ (R = Ph, Me) [E1a] with basic phosphines and $[RuCl_2(\eta^6\text{-}p\text{-cymene})]_2/P(Fur)_3$ [E9] with its electron-poor phosphine we could not find a general trend concerning basicity or steric factors under reaction conditions used by us (Figure 3). We believe that it is a combination of both issues, whereas electron-poor ligands at the phosphorus atom are best suited, which is achieved by the introduction of an

ethynylferrocenyl functionality. Moderate electron-rich species are only effective catalysts, when they possess at the same time bulky ligands, *e. g*. *ortho*-tolyl groups (Figure E3). Also, some of our systems need longer reaction times and therefore, suffer from deactivation due to decomposition of the active species. Finally, it must be noted that, however, our catalysts only work at temperatures at 80 °C, which differs from literature known species described by, for example, Dixneuf [E1] or Goosen. [E9]

4 Conclusions

In this work, we presented the synthesis of novel heterobimetallic dinuclear and tetranuclear complexes of type (FcC≡C)R_2P($RuCl_2$(η^6-*p*-cymene)) (R = Ph, *o*-Tol, Fur, *t*-Bu, Cy; *p*-cymene = 1-*i*-Pr-4-Me-C_6H_4; Fc = Fe(η^5-C_5H_4)(η^5-C_5H_5)) and ($RuCl_2$(η^6-*p*-cymene))(FcC≡C)-P(C≡CPPh_2($RuCl_2$(η^6-*p*-cymene)))$_2$, respectively. All molecules were used as catalysts in the formation of *β*-oxopropyl benzoate by treatment of propargyl alcohol with benzoic acid. All complexes show a catalytic activity with moderate to good conversions (23 – 58 %). However, neither electronic properties nor steric factors alone are responsible for the catalytic performance, which differs from statements recently made. [E1,E9] We believe that it is more or less a combination of both criteria, whereas electron-poor ligands R are best suited. Moderate electron-rich species are only effective catalysts, when they possess bulky ligands.

5 Supporting Information

CCDC 843924, CCDC 843923 and CCDC 843922 contain the supplementary crystallographic data for complexes **3b**, **3c** and **10**. These data can be obtained free of charge from the Cambridge Crystallographic Database *via* www.ccdc.cam.ac.uk/products/csd/request/.

6 Acknowledgement

We are grateful to the Deutsche Forschungsgemeinschaft and the Fonds der Chemischen Industrie for financial support.

7 References

[E1] a) D. Devanne, C. Ruppin, P. H. Dixneuf *J. Org. Chem*. **1988**, *53*, 925; b) C. Bruneau, P. H. Dixneuf *Angew. Chem. Int. Ed*. **2006**, *45*, 2176.

[E2] a) C. Bruneau, Z. Kabouche, M. Neveux, B. Seiller, P. H. Dixneuf *Inorg. Chim. Acta* **1994**, *222*, 155; b) M. Neveux, B. Seiller, F. Hagedorn, C. Bruneau, P. H. Dixneuf *J. Organomet. Chem*. **1993**, *451*, 133.

[E3] V. Cadierno, J. Francos, J. Gimeno *Green Chem*. **2010**, *12*, 135.

[E4] D. W. Hansen, Jr., R. Pappo, R. B. Garland *J. Org. Chem*. **1988**, *53*, 4244.

[E5] P. Yates, R. S. Grewal, P. C. Hayes, J. F. Sawyer *Can. J. Chem*. **1988**, *66*, 2805.

[E6] S. Costin, N. P. Rath, E. B. Bauer *Adv. Synth. Catal*. **2008**, *350*, 2414.

[E7] A. J. Fry, D. Herr *Tetrahedron Lett*. **1978**, *19*, 1721.

[E8] M. A. Ashraf, M. A. Jones, N. E. Kelly, A. Mullaney, J. S. Snaith, I. Williams *Tetrahedron Lett*. **2003**, *44*, 3151.

[E9] L. J. Goossen, J. Paetzold, D. Koley *Chem. Comm*. **2003**, 706.

[E10] A. D. Cort *J. Org. Chem*. **1991**, *56*, 6708.

[E11] R. C. Cambie, R. C. Hayward, J. L. Jurlina, P. S. Rutledge, P. D. Woodgate *J. Chem. Soc. Perkin Trans*. **1978**, *1*, 126.

[E12] S. Torii, T. Inokuchi, S. Misima, T. Kobayashi *J. Org. Chem*. **1980**, *45*, 2731.

[E13] S. Stavber, B. Sket, B. Zajc, M. Zupan *Tetrahedron* **1989**, *45*, 6003.

[E14] M. M. Salunkhe, A. R. Sande, A. S. Kanade, P. P. Wadgaonkarb *Synth. Commun*. **1997**, *27*, 2885.

[E15] M. Arfan Ashraf, A. G. Russell, C. W. Wharton, J. S. Snaith *Tetrahedron* **2007**, *63*, 586.

[E16] M. Rotem, Y. Shvo *Organometallics* **1983**, *2*, 1689.

[E17] a) C. Ruppin, P. H. Dixneuf *Tetrahedron Lett*. **1986**, *27*, 6323; b) C. Ruppin, P. H. Dixneuf, S. Lecolier *Tetrahedron Lett*. **1988**, *29*, 5365; c) K. Philippot, D. Devanne, P. H. Dixneuf *J. Chem. Soc. Chem. Commun*. **1990**, 1199.

[E18] R. Packheiser, H. Lang *Eur. J. Inorg. Chem*. **2007**, 3786.

[E19] P. Štěpnička, J. Demel, J. Cejka *J. Molec. Catal. A: Chem*. **2004**, *224*, 161.

[E20] B. Milde, D. Schaarschmidt, P. Ecorchard, H. Lang *J. Organomet. Chem*. **2012**, *706-707*, 52 – 65.

[E21] T. Baumgartner, M. Fiege, F. Pontzen, R. Arteaga-Müller *Organometallics* **2006**, *25*, 5657.

[E22] V. Huc, A. Balueva, R.-M. Sebastian, A.-M. Caminade, J.-P. Majoral *Synthesis* **2000**, *5*, 726.

[E23] S.-Z. Luo, Y.-M. Li, Z.-Z. Chen, H. Abe, L.-P. Cui, H. Nakanishi, X.-R. Qin, Y.-F. Zhao *Letters in Peptide Science* **2003**, *10*, 57.

[E24] S. Suravajjala, J. R. Polam, L. C. Porter *J. Organomet. Chem*. **1993**, *461*, 201.

[E25] G. M. Sheldrick *Acta Cryst. Sect. A* **1990**, *46*, 467.

[E26] G. M. Sheldrick, *SHELXL-97, Program for Crystal Structure Refinement*, University of Göttingen, **1997**.

[E27] A. Jakob, B. Milde, P. Ecorchard, C. Schreiner, H. Lang *J. Organomet. Chem*. **2008**, *693*, 3821.

[E28] C. Schreiner, *Ph.D. Thesis* **2010**, TU Chemnitz/Germany.

[E29] V. Hornillos, J. Guerra, A. de Cozar, P. Prieto, S. Merino, M. A. Maestro, E. Diez-Barra, J. Tejeda *Dalton Trans*. **2011**, *40*, 4095.

[E30] M. T. Reetz, G. Lohmer, R. Schwickardi *Angew. Chem. Inl. Ed. Engl*. **1997**, *36*, 1526.

[E31] S. Dietrich, A. Nicolai, H. Lang *J. Organomet. Chem*. **2011**, *696*, 739.

[E32] J. W. J. Kapen, A. W. van der Made, J. C. de Wilde, P. W. N. M. van Leeuwen, P. Wijkens, D. M. Grove, G. van Koten *Nature* **1994**, *372*, 659.

[E33] E. K. van den Beuken, B. L. Feringa *Tetrahedron* **1998**, *54*, 12985.

[E34] B. Coq, F. Figueras *Coord. Chem. Rev*. **1998**, *178–180*, 1753.

[E35] V. Cadierno, J. Francos, J. Gimeno *Organometallics* **2011**, *30*, 852.

F Phosphino Imidazoles and Imidazolium Salts for Suzuki-Miyaura *C,C* Coupling Reactions

Bianca Milde, Dieter Schaarschmidt, Tobias Rüffer, and Heinrich Lang*

Published in *Dalton Trans*. **2012**, *41*, 5377 – 5390.

1 Introduction

Imidazole- and imidazolium-functionalized phosphines represent an interesting family of molecules because they can act as ambivalent *P,N* donors which allow the coordination of either hard or soft transition metals. [F1] These species can be applied, for example, as model systems imitating the catalytically active site in bio-inorganic molecules. [F1c,F2] In addition, they can be used as easily tuneable ligands with good performance in palladium-catalyzed *C-C* coupling reactions. [F1a,d,F3] Imidazolium phosphines contain structural elements of an ionic liquid and have been obtained by selective *N*-protonation or *N*-alkylation of the appropriate neutral molecules. Their application in 2-phase catalytic reactions is advantageous since they allow facile recycling and easy separation of the catalyst from the products. [F1b,d,e,F3a,F3c,F4,F6] During the last years, this field of chemistry developed rapidly, however, only little is known about aryl-substituted imidazoles [F2b,d,F3b,e,F5a,e] and imidazolium salts, [F3a,d,F5] which is attributed to their elaborate multistep preparation procedures. Compared to classical monodentate ligands, such as phosphines, phosphino imidazoles and imidazolium salts are advantageous due to their flexible coordination behavior and their ability to reduce metal leaching in homogeneous multiphase catalysis. [F1e,F6] Recently, it was reported that, for example, dialkylphosphino imidazoles can be used in the Sonogashira [F3e] and Suzuki-Miyaura [F3b] *C;C* as well as Buchwald-Hartwig [F3b] *C;N* coupling.

This prompted us to develop straightforward consecutive synthesis methodologies for the preparation of organic- and organometallic-functionalized aryl phosphino imidazoles which were converted into the appropriate imidazolium salts to study the electronic influence of the *N*-heterocyclic component to the phosphino group. The use of the appropriate phosphines in carbon-carbon cross-couplings is reported both in organic solvents and ionic liquids.

2 Results and Discussion

2.1 Synthesis

As starting molecule 1-(4-X-C_6H_4)-4,5-R_2-^{c}C_3HN_2 (**3a**, X = Br, R = H; **3b**, X = I, R = Me, **3c** [F19], X = H, R = Me) was chosen which was synthesised by a modified reaction protocol as described by Zhang and co-workers [F2d] (Scheme F1). These species can further be functionalized by applying *C-C* cross-couplings including the palladium-promoted Negishi, Sonogashira and Suzuki-Miyaura reactions. Compound 1-(4-Fc-C_6H_4)-^{c}$C_3H_3N_2$ (**5**) (Fc = Fe(η^5-C_5H_4)(η^5-C_5H_5)) was accessible by Negishi ferrocenylation of the appropriate bromo-substituted imidazole **3a** with FcZnCl (**4**), available by mono-lithiation of ferrocene according to Müller-Westerhoff [F7] followed by treatment with dry [$ZnCl_2(thf)_2$], in presence of catalytic amounts of [$Pd(PPh_3)_4$] (Scheme F1). Imidazole 1-(4-FcC≡C-C_6H_4)-^{c}$C_3H_3N_2$ (**7**) was obtained by the reaction of **3a** with ethynyl ferrocene (**6**) in presence of catalytic amounts of [CuI] and [$PdCl_2(PPh_3)_2$] in NEt_3 under Sonogashira cross-coupling conditions. Suzuki-Miyaura *C-C* coupling of **3b** with phenylboronic acid, potassium carbonate as base and [Pd(dppf)Cl_2] (dppf = 1,1'-bis(diphenylphosphino)ferrocene) as catalyst afforded 1-(4-Ph-C_6H_4)-4,5-Me_2-^{c}C_3HN_2 (**9**) (Scheme F1, Experimental Section).

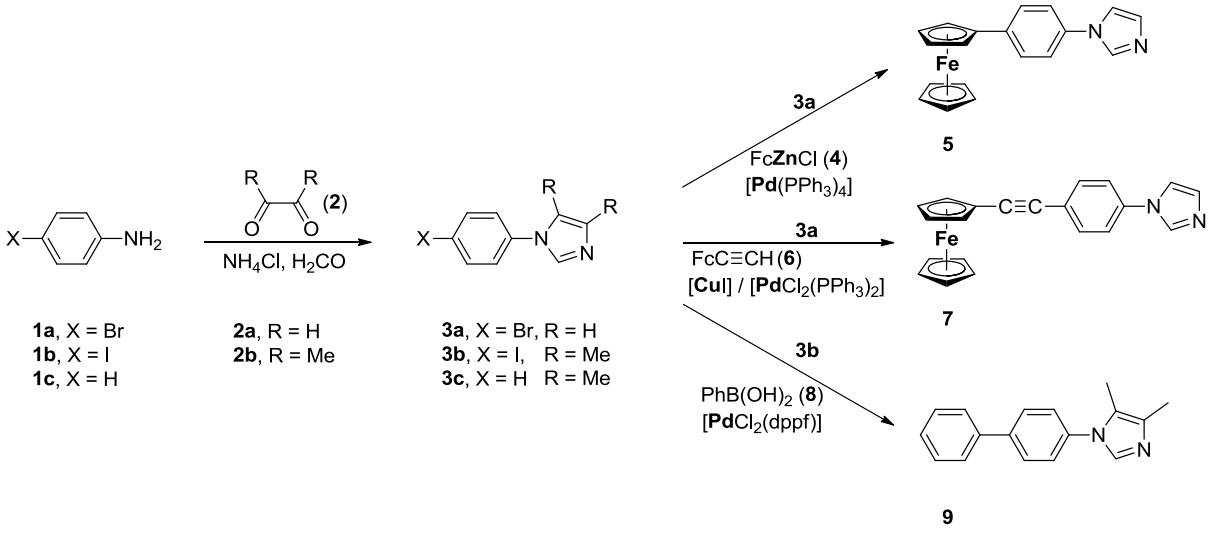

Scheme F1. Synthesis of imidazoles **3a** – **c**, **5**, **7** and **9** (Fc = Fe(η^5-C_5H_4)(η^5-C_5H_5), dppf = 1,1'bis(diphenylphosphino)ferrocene).

Imidazoles **3**, **5**, **7** and **9** could be converted to the appropriate phosphino imidazoles 1-(4-X-C_6H_4)-2-PR'$_2$-4,5-R_2-^{c}C_3N_2 (**11a** – **k**; X = Br; I, Fc, FcC≡C, Ph; R = H, Me; R' = Ph, Cy, Fur) (Scheme F2, Table F1) by the consecutive reaction of either lithium di-*i*-propylamide or *n*-butyl lithium followed by addition of phosphines PR'$_2$Cl (**10**) in tetrahydrofuran (LDA) or

diethyl ether solutions (*n*-BuLi). Reaction of **11a** – **k** with alkyl iodides R"I (R'' = *n*-Bu, *n*-Oct) did result in the formation of a mixture of compounds **13** – **15**, from which desired **13** could not be isolated in pure form, neither by chromatography nor crystallization (Scheme F2, Experimental Section).

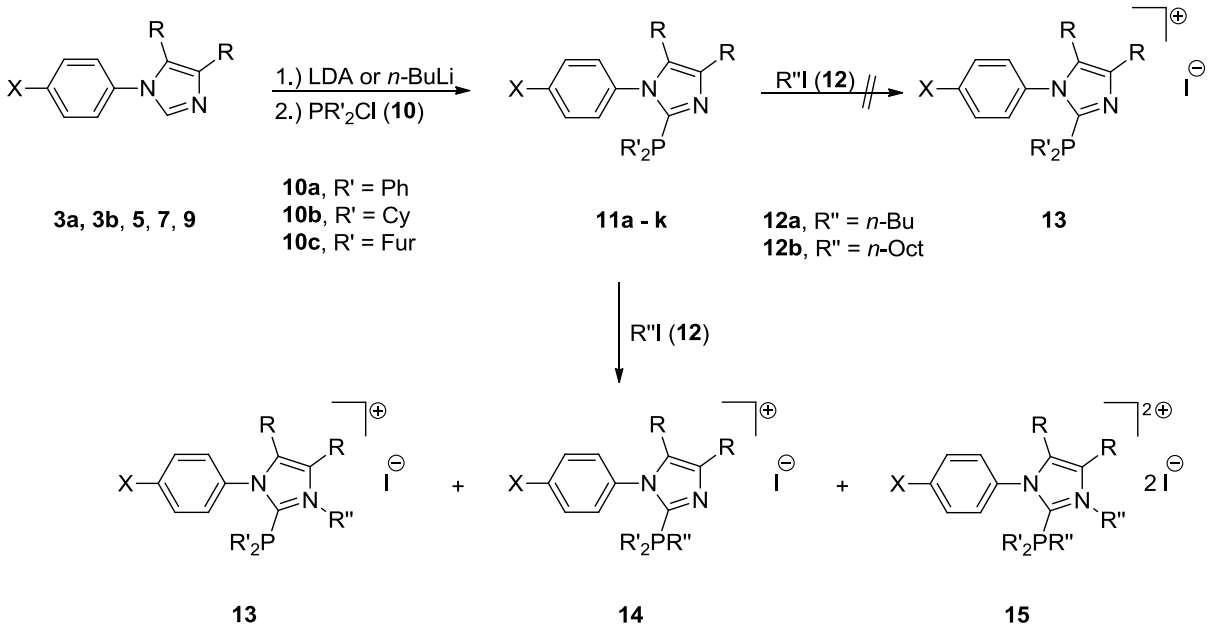

Scheme F2. Synthesis of phosphino imidazoles and imidazolium salts **11a** – **k** and **13** – **15**.

Table F1. Synthesis of phosphino imidazoles **11a** – **k**.

Compd.	X	R	R'	Yield [a] [%]
11a	Br	H	Ph	60
11b	Br	H	Cy	49
11c	Br	H	Fur	52
11d	I	Me	Ph	65
11e	I	Me	Cy	55
11f	I	Me	Fur	55
11g	Fc [b]	H	Ph	63
11h	FcC≡C [b]	H	Ph	44
11i	Ph	Me	Ph	67
11j	Ph	Me	Cy	61
11k	Ph	Me	Fur	72

a) Based on **3a** and **3b**, respectively; b) Fc = Fe(η^5-C_5H_4)(η^5-C_5H_5).

Since no separation of molecules **13** – **15** from each other was possible, another synthesis procedure had to be developed. The crucial step was the quaternisation of **3a** and **3b** with **12** yielding the imidazolium salts [1-(4-X-C_6H_4)-3-R''-4,5-R_2-^{c}C_3HN_2]I (**16a**; X = Br, R = H, R'' = *n*-Bu; **16b**, X = Br, R = H, R'' = *n*-Oct; **16c**, X = I, R = Me, R'' = *n*-Oct; **16d**, X = H, R =

Me, R'' = *n*-Oct) (Scheme F3). Decreasing the melting point of imidazolium salts by longer alkyl chains, [F6d] results in the formation of ionic liquids. For this reason, we chose **16c** as a starting compound for the synthesis of ionic phosphines. Therefore, **16c** was deprotonated with *n*-BuLi followed by the reaction of **16c·Li** with PR'_2Cl to give after anion exchange with $K[PF_6]$ a mixture of $[1\text{-}(4\text{-}I\text{-}C_6H_4)\text{-}2\text{-}PR'_2\text{-}3\text{-}R''\text{-}4,5\text{-}Me_2\text{-}^cC_3N_2]PF_6$ (**13a**: R' = Ph, R'' = *n*-Oct; **13b**: R' = Cy, R'' = *n*-Oct) and $[1\text{-}Ph\text{-}2\text{-}PR'_2\text{-}3\text{-}R''\text{-}4,5\text{-}Me_2\text{-}^cC_3N_2]PF_6$ (**17a**: R' = Ph, R'' = *n*-Oct; **17b**: R' = Cy, R'' = *n*-Oct), respectively (Scheme F3). However, these mixtures could, as **13** – **15** (*vide supra*), not be separated. Nevertheless, a straightforward synthesis procedure to produce pure **17a** and **17b** starts from halide-free $1\text{-}Ph\text{-}4,5\text{-}Me_2\text{-}^cC_3HN_2$ (**3c**) applying the same reaction sequence as just described (Scheme F3). Quaternization of **3c** with **12b** gave **16d**, which on subsequent reaction with LDA, PR'_2Cl and $K[PF_6]$ produced **17a** and **17b** (Scheme F3). After appropriate work-up, **17a** and **17b** could be isolated as colorless solids in an overall yield of 66 and 71 %, respectively (Experimental Section).

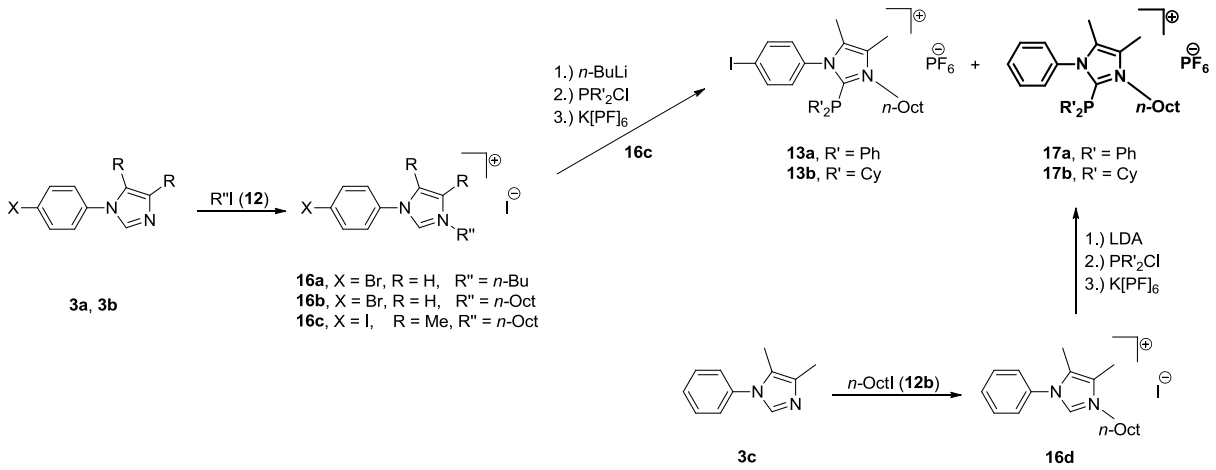

Scheme F3. Synthesis of **13**, **16** and **17**.

On the other hand, a diphenyl phosphino group could successfully be introduced at the phenyl imidazolium building block using a synthesis protocol first described by Stelzer [F8] as demonstrated in Reaction (F1). After appropriate work-up, the corresponding imidazolium salt $[1\text{-}(4\text{-}PPh_2\text{-}C_6H_4)\text{-}3\text{-}n\text{-}Oct\text{-}4,5\text{-}Me_2\text{-}^cC_3HN_2]PF_6$ (**20**) could be isolated as a colorless solid in 63 % yield (Experimental Section).

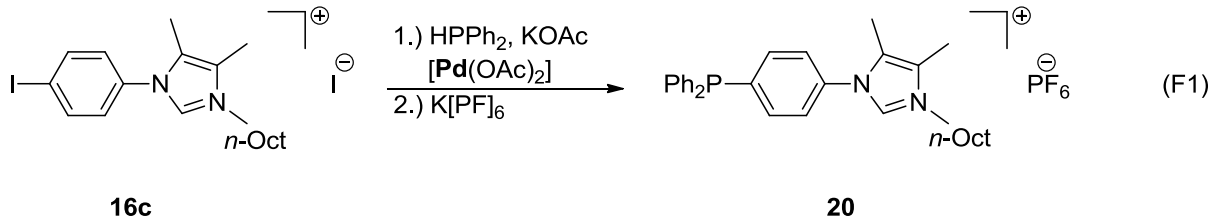

(F1)

To verify the σ donor properties of the newly synthesized phosphines **11a** – **f** we converted them into the appropriate seleno phosphines **11a-Se** – **f-Se** by addition of a 2-fold excess of elemental selenium in toluene at 100 °C (Reaction (F2)). In general, the σ donor ability of phosphines toward selenium acceptors can be quantified by the phosphorus-selenium coupling constant as indicated by $^{31}P\{^{1}H\}$ NMR spectroscopy. [F9] Electron-withdrawing groups increase $^{1}J_{PSe}$, due to the increased s character of the phosphorus orbital involved in the P=Se bonding. This results in shorter bond distances between the phosphorus and the acceptor carbon atoms, which directly affects the steric demand around the P atom resulting in marked changes in the behavior of the respective transition metal complexes.

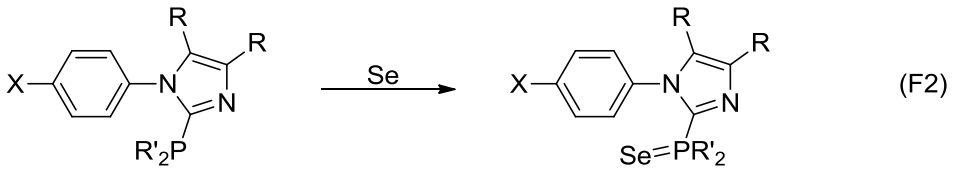

(F2)

11a - f **11a-Se - f-Se**

The chemistry of *N*-heterocyclic carbenes developed rapidly during the last years due to their outstanding potential as supporting ligands in homogeneous catalysis. [F10] For this reason, we did react the imidazolium salts **16a** – **c** with $[PdCl_2(cod)]$ (cod = cycloocta-1,5-diene) as palladium source and KO(*t*-Bu) as deprotonting agent (Reaction (F3)). Although the reactants were readily consumed only in case of **16a** we succeeded in isolating a pure palladium carbene complex. By halide exchange the mononuclear palladium carbene complex **19** could be isolated in minor yield (Experimental Section). The obtained few crystals were characterized by X-ray diffraction studies indicating that **19** was formed both in the *cis* and *trans* configuration (Figure F2). Due to the very low yield of **19** no further analytical characterizations could be performed.

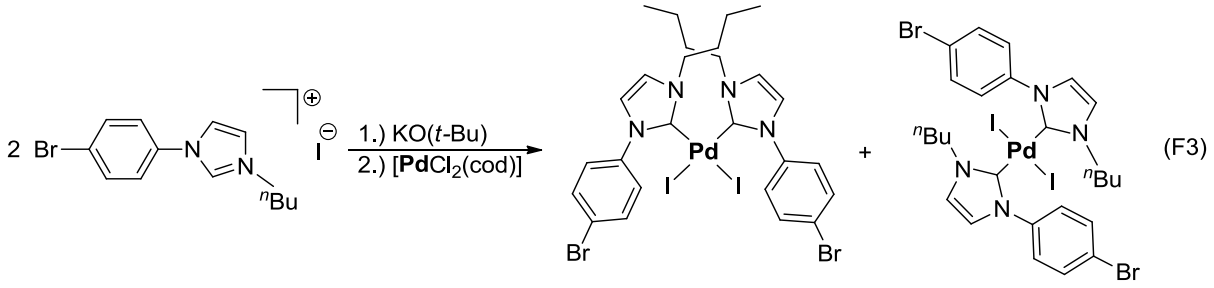

(F3)

16a *cis*-**19** *trans*-**19**

It is important to note that all compounds are sensitive toward light and quickly turn yellow. Furthermore, the phosphine carrying imidazoles are sensitive toward air and the

phosphino imidazolium salts are hygroscopic. Therefore, rapid work-up and storage under argon is mandatory.

2.2 Characterization

The identities of all newly synthesized imidazoles **3b**, **5**, **7** and **9**, phosphino imidazoles **11a** – **k** and **11a-Se** – **f-Se** and imidazolium salts **16a** – **d**, **17a**, **17b** and **20** have been confirmed by elemental analysis, IR and NMR spectroscopy (^{1}H, ^{13}C{^{1}H}, ^{31}P{^{1}H}) as well as high-resolution mass spectrometry (Experimental Section). Cyclovoltammetric measurements of **5**, **7** and the halide derivatives **3a** and **3b** were additionally carried out. The structures of **11a-Se** and **19** in the solid state were determined by single crystal X-ray structure analysis.

The IR spectra of the newly prepared molecules are less expressive with exception of the imidazole and imidazolium C=N and C=C vibrations (Experimental Section). The introduction of phosphino groups resulted in the visibility of characteristic P-C stretching frequencies and for the appropriate seleno derivatives additional $\tilde{\upsilon}_{P=Se}$ absorptions are observed. Apparently there is nearly no influence on the C≡C vibration, when the imidazole ring is functionalized by a PPh_2 group as given in **7** ($\tilde{\upsilon}_{C\equiv C}$ = 2206 cm^{-1}) and **11h** ($\tilde{\upsilon}_{C\equiv C}$ = 2204 cm^{-1}), respectively.

Contrastingly, the NMR spectra of the respective imidazole and imidazolium species are in some extend more meaningful. A striking feature in the ^{1}H NMR spectra is the shift of the $^{c}C_3HN_2$ core proton in position 2 to lower field, when changing from the imidazoles to the appropriate imidazolium salts, *i. e.* **3b**, 7.45 ppm and **16c**, 9.82 ppm (Experimental Section). For the phenylene C_6H_4 units, as expected, a characteristic AA'XX' coupling pattern with $^{3}J_{HH}$ = 8.7 Hz is found, which splits into a more complex pattern, when a phosphorus atom is attached to the heterocyclic core as given in **11a** – **k** and **11a-Se** – **f-Se** (Experimental Section). For the ferrocenyl-containing molecules **5**, **7** and **11g** and **11h** a singlet as well as two pseudo-triplets are observed between 4.0 (C_5H_5) and 4.7 ppm (C_5H_4), respectively, resulting from the cyclopentadienyl ring protons. For the two methyl groups in **3b**, **9**, **11d** –**f**, **11d-Se** –**f-Se**, **16c**, **16d**, **17a**, **17b** and **20** two individual singlets due to the asymmetry of the $^{c}C_3N_2$ core unit are characteristic.

The interpreting of the ^{13}C{^{1}H} NMR spectra of all imidazoles and imidazolium salts is somewhat more complex due to the presence of *ipso*-carbon atoms. However, when phosphino groups are attached either to the $^{c}C_3N_2$ or C_6H_4 unit the spectra became more

simplified, since characteristic P-C couplings appear (Experimental Section). Very distinctive is the signal of the heterocyclic C-2 carbon atom at ca. 135 ppm (**3**, **16**) which is shifted to 140 – 147 ppm in the phosphino-containing species **11** and **17**. Conspicuous in **11a**, **11c**, **11d** and **11f** and the corresponding selenium derivatives **11a-Se** – **e-Se** is that C-5 shows a $^{3}J_{CP}$ coupling, while C-4 appears as singlet. All other molecules of **11** solely show a singlet. Also very characteristic is the *meta*-carbon C_6H_4 atom in **11a** – **k**, **17** and **20** emerging as a doublet with a $^{4}J_{CP}$ coupling of 3 – 6 Hz at ca. 130 ppm.

$^{31}P\{^{1}H\}$ NMR spectroscopy can be used to monitor the progress of the reaction of lithiated **3**, **5**, **7**, **9** and **16** with the respective chloro phosphines PR'_2Cl (**10a** – **c**) since a singlet of the phosphorus atom appears between -73 – 5 ppm depending on the nature of the organic groups R' (Experimental Section). In addition, the donor properties of the phosphino imidazoles **11a** – **f** can be quantified by the coupling constant $^{1}J_{PSe}$ of the appropriate seleno phosphines **11a-Se** – **f-Se**. An electron-withdrawing group at P increases $^{1}J_{PSe}$ as result of the increased s character of the phosphorus orbital involved in the phosphorus-selenium bonding. As consequence thereof, a shorter bond length between the phosphorus and the acceptor R' units is observed. [F9] This electronic impact has direct influence on the P donor ability. The $^{31}P\{^{1}H\}$ NMR data together with the $^{1}J_{PSe}$ coupling constant for the seleno phosphines **11a-Se** – **f-Se** are summarized in Table F2.

Table F2. Chemical shifts and $^{1}J_{PSe}$ values of **11a-Se** – **f-Se**.

Compd.	δ / ppm	$^{1}J_{PSe}$ / Hz	Compd.	δ / ppm	$^{1}J_{PSe}$ / Hz
11a-Se	19.1	753	**11d-Se**	17.6	745
11b-Se	41.6	725	**11e-Se**	41.2	718
11c-Se	-20.7	790	**11f-Se**	-21.4	781

From Table F2 it can be seen that the seleno phosphines **11a-Se** – **c-Se** show higher coupling constants than the respective **11d-Se** – **f-Se** derivatives featuring methyl groups in positions 4 and 5 indicating that the latter three molecules are the better σ donors. The most electron-donating systems are the aliphatic cyclohexyl seleno phosphines **11b-Se** and **11e-Se** with $^{1}J_{PSe}$ of 718 and 725 Hz, respectively (Table F2). In summary, the σ donor ability decreases in the series **11e** > **11b** > **11d** > **11a** > **11f** > **11c**. The data summarized in Table F2 are indicative to classify the suitability of the phosphino imidazoles as suitable ligands in palladium-promoted Suzuki-Miyaura *C,C* cross-couplings (*vide infra*).

Complexes **5** and **7** contain a redox-active ferrocenyl group and hence they have been subjected to cyclovoltammetric measurements in dry dichloromethane solutions utilizing [(*n*-Bu)$_4$N][B(C$_6$F$_5$)$_4$] as supporting electrolyte. [F11] The cyclovoltammetric studies were carried out at scan rates of 100 mV·s^{-1}. All potentials are referenced to the FcH/FcH$^+$ redox couple as internal standard as recommended by IUPAC. [F12] The cyclovoltammetric data are summarized in Table F3 and the cyclovoltammograms (= CV) of **5** and **7** are shown in Figure F3 in the Supporting Information.

Table F3. Cyclovoltammetric data (potentials *vs.* FcH/FcH$^+$), scan rate 100 mV·s^{-1} at a glassy-carbon electrode of 1.0 mmol·L^{-1} solutions of **3a**, **3b**, **5**, and **7** in dry dichloromethane containing 0.1 mol·L^{-1} of [(*n*-Bu)$_4$N][B(C$_6$F$_5$)$_4$] as supporting electrolyte at 25 °C.

Compd.	$E_{\text{red-irrev}}$ / V	Compd.	E^0 (ΔE_p) / V	$E_{\text{red-irrev}}$ / V
3a	-1.22	**5**	0.108 (0.114)	-1.48
3b	-1.23	**7**	0.183 (0.102)	-1.52

E^0 = redox potential, ΔE_p = difference between oxidation and reduction potential, $E_{\text{red-irrev}}$ = irreversible reduction potential.

One ferrocenyl-related oxidation half reaction in the anodic CV sweep and reduction half reaction in the cathodic CV sweep could be observed. The ferrocenyl substituents showed a reversible electrochemical behavior (ΔE_p = 0.114 (**5**) and 0.102 V (**7**)), while for the imidazole unit one irreversible reduction event is observed at -1.48 V (**5**) and -1.52 V (**7**), respectively. From Table F3 it is obvious that molecule **7** with its alkynyl unit is more difficult to oxidize (**5**, E^0 = 0.108 V; **7**, E^0 = 0.183 V). The imidazole starting compounds **3a** and **3b** show only irreversible reduction events at -1.22 (**3a**) and -1.23 V (**3b**) for the heterocyclic core (Supporting Information, Figure F3, Table F3).[F13] This indicates that, as expected, organometallics **5** and **7** are more electron rich due to the electron donating ferrocenyl groups present.

An advantage of the seleno phosphines is their tendency to crystallize easier than the appropriate phosphino imidazoles or imidazolium salts. Exemplary, the molecular structure of **11a-Se** in the solid state was established by single crystal X-ray structure analysis. Suitable crystals were obtained by slow evaporation of a saturated dichloromethane solution containing **11a-Se** at ambient temperature. The ORTEP diagram, selected bond distances (Å) and angles (°) are shown in Figure F1. The crystal and structure refinement data are presented in the Experimental Section.

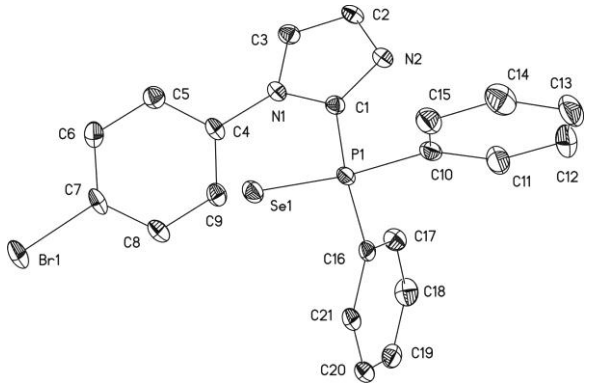

Figure F1. ORTEP diagram (50 % probability level) of the molecular structure of **11a-Se** with the atom numbering scheme. (Hydrogen atoms are omitted for clarity.) Standard uncertainties of the last significant digit(s) are shown in parenthesis. Selected bond distances (Å) and angles (°): P1-Se1 = 2.1032(6), P1-C1 = 1.813(2), P1-C10 = 1.813(2), P1-C16 = 1.820(2), N1-C1 = 1.373(3), N1-C3 = 1.371(3), N2-C1 = 1.321(3), N2-C2 = 1.372(3), C2-C3 = 1.368(3); C1-P1-Se1 = 113.56(8), C10-P1-Se1 = 113.18(8), C16-P1-Se1 = 114.43(8), C1-P1-C10 = 103.02(10), C1-P1-C16 = 105.16(11), C16-P1-C10 = 106.48(11).

Seleno phosphine **11a-Se** crystallizes in the monoclinic space group $P2_1/n$. The molecular structure of **11a-Se** is set-up by two phenyl groups, the imidazole unit and one selenium atom which are bound to the phosphorus atom resulting in a tetrahedrally distorted geometry (Figure F1). The phosphorus-carbon bond separations with 1.813(2) (P1-C1 / P1-C10) and 1.820(2) Å (P1-C16) are representative for P-C_{aryl} bond distances. [F9c,g,h] Very characteristic is the P-Se bond of 2.1032(6) Å, which is similar to other seleno phosphines, *i. e.* 1-*tert*-butyl-2-(diphenylphosphino selenide)-*1H*-imidzole [F1c] and triphenyl seleno phosphine. [F14] The C-P-C angles at P1 (Figure F1) are with 103.02(10) - 106.48(11)° in the typical range of tertiary seleno phosphines. [F1c,F9c,g,h,F14] The imidazole core entity with atoms N1, N2 and C1 – C3 is planar (r. m. s. deviation 0.0006 Å, highest deviation from planarity observed for C3 with 0.0010 Å). The C_6H_4Br moiety of the imidazole unit is rotated by 58.1° with respect to the imidazole core entity.

As outlined earlier, from palladium complex **19** single crystals could be separated in minor yield by slow evaporation of a chloroform solution below 0 °C. Complex *trans*-**19** crystallizes in form of pale yellow plates, whereas *cis*-**19** crystallizes as colorless needles. For *trans*-**19** the structure determination by X-ray crystallography proceeds unproblematic by the use of Mo K_α radiation. In case of *cis*-**19** the needles were extremely tiny and Cu K_α radiation had to be used with comparatively long exposure times. Due to this, an "icing" of the crystal occurred at higher diffraction angles and the data set obtained so far did not reach full

completeness (Table F7, Experimental Section). As no further suitable crystals of *cis*-**19** could be selected the incomplete data set has been used for refining. Thus, Figure F2 displays the molecular structure of *cis*-**19** and selected bond ranges, without further discussion (Experimental Section). Figure F2 presents further the molecular structure of *trans*-**19** (right). Important bond distances (Å) and bond angles (°) for *trans*-**19** are summarized in the caption of this Figure. Crystal and structure refinement data are presented in the Experimental Section.

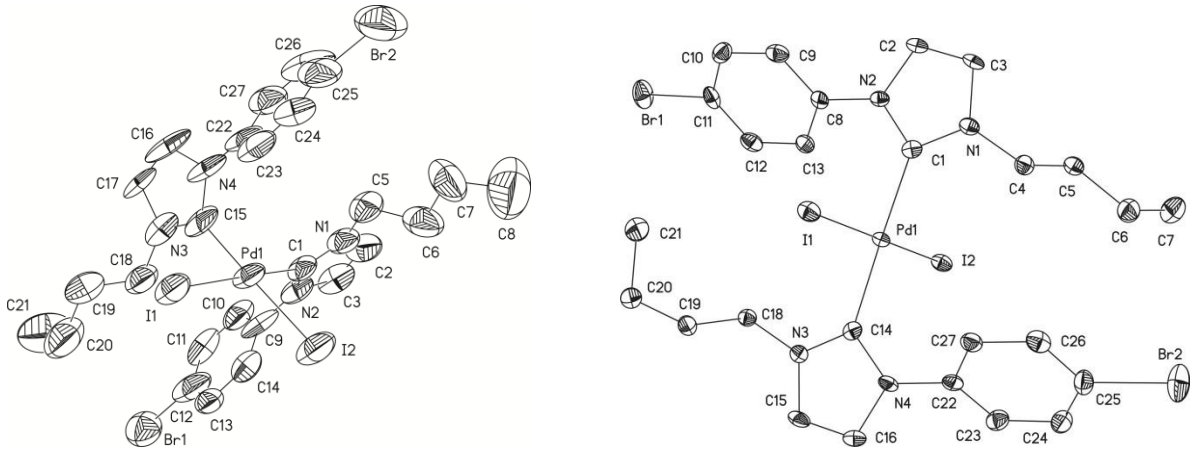

Figure F2. ORTEP diagram (50 % probability level) of the molecular structure of *cis*-**19** (left), showing only one molecule, and *trans*-**19** (right) with the atom-numbering scheme. For *cis*-**19** and *trans*-**19** all hydrogen atoms and one molecule of the packing solvent chloroform (*cis*-**19**) have been omitted for clarity. Selected bond distances (Å), angles (°) and torsion angles (°) for *trans*-**19**: Pd1-I1 = 2.6152(4), Pd1-I2 = 2.6092(4), Pd1-C1 = 2.031(3), Pd1-C14 = 2.032(3), N1-C1 = 1.341(4), N1-C3 = 1.390(4), N1-C4 = 1.463(4), N2-C1 = 1.367(4), N2-C2 = 1.395(4), N2-C8 = 1.422(4), N3-C14 = 1.335(4), N3-C15 = 1.393(4), N3-C18 = 1.463(4), N4-C14 = 1.376(4), N4-C16 = 1.386(4), N4-C22 = 1.422(4), C2-C3 = 1.343(5), C15-C16 = 1.341(5); C1-Pd1-C14 = 178.49(12), I1-Pd1-I2 = 178.963(13), I1-Pd1-C1 = 89.48(9), I1-Pd-C14 = 91.66(9), I2-Pd1-C1 = 90.34(9), I2-Pd1-C14 = 88.54(9), N1-C1-N2 = 104.8(3), N3-C14-N4 = 104.8(3). Range of bond distances for *cis*-**19**: Pd-I = 2.601(4) – 2.68(4), Pd-C_{sp2} = 1.91(2) – 2.07(2).

Both isomers of complex **19** crystallize in the triclinic space group $P\bar{1}$. The Pd1 atom of *trans*-**19** possesses a planar PdC_2I_2 coordination set-up (r. m. s. deviation 0.0169 Å, highest deviation from planarity observed for I2 with -0.0213 Å) with *trans*-oriented I1-Pd1-I2 and C1-Pd1-C14 angles of 178.963(13) and 178.49(12)°, respectively (Figure F2). As expected, the imidazole units show planarity (r. m. s. deviation 0.0025 and 0.0020 Å) and are twisted to

the C_6H_4Br moieties with angles of 47.1 and 47.3°, respectively. The main structural features of the imidazole ligands is the slightly decreased N1-C1-N2 angle (104.8(3)°) which is attributed to the extent of electronic delocalization. A similar behavior was found for other palladium imidazole species. [F15] The Pd-I, Pd-C_{sp2} and the bond distances of the imidazole and phenyl units correspond to bond lengths of related molecules, *i. e.* [(1,3-Me_2-$^cC_3H_2N_2)_2PdI_2$]. [F15a] The formation of both the kinetic and thermodynamic product might be attributed to the isolation method of crystals of **19** (Experimental Section).

2.3 Catalysis

The application of phosphino imidazoles **11a** – **k** and phosphino imidazolium salts **17** and **20** in the homogeneous palladium-catalyzed Suzuki-Miyaura *C-C* cross-coupling of 2-bromo toluene with phenylboronic acid was studied as model systems. The catalytic active species was *in situ* generated by applying mixtures of [$Pd(OAc)_2$] and the respective phosphines **11a** – **k**, **17** and **20** in the ratio of 1:2 (Reaction (F4)). The catalytic reactions were carried out in 1,4-dioxane-water mixtures of ratio 2:1 (*v*:*v*) in presence of potassium carbonate at 100 °C using 0.5 mol% of the appropriate phosphine and 0.25 mol% of the palladium source. Acetyl ferrocene as standard was added to the appropriate reaction solution to determine the rate of conversion by ^{1}H NMR spectroscopy. [F16] The obtained conversions equal ^{1}H NMR spectroscopic yields and are based on the respective aryl halides.

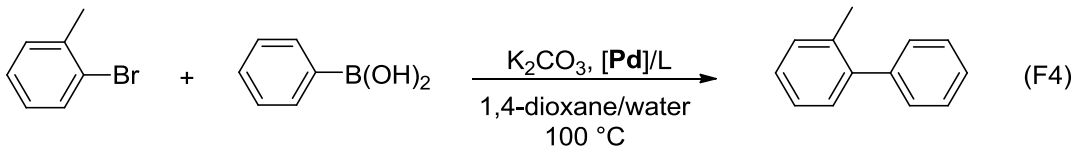

(F4)

As it can be seen from Table F4 and Figures F4 – F7 (Supporting Information) all in *in situ* generated palladium phosphines are catalytically active of which the cyclohexyl-substituted phosphines **11b**, **11e**, **11j** and **17b** are significantly more productive and active as the others (Table F4; entries 2, 5, 9 and 13), which originates from the electron-richness and bulkiness of these compounds. Comparing the alkyl- and aryl-functionalized phosphines among each other following trend concerning the activity and productivity of their palladium complexes can be seen: **11b** > **11a** > **11c** > and **11e** > **11d** > **11f**. In general, the dimethyl functionalized phosphino imidazole systems (Table F4; entries 4 – 6), which also are more easily and in better yields accessible (*vide supra*), are by far more productive than the *non*-substituted derivatives **11a** – **c** (Table F4; entries 1 – 3), explainable by the more electron-donating

capability of the imidazole rings. Since these compounds possess with the bromo and iodo substituents reactive functionalities, we decided to introduce organic and organometallic catalytic inert groups at the phenylene building block. This led to derivatives **11i** – **k**. It was found that the productivities of these species are similar to their halide counter parts (Table F4; entries 4 – 6 and 9 – 11). However, their activities are considerably higher (Figure F5, Supporting Information; Table F4) indicating that the halide carrying phosphines **11a** – **f** are involved in the catalytic reactions. In addition, the reaction profiles (Figure F5, Supporting Information) indicate that the influence of the halide is less prominent when electron-deficient phosphino groups are present explainable by the slower oxidative addition. Comparing the biphenyl- and ferrocenyl-functionalized molecules with each other it is obvious that the organometallic compounds **11g** and **11h** are superior ligands in catalysis, however, less active than the respective cyclohexyl phosphines.

From Table F4 it further becomes clear that the neutral as well as the ionic cyclohexyl phosphino systems show the same productivity with a slightly higher activity for **11e**. In the case of the molecules featuring phenyl groups it is obvious that the imidazolium derivative **17a** gives a more active and productive catalyst than **11d** (Table F4; entries 4 and 12; Figure F7, Supporting Information)) most likely attributed to the better solubility of ionic **17a**. The palladium complex carrying the imidazolium salt **20** with the phosphino donating group located at the phenylene unit is compared with ligand **17a** more active and productive, which can be explained by the better σ donor ability of the triphenylphosphine derivative. Compared with the respective neutral phosphino imidazole molecule, [F17] the imidazolium salt **20** is a better ligand for *C-C* couplings.

Table F4. Reaction of 2-bromo toluene with phenylboronic acid to give 2-methyl biphenyl. [a)]

Entry	Compd.	Conversion / %	Entry	Compd.	Conversion / %
1	**11a**	7	8	**11h**	60
2	**11b**	80	9	**11i**	24
3	**11c**	0	10	**11j**	100
4	**11d**	20	11	**11k**	5
5	**11e**	100	12	**17a**	55
6	**11f**	5	13	**17b**	97
7	**11g**	32	14	**20**	66

a) Reaction conditions[F16]: 2-bromo toluene (1.0 eq), phenylboronic acid (1.5 eq), K_2CO_3 (3.0 eq), 1,4-dioxane-water (ratio 2:1, *v*:*v*) (10 mL·mmol^{-1}), [$Pd(OAc)_2$]/phosphine (0.25 mol% [Pd], 0.5 mol% phosphine, 100 °C, 1 h. Reaction times were not minimized.

We also studied the ability of our systems *i*) to couple *non*-activated 4-chloro toluene using low palladium loadings, and *ii*) the ability to convert sterically hindered biaryls at only 50 °C (Table F5). As it can be seen from Table F5, the reaction of 4-chloro toluene with phenylboronic acid in the presence of phosphines **11d** and **11e** gave 28 and 88 % conversion, respectively, using only 0.01 mol% [$Pd(OAc)_2$] (Table F5; entries 1 and 2). Especially the cyclohexyl derivative **11e** can compete under these reaction conditions with TONs up to 8800 with the di-*t*-butylphosphino-substituted benzimidazole (TON: 8600) and shows excellent results compared to the dicyclohexylphosphino imidazole (TON: 1500 – 6600) reported by Beller and co-workers [F3b] (Table F5; entries 3 and 4). In comparison with the biphenyl ligand, first described by Buchwald, [F18a,d] significantly higher conversions can be achieved using 0.01 mol% palladium (Table F5, entry 6). [F18b] However, comparison with the trialkyl phosphino ligands by Fu [F18c] and Beller[F18b] showed a slightly lower conversion under the applied reaction conditions. [F18b]

Another challenge in organic synthesis is the preparation of sterically hindered biaryls especially under mild reaction conditions. As it can be seen from Table F5 the coupling of aryl bromides with one or two *ortho*-substituents proves the successful use of only 0.05 mol% palladium at 50 °C (Table F5; entries 9 – 12). Even highly congested 1,3,5-tri-*i*-pr-2-bromo benzene can be coupled with good conversions of 76 % (Table F5; entry 12). Compared to previously reported catalyst systems suitable for these couplings, *i. e*. Fe(η^5-(1-(4-*t*-Bu-C_6H_4)-2-P(*o*-Tol)$_2C_5H_3$))(η^5-C_5H_5)/[$Pd_2(dba)_3$] [F19a] (dba = dibenzylideneacetone) [F19] only half the amount of palladium is required to achieve good to excellent results. In comparison with the established biphenyl catalyst system by Buchwald [F18d] (Table F5, entry 13) higher catalyst loadings and longer reaction times are necessary, yet, the catalytic reaction can be performed at considerably lower temperature (50 °C *vs*. 100 °C).

Table F5. Suzuki-Miyaura coupling of 4-chloro toluene and sterically hindered aryl bromides.

Entry	Aryl Halide	Ligand	Catalyst / mol%	Conversion / %	TON
1	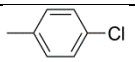	**11d**	0.01	28 [a)]	2800
2		**11e**	0.01	88 [a)]	8800
3		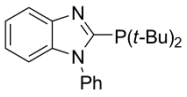	0.01	86 [a,b)]	8600
4		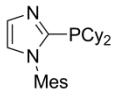	0.01	15 – 66 [a,b)]	1500 – 6600

5		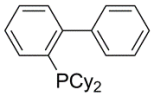	0.05	99 [c,d]	1860
6			0.01	47 [c,d]	4700
7		$P(t\text{-Bu})_3$	0.01	92 [c,d]	9200
8		$P(n\text{-Bu})Ad_2$	0.01	94 [c,d]	9400
9	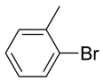	**11e**	0.05	100 [e]	2000
10	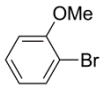	**11e**	0.05	43 [e]	860
11	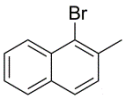	**11e**	0.05	100 [e]	2000
12	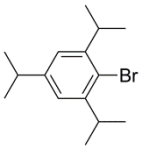	**11e**	0.05	76 [e]	1520
13		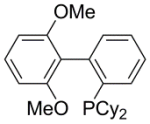	0.01	97 [e,f]	9700

a) Reaction conditions [F3b]: 4-chloro toluene (3.0 mmol, 1.0 eq), phenylboronic acid (4.5 mmol, 1.5 eq), K_3PO_4 (6.0 mmol, 3.0 eq), toluene (6 mL), $[Pd(OAc)_2]$/phosphine (0.01 mol% [Pd], 0.1 mol% phosphine, 100 °C, 20 h; b) Ligand from reference [F3b]; c) Ligands from reference [F18b]; d) Reaction conditions [F18b]: 4-chloro toluene (3.0 mmol, 1.0 eq), phenylboronic acid (4.5 mmol, 1.5 eq), K_3PO_4 (6.0 mmol, 3.0 eq), toluene (6 mL), [Pd]:P = 1:2, 100 °C, 20 h; e) Reaction conditions [F19]: aryl halide (1.0 mmol, 1.0 eq), phenylboronic acid (1.5 mmol, 1.5 eq), K_3PO_4 (3.0 mmol, 3.0 eq), toluene (2 mL), $[Pd_2(dba)_3]$/phosphine (0.05 mol% [Pd], 0.1 mol% phosphine, 50 °C, 24 h; f) Ligand from reference [F18d], T = 100 °C, 16 h.

Ionic phosphines **17b** and **20** were additionally tested under similar catalytic conditions (*vide supra*) in the coupling of 2-bromo toluene with phenylboronic acid but exchanging the organic solvent (1,4-dioxane) with the ionic liquid [BMIM][PF_6] (BMIM = 1-*n*-butyl-3-methylimidazolium) due to its structural similarity to the phosphines which should provide excellent solubility. It is well-stated that ionic liquids in homogeneous catalysis show some benefits including better solubility, stability under catalytic conditions and easier separation of the organic coupling products from the catalytic active species. [F6] The results thereof are shown in Table F6. To our surprise, the conversions in the first run are lower, when compared to the reaction in 1,4-dioxane (Table F6; entry 1 and 4). Furthermore, recycling proved unsuccessful and almost no conversion could be detected in further runs (Table F6; entries 2, 3, 5 and 6). These inactivity of our systems might be caused by the formation of 1,3-

dialkylimidazole-2-ylidene palladium complexes, which can lead, due to their stability regarding dissociation, to inactive polycarbene palladium complexes. [F20] To rule out the possibility of the formation of inactive complexes, we chose 1-*n*-butyl-2,3-dimethylimidazolium tetrafluoroborate ([BDMIM][BF_4]) as ionic liquid. However, the Suzuki-Miyaura reaction in [BDMIM][BF_4] resulted in even lower conversions after 1 h when compared to the couplings in [BMIM][PF_6] or 1,4-dioxane (Table F6; entries 7 and 8). Furthermore, precipitation of metallic palladium occurred during the catalytic reaction, which could not be suppressed by carrying out the reaction at 75 °C but with 0.5 mol% of palladium (Table F6; entries 9 and 10). These obtained results show that the catalytic species is only active for a short time leading to rapid decomposition, most probably attributed to the lower σ donor ability of the ionic phosphines and hence insufficient stabilisation of the active species.

Table F6. Reaction of 2-bromo toluene with phenylboronic acid in ionic liquid.

Entry	Run	Compd.	Conversion / %	Entry	Run	Compd.	Conversion / %
1	1	**17b** [a)]	65	7	1	**17b** [b)]	26
2	2		5	8	2		3
3	3		1				
				9	1	**17b** [c)]	36
4	1	**20** [a)]	55	10	2		3
5	2		1				
6	3		0				

a) Reaction conditions: 2-bromo toluene (1.0 eq), phenylboronic acid (1.5 eq), K_2CO_3 (3.0 eq), water (10 mL), [BMIM][PF_6] (7 g, 24.6 mmol), [$Pd(OAc)_2$]/phosphine (0.25 mol% [Pd], 0.5 mol% phosphine, 100 °C, 1 h; b) Reaction conditions: 2-bromo toluene (1.0 eq), phenylboronic acid (1.5 eq), K_2CO_3 (3.0 eq), water (10 mL), [BDMIM][BF_4] (6 g, 25.0 mmol), [$Pd(OAc)_2$]/phosphine (0.25 mol% [Pd], 0.5 mol% phosphine, 100 °C, 1 h; c) Reaction conditions: 2-bromo toluene (1.0 eq), phenylboronic acid (1.5 eq), K_2CO_3 (3.0 eq), water (10 mL), [BDMIM][BF_4] (6 g, 25.0 mmol), [$Pd(OAc)_2$]/phosphine (0.5 mol% [Pd], 1.0 mol% phosphine, 75 °C, 1 h.

3 Conclusions

Within this study the synthesis and characterization (IR, NMR, HRMS, electrochemistry, elemental analysis) of a series of imidazoles 1-(4-X-C_6H_4)-4,5-R_2-^{c}C_3HN_2 (X = Br, I, Fc, FcC≡C, Ph; R = H; Me; Fc = Fe(η^5-C_5H_4)(η^5-C_5H_5)), phosphino imidazoles 1-(4-X-C_6H_4)-2-PR'$_2$-4,5-R_2-^{c}C_3N_2 (X = Br, I, Fc, FcC≡C, Ph; R = H; Me; R' = Ph, Cy, Fur), imidazolium [1-(4-X-C_6H_4)-3-R''-4,5-R_2-^{c}C_3HN_2]I (X = Br, I; R = H, Me; R'' = *n*-Bu, *n*-Oct) and phosphino imidazolium salts [1-C_6H_5-2-PR'$_2$-3-*n*-Oct-4,5-Me_2-^{c}C_3N_2]PF_6 (R' = Ph, Cy) or [1-(4-PPh_2-C_6H_4)-3-*n*-Oct-4,5-Me_2-^{c}C_3HN_2]PF_6, and their selenium derivatives 1-(4-X-C_6H_4)-2-

P(=Se)R'$_2$-4,5-R$_2$-^{c}C$_3$N$_2$ (X = Br, I; R = H, Me; R' = Ph, Cy, Fur) are reported. They have been prepared by straightforward synthesis methodologies including alkylation, metallation, *P,C* coupling (Stelzer) and *C,C* cross-coupling reactions (Suzuki-Miyaura, Negishi, Sonogashira). To verify the σ donor ability of the phosphino imidazoles the appropriate selenium derivatives have been prepared by addition of selenium in its elemental form. High $^1J_{PSe}$ values indicate electron-poor phosphines and hence less electron donating σ donors. [F9] The structure of 1-(4-Br-C$_6$H$_4$)-2-P(=Se)Ph$_2$-^{c}C$_3$H$_2$N$_2$ in the solid state was confirmed by single crystal X-ray diffraction studies showing the pseudo-tetrahedral environment about the phosphorus atom. The reaction of [1-(4-Br-C$_6$H$_4$)-3-*n*-Bu-^{c}C$_3$H$_3$N$_2$]I toward [PdCl$_2$(cod)] (cod = cyclo-1,5-octadiene) gave the respective *cis*- and *trans*-palladium carbene complexes [Pd(1-(4-Br-C$_6$H$_4$)-3-*n*-Bu-^{c}C$_3$H$_2$N$_2$)$_2$I$_2$], which were characterized by single crystal X-ray structure measurements confirming the molecular square-planar coordination about Pd and additionally shows the structural characteristics typical for palladium-carbene complexes. [F15] Furthermore, the phosphino imidazoles and imidazolium salts were applied in the palladium-promoted Suzuki-Miyaura *C,C* cross-coupling. As model reaction the conversion of 2-bromo toluene and phenylboronic acid as organic substrates and potassium carbonate as base were chosen. All *in situ* generated phosphino palladium species showed catalytic activity toward the formation of 2-methyl biphenyl. It was found that the more electron-rich the phosphines are, the more active and productive the catalytic system is. This was impressively demonstrated by the cyclohexyl-functionalized derivatives. Additionally, the phosphino imidazolium species showed higher activity and productivity than their neutral derivatives. Also it is obvious that the halide ligands at the phenylene units should be replaced by innocent organic or organometallic moieties since otherwise the C-Br or C-I bonds are involved in the catalytic reactions. Compared with, for example, dialkylphosphino-functionalized imidazoles and benzimidazoles applying [Pd(OAc)$_2$] [F3b] as palladium source, the compounds described within this study show excellent productivities with TONs up to 8800. Furthermore, the cyclohexyl-functionalized phosphino imidazole 1-(4-I-C$_6$H$_4$)-2-PCy$_2$-4,5-Me$_2$-^{c}C$_3$N$_2$ was used in the synthesis of sterically hindered biphenyls showing good to excellent results at 50 °C and catalyst loadings of only 0.05 mol%. In further studies *C,C* coupling reactions of the appropriate imidazolium molecules in presence of the ionic liquid [BMIM][PF$_6$] were carried out. Surprisingly, the conversions were lower, when compared to the reaction in 1,4-dioxane and recycling was not possible. These observations are most likely attributed to a deactivation of the catalyst due to the formation of stable, inactive polycarbene palladium complexes. [F20] To avoid this type of reaction we carried out the Suzuki-Miyaura catalysis in [BDMIM][BF$_4$].

Nevertheless, the observed conversion were even lower, when compared to [BMIM][PF_6] or 1,4-dioxane. In addition, the formation of "palladium-black" was observed leading to the assumption that the phosphino imidazolium salts are not suited to stabilise the active species due to their lower σ donor ability.

4 Experimental Section

4.1 General Procedures

All reactions were carried out under an atmosphere of argon using standard Schlenk techniques. Toluene and tetrahydrofuran were purified by distillation from sodium/benzophenone; triethylamine was purified by distillation from calcium hydride. Diethyl ether and dichloromethane were received from a MBRAUN (MB-SPS 800) solvent drying and purification system. For filtrations Celite (purified and annealed, Erg. B.6, Riedel de Haen) was used. Column chromatography was carried out using either alumina with a particle size of 90 μm (standard, Merck KGaA) or Silica with a particle size of 40 – 60 μm (230 – 400 mesh (ASTM), Becker).

NMR spectra were recorded with a Bruker Avance III 500 spectrometer. The ^{1}H NMR spectra were recorded at 500.3 MHz, the $^{13}C\{^{1}H\}$ and $^{31}P\{^{1}H\}$ NMR spectra at 125.7 MHz and 202.5 MHz, respectively. Chemical shifts are reported in δ units (parts per million) downfield from tetramethylsilane with the solvent as reference signal (^{1}H NMR: standard internal $CDCl_3$, δ 7.26; $^{13}C\{^{1}H\}$ NMR: standard internal $CDCl_3$, δ 77.16; $^{31}P\{^{1}H\}$ NMR: standard external rel. 85 % H_3PO_4, δ 0.0; $P(OMe)_3$, δ 139.0, respectively). High resolution mass spectra were recorded with a Bruker Daltonik micrOTOF-QII spectrometer (ESI-TOF). Elemental analyses were carried out with a Thermo FlashAE 1112 series instrument. Melting points of analytical pure samples were determined by a Gallenkamp MFB 595 010 M melting point apparatus. FT IR spectra were recorded with a Thermo Nicolet IR 200 spectrometer using either KBr pellets or NaCl plates. Cyclovoltammetric measurements of dry degassed dichloromethane solutions (1.0 mmol·L^{-1}) of **3a**, **3b**, **5** and **7** containing [(*n*-Bu)$_4$N][$B(C_6F_5)_4$] (0.1 mol·L^{-1}) as supporting electrolyte were conducted under a blanket of purified argon at 25 °C utilising a Radiometer Voltalab PGZ 100 electrochemical workstation interfaced with a personal computer. A three electrode cell, which utilised a Pt auxiliary electrode, a glassy carbon working electrode (surface area 0.031 cm^2) and an Ag/Ag^+ (0.01 mol·L^{-1} [$AgNO_3$]) reference electrode mounted on a luggin capillary was used. The working electrode was pre-treated by polishing on a Buehler microcloth first with 1 micron and then with a ¼ micron

diamond paste. The reference electrode was constructed from a silver wire and inserted into a acetonitrile solution containing [$AgNO_3$] (0.01 mol·L^{-1}) and [(n-Bu)$_4$N][B(C_6F_5)$_4$] (0.1 mol·L^{-1}), in a luggin capillary with a vycor tip. This luggin capillary was inserted into a second luggin capillary with vycor tip filled with a 0.1 mol·L^{-1} [(n-Bu)$_4$N][B(C_6F_5)$_4$] solution in dichloromethane. Experimentally potentials were referenced against an Ag/Ag^+ reference electrode but results are presented referenced against ferrocene as an internal standard as required by IUPAC. [F12] Data were manipulated on a Microsoft Excel worksheet to set the formal reduction potentials of the FcH/FcH^+ couple to 0.0 V (FcH = Fe(η^5-C_5H_5)$_2$). Under our conditions the FcH/FcH^+ redox couple was at 320 mV *vs*. Ag/Ag^+.

All starting materials were obtained from commercial suppliers and used without further purification. 1-(4-Bromophenyl)-1*H*-imidazole (**3a**), [F5a] 1-phenyl-1*H*-imidazole (**3c**), [F21] [$PdCl_2(PPh_3)_2$], [F22] [$PdCl_2$(cod)], [F23] ethynylferrocene (**6**), [F24] diphenylphosphine [F25] and the chlorophosphines **10b** [F26] and **10c** [F27] were prepared according to published procedures.

4.2 Synthesis of 1-(4-iodophenyl)-4,5-dimethyl-1*H*-imidazole (3b)

Following the synthesis procedure described by Zhang *et al.* [F2d], 4-iodoaniline (10.95 g, 0.05 mol) dissolved in methanol (300 mL) was reacted with 2,3-butanedione (4.4 mL, 0.05 mol). After stirring for 16 h at ambient temperature, ammonium chloride (5.35 g, 0.1 mol) and 30 % aq. formaldehyde (10 mL, 0.1 mol) was added and the mixture was refluxed for 2 h. Afterwards, phosphoric acid (7 mL) was added in a single portion and the reaction mixture was refluxed for additional 6 h. After cooling to ambient temperature all volatiles were removed in vacuum and the dark brown residue was poured onto ice and neutralised with potassium hydroxide until pH ≈ 9 was reached. The resulting mixture was extracted with dichloromethane (300 mL) and dried over magnesium sulfate. The solvent was removed in vacuum and the residue was purified on Silica (column size: 15 × 5 cm) using diethyl ether as eluent. Product **3b** was obtained as pale yellow solid. Yield: 4.3 g (14.4 mmol, 29 % based on 4-iodoaniline). Anal. Calcd. for $C_{11}H_{11}IN_2$ (298.12 g/mol): C, 44.32; H, 3.72; N, 9.40. Found: C, 45.34; H, 3.90; N, 8.75.[*)] Mp.: 86 °C. IR (KBr, $\tilde{\upsilon}$/cm^{-1}): 1495 (m, N=C), 1588 (w, C=C), 2854/2917/2959 (w, C-H), 3060/3105 (w, =C-H). ^{1}H NMR (500.30 MHz, $CDCl_3$, δ): 2.08 (s, 3 H, CH_3), 2.21 (s, 3 H, CH_3), 7.01 (dpt, $^3J_{HH}$ = 8.7 Hz, 2 H, H^o/C_6H_4), 7.45 (s, 1 H, H^2/C_3HN$_2$), 7.80 (dpt, $^3J_{HH}$ = 8.7 Hz, 2 H, H^m/C_6H_4). ^{13}C{^{1}H} NMR (125.81 MHz, $CDCl_3$, δ): 9.2 (s, CH$_3$), 12.9 (s, CH$_3$), 93.2 (C^p/C_6H$_4$), 122.8 (s, C^4/C_3HN$_2$), 127.4 (s, C^o/C_6H$_4$), 135.0 (s, C^2/C_3HN$_2$), 135.1 (s, C^5/C_3HN$_2$), 136.8 (s, C^i/C_6H$_4$), 138.8 (s, C^m/C_6H$_4$). HRMS (ESI-TOF)

$C_{11}H_{11}IN_2$ $[M+H]^+$ *m/z*: calcd.: 299.0050, found: 299.0040. *) Please, notice that the results of the elemental analysis deviate from the calculated values due to decomposition of **3b** because this compound is highly light sensitive.

4.3 Synthesis of 1-(4-ferrocenylphenyl)-1*H*-imidazole (5)

Ferrocene (840 mg, 4.52 mmol) was dissolved in dry tetrahydrofuran (60 mL) and cooled to -78 °C. Then potassium *tert*-butoxide (64 mg, 0.57 mmol, 0.125 eq) was added in a single portion followed by dropwise addition of *t*-BuLi (5.6 mL, 8.96 mmol, 2 eq). After stirring the reaction mixture for 45 min at -78 °C, $[ZnCl_2(thf)_2]$ (1.4 g, 4.99 mmol, 1.1 eq) and **3a** (1.0 g, 4.48 mmol) was added in a single portion at 0 °C. The mixture was stirred for 30 min at this temperature, followed by addition of $[Pd(PPh_3)_4]$ (26 mg, 0.5 mol%). After heating the reaction mixture to 50 °C for 24 h, all volatiles were removed and the residue was purified by column chromatography on Silica (column size: 15 × 3.5 cm) using diethyl ether as eluent and then a mixture of diethyl ether-ethyl acetate (ratio 1:1, *v*:*v*). The product was obtained as an orange solid. Yield: 0.94 g (2.86 mmol, 63 % based on **3a**). Anal. Calcd. for $C_{19}H_{16}FeN_2$ (328.19 g/mol): C, 69.53; H, 4.91; N, 8.54. Found: C, 69.06; H, 5.06; N, 8.61. Mp.: 132 °C. IR (KBr, $\tilde{\upsilon}$/cm^{-1}): 1509/1532 (s, N=C), 1560 (w, C=C), 2868/2931 (w, C-H), 3124 (w, =C-H). ^{1}H NMR (500.30 MHz, CD_2Cl_2, δ): 4.04 (s, 5 H, C_5H_5), 4.38 (pt, $^3J_{HH}$ = 1.8 Hz, 2 H, C_5H_4), 4.69 (pt, $^3J_{HH}$ = 1.8 Hz, 2 H, C_5H_4), 7.35 (dpt, $^3J_{HH}$ = 8.6 Hz, 2 H, H^o/C_6H_4), 7.37 (pt, $^3J_{HH}$ = 1.5 Hz, 1 H, $H^4/C_3H_3N_2$), 7.43 (pt, $^3J_{HH}$ = 1.5 Hz, 1 H, $H^5/C_3H_3N_2$), 7.60 (dpt, $^3J_{HH}$ = 8.6 Hz, 2 H, H^m/C_6H_4), 8.33 (m, 1 H, $H^2/C_3H_3N_2$). ^{13}C{^{1}H} NMR (125.81 MHz, CD_2Cl_2, δ): 66.8 (s, C_5H_4), 69.8 (s, C_5H_4), 69.9 (s, C_5H_5), 83.2 (s, C^i/C_5H_4), 120.0 (s, $C^4/C_3H_3N_2$), 122.2 (s, C^o/C_6H_4), 127.3 (s, C^m/C_6H_4), 127.9 (s, $C^5/C_3H_3N_2$), 133.6 (s, C^i/C_6H_4), 136.8 (s, $C^2/C_3H_3N_2$), 141.2 (s, C^p/C_6H_4). HRMS (ESI-TOF) $C_{19}H_{16}FeN_2$ $[M+H]^+$ *m/z*: calcd.: 329.0715, found: 329.0736.

4.4 Synthesis of 1-(4-(ethynylferrocenyl)phenyl)-1*H*-imidazole (7)

Ethynylferrocene (**6**, 0.5 g, 2.38 mmol), **3a** (0.53 g, 2.38 mmol), [CuI] (45 mg, 10 mol%) and $[PdCl_2(PPh_3)_2]$ (83 mg, 5 mol%) were dissolved in dry triethylamine (60 mL) and stirred at 60 °C for 16 h. After removal of all volatiles in vacuum, the residue was purified by column chromatography on Silica (column size: 15 × 3.5 cm) using diethyl ether and then ethyl acetate as eluent. Product **7** was obtained as yellow solid. Yield: 0.37 g (1.05 mmol, 44 % based on **3a**). Anal. Calcd. for $C_{21}H_{16}FeN_2$ (352.21 g/mol): C, 71.61; H, 4.58; N, 7.95.

Found: C, 71.45; H, 4.60; N, 7.95. Mp.: 160 °C (dec.). IR (KBr, $\tilde{\upsilon}$/cm^{-1}): 1490 (w, N=C), 1524 (m, C=C), 2206 (w, C≡C), 2851/2921 (w, C-H), 3108 (w, =C-H). ^{1}H NMR (500.30 MHz, $CDCl_3$, δ): 4.26 (s, 5 H, C_5H_5), 4.27 (pt, $^{3}J_{HH}$ = 1.8 Hz, 2 H, C_5H_4), 4.52 (pt, $^{3}J_{HH}$ = 1.9 Hz, 2 H, C_5H_4), 7.24 (m, 1 H, $C_3H_3N_2$), 7.32 (m, 1 H, $C_3H_3N_2$), 7.35 (dpt, $^{3}J_{HH}$ = 8.5 Hz, 2 H, C_6H_4), 7.59 (dpt, $^{3}J_{HH}$ = 8.4 Hz, 2 H, C_6H_4), 7.89 (m, 1 H, $H^{2}/C_3H_3N_2$). $^{13}C\{^{1}H\}$ NMR (125.81 MHz, CD_2Cl_2, δ): 64.8 (s, C^{i}/C_5H_4), 69.2 (s. C_5H_4), 70.1 (s, C_5H_5), 71.6 (s, C_5H_4), 84.6 (s, C≡C), 90.2 (s, C≡C), 121.1 (s, $C^{4}/C_3H_2N_2$), 121.3 (s, C^{o}/C_6H_4), 123.2 (s, C^{p}/C_6H_4), 123.5 (s, $C^{5}/C_3H_2N_2$), 133.0 (s, C^{m}/C_6H_4), 133.2 (s, C^{i}/C_6H_4), 136.5 (s, $C^{2}/C_3H_3N_2$). HRMS (ESI-TOF) $C_{21}H_{16}FeN_2$ $[M+H]^+$ *m/z*: calcd.: 353.0719, found: 353.0736.

4.5 Synthesis of 1-(4-(1,1'-biphenyl))-4,5-dimethyl-1*H*-imidazole (9)

Imidazole **3b** (1.29 g, 6.5 mmol), phenylboronic acid (**8**, 0.95 g, 7.81 mmol, 1.2 eq), potassium carbonate (2.69 g, 19.5 mmol, 3 eq) and [$PdCl_2$(dppf)] (23 mg, 0.5 mol%) were dissolved in a 1,4-dioxane-water mixture (50 mL, ratio 2:1, *v*:*v*) and stirred at 100 °C for 16 h. After cooling to ambient temperature the organic phase was separated, dried over magnesium sulphate and purified by column chromatography on Silica (column size: 18 × 3.5 cm) using diethyl ether as eluent. Biphenyl **9** was obtained as a pale yellow solid. Yield: 1.31 g (5.3 mmol, 82 % based on **3b**). Anal. Calcd. for $C_{17}H_{16}N_2$ (248.32 g/mol): C, 82.22; H, 6.49; N, 11.28. Found: C, 81.61; H, 6.60; N, 11.13. Mp.: 103 °C. IR (KBr, $\tilde{\upsilon}$/cm^{-1}): 1450/1490 (s, N=C), 1595/1605 (w, C=C), 2860/2919 (w, C-H), 3033/3102 (w, =C-H). ^{1}H NMR (500.30 MHz, $CDCl_3$, δ): 2.12 (s, 3 H, CH_3), 2.24 (s, 3 H, CH_3), 7.30 (dpt, $^{3}J_{HH}$ = 8.4 Hz, 2 H, H^{3}/C_6H_5-C_6H_4), 7.36 (m, 1 H, $H^{4'}/C_6H_5$-C_6H_4), 7.45 (m, 2 H, $H^{3'}/C_6H_5$-C_6H_4), 7.51 (s, 1 H, H^{2}/C_3HN_2), 7.59 (m, 2 H, $H^{2'}/C_6H_5$-C_6H_4), 7.66 (dpt, $^{3}J_{HH}$ = 8.4 Hz, 2 H, H^{2}/C_6H_5-C_6H_4). $^{13}C\{^{1}H\}$ NMR (125.81 MHz, $CDCl_3$, δ): 9.2 (s, CH_3), 12.8 (s, CH_3), 122.9 (s, C^{i}), 125.7 (s, C^{3}/C_6H_5-C_6H_4), 127.1 (s, $C^{2'}/C_6H_5$-C_6H_4), 127.8 (s, $C^{4'}/C_6H_5$-C_6H_4), 128.1 (s, C^{2}/C_6H_5-C_6H_4), 128.9 (s, $C^{3'}/C_6H_5$-C_6H_4), 134.6 (s, C^{i}), 135.1 (s, C^{2}/C_3HN_2), 136.1 (s, C^{i}), 139.8 (s, C^{i}), 141.0 (s, C^{i}). HRMS (ESI-TOF) $C_{17}H_{16}N_2$ $[M+H]^+$ *m/z*: calcd.: 249.1386, found: 249.1381; $[M+Na]^+$ *m/z*: calcd.: 271.1206, found: 271.1206.

4.6 General Synthesis Procedure for Phosphines 11a – f

To 0.5 g of **3a** (2.24 mmol), **3b** (1.68 mmol), **5** (1.52 mmol), **7** (1.42 mmol) or **9** (2.01 mmol) dissolved in in dry diethyl ether (**3a**, **5**, **7**, **9**, 40 mL) or tetrahydrofuran (**3b**, 40 mL) one eq of a 2.5 M solution of *n*-BuLi (**3a**, **5**, **7**, **9**) or a 2.0 M solution of lithium di-*i*-

propylamide (**3b**) was added dropwise at -30 °C. After warming the solution to ambient temperature, it was again cooled to -30 °C and one eq of the chlorophosphines **10a** – **c** was added dropwise. The reaction mixture was stirred at ambient temperature for 2 h and the solvent was removed in vacuum. The crude product was purified by column chromatography on Silica or alumina and dried in vacuum.

4.6.1 Synthesis of 1-(4-bromophenyl))-2-(diphenylphosphino)-1*H*-imidazole (11a)

Following the general procedure described above, **3a** (0.5 g, 2.24 mmol) was reacted with *n*-BuLi (0.90 mL, 2.25 mmol) and chlorodiphenylphosphine (**10a**, 0.40 mL, 2.23 mmol). The residue was purified by column chromatography on Silica (column size: 12 × 3.5 cm) using a mixture of *n*-hexane-diethyl ether (ratio 1:1, *v*:*v*) as eluent. Phosphine **11a** was obtained as a colorless solid. Yield: 0.55 g (1.35 mmol, 60 % based on **3a**). Anal. Calcd. for $C_{21}H_{16}BrN_2P$ (407.24 g/mol): C, 61.93; H, 3.96; N, 6.88. Found: C, 61.85; H, 3.98; N, 6.87. Mp.: 170 °C. IR (KBr, $\tilde{\upsilon}$/cm^{-1}): 1432 (m, P-C), 1480 (s, N=C), 1582 (w, C=C), 3052/3138 (w, =C-H). ^{1}H NMR (500.30 MHz, $CDCl_3$, δ): 7.09 (dpt, $^3J_{HH}$ = 8.6 Hz, $^4J_{HH}$ = 2.1 Hz, 2 H, H^o/C$_6$*H*$_4$), 7.23 (dd, $^3J_{HH}$ = 1.2 Hz, $^4J_{HP}$ = 2.0 Hz, 1 H, H^4/C$_3$*H*$_2$N$_2$), 7.32 – 7.35 (m, 6 H, H^{m,p}/C$_6$*H*$_5$), 7.38 (d, $^3J_{HH}$ = 1.2 Hz, H^5/C$_3$*H*$_2$N$_2$), 7.41 – 7.45 (m, 4 H, H^o/C$_6$*H*$_5$), 7.52 (dpt, $^3J_{HH}$ = 8.6 Hz, $^4J_{HH}$ = 2.9 Hz, 2 H, H^m/C$_6$*H*$_4$). ^{13}C{^{1}H} NMR (125.81 MHz, $CDCl_3$, δ): 122.6 (s, C^p/*C*$_6$H$_4$), 123.7 (s, C^4/*C*$_3$H$_2$N$_2$), 128.0 (d, $^4J_{CP}$ = 3.7 Hz, C^o/*C*$_6$H$_4$), 128.6 (d, $^3J_{CP}$ = 7.5 Hz, C^m/*C*$_6$H$_5$), 129.3 (s, C^p/*C*$_6$H$_5$), 131.7 (d, $^3J_{CP}$ = 1.6 Hz, C^5/*C*$_3$H$_2$N$_2$), 132.4 (s, C^m/*C*$_6$H$_4$), 134.0 (d, $^2J_{CP}$ = 20.8 Hz, C^o/*C*$_6$H$_5$), 135.3 (d, $^1J_{CP}$ = 4.8 Hz, C^i/*C*$_6$H$_5$), 137.1 (d, $^3J_{CP}$ = 1.8 Hz, C^i/*C*$_6$H$_4$), 147.0 (d, $^1J_{CP}$ = 7.4 Hz, C^2/*C*$_3$H$_2$N$_2$). ^{31}P{^{1}H} NMR (202.5 MHz, $CDCl_3$, δ): -29.4 (s). HRMS (ESI-TOF) $C_{21}H_{16}BrN_2P$ $[M+H]^+$ *m/z*: calcd.: 407.0307, found: 407.0255.

4.6.2 Synthesis of 1-(4-bromophenyl))-2-(dicyclohexylphosphino)-1*H*-imidazole (11b)

Using the general procedure described above, **3a** (0.5 g, 2.24 mmol) was reacted with *n*-BuLi (0.90 mL, 2.25 mmol) and chlorodicyclohexylphosphine (**10b**, 0.50 mL, 2.26 mmol). The residue was purified by column chromatography on Silica (column size: 12 × 3.5 cm) using a mixture of *n*-hexane-diethyl ether (ratio 1:1, *v*:*v*) as eluent. Phosphine **11b** was obtained as a colorless solid. Yield: 0.46 g (1.10 mmol, 49 % based on **3a**). Anal. Calcd. for $C_{21}H_{28}BrN_2P$ (419.34 g/mol): C, 60.15; H, 6.73; N, 6.68. Found: C, 60.25; H, 6.62; N, 6.66. Mp.: 139 °C. IR (KBr, $\tilde{\upsilon}$/cm^{-1}): 1445 (m, P-C), 1481/1501 (m, N=C), 1586 (w, C=C), 2847/2922 (s, C-H), 3097/3150 (w, =C-H). ^{1}H NMR (500.30 MHz, $CDCl_3$, δ): 0.95 – 1.04

(m, 2 H, C_6H_{11}), 1.08 – 1.30 (m, 8 H, C_6H_{11}), 1.55 – 1.57 (m, 2 H, C_6H_{11}), 1.61 – 1.72 (m, 8 H, C_6H_{11}), 2.08 – 2.13 (m, 2 H, H^1/C_6H_{11}), 7.13 (dd, $^3J_{HH}$ = 1.1 Hz, $^4J_{HP}$ = 2.3 Hz, 1 H, $H^4/C_3H_2N_2$), 7.18 (dpt, $^3J_{HH}$ = 8.6 Hz, $^4J_{HH}$ = 2.0 Hz, $^5J_{HP}$ = 1.0 Hz, 2 H, H^o/C_6H_4), 7.33 (d, $^3J_{HH}$ = 1.0 Hz, 1 H, $H^5/C_3H_2N_2$), 7.57 (dpt, $^3J_{HH}$ = 8.6 Hz, $^4J_{HH}$ = 1.9 Hz, H^m/C_6H_4). $^{13}C\{^1H\}$ NMR (125.81 MHz, $CDCl_3$, δ): 26.5 (s, C_6H_{11}), 26.9 (d, J_{CP} = 8.1 Hz, C_6H_{11}), 27.1 (d, J_{CP} = 12.7 Hz, C_6H_{11}), 29.3 (d, J_{CP} = 7.1 Hz, C_6H_{11}), 30.4 (d, J_{CP} = 16.1 Hz, C_6H_{11}), 34.4 (d, $^1J_{CP}$ = 7.7 Hz, C^1/C_6H_{11}), 122.3 (s, C^p/C_6H_4), 123.1 (s, $C^4/C_3H_2N_2$), 128.9 (d, $^4J_{CP}$ = 4.3 Hz, C^o/C_6H_4), 130.9 (s, $C^5/C_3H_2N_2$), 132.2 (s, C^m/C_6H_4), 137.6 (d, $^3J_{CP}$ = 1.4 Hz, C^i/C_6H_4), 147.4 (d, $^1J_{CP}$ = 19.9 Hz, $C^2/C_3H_2N_2$). $^{31}P\{^1H\}$ NMR (202.5 MHz, $CDCl_3$, δ): -24.4 (s). HRMS (ESI-TOF) $C_{21}H_{28}BrN_2P$ $[M+H]^+$ *m/z*: calcd.: 419.1246, found: 419.1224.

4.6.3 Synthesis of 1-(4-bromophenyl))-2-(di-2-furylphosphino)-1*H*-imidazole (11c)

Based on the general procedure described above, **3a** (0.5 g, 2.24 mmol) was reacted with *n*-BuLi (0.90 mL, 2.25 mmol) and chlorodi-2-furylphosphine (**10c**, 0.45 g, 2.24 mmol). The residue was purified by column chromatography on Silica (column size: 12 × 3.5 cm) using diethyl ether as eluent. Phosphine **11c** was obtained as colorless solid. Yield: 0.45 g (1.16 mmol, 52 % based on **3a**). Anal. Calcd. for $C_{17}H_{12}BrN_2O_2P$ (387.17 g/mol): C, 52.74; H, 3.12; N, 7.24. Found: C, 52.83; H, 3.09; N, 7.24. Mp.: 146 °C. IR (KBr, $\tilde{\nu}$/cm^{-1}): 1007 (s, C-O), 1449 (m, P-C), 1483/1498 (m, N=C), 1546 (w, C=C), 3073/3094/3112/3137 (w, =C-H). ^1H NMR (500.30 MHz, $CDCl_3$, δ): 6.38 (dt $^4J_{HP}$ = 1.6 Hz, $^3J_{HH}$ = 3.3 Hz, $^3J_{HH}$ = 1.8 Hz, 2 H, H^4/C_4H_3O), 6.77 (m, 2 H, H^3/C_4H_3O), 7.07 (dpt, $^3J_{HH}$ = 8.6 Hz, $^4J_{HH}$ = 2.0 Hz, $^5J_{HP}$ = 1.1 Hz, 2 H, H^o/C_6H_4), 7.14 (pt, $^3J_{HH}$ = 1.4 Hz, $H^4/C_3H_2N_2$), 7.33 (d, $^3J_{HH}$ = 1.1 Hz, $H^5/C_3H_2N_2$), 7.51 (dpt, $^3J_{HH}$ = 8.6 Hz, $^4J_{HH}$ = 2.0 Hz, H^m/C_6H_4), 7.65 (m, 2 H, H^5/C_4H_3O). $^{13}C\{^1H\}$ NMR (125.81 MHz, $CDCl_3$, δ): 111.0 (d, $^3J_{CP}$ = 6.6 Hz, C^4/C_4H_3O), 122.5 (d, $^2J_{CP}$ = 26.3 Hz, C^3/C_4H_3O), 122.7 (s, C^p/C_6H_4), 123.8 (s, $C^4/C_3H_2N_2$), 127.8 (d, $^4J_{CP}$ = 3.5 Hz, C^o/C_6H_4), 131.7 (d, $^3J_{CP}$ = 3.5 Hz, $C^5/C_3H_2N_2$), 132.4 (s, C^m/C_6H_4), 136.9 (m, C^i/C_6H_4), 143.7 (d, $^1J_{CP}$ = 7.8 Hz, C^2/C_4H_3O), 147.6 (m, $C^2/C_3H_2N_2$), 148.0 (d, $^4J_{CP}$ = 2.9 Hz, C^5/C_4H_3O). $^{31}P\{^1H\}$ NMR (202.5 MHz, $CDCl_3$, δ): -73.0 (s). HRMS (ESI-TOF) $C_{17}H_{12}BrN_2O_2P$ $[M+H]^+$ *m/z*: calcd.: 386.9893, found: 386.9882; $[M+Na]^+$ *m/z*: calcd.: 408.9712, found: 408.9698.

4.6.4 Synthesis of 1-(4-iodophenyl)-2-(diphenylphosphino)-4,5-dimethyl-1*H*-imidazole (11d)

Compound **3b** (0.5 g, 1.68 mmol) was reacted with lithium di-*iso*-propylamide (0.84 mL, 1.68 mmol) and chlorodiphenylphosphine (**10a**, 0.31 mL, 1.73 mmol) as described earlier. The crude product was purified by column chromatography on Silica (column size: 12 × 3.5 cm) using a mixture of *n*-hexane-diethyl ether (ratio 1:1, *v*:*v*) as eluent. Phosphine **11d** was obtained as a colorless solid. Yield: 0.53 g (1.10 mmol, 65 % based on **3b**). Anal. Calcd. for $C_{23}H_{20}IN_2P$ (482.30 g/mol): C, 57.28; H, 4.18; N, 5.81. Found: C, 56.86; H, 4.36; N, 5.49. Mp.: 189 °C. IR (KBr, $\tilde{\upsilon}$/cm^{-1}): 1433 (m, P-C), 1479/1487 (s, N=C), 1581 (w, C=C), 2913 (w, C-H), 3048 (w, =C-H). ^{1}H NMR (500.30 MHz, $CDCl_3$, δ): 1.96 (s, 3 H, CH_3), 2.25 (s, 3 H, CH_3), 6.77 (dpt, $^3J_{HH}$ = 8.5 Hz, $^4J_{HH}$ = 1.9 Hz, $^5J_{HP}$ = 0.9 Hz, 2 H, H^o/C$_6H_4$), 7.28 – 7.30 (m, 6 H, H^{m,p}/C$_6H_5$), 7.40 – 7.44 (m, 4 H, H^o/C$_6H_5$), 7.70 (dpt, $^3J_{HH}$ = 8.5 Hz, $^4J_{HH}$ = 1.9 Hz, H^m/C$_6H_4$). ^{13}C{^{1}H} NMR (125.81 MHz, $CDCl_3$, δ): 9.7 (s, *C*H$_3$), 13.2 (s, *C*H$_3$), 94.5 (s, C^p/*C*$_6$H$_4$), 127.1 (s, C^4/*C*$_3$N$_2$), 128.5 (d, $^3J_{CP}$ = 7.6 Hz, C^m/*C*$_6$H$_5$), 128.9 (s, C^p/*C*$_6$H$_5$), 130.1 (d, $^4J_{CP}$ = 2.7 Hz, C^o/*C*$_6$H$_4$), 133.8 (d, $^2J_{CP}$ = 20.1 Hz, C^o/*C*$_6$H$_5$), 136.1 (d, $^1J_{CP}$ = 5.4 Hz, C^i/C$_6$H$_5$), 136.7 (d, $^3J_{CP}$ = 2.0 Hz, C^5/*C*$_3$N$_2$), 137.1 (d, $^3J_{CP}$ = 2.3 Hz, C^i/C$_6$H$_4$), 138.4 (s, C^m/*C*$_6$H$_4$), 143.9 (d, $^1J_{CP}$ = 2.6 Hz, C^2/(CH$_3$)$_2$*C*$_3$N$_2$). ^{31}P{^{1}H} NMR (202.5 MHz, $CDCl_3$, δ): -29.1 (s). HRMS (ESI-TOF) $C_{23}H_{20}IN_2P$ [M+H]$^+$ *m/z*: calcd.: 483.0482, found: 483.0479.

4.6.5 Synthesis of 1-(4-iodophenyl))-2-(dicyclohexylphosphino)-4,5-dimethyl-1*H*-imidazole (11e)

Compound **3b** (0.5 g, 1.68 mmol) was reacted with lithium di-*iso*-propylamide (0.84 mL, 1.68 mmol) and chlorodicyclohexylphosphine (**10b**, 0.37 mL, 1.68 mmol) as described earlier. The residue was purified by column chromatography on Silica (column size: 12 × 3.5 cm) using a mixture of *n*-hexane-diethyl ether (ratio 1:1, *v*:*v*) as eluent. Molecule **11e** was obtained as a colorless solid. Yield: 0.46 g (0.93 mmol, 55 % based on **3b**). Anal. Calcd. for $C_{23}H_{32}IN_2P$ (494.39 g/mol): C, 55.88; H, 6.52; N, 5.67. Found: C, 56.19; H, 6.62; N, 5.65. Mp.: 181 °C. IR (KBr, $\tilde{\upsilon}$/cm^{-1}): 1435 (m, P-C), 1459 (s, N=C), 1582 (w, C=C), 2855/2914/2936 (w, C-H), 3049/3070 (w, =C-H). ^{1}H NMR (500.30 MHz, $CDCl_3$, δ): 0.97 – 1.06 (m, 2 H, C$_6H_{11}$), 1.09 – 1.30 (m, 8 H, C$_6H_{11}$), 1.56 – 1.58 (m, 2 H, C$_6H_{11}$), 1.61 – 1.72 (m, 8 H, C$_6H_{11}$), 1.93 (s, 3 H, CH_3), 2.07 – 2.12 (m, 2 H, H^1/C$_6H_{11}$), 2.25 (s, 3 H, CH_3), 6.85 (dpt, $^3J_{HH}$ = 8.5 Hz, $^4J_{HH}$ = 1.9 Hz, $^5J_{HP}$ = 0.7 Hz, 2 H, H^o/C$_6H_4$), 7.78 (dpt, $^3J_{HH}$ = 8.5 Hz, $^4J_{HH}$ = 1.9 Hz, 2 H, H^m/C$_6H_4$). ^{13}C{^{1}H} NMR (125.81 MHz, $CDCl_3$, δ): 9.8 (s, *C*H$_3$), 13.1 (s,

CH_3), 26.5 (s, C_6H_{11}), 27.0 (d, J_{CP} = 8.7 Hz, C_6H_{11}), 27.1 (d, J_{CP} = 13.5 Hz, C_6H_{11}), 29.5 (d, J_{CP} = 7.7 Hz, C_6H_{11}), 30.6 (d, J_{CP} = 16.6 Hz, C_6H_{11}), 34.5 (d, $^1J_{CP}$ = 7.3 Hz, C^1/C_6H_{11}), 94.3 (s, C^p/C_6H_4), 125.8 (s, C^4/C_3N_2), 130.8 (d, $^4J_{CP}$ = 2.7 Hz, C^o/C_6H_4), 135.8 (s, C^5/C_3N_2), 137.7 (s, C^i/C_6H_4), 138.3 (s, C^m/C_6H_4), 144.9 (d, $^1J_{CP}$ = 13.4 Hz, C^2/C_3N_2). $^{31}P\{^1H\}$ NMR (202.5 MHz, $CDCl_3$, δ): -23.6 (s). HRMS (ESI-TOF) $C_{23}H_{32}IN_2P$ $[M+H]^+$ *m/z*: calcd.: 495.1421, found: 495.1380.

4.6.6 Synthesis of 1-(4-iodophenyl))-2-(di-2-furylphosphino)-4,5-dimethyl-1*H*-imidazole (11f)

Following the synthesis methodology described above, **3b** (0.5 g, 1.68 mmol) was reacted with lithium di-*i*-propylamide (0.84 mL, 1.68 mmol) and chlorodi-2-furylphosphine (**10c**, 0.37 mL, 1.68 mmol). The crude product was purified by column chromatography on Silica (column size: 12 × 3.5 cm) using diethyl ether as eluent. Product **11f** was obtained as colorless solid. Yield: 0.52 g (1.13 mmol, 55 % based on **3b**). Anal. Calcd. for $C_{19}H_{16}IN_2O_2P$ (462.22 g/mol): C, 49.37; H, 3.49; N, 6.06. Found: C, 49.37; H, 3.65; N, 5.83. Mp.: 132 °C. IR (KBr, $\tilde{\upsilon}$/cm^{-1}): 1006 (s, C-O), 1454 (m, P-C), 1488 (s, N=C), 1550/1589 (w, C=C), 2914 (w, C-H), 3031/3045/3077 (w, =C-H). ^1H NMR (500.30 MHz, $CDCl_3$, δ): 1.92 (s, 3 H, CH_3), 2.23 (s, 3 H, CH_3), 6.35 (dt $^4J_{HP}$ = 1.6 Hz, $^3J_{HH}$ = 3.3 Hz, $^3J_{HH}$ = 1.7 Hz, 2 H, H^4/C_4H_3O), 6.71 (m, 2 H, H^3/C_4H_3O), 6.80 (dpt, $^3J_{HH}$ = 8.6 Hz, $^4J_{HH}$ = 2.0 Hz, $^5J_{HP}$ = 0.9 Hz, 2 H, H^o/C_6H_4), 7.62 (m, 2 H, H^5/C_4H_3O), 7.72 (dpt, $^3J_{HH}$ = 8.5 Hz, $^4J_{HH}$ = 1.9 Hz, H^m/C_6H_4). $^{13}C\{^1H\}$ NMR (125.81 MHz, $CDCl_3$, δ): 9.5 (s, CH_3), 13.2 (s, CH_3), 94.4 (s, C^p/C_6H_4), 111.0 (d, $^3J_{CP}$ = 6.9 Hz, C^4/C_4H_3O), 121.9 (d, $^2J_{CP}$ = 26.4 Hz, C^3/C_4H_3O), 127.4 (s, C^4/C_3N_2), 129.8 (d, $^4J_{CP}$ = 2.5 Hz, C^o/C_6H_4), 136.7 (d, $^3J_{CP}$ = 4.3 Hz, C^5/C_3N_2), 136.8 (d, $^3J_{CP}$ = 1.3 Hz, C^i/C_6H_4), 138.4 (s, C^m/C_6H_4), 140.4 (d, $^1J_{CP}$ = 12.1 Hz, C^2/C_3N_2), 147.7 (d, $^4J_{CP}$ = 2.7 Hz, C^5/C_4H_3O), 148.1 (d, $^1J_{CP}$ = 3.0 Hz, C^2/C_4H_3O). $^{31}P\{^1H\}$ NMR (202.5 MHz, $CDCl_3$, δ): -72.9 (s). HRMS (ESI-TOF) $C_{19}H_{16}IN_2O_2P$ $[M+H]^+$ *m/z*: calcd.: 463.0066, found: 463.0067.

4.6.7 Synthesis of 1-(4-ferrocenylphenyl))-2-(diphenylphosphino)-1*H*-imidazole (11g)

Molecule **5** (0.5 g, 1.52 mmol) was reacted with *n*-BuLi (0.61 mL, 1.53 mmol) and chlorodiphenylphosphine (**10a**, 0.28 mL, 1.56 mmol) as described above. The crude product was purified by column chromatography on Silica (column size: 12 × 3.5 cm) using a mixture of *n*-hexane-diethyl ether (ratio 2:5, *v*:*v*) as eluent. The title compound **11g** was obtained as an orange solid. Yield: 0.49 g (0.96 mmol, 63 % based on **5**). Anal. Calcd. for $C_{31}H_{25}FeN_2P$

(512.36 g/mol): C, 72.67; H, 4.92; N, 5.47. Found: C, 72.24; H, 5.25; N, 5.39. Mp.: 171 °C. IR (KBr, $\tilde{\upsilon}$/cm^{-1}): 1431 (m, P-C), 1458/1475 (m, N=C), 1531/1537 (m, C=C), 2852/2923/2957 (w, C-H), 3043/3082 (w, =C-H). ^{1}H NMR (500.30 MHz, $CDCl_3$, δ): 4.05 (s, 5 H, C_5H_5), 4.35 (pt, $^{3}J_{HH}$ = 1.8 Hz, C_5H_4), 4.64 (pt, $^{3}J_{HH}$ = 1.8 Hz, C_5H_4), 7.13 (dpt, $^{3}J_{HH}$ = 8.4 Hz, $^{4}J_{HH}$ = 2.0 Hz, $^{5}J_{HP}$ = 1.3 Hz, 2 H, H^{o}/C_6H_4), 7.28 (dd, $^{3}J_{HH}$ = 1.2 Hz, $^{4}J_{HP}$ = 2.0 Hz, 1 H, $H^{5}/C_3H_2N_2$), 7.33 – 7.44 (m, 6 H, $H^{m,p}/C_6H_5$), 7.39 (d, $^{3}J_{HH}$ = 1.1 Hz, $H^{4}/C_3H_2N_2$), 7.42 – 7.47 (m, 6 H, H^{o}/C_6H_5 + H^{m}/C_6H_4). ^{13}C{^{1}H} NMR (125.81 MHz, $CDCl_3$, δ): 66.8 (s, C_5H_4), 69.5 (s, C_5H_4), 69.9 (s, C_5H_5), 84.0 (s, C^{i}/C_5H_4), 123.9 (s, $C^{4}/C_3H_2N_2$), 126.4 (d, $^{4}J_{CP}$ = 3.9 Hz, C^{o}/C_6H_4), 126.5 (s, C^{p}/C_6H_5), 128.6 (d, $^{3}J_{CP}$ = 7.4 Hz, C^{m}/C_6H_5), 129.2 (s, C^{m}/C_6H_4), 131.5 (d, $^{3}J_{CP}$ = 1.7 Hz, $C^{5}/C_3H_2N_2$), 134.1 (d, $^{2}J_{CP}$ = 20.8 Hz, C^{o}/C_6H_5), 135.6 (d, $^{3}J_{CP}$ = 1.7 Hz, C^{i}/C_6H_4), 135.7 (d, $^{1}J_{CP}$ = 5.5 Hz, C^{i}/C_6H_5), 140.2 (s, C^{p}/C_6H_4), 146.9 (d, $^{1}J_{CP}$ = 6.6 Hz, $C^{2}/C_3H_2N_2$). ^{31}P{^{1}H} NMR (202.5 MHz, $CDCl_3$, δ): -28.0 (s). HRMS (ESI-TOF) $C_{31}H_{25}FeN_2P$ $[M+H]^+$ *m/z*: calcd.: 513.1159, found: 513.1178.

4.6.8 Synthesis of 1-(4-(ethynylferrocenyl)phenyl))-2-(diphenylphosphino)-1*H*-imidazole (11h)

7 (0.5 g, 1.42 mmol) was reacted with *n*-BuLi (0.57 mL, 1.43 mmol) and chlorodiphenylphosphine (**10a**, 0.26 mL, 1.45 mmol) as described earlier. The residue was purified by column chromatography on Silica (column size: 12 × 3.5 cm) using diethyl ether as eluent. The product **11h** was obtained as orange solid. Yield: 0.34 g (0.63 mmol, 44 % based on **7**). Anal. Calcd. for $C_{33}H_{25}FeN_2P$ (536.38 g/mol): C, 73.89; H, 4.70; N, 5.22. Found: C, 73.34; H, 4.85; N, 5.15. Mp.: 139 °C. IR (KBr, $\tilde{\upsilon}$/cm^{-1}): 1433 (m, P-C), 1477 (w, N=C), 1519 (m, C=C), 2204 (w, C≡C), 2852/2922 (w, C-H), 3050 (w, =C-H). ^{1}H NMR (500.30 MHz, $CDCl_3$, δ): 4.25 (s, 5 H, C_5H_5), 4.27 (pt, $^{3}J_{HH}$ = 1.8 Hz, C_5H_4), 4.52 (pt, $^{3}J_{HH}$ = 1.8 Hz, C_5H_4), 7.18 (dpt, $^{3}J_{HH}$ = 8.5 Hz, $^{4}J_{HH}$ = 1.8 Hz, $^{5}J_{HP}$ = 1.3 Hz, 2 H, H^{o}/C_6H_4), 7.26 (m, 1 H, $H^{5}/C_3H_2N_2$), 7.33 – 7.36 (m, 6 H,), 7.39 (d, $^{3}J_{HH}$ = 0.9 Hz, $H^{4}/C_3H_2N_2$), 7.43 – 7.46 (m, 6 H, $H^{m,p}/C_6H_5$), 7.49 (dpt, $^{3}J_{HH}$ = 8.5 Hz, $^{4}J_{HH}$ = 1.8 Hz, 2 H, H^{m}/C_6H_4). ^{13}C{^{1}H} NMR (125.81 MHz, $CDCl_3$, δ): 64.8 (s, C^{i}/C_5H_4), 69.2 (s, C_5H_4), 70.2 (s, C_5H_5), 71.6 (s, C_5H_4), 84.8 (s, C≡C), 90.4 (s, C≡C), 123.7 (s, $C^{4}/C_3H_2N_2$), 124.6 (s, C^{p}/C_6H_4), 126.4 (d, $^{4}J_{CP}$ = 4.2 Hz, C^{o}/C_6H_4), 128.6 (d, $^{3}J_{CP}$ = 7.8 Hz, C^{m}/C_6H_5), 129.2 (s, C^{p}/C_6H_5), 131.7 (d, $^{3}J_{CP}$ = 1.3 Hz, $C^{5}/C_3H_2N_2$), 132.1 (s, C^{m}/C_6H_4), 134.0 (d, $^{2}J_{CP}$ = 20.9 Hz, C^{o}/C_6H_5), 135.6 (d, $^{3}J_{CP}$ = 5.1 Hz, C^{i}/C_6H_5), 137.1 (d, $^{1}J_{CP}$ = 1.7 Hz, C^{i}/C_6H_4), 146.9 (d, $^{1}J_{CP}$ = 7.8 Hz, $C^{2}/C_3H_2N_2$). ^{31}P{^{1}H} NMR (202.5 MHz, $CDCl_3$,

δ): -29.1 (s). HRMS (ESI-TOF) $C_{33}H_{25}FeN_2P$ $[M+H]^+$ *m/z*: calcd.: 537.1109, found: 537.1178.

4.6.9 Synthesis of 1-(4-(1,1'-biphenyl))-2-(diphenylphosphino)-4,5-dimethyl-1*H*-imidazole (11i)

Based on the general procedure described earlier, **9** (0.5 g, 2.01 mmol) was reacted with *n*-BuLi (0.80 mL, 2.00 mmol) and chlorodiphenylphosphine (**10a**, 0.36 mL, 2.01 mmol). The residue was purified by column chromatography on alumina (column size: 12 × 3.5 cm) using a mixture of *n*-hexane-diethyl ether (ratio 1:1, *v*:*v*) as eluent. Phosphine **11i** was obtained as a colorless solid. Yield: 0.58 g (1.34 mmol, 67 % based on **9**). Anal. Calcd. for $C_{29}H_{25}N_2P$ (432.50 g/mol): C, 80.53; H, 5.83; N, 6.48. Found: C, 80.35; H, 5.98; N, 6.48. Mp.: 151 °C. IR (KBr, $\tilde{\upsilon}$/cm^{-1}): 1432 (m, P-C), 1488 (s, N=C), 1587 (m, C=C), 2850/2916 (w, C-H), 3045/3062 (w, =C-H). ^{1}H NMR (500.30 MHz, $CDCl_3$, *δ*): 2.02 (s, 3 H, C*H*$_3$), 2.29 (s, 3 H, C*H*$_3$), 7.12 (dpt, $^3J_{HH}$ = 8.5 Hz, $^4J_{HH}$ = 1.9 Hz, $^5J_{HP}$ = 0.8 Hz, 2 H, H^{3}/C$_6$H$_5$-C$_6$*H*$_4$), 7.28 – 7.31 (m, 6 H, H^{m,p}/C$_6$*H*$_5$), 7.39 (m, 1 H, H$^{4'}$/C$_6$*H*$_5$-C$_6$H$_4$), 7.45 – 7.49 (m, 6 H, H$^{3'}$/C$_6$*H*$_5$-C$_6$H$_4$+H^{o}/C$_6$*H*$_5$), 7.60 (dpt, $^3J_{HH}$ = 8.4 Hz, $^4J_{HH}$ = 1.9 Hz, 2 H, H$^{2'}$/C$_6$*H*$_5$-C$_6$H$_4$), 7.62 (dpt, $^3J_{HH}$ = 8.4 Hz, $^4J_{HH}$ = 1.9 Hz, 2 H, H^{2}/C$_6$*H*$_4$). ^{13}C{^{1}H} NMR (125.81 MHz, $CDCl_3$, *δ*): 9.8 (s, *C*H$_3$), 13.3 (s, *C*H$_3$), 127.3 (s, C$^{2'}$/*C*$_6$H$_5$-C$_6$H$_4$), 127.3 (s, C^{i}), 127.8 (s, C^{2}/C$_6$H$_5$-*C*$_6$H$_4$), 127.9 (s, C$^{4'}$/*C*$_6$H$_5$-C$_6$H$_4$), 128.4 (d, $^3J_{CP}$ = 7.6 Hz, C^{m}/*C*$_6$H$_5$), 128.6 (d, $^4J_{CP}$ = 2.7 Hz, C^{3}/C$_6$H$_5$-*C*$_6$H$_4$), 128.7 (s, C$^{3'}$/*C*$_6$H$_5$-C$_6$H$_4$), 129.0 (s, C^{p}/*C*$_6$H$_5$), 133.8 (d, $^2J_{CP}$ = 20.6 Hz, C^{o}/*C*$_6$H$_5$), 136.5 (s, C^{i}), 136.5 (d, $^3J_{CP}$ = 1.5 Hz, C^{4}/ C$_6$H$_5$-*C*$_6$H$_4$), 136.5 (d, $^1J_{CP}$ = 2.4 Hz, C^{i}/C$_6$H$_5$), 140.1 (s, C^{i}), 141.6 (s, C^{i}), 144.0 (d, $^1J_{CP}$ = 1.2 Hz, C^{2}/*C*$_3$N$_2$). ^{31}P{^{1}H} NMR (202.5 MHz, $CDCl_3$, *δ*): -28.9 (s). HRMS (ESI-TOF) $C_{29}H_{25}N_2P$ $[M+H]^+$ *m/z*: calcd.: 433.1783, found: 433.1828.

4.6.10 Synthesis of 1-(4-(1,1'-biphenyl))-2-(dicyclohexylphosphino)-4,5-dimethyl-1*H*-imidazole (11j)

Using the general synthesis methodology described above, **9** (0.5 g, 2.01 mmol) was reacted with *n*-BuLi (0.80 mL, 2.00 mmol) and chlorodicyclohexylphosphine (**10b**, 0.44 mL, 1.99 mmol). The residue was purified by column chromatography on alumina (column size: 12 × 3.5 cm) using a mixture of *n*-hexane-diethyl ether (ratio 2:1, *v*:*v*) as eluent. Phosphine **11j** was obtained as a colorless solid. Yield: 0.54 g (1.21 mmol, 61 % based on **9**). Anal. Calcd. for $C_{29}H_{37}N_2P$ (444.59 g/mol): C, 78.34; H, 8.39; N, 6.30. Found: C, 78.77; H, 8.61; N, 6.14. Mp.: 131 °C. IR (KBr, $\tilde{\upsilon}$/cm^{-1}): 1442 (m, P-C), 1488/1518 (m, N=C), 1591 (w, C=C),

2846/2922 (s, C-H), 3034 (w, =C-H). ^{1}H NMR (500.30 MHz, $CDCl_3$, δ): 1.06 – 1.31 (m, 10 H, C_6H_{11}), 1.62 – 1.75 (m, 10 H, C_6H_{11}), 1.97 (s, 3 H, CH_3), 2.10 – 2.16 (m, 2 H, H^{1}/C_6H_{11}), 2.28 (s, 3 H, CH_3), 7.18 (m, 2 H, H^{3}/C_6H_5-C_6H_4), 7.37 (tt, $^{3}J_{HH}$ = 7.4 Hz, $^{4}J_{HH}$ = 1.8 Hz, 1 H, $H^{4'}/C_6H_5$-C_6H_4), 7.46 (m, 2 H, $H^{3'}/ C_6H_5$-C_6H_4), 7.64 (dpt, $^{3}J_{HH}$ = 8.0 Hz, $^{4}J_{HH}$ = 1.9 Hz, 2 H, $H^{2'}/C_6H_5$-C_6H_4), 7.68 (dpt, $^{3}J_{HH}$ = 8.4 Hz, $^{4}J_{HH}$ = 1.9 Hz, 2 H, H^{2}/C_6H_5-C_6H_4). ^{13}C{^{1}H} NMR (125.81 MHz, $CDCl_3$, δ): 9.8 (s, CH_3), 13.2 (s, CH_3), 26.6 (s, C_6H_{11}), 27.0 (d, J_{CP} = 8.4 Hz, C_6H_{11}), 27.1 (d, J_{CP} = 12.6 Hz, C_6H_{11}), 29.6 (d, J_{CP} = 8.0 Hz, C_6H_{11}), 30.5 (d, J_{CP} = 16.9 Hz, C_6H_{11}), 34.6 (d, J_{CP} = 7.4 Hz, C^{1}/C_6H_{11}), 126.0 (s, C^{i}), 127.3 (s, $C^{2'}/C_6H_5$-C_6H_4), 127.7 (s, C^{2}/C_6H_5-C_6H_4), 127.8 (s, $C^{4'}/C_6H_5$-C_6H_4), 129.0 (s, $C^{3'}/C_6H_5$-C_6H_4), 129.2 (d, $^{4}J_{CP}$ = 2.7 Hz, C^{3}/C_6H_5-C_6H_4), 135.6 (s, C^{i}), 137.1 (d, $^{3}J_{CP}$ = 2.3 Hz, C^{4}/C_6H_5-C_6H_4), 140.2 (s, C^{i}), 141.3 (s, C^{i}), 144.9 (d, $^{1}J_{CP}$ = 12.1 Hz, C^{2}/C_3N_2). ^{31}P{^{1}H} NMR (202.5 MHz, $CDCl_3$, δ): -23.5 (s). HRMS (ESI-TOF) $C_{29}H_{37}N_2P$ $[M+H]^+$ *m/z*: calcd.: 445.2725, found: 445.2767.

4.6.11 Synthesis of 1-(4-(1,1'-biphenyl))-2-(di-2-furyl-phosphino)-4,5-dimethyl-1*H*-imidazole (11k)

Following the general synthesis methodology described above, **9** (0.5 g, 2.01 mmol) was reacted with *n*-BuLi (0.80 mL, 2.00 mmol) and chlorodi-2-furylphosphine (**10c**, 0.40 g, 1.99 mmol). The residue was purified by column chromatography on alumina (column size: 12 × 3.5 cm) using diethyl ether as eluent. Phosphine **11k** was obtained as a colorless solid. Yield: 0.59 g (1.43 mmol, 72 % based on **9**). Anal. Calcd. for $C_{25}H_{21}N_2O_2P$ (412.42 g/mol): C, 72.81; H, 5.13; N, 6.79. Found: C, 72.87; H, 5.27; N, 6.47. Mp.: 126 °C. IR (KBr, $\tilde{\upsilon}$/cm^{-1}): 1006 (s, C-O), 1449 (m, P-C), 1486/1518 (s, N=C), 1548/1584 (w, C=C), 2918 (w, C-H), 3029/3078/3100/3125 (w, =C-H). ^{1}H NMR (500.30 MHz, $CDCl_3$, δ): 1.98 (s, 3 H, CH_3), 2.29 (s, 3 H, CH_3), 6.34 (dt $^{4}J_{HP}$ = 1.6 Hz, $^{3}J_{HH}$ = 3.4 Hz, $^{3}J_{HH}$ = 1.8 Hz, 2 H, H^{4}/C_4H_3O), 6.74 (m, 2 H, H^{3}/C_4H_3O), 7.14 (dpt, $^{3}J_{HH}$ = 8.4 Hz, $^{4}J_{HH}$ = 1.9 Hz, $^{5}J_{HP}$ = 0.8 Hz, 2 H, H^{3}/C_{65}-C_6H_4), 7.38 (tt, $^{3}J_{HH}$ = 7.3 Hz, $^{4}J_{HH}$ = 1.8 Hz, 2 H, $H^{4'}/C_6H_5$-C_6H_4), 7.47 (m, 2 H, $H^{3'}/C_6H_5$-C_6H_4), 7.60 – 7.63 (m, 6 H, H^{5}/C_4H_3O + H^{2}/C_6H_5-C_6H_4 + $H^{2'}/C_6H_5$-C_6H_4). ^{13}C{^{1}H} NMR (125.81 MHz, $CDCl_3$, δ): 6.4 (s, CH_3), 13.2 (s, CH_3), 110.7 (d, $^{3}J_{CP}$ = 6.8 Hz, C^{4}/C_4H_3O), 121.6 (d, $^{1}J_{CP}$ = 25.9 Hz, C^{3}/C_4H_3O), 127.1 (s, C^{2}/C_6H_5-C_6H_4), 127.4 (s, C^{4}/C_3N_2), 127.6 (s, $C^{2'}/C_6H_5$-C_6H_4), 127.8 (s, $C^{4'}/C_6H_5$-C_6H_4), 128.1 (d, $^{4}J_{CP}$ = 2.5 Hz, C^{3}/C_6H_5-C_6H_4), 128.9 (s, $C^{3'}/C_6H_5$-C_6H_4), 136.0 (m, C^{5}/C_3N_2), 136.4 (d, $^{3}J_{CP}$ = 3.8 Hz, C^{4}/C_6H_5-C_6H_4), 139.9 (s, $C^{1,1'}/C_6H_5$-C_6H_4), 140.3 (d, $^{1}J_{CP}$ = 13.5 Hz, C^{2}/C_3N_2), 141.5 (s, $C^{1,1'}/C_6H_5$-C_6H_4), 147.4 (d, $^{4}J_{CP}$ = 2.8 Hz,

C^5/C_4H_3O), 148.3 (d, $^1J_{CP}$ = 3.1 Hz, C^1/C_4H_3O). HRMS (ESI-TOF) $C_{25}H_{21}N_2O_2P$ $[M+H]^+$ *m/z*: calcd.: 413.1365, found: 413.1413.

4.7 General Procedure for the Synthesis of Seleno Phosphines 11a-Se – f-Se

To a toluene solution of **11a** – **f** (100 mg), 2 eq of elemental selenium was added in a single portion and stirred for 2 h at 100 °C. After cooling to ambient temperature, the solvent was removed in membrane-pump vacuum and the respective seleno phosphines were purified by column chromatography on Silica (column size: 2.5 × 8 cm) and dried in membrane-pump vacuum.

4.7.1 Synthesis of 1-(4-bromophenyl))-2-(diphenylphosphino selenide)-1*H*-imidazole (11a-Se)

Using the general procedure described above, **11a** (100 mg, 0.25 mmol) was reacted with elemental selenium (40 mg, 0.51 mmol, 2 eq). The crude product was purified by column chromatography using a mixture of *n*-hexane-diethyl ether (ratio 1:1, *v*:*v*) as eluent. Compound **11a-Se** was obtained as a colorless solid. Yield: 0.10 g (0.21 mmol, 84 % based on **11a**). Anal. Calcd. for $C_{21}H_{16}BrN_2PSe$ (486.20 g/mol): C, 51.88; H, 3.32; N, 5.76. Found: C, 52.28; H, 3.31; N, 5.74. Mp.: 160 °C. IR (KBr, $\tilde{\nu}$/cm^{-1}): 576 (s, P-Se), 1435 (m, P-C), 1484/1497 (m, N=C), 1560 (w, C=C), 3046/3069/3145 (w, =C-H). ^{1}H NMR (500.30 MHz, $CDCl_3$, δ): 7.00 (dpt, $^3J_{HH}$ = 8.6 Hz, $^4J_{HH}$ = 2.0 Hz, 2 H, H^o/C_6H_4), 7.17 (dd, $^3J_{HH}$ = 1.2 Hz, $^4J_{HP}$ = 1.7 Hz, 1 H, $H^4/C_3H_2N_2$), 7.30 (dpt, $^3J_{HH}$ = 8.7 Hz, $^4J_{HH}$ = 2.1 Hz, 2 H, H^m/C_6H_4), 7.33 (pt, $^3J_{HH}$ = 1.0 Hz, $H^5/C_3H_2N_2$), 7.40 – 7.44 (m, 4 H, H^m/C_6H_5), 7.47 – 7.51 (m, 2 H, H^p/C_6H_5), 7.82 – 7.87 (m, 4 H, H^o/C_6H_5). ^{13}C{^{1}H} NMR (125.81 MHz, $CDCl_3$, δ): 123.1 (s, C^p/C_6H_4), 126.8 (d, $^3J_{CP}$ = 1.8 Hz, $C^4/C_3H_2N_2$), 128.5 (d, $^3J_{CP}$ = 13.4 Hz, C^m/C_6H_5), 129.0 (s, C^o/C_6H_4), 130.3 (d, $^3J_{CP}$ = 43.1 Hz, $C^5/C_3H_2N_2$), 130.6 (d, $^1J_{CP}$ = 54.4 Hz, C^i/C_6H_5), 131.8 (s, C^m/C_6H_4), 132.0 (d, $^4J_{CP}$ = 3.3 Hz, C^p/C_6H_5), 132.9 (d, $^2J_{CP}$ = 11.3 Hz, C^o/C_6H_5), 136.4 (s, C^i/C_6H_4), 139.7 (d, $^1J_{CP}$ = 120.8 Hz, $C^2/C_3H_2N_2$). ^{31}P{^{1}H} NMR (202.5 MHz, $CDCl_3$, δ): 19.1 ($^1J_{PSe}$ = 753.4 Hz). HRMS (ESI-TOF) $C_{21}H_{16}BrN_2PSe$ $[M+H]^+$ *m/z*: calcd.: 486.9470, found: 486.9413; $[M+Na]^+$ *m/z*: calcd.: 508.9290, found: 508.9222; $[2M+Na]^+$ *m/z*: calcd.: 994.8681, found: 994.8595.

4.7.2 Synthesis of 1-(4-bromophenyl))-2-(dicyclohexylphosphino selenide)-1*H*-imidazole (11b-Se)

Using the synthesis methodology described earlier, **11b** (100 mg, 0.24 mmol) was reacted with elemental selenium (38 mg, 0.48 mmol, 2 eq). The crude product was purified by column chromatography using mixture of *n*-hexane-diethyl ether (ratio 10:1, *v*:*v*) as eluent. Molecule **11b-Se** was obtained as colorless solid. Yield: 0.11 g (0.22 mmol, 92 % based on **11b**). Anal. Calcd. for $C_{21}H_{28}BrN_2PSe$ (498.30 g/mol): C, 50.62; H, 5.66; N, 5.62. Found: C, 50.60; H, 5.64; N, 5.52. Mp.: 170 °C. IR (KBr, $\tilde{\upsilon}$/cm^{-1}): 558 (s, P-Se), 1445 (m, P-C), 1481/1497 (m, N=C), 1589 (w, C=C), 2928/2846 (s, C-H), 3133/3108 (w, =C-H). ^{1}H NMR (500.30 MHz, $CDCl_3$, δ): 1.11 – 1.19 (m, 2 H, C_6H_{11}), 1.20 – 1.36 (m, 6 H, C_6H_{11}), 1.49 – 1.58 (m, 2 H, C_6H_{11}), 1.61 – 1.67 (m, 4 H, C_6H_{11}), 1.76 – 1.82 (m, 4 H, C_6H_{11}), 1.91 – 1.93 (m, 2 H, H^1/C_6H_{11}), 2.41 – 2.48 (m, 2 H, H^1/C_6H_{11}), 7.06 (pt, $^3J_{HH}$ = 1.2 Hz, 1 H, H^4/$C_3H_2N_2$), 7.19 (dpt, $^3J_{HH}$ = 8.6 Hz, $^4J_{HH}$ = 2.0 Hz, 2 H, H^o/C_6H_4), 7.33 (pt, $^3J_{HH}$ = 0.8 Hz, 1 H, H^5/$C_3H_2N_2$), 7.53 (dpt, $^3J_{HH}$ = 8.6 Hz, $^4J_{HH}$ = 2.0 Hz, H^m/C_6H_4). ^{13}C{^{1}H} NMR (125.81 MHz, $CDCl_3$, δ): 26.9 (d, J_{CP} = 1.3 Hz, C_6H_{11}), 26.1 (s, C_6H_{11}), 26.2 (d, J_{CP} = 8.0 Hz, C_6H_{11}), 26.4 (d, J_{CP} = 7.0 Hz, C_6H_{11}), 26.7 (d, J_{CP} = 3.8 Hz, C_6H_{11}), 39.9 (d, $^1J_{CP}$ = 45.3 Hz, C^1/C_6H_{11}), 123.5 (s, C^p/C_6H_4), 126.9 (s, C^4/$C_3H_2N_2$), 129.4 (d, $^3J_{CP}$ = 12.6 Hz, C^5/$C_3H_2N_2$), 130.2 (s, C^o/C_6H_4), 131.6 (s, C^m/C_6H_4), 135.4 (d, $^1J_{CP}$ = 92.3 Hz, C^2/$C_3H_2N_2$), 136.8 (s, C^i/C_6H_4). ^{31}P{^{1}H} NMR (202.5 MHz, $CDCl_3$, δ): 41.6 ($^1J_{PSe}$ = 724.5 Hz). HRMS (ESI-TOF) $C_{21}H_{28}BrN_2PSe$ $[M+H]^+$ *m/z*: calcd.: 499.0409, found: 499.0363; $[M+Na]^+$ *m/z*: calcd.: 521.0229, found: 521.0195; $[2M]^+$ *m/z*: calcd.: 996.0662, found: 996.0560.

4.7.3 Synthesis of 1-(4-bromophenyl))-2-(di-2-furylphosphino selenide)-1*H*-imidazole (11c-Se)

Reaction of **11c** (100 mg, 0.26 mmol) with elemental selenium (41 mg, 0.52 mmol, 2 eq) gave, after purification by column chromatography using diethyl ether as eluent, **11c-Se** as a colorless solid. Yield: 0.11 g (0.24 mmol, 92 % based on **11c**). Anal. Calcd. for $C_{17}H_{12}BrN_2O_2PSe$ (466.13 g/mol): C, 43.80; H, 2.59; N, 6.01. Found: C, 43.76; H, 2.59; N, 5.82. Mp.: 128 °C. IR (KBr, $\tilde{\upsilon}$/cm^{-1}): 587 (s, P-Se), 1010 (s, C-O), 1455 (m, P-C), 1483/1494 (m, N=C), 1547 (w, C=C), 3090/3107/3128/3145 (w, =C-H). ^{1}H NMR (500.30 MHz, $CDCl_3$, δ): 6.43 (dt $^4J_{HP}$ = 1.7 Hz, $^3J_{HH}$ = 3.5 Hz, $^3J_{HH}$ = 1.8 Hz, 2 H, H^4/C_4H_3O), 7.14 (dd, $^3J_{HH}$ = 1.0 Hz, $^4J_{HP}$ = 1.8 Hz, 1 H, H^4/$C_3H_2N_2$), 7.20 (dpt, $^3J_{HH}$ = 8.6 Hz, $^4J_{HH}$ = 2.0 Hz, 2 H, H^o/C_6H_4), 7.24 (m, 2 H, H^3/C_4H_3O), 7.32 (pt, $^3J_{HH}$ = 1.0 Hz, H^5/$C_3H_2N_2$), 7.39 (dpt, $^3J_{HH}$ = 8.6 Hz, $^4J_{HH}$

= 1.9 Hz, H^{m}/C$_6$*H*$_4$), 7.67 (m, 2 H, H^{5}/C$_4$*H*$_3$O). ^{13}C{^{1}H} NMR (125.81 MHz, $CDCl_3$, δ): 111.7 (d, $^{3}J_{CP}$ = 10.2 Hz, C^{4}/*C*$_4$H$_3$O), 123.2 (s, C^{p}/*C*$_6$H$_4$), 125.6 (d, $^{2}J_{CP}$ = 24.9 Hz, C^{3}/*C*$_4$H$_3$O), 126.5 (s, C^{4}/*C*$_3$H$_2$N$_2$), 128.4 (s, C^{o}/*C*$_6$H$_4$), 131.3 (d, $^{3}J_{CP}$ = 18.2 Hz, C^{5}/*C*$_3$H$_2$N$_2$), 131.9 (s, C^{m}/*C*$_6$H$_4$), 135.5 (s, C^{i}/*C*$_6$H$_4$), 138.6 (d, $^{1}J_{CP}$ = 139.9 Hz, C^{2}/*C*$_3$H$_2$N$_2$), 143.7 (d, $^{1}J_{CP}$ = 121.8 Hz, C^{2}/*C*$_4$H$_3$O), 149.3 (d, $^{4}J_{CP}$ = 7.3 Hz, C^{5}/*C*$_4$H$_3$O). ^{31}P{^{1}H} NMR (202.5 MHz, $CDCl_3$, δ): -20.7 ($^{1}J_{PSe}$ = 789.9 Hz). HRMS (ESI-TOF) $C_{17}H_{12}BrN_2O_2PSe$ $[M+H]^+$ *m/z*: calcd.: 466.9055, found: 466.9056.

4.7.4 Synthesis of 1-(4-iodophenyl)-2-(diphenylphosphino selenide)-4,5-dimethyl-1*H*-imidazole (11d-Se)

Compound **11d** (100 mg, 0.21 mmol) was reacted with elemental selenium (33 mg, 0.42 mmol, 2 eq) as described earlier. The residue was purified by column chromatography using a mixture of *n*-hexane-diethyl ether (ratio 1:2, *v*:*v*) as eluent. Seleno phosphine **11d-Se** was obtained as colorless solid. Yield: 0.10 g (0.18 mmol, 86 % based on **11d**). Anal. Calcd. for $C_{23}H_{20}IN_2PSe$ (561.26 g/mol): C, 49.22; H, 3.59; N, 4.99. Found: C, 48.91; H, 3.65; N, 4.91. Mp.: 86 °C. IR (KBr, $\tilde{\upsilon}$/cm^{-1}): 557 (s, P-Se), 1435 (m, P-C), 1488 (m, N=C), 1580 (w, C=C), 2910/2965 (s, C-H), 3048 (w, =C-H). ^{1}H NMR (500.30 MHz, $CDCl_3$, δ): 1.87 (s, 3 H, C*H*$_3$), 2.23 (s, 3 H, C*H*$_3$), 6.68 (dpt, $^{3}J_{HH}$ = 8.6 Hz, $^{4}J_{HH}$ = 2.0 Hz, 2 H, H^{o}/C$_6$*H*$_4$), 7.35 – 7.39 (m, 4 H, H^{m}/C$_6$*H*$_5$), 7.43 – 7.45 (m, 2 H, H^{p}/C$_6$*H*$_5$), 7.47 (dpt, $^{3}J_{HH}$ = 8.6 Hz, $^{4}J_{HH}$ = 2.0 Hz, H^{m}/C$_6$*H*$_4$), 7.81 – 7.86 (m, 4 H, H^{o}/C$_6$*H*$_5$). ^{13}C{^{1}H} NMR (125.81 MHz, $CDCl_3$, δ): 9.5 (s, *C*H$_3$), 13.1 (s, *C*H$_3$), 94.8 (s, C^{p}/*C*$_6$H$_4$), 128.3 (d, $^{3}J_{CP}$ = 12.9 Hz, C^{m}/*C*$_6$H$_5$), 130.1 (s, C^{4}/*C*$_3$N$_2$), 130.7 (s, C*o*/*C*$_6$H$_4$), 130.9 (d, $^{1}J_{CP}$ = 81.6 Hz, C^{i}/*C*$_6$H$_5$), 131.6 (d, $^{4}J_{CP}$ = 2.8 Hz, C^{p}/C$_6$H$_5$), 133.0 (d, $^{2}J_{CP}$ = 11.4 Hz, C^{o}/*C*$_6$H$_5$), 135.8 (s, C^{i}/*C*$_6$H$_4$), 136.1 (d, $^{3}J_{CP}$ = 14.8 Hz, C^{5}/*C*$_3$N$_2$), 136.5 (d, $^{1}J_{CP}$ = 125.8 Hz, C^{2}/C$_3$N$_2$), 137.9 (s, C^{m}/*C*$_6$H$_4$). ^{31}P{^{1}H} NMR (202.5 MHz, $CDCl_3$, δ): 17.6 ($^{1}J_{PSe}$ = 745.4 Hz). HRMS (ESI-TOF) $C_{23}H_{20}IN_2PSe$ $[M+H]^+$ *m/z*: calcd.: 562.9648, found: 562.9607; $[M+Na]^+$ *m/z*: calcd.: 584.9467, found: 584.9415; $[2M+Na]^+$ *m/z*: calcd.: 1146.9051, found: 1146.8976.

4.7.5 Synthesis of 1-(4-iodophenyl))-2-(dicyclohexylphosphino selenide)-4,5-dimethyl-1*H*-imidazole (11e-Se)

Molecule **11e** (100 mg, 0.20 mmol) was reacted with elemental selenium (32 mg, 0.41 mmol, 2 eq) as described above. The crude product was purified by column chromatography using a mixture of *n*-hexane-diethyl ether (ratio 1:1, *v*:*v*) as eluent. Molecule **11e-Se** was

obtained as colorless solid. Yield: 0.11 g (0.19 mmol, 95 % based on **11e**). Anal. Calcd. for $C_{23}H_{32}IN_2PSe$ (573.35 g/mol): C, 48.18; H, 5.63; N, 4.89. Found: C, 47.91; H, 5.79; N, 4.79. Mp.: 210 °C. IR (KBr, $\tilde{\upsilon}$/cm^{-1}): 576 (m P-Se), 1444 (m, P-C), 1488 (m, N=C), 1590 (w, C=C), 2848/2926 (s, C-H). ^{1}H NMR (500.30 MHz, $CDCl_3$, δ): 1.12 –1.33 (m, 8 H, C_6H_{11}), 1.48 – 1.56 (m, 2 H, C_6H_{11}), 1.61 – 1.67 (m, 4 H, C_6H_{11}), 1.75 – 1.80 (m, 4 H, C_6H_{11}), 1.83 (s, 3 H, CH_3), 1.88 – 1.90 (m, 2 H, C_6H_{11}), 2.23 (s, 3 H, CH_3), 2.39 – 2.45 (m, 2 H, C_6H_{11}), 6.90 (dpt, $^3J_{HH}$ = 8.5 Hz, $^3J_{HH}$ = 2.6 Hz, $^4J_{HH}$ = 1.9 Hz, 2 H, H^o/C_6H_4), 7.74 (dpt, $^3J_{HH}$ = 8.5 Hz, $^3J_{HH}$ = 2.6 Hz, $^4J_{HH}$ = 1.9 Hz, 2 H, H^m/C_6H_4). ^{13}C{^{1}H} NMR (125.81 MHz, $CDCl_3$, δ): 9.6 (s, CH_3), 13.0 (s, CH_3), 26.0 (d, J_{CP} = 1.4 Hz, C_6H_{11}), 26.2 (d, J_{CP} = 6.8 Hz, C_6H_{11}), 26.3 (d, J_{CP} = 8.4 Hz, C_6H_{11}), 26.4 (d, J_{CP} = 14.3 Hz, C_6H_{11}), 26.8 (d, J_{CP} = 3.7 Hz, C_6H_{11}), 39.9 (d, $^1J_{CP}$ = 45.7 Hz, C^1/C_6H_{11}), 95.0 (s, C^p/C_6H_4), 131.4 (s, C^o/C_6H_4), 129.3 (s, C^4/C_3N_2), 132.6 (d, $^1J_{CP}$ = 97.8 Hz, C^2/C_3N_2), 135.2 (d, $^3J_{CP}$ = 10.3 Hz, C^5/C_3N_2), 136.7 (s, C^i/C_6H_4), 137.9 (s, C^m/C_6H_4). ^{31}P{^{1}H} NMR (202.5 MHz, $CDCl_3$, δ): 41.2 ($^1J_{PSe}$ = 717.5 Hz). HRMS (ESI-TOF) $C_{23}H_{32}IN_2PSe$ $[M+H]^+$ *m/z*: calcd.: 575.0587, found: 575.0521.

4.7.6 Synthesis of 1-(4-iodophenyl))-2-(di-2-furylphosphino selenide)-4,5-dimethyl-1*H*-imidazole (11f-Se)

Phosphine **11f** (100 mg, 0.22 mmol) was reacted with elemental selenium (35 mg, 0.44 mmol, 2 eq) as described earlier. The crude product was purified by column chromatography using diethyl ether as eluent. Compound **11f-Se** was obtained as colorless solid. Yield: 0.11 g (0.20 mmol, 91 % based on **11f**). Anal. Calcd. for $C_{19}H_{16}IN_2O_2PSe$ (541.18 g/mol): C, 42.17; H, 2.98; N, 5.18. Found: C, 42.32; H, 3.10; N, 5.07. Mp.: 142 °C. IR (NaCl, $\tilde{\upsilon}$/cm^{-1}): 583 (s, P-Se), 1004 (s, C-O), 1456 (m, P-C), 1488 (s, N=C), 1550/1578 (w, C=C), 2918 (w, C-H), 3120 (w, =C-H). ^{1}H NMR (500.30 MHz, $CDCl_3$, δ): 1.90 (s, 3 H, CH_3), 2.22 (s, 3 H, CH_3), 6.41 (dt $^4J_{HP}$ = 1.7 Hz, $^3J_{HH}$ = 3.5 Hz, $^3J_{HH}$ = 1.8 Hz, 2 H, H^4/C_4H_3O), 6.90 (dpt, $^3J_{HH}$ = 8.6 Hz, $^3J_{HH}$ = 2.6 Hz, $^4J_{HH}$ = 2.0 Hz, 2 H, H^o/C_6H_4), 7.19 (m, 2 H, H^3/C_4H_3O), 7.58 (dpt, $^3J_{HH}$ = 8.7 Hz, $^3J_{HH}$ = 2.6 Hz, $^4J_{HH}$ = 2.1 Hz, H^m/C_6H_4), 7.65 (m, 2 H, H^5/C_4H_3O). ^{13}C{^{1}H} NMR (125.81 MHz, $CDCl_3$, δ): 9.3 (s, CH_3), 13.1 (s, CH_3), 94.9 (s, C^p/C_6H_4), 111.6 (d, $^3J_{CP}$ = 10.1 Hz, C^4/C_4H_3O), 125.4 (d, $^2J_{CP}$ = 24.5 Hz, C^3/C_4H_3O), 129.9 (s, C^o/C_6H_4), 130.4 (s, C^4/C_3N_2), 135.4 (s, C^i/C_6H_4), 135.9 (s, C^5/C_3N_2), 137.1 (d, $^3J_{CP}$ = 17.2 Hz, C^2/$(CH_3)_2C_3N_2$), 138.1 (s, C^m/C_6H_4), 144.2 (d, $^1J_{CP}$ = 120.8 Hz, C^2/C_4H_3O), 149.0 (d, $^4J_{CP}$ = 7.3 Hz, C^5/C_4H_3O). ^{31}P{^{1}H} NMR (202.5 MHz, $CDCl_3$, δ): -21.4 ($^1J_{PSe}$ = 781.0 Hz). HRMS (ESI-TOF) $C_{19}H_{16}IN_2O_2PSe$

$[M+H]^+$ *m/z*: calcd.: 542.9233, found: 542.9206; $[M+Na]^+$ *m/z*: calcd.: 564.9052, found: 564.9003.

4.8 General Procedure for the Synthesis of Imidazolium Salts 16a – 16d

To **3a** – **c** (0.5 g) dissolved in acetonitrile (50 mL) one eq of *n*-BuI (**12a**) or *n*-OctI (**12b**) was added in a single portion and the reaction mixture was stirred at 70 °C for 5 (**12a**) or 14 (**12b**) days. The progress of the reaction was monitored by ^{1}H NMR spectroscopy. After completion of the reaction the solvent was removed in membrane-pump vacuum. The crude product was washed five times with diethyl ether (10 mL portions) and dried in membrane-pump vacuum.

4.8.1 Synthesis of 1-(4-bromophenyl)-3-*n*-butyl-1*H*-imidazolium iodide (16a)

Following the synthesis methodology described above, **3a** (0.5 g, 2.24 mmol) was reacted with *n*-BuI (**12a**, 0.30 mL, 2.64 mmol, 1.2 eq). After appropriate work-up, the product was obtained as pale beige solid. Yield: 0.90 g (2.21 mmol, 99 % based on **3a**). Anal. Calcd. for $C_{13}H_{16}BrIN_2$ (407.09 g/mol): C, 38.36; H, 3.96; N, 6.88. Found: C, 38.40; H, 3.92; N, 6.64. Mp.: 120 °C. IR (KBr, $\tilde{\nu}$/cm^{-1}): 1496/1550 (s, N=C), 1590 (m, C=C), 2851/2872/2891/2932/2963/2995 (m – s, C-H), 3045/3073/3155 (w, =C-H). ^{1}H NMR (500.30 MHz, $CDCl_3$, δ): 0.93 (t, $^3J_{HH}$ = 7.4 Hz, 3 H, $CH_2CH_2CH_2CH_3$), 1.39 (sext, $^3J_{HH}$ = 7.6 Hz, 2 H, $CH_2CH_2CH_2CH_3$), 1.95 (quint, $^3J_{HH}$ = 7.5 Hz, 2 H, $CH_2CH_2CH_2CH_3$), 4.50 (t, $^3J_{HH}$ = 7.4 Hz, 2 H, $CH_2CH_2CH_2CH_3$), 7.63 (dpt, $^3J_{HH}$ = 8.9 Hz, $^4J_{HH}$ = 2.2 Hz, 2 H, $H^{o,m}/C_6H_4$), 7.76 (pt, $^3J_{HH}$ = 1.8 Hz, 1 H, $C_3H_3N_2$), 7.78 (dpt, $^3J_{HH}$ = 8.9 Hz, $^4J_{HH}$ = 2.1 Hz, 2 H, $H^{o,m}/C_6H_4$), 7.92 (pt, $^3J_{HH}$ = 1.9 Hz, 1 H, $C_3H_3N_2$), 10.54 (pt, $^4J_{HH}$ = 1.5 Hz, 1 H, $H^2/C_3H_3N_2$). ^{13}C{^{1}H} NMR (125.81 MHz, $CDCl_3$, δ): 13.5 (s, $CH_2CH_2CH_2CH_3$), 19.5 (s, $CH_2CH_2CH_2CH_3$), 32.1 (s, $CH_2CH_2CH_2CH_3$), 50.4 (s, $CH_2CH_2CH_2CH_3$), 121.3 (s, $C_3H_3N_2$), 123.6 (s, $C_3H_3N_2$), 123.8 (s, C^o/C_6H_4), 124.3 (s, C^p/C_6H_4), 133.3 (s, C^i/C_6H_4), 133.6 (s, C^m/C_6H_4), 135.0 (s, $C^2/C_3H_3N_2$). HRMS (ESI-TOF) $[C_{13}H_{16}BrN_2]^+$ $[M]^+$ *m/z*: calcd.: 279.0494, found: 279.0491.

4.8.2 Synthesis of 1-(4-bromophenyl)-3-*n*-octyl-1*H*-imidazolium hexafluorophosphate ([16b]PF$_6$)

Compound **3a** (0.5 g, 2.24 mmol) was reacted with *n*-OctI (**12b**, 0.41 mL, 2.27 mmol) as described earlier giving, after appropriate work-up, the imidazolium salt **16b** as yellow solid.

Please, notice that due to the long reaction time, impurities were present which could not be removed, neither by chromatography nor precipitation. Therefore, the hexafluorophosphate salt was prepared by addition of a solution of potassium hexafluorophosphate (0.20 g, 1.09 mmol) in water (20 mL) to **16b** (0.5 g, 1.08 mmol) dissolved in acetone (20 mL). After stirring at ambient temperature for 1 h, the solvent was removed in membrane-pump vacuum and the crude product was purified by column chromatography on Silica (column size: 10 × 2 cm) using acetone as eluent. Compound **[16b]PF_6** was obtained as a pale yellow solid. Yield: 0.45 g (0.94 mmol, 87 % based on **3a**). Anal. Calcd. for $C_{17}H_{24}BrF_6N_2P$ (481.25 g/mol): C, 42.43; H, 5.03; N, 5.82. Found: C, 42.23; H, 4.95; N, 5.73. Mp.: 101 °C. IR (KBr, $\tilde{\upsilon}$/cm^{-1}): 1493 (m, N=C), 1549/1561 (m, C=C), 2851/2921/2950 (s, C-H), 3042/3060 (m, =C-H). ^{1}H NMR (500.30 MHz, $CDCl_3$, δ): 0.80 (t, $^3J_{HH}$ = 7.1 Hz, 3 H, $CH_2(CH_2)_6CH_3$), 1.15 – 1.23 (m, 6 H, $CH_2(CH_2)_6CH_3$), 1.26 – 1.37 (m, 4 H, $CH_2(CH_2)_6CH_3$), 1.95 (pent, $^3J_{HH}$ = 7.3 Hz, 2 H, $CH_2(CH_2)_6CH_3$), 4.47 (t, $^3J_{HH}$ = 7.4 Hz, 2 H, $CH_2(CH_2)_6CH_3$), 7.62 (m, 2 H, H^o/C_6H_4), 7.71 (m, 1 H, H^{4,5}/$C_3H_3N_2$), 7.78 (m, 2 H, H^m/C_6H_4), 7.94 (m, 1 H, H^{4,5}/$C_3H_3N_2$), 10.52 (s, 1 H, H^2/C_3H_3N2). ^{13}C{^{1}H} NMR (125.81 MHz, $CDCl_3$, δ): 14.0 (s, $CH_2(CH_2)_6CH_3$), 22.5 (s, $CH_2(CH_2)_6CH_3$), 26.2 (s, $CH_2(CH_2)_6CH_3$), 28.9 (s, $CH_2(CH_2)_6CH_3$), 29.0 (s, $CH_2(CH_2)_6CH_3$), 30.2 (s, $CH_2(CH_2)_6CH_3$), 31.6 (s, $CH_2(CH_2)_6CH_3$), 50.7 (s, $CH_2(CH_2)_6CH_3$), 121.3 (s, $C_3H_3N_2$), 123.5 (s, $C_3H_3N_2$), 123.8 (s, C^o/C_6H_4), 124.3 (s, C^p/C_6H_4), 133.3 (s, C^i/C_6H_4), 133.6 (s, C^m/C_6H_4), 134.9 (s, C^2/$C_3H_3N_2$). ^{31}P{^{1}H} NMR (202.5 MHz, $CDCl_3$, δ): -144.5 (sept, $^1J_{PF}$ = 712.6 Hz, PF_6). HRMS (ESI-TOF) $[C_{17}H_{24}BrN_2]^+$ $[M]^+$ *m/z*: calcd.: 335.1107, found: 335.1117.

4.8.3 Synthesis of 1-(4-iodophenyl)-3-*n*-octyl-4,5-dimethyl-1*H*-imidazolium iodide (16c)

Using the synthesis procedure described above, **3b** (0.5 g, 1.68 mmol) was reacted with *n*-OctI (**12b**, 0.31 mL, 1.72 mmol). After appropriate work-up, **16c** was obtained as pale beige solid. Yield: 0.90 g (1.67 mmol, 99 % based on **3b**). Anal. Calcd. for $C_{19}H_{28}I_2N_2$ (538.25 g/mol): C, 42.40; H, 5.24; N, 5.20. Found: C, 42.19; H, 5.24; N, 4.93. Mp.: 175 °C. IR (KBr, $\tilde{\upsilon}$/cm^{-1}): 1560 (s, N=C), 1636/1655 (m, C=C), 2855/2923/2974 (m, C-H), 3116 (w, =C-H).^{1}H NMR (500.30 MHz, $CDCl_3$, δ): 0.87 (t, $^3J_{HH}$ = 7.1 Hz, 3 H, $CH_2(CH_2)_6CH_3$), 1.26 – 1.41 (m, 10 H, $CH_2(CH_2)_6CH_3$), 1.93 (pent, $^3J_{HH}$ = 7.6 Hz, 2 H, $CH_2(CH_2)_6CH_3$), 2.17 (s, 3 H, CH_3), 2.33 (s, 3 H, CH_3), 4.37 (t, $^3J_{HH}$ = 7.7 Hz, 2 H, $CH_2(CH_2)_6CH_3$), 7.41 (dpt, $^3J_{HH}$ = 8.7 Hz, $^4J_{HH}$ = 2.0 Hz, 2 H, H^o/C_6H_4), 7.92 (dpt, $^3J_{HH}$ = 8.7 Hz, $^4J_{HH}$ = 2.0 Hz, 2 H, H^m/C_6H_4), 9.82 (s, 1 H,

H^2/$(CH_3)_2C_3HN_2$). $^{13}C\{^1H\}$ NMR (125.81 MHz, $CDCl_3$, δ): 9.1 (s, CH_3), 9.6 (s, CH_3), 14.1 (s, $CH_2(CH_2)_6CH_3$), 22.6 (s, $CH_2(CH_2)_6CH_3$), 26.4 (s, $CH_2(CH_2)_6CH_3$), 29.0 (s, $CH_2(CH_2)_6CH_3$), 29.0 (s, $CH_2(CH_2)_6CH_3$), 29.9 (s, $CH_2(CH_2)_6CH_3$), 31.7 (s, $CH_2(CH_2)_6CH_3$), 47.9 (s, $CH_2(CH_2)_6CH_3$), 97.1 (s, C^p/C_6H_4), 127.2 (s, C_3HN_2), 127.4 (s, C_3HN_2), 127.9 (s, C^o/C_6H_4), 132.7 (s, C^i/C_6H_4), 134.7 (s, C^2/C_3HN_2), 139.4 (s, C^m/C_6H_4). HRMS (ESI-TOF) $[C_{19}H_{28}IN_2]I$ $[M]^+$ *m/z*: calcd.: 411.1250, found: 411.1292.

4.8.4 Synthesis of 1-phenyl-3-*n*-octyl-4,5-dimethyl-1*H*-imidazolium iodide (16d)

Using the synthesis methodology described above, **3c** (0.5 g, 2.90 mmol) was reacted with *n*-$C_8H_{17}I$ (**12b**, 0.54 mL, 2.99 mmol). After appropriate work-up, **16d** could be isolated as yellow oil. Yield: 1.17 g (2.84 mmol, 98 % based on **3c**). Anal. Calcd. for $C_{19}H_{29}IN_2$ (412.35 g/mol): C, 55.34; H, 7.09; N, 6.79. Found: C, 55.04; H, 7.24; N, 6.21. IR (KBr, $\tilde{\upsilon}$/cm^{-1}): 1460 (m, P-C), 1498/1555 (s, N=C), 1596/1631 (m, C=C), 2854/2926/2954 (s, C-H), 3111 (w, =C-H).^{1}H NMR (500.30 MHz, $CDCl_3$, δ): 0.77 (t, $^3J_{HH}$ = 7.1 Hz, 3 H, $CH_2(CH_2)_6CH_3$), 1.14 – 1.35 (m, 10 H, $CH_2(CH_2)_6CH_3$), 1.84 (quint, $^3J_{HH}$ = 7.6 Hz, $CH_2(CH_2)_6CH_3$), 2.11 (s, 3 H, CH_3), 2.28 (s, 3 H, CH_3), 4.30 (t, $^3J_{HH}$ = 7.7 Hz, $CH_2(CH_2)_6CH_3$), 7.47 – 7.50 (m, 5 H, C_6H_5), 9.55 (s, 1 H, $(CH_3)_3C_3HN_2$). $^{13}C\{^1H\}$ NMR (125.81 MHz, $CDCl_3$, δ): 9.0 (s, CH_3), 9.4 (s, CH_3), 13.9 (s, $CH_2(CH_2)_6CH_3$), 22.4 (s, $CH_2(CH_2)_6CH_3$), 26.2 (s, $CH_2(CH_2)_6CH_3$), 28.9 (s, $CH_2(CH_2)_6CH_3$), 28.9 (s, $CH_2(CH_2)_6CH_3$), 29.8 (s, $CH_2(CH_2)_6CH_3$), 31.5 (s, $CH_2(CH_2)_6CH_3$), 47.7 (s, $CH_2(CH_2)_6CH_3$), 125.9 (s, C^o/C_6H_5), 127.1 (s, C_3HN_2), 127.3 (s, C_3HN_2), 130.1 (s, C^m/C_6H_5), 130.6 (s, C^p/C_6H_5), 133.0 (s, C^i/C_6H_5), 134.4 (s, C^2/C_3HN_2). HRMS (ESI-TOF) $[C_{19}H_{29}N_2]I$ $[M]^+$ *m/z*: calcd.: 285.2325, found: 285.2322.

4.9 Synthesis of 1-phenyl-2-(diphenylphosphino)-3-*n*-octyl-4,5-dimethyl-1*H*-imidazolium hexafluorophosphate (17a)

To **16d** (0.30 g, 0.73 mmol) in dry dichloromethane (30 mL), *n*-BuLi (0.30 mL, 0.75 mmol) was added dropwise at -78 °C. The reaction mixture was stirred for 45 min at this temperature followed by dropwise addition of chlorodiphenylphosphine (0.14 mL, 0.78 mmol). After warming the mixture to ambient temperature, all volatile materials were removed in membrane-pump vacuum and the residue was dissolved in acetone (20 mL). Then a solution of potassium hexafluorophosphate (0.14 g, 0.76 mmol) in water (20 mL) was added in a single portion and the mixture was stirred at ambient temperature for an additional hour. After removal of all volatiles, the residue was purified by column chromatography (column

size: 2.5 × 12 cm) on Silica using diethyl ether as eluent. Phosphine **17a** was obtained as a colorless solid. Yield: 0.30 g (0.49 mmol, 67 % based on **16d**). Anal. Calcd. for $C_{31}H_{38}F_6N_2P$ (614.58 g/mol): C, 60.58; H, 6.23; N, 4.56. Found: C, 60.50; H, 6.53; N, 4.25. Mp.: 92 °C. IR (KBr, $\tilde{\upsilon}$/cm^{-1}): 1436 (m, P-C), 1499 (m, N=C), 1595/1632 (w, C=C), 2855/2927/2953 (m, C-H), 3058 (w, =C-H). ^{1}H NMR (500.30 MHz, $CDCl_3$, δ): 0.86 (t, $^3J_{HH}$ = 7.2 Hz, 3 H, $CH_2(CH_2)_6CH_3$), 1.07 – 1.25 (m, 10 H, $CH_2(CH_2)_6CH_3$), 1.35 – 1.41 (m, 2 H, $CH_2(CH_2)_6CH_3$), 1.97 (s, 3 H, CH_3), 2.41 (s, 3 H, CH_3), 4.15 (m, 2 H, $CH_2(CH_2)_6CH_3$), 6.99 (dpt, $^3J_{HH}$ = 8.5 Hz, $^4J_{HH}$ = 1.9 Hz, $^5J_{HP}$ = 1.2 Hz, 2 H, H^o/C_6H_4), 7.18 – 7.23 (m, 6 H, H^{m,p}/C_6H_5-P), 7.33 – 7.37 (m, 7 H, H^o/C_6H_5-P + H^{m,p}/C_6H_5). ^{13}C{^{1}H} NMR (125.81 MHz, $CDCl_3$, δ): 9.5 (s, CH_3), 9.7 (s, CH_3), 14.2 (s, $CH_2(CH_2)_6CH_3$), 22.7 (s, $CH_2(CH_2)_6CH_3$), 26.6 (s, $CH_2(CH_2)_6CH_3$), 28.9 (s, $CH_2(CH_2)_6CH_3$), 29.0 (s, $CH_2(CH_2)_6CH_3$), 29.7 (s, $CH_2(CH_2)_6CH_3$), 31.7 (s, $CH_2(CH_2)_6CH_3$), 47.9 (d, $^3J_{CP}$ = 10.6 Hz, $CH_2(CH_2)_6CH_3$), 127.7 (s, C^4/C_3N_2), 128.8 (d, $^4J_{CP}$ = 6.6 Hz, C^o/C_6H_5), 129.6 (d, $^3J_{CP}$ = 7.3 Hz, C^m/C_6H_5-P), 129.9 (s, C^p/C_6H_5), 130.4 (s, C^m/C_6H_5), 130.5 (s, C^p/C_6H_5-P), 131.0 (s, C^5/C_3N_2), 132.9 (d, $^2J_{CP}$ = 20.2 Hz, C^o/C_6H_5-P), 133.0 (m, C^i/C_6H_5-P), 133.9 (d, $^3J_{CP}$ = 1.2 Hz, C^i/C_6H_5), 141.1 (d, $^1J_{CP}$ = 54.0 Hz, C^2/C_3N_2). ^{31}P{^{1}H} NMR (202.5 MHz, $CDCl_3$, δ): -144.6 (sept, $^1J_{PF}$ = 712.5 Hz, PF_6), -23.5 (s, $P(C_6H_5)_2$). HRMS (ESI-TOF) $[C_{31}H_{38}N_2P]PF_6$ $[M]^+$ *m/z*: calcd.: 469.2767, found: 469.2767.

4.10 Synthesis of 1-phenyl-2-(dicyclohexylphosphino)-3-*n*-octyl-4,5-dimethyl-1*H*-imidazolium hexafluorophosphate (17b)

Compound **16d** (0.50 g, 1.21 mmol) was dissolved in dry dichloromethane (40 mL) and cooled to -78 °C. *n*-BuLi (0.48 mL, 1.20 mmol) was added dropwise and the reaction mixture was stirred for 45 min at this temperature. After dropwise addition of chlorodicyclohexylphosphine (0.27 mL, 1.22 mmol) the reaction mixture was warmed to ambient temperature. Then all volatiles were removed in vacuum and the residue was dissolved in acetone (20 mL). A solution of potassium hexafluorophosphate (0.22 g, 1.20 mmol) in water (20 mL) was added dropwise and the mixture was stirred at ambient temperature for 1 h. The solvent was removed in membrane-pump vacuum and the crude product was purified by column chromatography (column size: 2.5 × 12 cm) on Silica using diethyl ether as eluent. Phosphine **17b** was obtained as a colorless solid. Yield: 0.54 g (0.86 mmol, 72 % based on **16d**). Anal. Calcd. for $C_{31}H_{50}F_6N_2P$ (626.68 g/mol): C, 59.41; H, 8.04; N, 4.47. Found: C, 59.58; H, 8.21; N, 4.32. Mp.: 58 °C. IR (NaCl, $\tilde{\upsilon}$/cm^{-1}): 1450 (m, P-C),

1500 (m, N=C), 1595/1635 (w, C=C), 2853/2927 (s, C-H), 3067 (w, =C-H). ^{1}H NMR (500.30 MHz, $CDCl_3$, δ): 0.86 (t, $^{3}J_{HH}$ = 7.1 Hz, 3 H, $CH_2(CH_2)_6CH_3$), 1.05 – 1.19 (m, 10 H, $CH_2(CH_2)_6CH_3$ + C_6H_{11}), 1.27 – 1.44 (m, 12 H, $CH_2(CH_2)_6CH_3$ + C_6H_{11}), 1.60 – 1.65 (m, 8 H, $CH_2(CH_2)_6CH_3$ + C_6H_{11}), 1.74 – 1.78 (m, 4 H, $CH_2(CH_2)_6CH_3$ + C_6H_{11}), 1.92 (s, 3 H, C_3N_2), 2.34 (s, 3 H, C_3N_2), 4.31 (m, 2 H, $CH_2(CH_2)_6CH_3$), 7.29 (d, $^{3}J_{HH}$ = 7.4 Hz, 2 H, H^{o}/C_6H_5), 7.60 – 7.66 (m, 3 H, $H^{m,p}/C_6H_5$). ^{13}C{^{1}H} NMR (125.81 MHz, $CDCl_3$, δ): 9.4 (s, CH_3), 9.4 (s, CH_3), 14.1 (s, $CH_2(CH_2)_6CH_3$), 22.6 (s, $CH_2(CH_2)_6CH_3$), 25.6 (s, C_6H_{11}), 26.2 (d, J_{CP} = 1.3 Hz, C_6H_{11}), 26.3 (d, J_{CP} = 6.9 Hz, C_6H_{11}), 26.5 (s, $CH_2(CH_2)_6CH_3$), 28.9 (s, $CH_2(CH_2)_6CH_3$), 29.0 (s, $CH_2(CH_2)_6CH_3$), 30.2 (s, $CH_2(CH_2)_6CH_3$), 31.1 (d, J_{CP} = 9.1 Hz, C_6H_{11}), 31.7 (d, J_{CP} = 23.5 Hz, C_6H_{11}), 31.7 (s, $CH_2(CH_2)_6CH_3$), 35.0 (d, $^{1}J_{CP}$ = 11.2 Hz, C^{1}/C_6H_{11}), 47.4 (d, $^{3}J_{CP}$ = 17.1 Hz, $CH_2(CH_2)_6CH_3$), 127.4 (m, C^{o}/C_6H_5), 129.9 (s, C^{p}/C_6H_5), 130.3 (s, C^{m}/C_6H_5), 131.6 (m, C^{4}/C_3N_2), 132.3 (d, $^{3}J_{CP}$ = 1.7 Hz, C^{5}/C_3N_2), 134.1 (m, C^{i}/C_6H_5), 143.3 (d, $^{1}J_{CP}$ = 61.7 Hz, C^{2}/C_3N_2). ^{31}P{^{1}H} NMR (202.5 MHz, $CDCl_3$, δ): -144.6 (sept, $^{1}J_{PF}$ = 712.5 Hz, PF_6), -13.8 (s, $P(C_6H_5)_2$). HRMS (ESI-TOF) $[C_{31}H_{50}N_2P]PF_6$ $[M]^{+}$ *m/z*: calcd.: 481.3706, found: 481.3679.

4.11 Synthesis of [(1-(4-Br-C_6H_4)-$^{c}C_3H_2N_2$-3-*n*-Bu)$_2$$PdI_2$] (19)

To **16a** (106 mg, 0.26 mmol) dissolved in dry tetrahydrofuran (10 mL) a solution of potassium *tert*-butoxide (58 mg, 0.53 mmol, 2 eq) in dry tetrahydrofuran (5 mL) was added dropwise at ambient temperature. After stirring the solution for 2 h, $[PdCl_2(cod)]$ (37 mg, 0.13 mmol) was added in a single portion and the mixture was stirred for additional 16 h. All volatiles were removed in membrane-pump vacuum and the residue was dissolved in chloroform and filtered through a pad of Celite. By slow evaporation in membrane-pump vacuum at 0 °C two different types of crystals (pale yellow plates and colorless needles) suitable for X-ray diffraction analysis could be isolated.

4.12 Synthesis of 1-(4-(diphenylphosphino)phenyl)-3-*n*-octyl-4,5-dimethyl-1*H*-imidazolium hexafluorophosphate (20)

Diphenylphosphine (0.18 mL, 1.03 mmol) was added in a single portion to a dimethyl acetamide solution (30 mL) containing **16c** (0.5 g, 0.93 mmol), potassium acetate (109 mg, 1.11 mmol, 1.2 eq) and $[Pd(OAc)_2]$ (2.1 mg, 1.0 mol%) and stirred for 2 h at 130 °C. After cooling the reaction mixture to ambient temperature, all volatile materials were removed in vacuum and the residue was dissolved in acetone (10 mL). Then a solution of potassium

hexafluorophosphate (172 mg, 0.93 mmol) in water (10 mL) was added in a single portion and the mixture was stirred at ambient temperature for 1 h. The solvent was removed in membrane-pump vacuum and the residue was purified by column chromatography (column size: 2.5 × 12 cm) on Silica using a mixture of acetone-diethyl ether (ratio 1:1, *v*:*v*). Ionic phosphine **20** could be isolated as colorless solid. Yield: 0.36 g (0.59 mmol, 63 % based on **16c**). Anal. Calcd. for $C_{31}H_{38}F_6N_2P$ (614.58 g/mol): C, 60.58; H, 6.23; N, 4.56. Found: C, 60.60; H, 6.24; N, 4.31. Mp.: 138 °C. IR (KBr, $\tilde{\upsilon}$/cm^{-1}): 1434 (m, P-C), 1560 (s, N=C), 1595/1634 (w, C=C), 2855/2925/2951 (s, C-H), 3056/3070/3160 (w, =C-H). ^{1}H NMR (500.30 MHz, $CDCl_3$, δ): 0.86 (t, $^3J_{HH}$ = 7.2 Hz, 3 H, $CH_2(CH_2)_6CH_3$), 1.20 – 1.38 (m, 10 H, $CH_2(CH_2)_6CH_3$), 1.84 (pent, $^3J_{HH}$ = 7.3 Hz, 2 H, $CH_2(CH_2)_6CH_3$), 2.13 (s, 3 H, CH_3), 2.29 (s, 3 H, CH_3), 4.10 (t, $^3J_{HH}$ = 7.8 Hz, 2 H, $CH_2(CH_2)_6CH_3$), 7.31 – 7.38 (m, 12 H, $H^{o,m,p}/C_6H_5$+H^m/C_6H_4), 7.40 – 7.43 (m, 2 H, H^o/C_6H_4). ^{13}C{^{1}H} NMR (125.81 MHz, $CDCl_3$, δ): 8.5 (s, CH_3), 9.1 (s, CH_3), 14.1 (s, $CH_2(CH_2)_6CH_3$), 22.7 (s, $CH_2(CH_2)_6CH_3$), 26.4 (s, $CH_2(CH_2)_6CH_3$), 29.0 (s, $CH_2(CH_2)_6CH_3$), 29.1 (s, $CH_2(CH_2)_6CH_3$), 29.5 (s, $CH_2(CH_2)_6CH_3$), 31.8 (s, $CH_2(CH_2)_6CH_3$), 47.8 (s, $CH_2(CH_2)_6CH_3$), 125.9 (d, $^3J_{CP}$ = 6.3 Hz, C^o/C_6H_4), 127.7 (s, C_3N_2), 128.0 (s, C_3N_2), 129.0 (d, $^3J_{CP}$ = 7.3 Hz, C^m/C_6H_5), 129.5 (s, C^p/C_6H_5), 133.2 (s, C^i/C_6H_4), 133.3 (s, C^2/C_3N_2), 134.1 (d, $^2J_{CP}$ = 20.1 Hz, C^o/C_6H_5), 134.9 (d, $^2J_{CP}$ = 19.2 Hz/C^m/C_6H_4), 135.8 (d, $^1J_{CP}$ = 10.6 Hz, C^i/C_6H_5), 142.3 (d, $^1J_{CP}$ = 16.5 Hz, C^p/C_6H_4). ^{31}P{^{1}H} NMR (202.5 MHz, $CDCl_3$, δ): -144.5 (sept, $^1J_{PF}$ = 712.6 Hz, PF_6), -5.4 (s, $P(C_6H_5)_2$). HRMS (ESI-TOF) $[C_{31}H_{38}N_2P]^+$ $[M]^+$ *m/z*: calcd.: 469.2767, found: 469.2739.

4.13 General Procedure for the Suzuki-Miyaura Reaction

2-Bromo toluene (500 mg, 2.92 mmol), phenylboronic acid (470 mg, 3.85 mmol), potassium carbonate (1.21 g, 8.76 mmol) and acetyl ferrocene (111 mg, 0.49 mmol) were dissolved in a 1,4-dioxane-water mixture (10 mL, ratio 2:1, *v*:*v*). After addition of 0.25 mol% of $[Pd(OAc)_2]$ and 0.5 mol% of the appropriate phosphine (**11**, **17**, **20**), the reaction mixture was stirred for 1 h at 100 °C. Samples of 1 mL were taken after 2.5, 5, 10, 20, 30, and 60 min and chromatographed on Silica gel (column size: 6 × 2.5 cm) using diethyl ether as eluent. All volatiles were evaporated under reduced pressure and the conversions were determined by ^{1}H NMR spectroscopy.

4.14 General Procedure for the Suzuki-Miyaura Reaction in Ionic Liquids

Phenylboronic acid (470 mg, 3.85 mmol), potassium carbonate (1.21 g, 8.76 mmol), acetyl ferrocene (111 mg, 0.49 mmol), 0.25 mol% of [$Pd(OAc)_2$] and 0.5 mol% of the appropriate phosphine (**17b**, **20**) were dissolved in [BMIM][PF_6] (7.0 g, 24.6 mmol) or [BDMIM][BF_4] (6.0 g, 25.0 mmol), followed by the addition of degassed water (5 mL). After stirring of the reaction mixture for 5 min at ambient temperature, 2-bromo toluene (500 mg, 2.92 mmol) was added in a single portion and the mixture was stirred for 60 min at 100 °C. After cooling to ambient temperature the reaction mixture was continuously extracted with *n*-pentane until no more colouring of the solution was observable. In the case of [BMIM][PF_6], the water layer was removed and the ionic liquid was washed once with water (10 mL) and then was used in the next run. The [BDMIM][BF_4] solution was used without further purification in the 2nd run. Finally, the *n*-pentane solution was evaporated in membrane-pump vacuum and the conversion was determined by ^{1}H NMR spectroscopy.

4.15 General Procedure for the Suzuki-Miyaura Coupling of Aryl Chlorides

4-Chloro toluene (379 mg, 3.0 mmol), phenylboronic acid (550 mg, 4.5 mmol, 1.5 eq), potassium phosphate (1.27 g, 6.0 mmol, 3 eq) and acetyl ferrocene (114 mg, 0.50 mmol) were dissolved in toluene (6 mL). After addition of 0.01 mol% [$Pd(OAc)_2$] and 0.1 mol% of the appropriate phosphine (**11d**, **11e**), the reaction mixture was stirred for 20 h at 100 °C. Afterwards, a sample of 2 mL was taken and filtered through a pad of Celite. After evaporation of all volatiles under reduced pressure, the conversions were determined by ^{1}H NMR spectroscopy.

4.16 General Procedure for the Synthesis of Sterically Hindered Biaryls

Phenylboronic acid (183 mg, 1.5 mmol, 1.5 eq), potassium phosphate (0.64 g, 3.0 mmol, 3.0 eq), acetyl ferrocene (114 mg, 0.50 mmol) 0.05 mol% [$Pd_2(dba)_3$] and 0.1 mol% of **11e** were dissolved in toluene (2 mL). Afterwards, the appropriate aryl bromide (1.0 mmol, 1.0 eq) was added in a single portion and the reaction mixture was stirred for 24 h at 50 °C. Afterwards, the reaction mixture was filtered through a pad of Celite and the solvent was removed in membrane-pump vacuum. The conversions were determined by ^{1}H NMR spectroscopy.

4.17 Crystal Structure Determination

The crystal and intensity collection data for **11a-Se**, *trans*-**19** and *cis*-**19** are summarized in Table F5. All data were collected on an Oxford Gemini S diffractometer with graphite monochromatised Mo K_α radiation (λ = 0.71073 Å) at 105 K (*trans*-**19**) and graphite monochromatised Cu K_α radiation (λ = 1.54184 Å) at 100 K (**11a**-**Se**, *cis*-**19**). The structures were solved by direct methods using *SHELXS-91* [F28] and refined by full-matrix least-square procedures on F^2 using *SHELXL-97*. [F29] All *non*-hydrogen atoms were refined anisotropically and a riding model was employed in the refinement of the hydrogen atom positions. For *cis*-**19** the crystal available for measuring was comparatively tiny and needed the use of Cu K_α radiation in order to get reasonable results. At higher diffraction angles large exposure times have been used, leading to an 'icing' of the crystal. The measurement was therefore stopped and hence, the ratio between unique to observed reflections is almost poor. As no further crystals were available no re-measurement could be performed. Despite this, all non-hydrogen atoms could be refined anisotropically and a number of fragments could be refined disordered over two positions. Occupation factors: 0.17/0.83 for Pd3, I5, I6/Pd3', I5', I6'. 0.49/0.51 for C71 - C73/C71' - C73'. 0.75/0.25 for C33, C34/C33'/C34'. 0.48/0.52 for C58 - C60/C58' - C60'. 0.39/0.61 for C80, Cl1 - Cl3/C80', Cl1' - Cl3'. Trials to introduce further disordered fragments did not give reliable results, which is attributed to the already poor data-to-parameter ratio.

Table F7. Crystal and intensity collection data for **11a-Se**, *trans*-**19** and *cis*-**19**.

	11a-Se	*trans*-**19**	*cis*-**19**
Formula weight	486.20	918.56	1037.93
Chemical formula	$C_{21}H_{16}BrN_2PSe$	$C_{26}H_{30}Br_2I_2N_4Pd$	$C_{27}H_{31}Br_2Cl_3I_2N_4Pd$
Crystal system	monoclinic	triclinic	triclinic
Space group	$P2_1/n$	$P\bar{1}$	$P\bar{1}$
a (Å)	14.6515(2)	8.7047(5)	16.3428(11)
b (Å)	6.86120(10)	12.7269(6)	16.6465(12)
c (Å)	19.3482(3)	14.2494(7)	19.6587(15)
α (°)		78.787(4)	88.435(6)
β (°)	96.639(2)	82.971(4)	79.579(6)
γ (°)		74.495(4)	79.799(6)
V (Å³)	1931.97(5)	1487.97(13)	5176.7(6)
ρ_{calc} (mg m^{-3})	1.672	2.050	1.998
F(000)	960	872	2964
Crystal dimensions	0.4 × 0.2 × 0.2	0.35 × 0.35 × 0.08	0.10 × 0.03 × 0.02

(mm)			
Z	4	2	6
Max. and min. transmission	1.00000, 0.37259	1.00000, 0.55328	1.00000, 0.25423
Absorption coefficient (λ, mm^{-1})	5.885	5.405	23.419
Scan range (°)	4.60 – 62.00	3.20 – 26.12	3.28 – 62.00
Index ranges	$-16 \le h \le 16$ $-7 \le k \le 7$ $-21 \le l \le 22$	$-9 \le h \le 10$ $-15 \le k \le 14$ $-11 \le l \le 17$	$-11 \le h \le 18$ $-12 \le k \le 19$ $-22 \le l \le 22$
Total reflections	7108	9837	23957
Unique reflections	2999	5836	14330
R_{int}	0.0191	0.0237	0.0603
Data/restraints/parameters	2999 / 0 / 235	5836 / 0 / 316	14330 / 670 / 1112
Goodness-of-fit on F^2	1.060	0.927	0.893
R_1[a], wR_2[a] [I $2\sigma(I)$]	0.0253, 0.0659	0.0248, 0.0519	0.0997, 0.2499
R_1[a], wR_2[a] (all data)	0.0283, 0.0671	0.0344, 0.0531	0.1714, 0.2796
Largest differences in peak and hole peak in final Fourier map (e $Å^{-3}$)	0.669, -0.620	0.757, -0.668	3.955, -1.841

[a] $R_1 = [\Sigma(||F_o| - |F_c||)/\Sigma|F_o|]$; $wR_2 = [\Sigma(w(F_o^2 - F_c^2)^2)/\Sigma(wF_o^4)]^{1/2}$; $S = [\Sigma w(F_o^2 - F_c^2)^2]/(n - p)^{1/2}$. n = number of reflections, p = parameters used.

5 Supporting Information

Reaction profiles for the Suzuki-Miyaura cross-couplings in the presence of phosphines **11**, **17**, **20** and [$Pd(OAc)_2$] are given. Crystallographic data of **11a-Se** (CCDC 848041), *trans*-**19** (CCDC 848043) and *cis*-**19** (CCDC 848042) are available as *CIF* files free of charge from the Cambridge Crystallographic Database *via* www.ccdc.cam.ac.uk/products/csd/-request/.

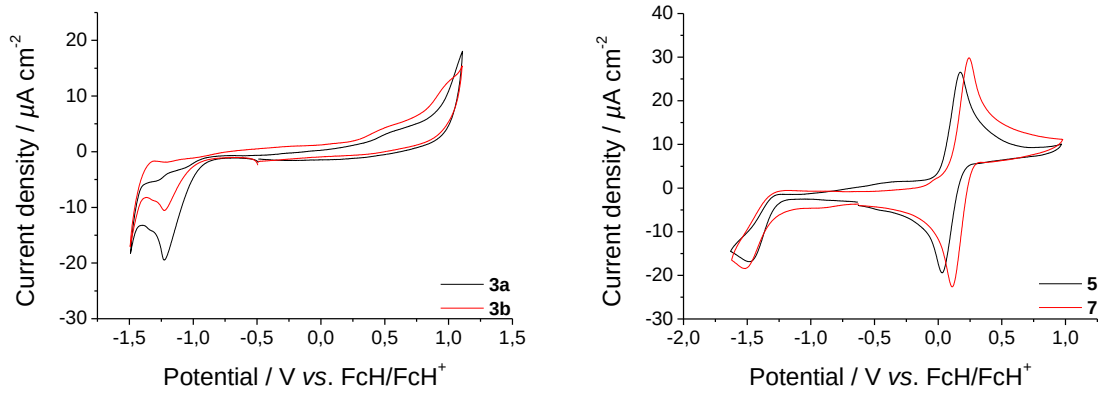

Figure F3. Cyclovoltammograms of **3a** and **3b** (left) and **5** and **7** (right) in dichloromethane solutions **(**1.0 mmol·dm^{-3}**)** at 25 °C, supporting electrolyte [(*n*-Bu)$_4$N][B(C$_6$F$_5$)$_4$] **(**0.1 mol·dm^{-3}**)** with a scan rate of 100 mV·s^{-1}.

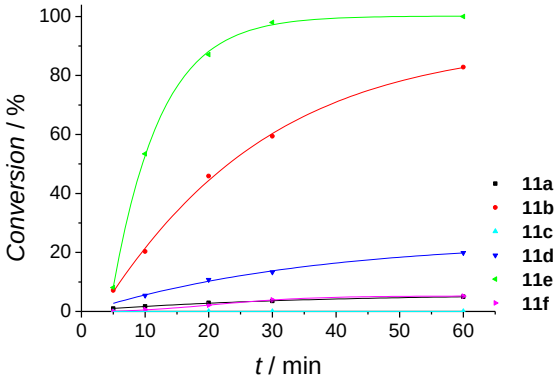

Figure F4. Reaction profile for the coupling of 2-bromo toluene (2.92 mmol) with phenyl boronic acid (3.85 mmol) to give 2-methyl biphenyl using [Pd(OAc)$_2$] / **11a** – **f** (0.25 mol% [Pd], 0.5 mol% **11a** – **f**) in the presence of K_2CO_3 (8.76 mmol) in a 1,4-dioxane-water mixture (ratio 2:1, *v*:*v*) at 100 °C.

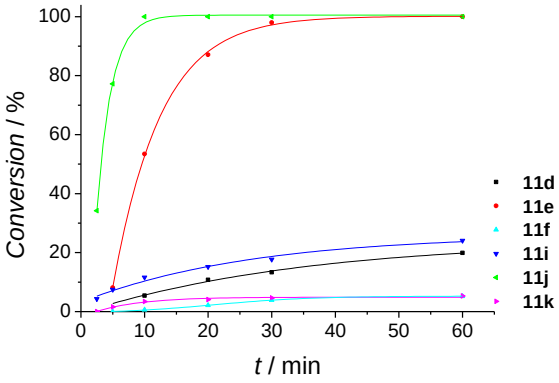

Figure F5. Reaction profile for the coupling of 2-bromo toluene (2.92 mmol) with phenyl boronic acid (3.85 mmol) to give 2-methyl biphenyl using [Pd(OAc)$_2$] / **11d** – **f**, **11i** – **k** (0.25 mol% [Pd], 0.5 mol% **11d** – **f**, **11i** – **k**) in the presence of K_2CO_3 (8.76 mmol) in a 1,4-dioxane-water mixture (ratio 2:1, *v*:*v*) at 100 °C.

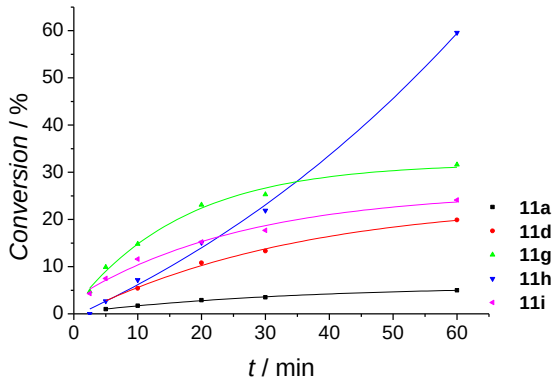

Figure F6. Reaction profile for the coupling of 2-bromo toluene (2.92 mmol) with phenyl boronic acid (3.85 mmol) to give 2-methyl biphenyl using [Pd(OAc)$_2$] / **11a** – **f** (0.25 mol% [Pd], 0.5 mol% **11a**, **11d**, **11g** – **i**) in the presence of K_2CO_3 (8.76 mmol) in a 1,4-dioxane-water mixture (ratio 2:1, *v*:*v*) at 100 °C.

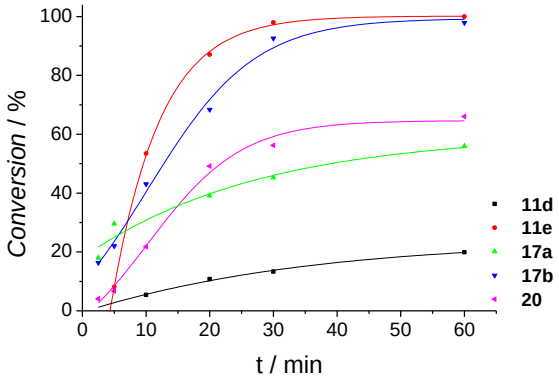

Figure F7. Reaction profile for the coupling of 2-bromo toluene (2.92 mmol) with phenyl boronic acid (3.85 mmol) to give 2-methyl biphenyl using [Pd(OAc)$_2$] / **11a** – **f** (0.25 mol% [Pd], 0.5 mol% **11d**, **11e**, **17a**, **17b**, **20**) in the presence of K_2CO_3 (8.76 mmol) in a 1,4-dioxane-water mixture (ratio 2:1, *v*:*v*) at 100 °C.

6 Acknowledgement

We are grateful to the Deutsche Forschungsgemeinschaft and the Fonds der Chemischen Industrie for generous financial support. Furthermore, we would like to thank Sabrina Krauße and Martina Steinert for assistance in the lab.

7 References

[F1] a) H. Willms, W. Frank, C. Ganter *Organometallics* **2009**, *28*, 3049; b) J. Li, J. Peng, Y. Bai, G. Zhang, G. Lai, X. Li *J. Organomet. Chem.* **2010**, *695*, 431; c) S. Sauerbrey, P. K. Majhi, J. Daniels, G. Schnakenburg, G. M. Brändle, K. Scherer, R. Streubel *Inorg. Chem.* **2011**, *50*, 793; d) Q.-X. Wan, Y. Liu, Y.-Q. Cai *Catal. Lett.* **2009**, *127*, 386; e) D. J. Brauer, K. W. Kottsieper, C. Liek, O. Stelzer, H. Waffenschmidt, P.Wasserscheid *J. Organomet. Chem.* **2001**, *630*, 177; f) S. S. Moore, G. M. Whitesides *J. Org. Chem.* **1982**, *47*, 1489; g) V. Diez, G. Espino, F. A. Jalon, B. R. Manzano, M. Perez-Manrique *J. Organomet. Chem.* **2007**, *692*, 1482; h) M. A. Jalil, S. Fujinami, T. Honjo, H. Nishikawa *Polyhedron* **2001**, *20*, 1071.

[F2] a) T. L. Gilchrist, *Heterocyclenchemie*, ed. H. Neunhoeffer, Weinheim, Wiley-VCH, **1995**, pp. 300; b) T. Schulz, C. Torborg, B. Schäffner, J. Huang, A. Zapf, R. Kadyrov, A. Börner, M. Beller *Angew. Chem. Int. Ed.* **2009**, *48*, 918; c) M. R.

Grimmett, in *Science of Synthesis-Five membered Heteroarenes with two Nitrogen or Phosphorus Atoms*, Vol.-ed. R. Neier, Thieme, Stuttgart-New York, **2002**, Vol. 12, pp. 325; d) J. Liu, J. Chen, J. Zhao, Y. Zhao, L. Li, H. Zhang *Synthesis* **2003**, *17*, 2661.

[F3] For example: a) A. Dumrath, X.-F. Wu, H. Neumann, A. Spannenberg, R. Jackstell, M. Beller *Angew. Chem. Int. Ed*. **2010**, *49*, 8988; b) S. Harkal, F. Rataboul, A. Zapf, C. Fuhrmann, T. Riermeier, A. Monsees, Matthias Beller *Adv. Synth. Catal*. **2004**, *346*, 1742; c) J. Sirieix, M. Oßberger, B. Betzemeier, P. Knochel *Synlett* **2000**, *11*, 1613; d) N. Debono, Y. Canac, C. Duhayon, R. Chauvin *Eur. J. Inorg. Chem*. **2008**, 2991; e) C. Torborg, J. Huang, T. Schulz, B. Schäffner, A. Zapf, A. Spannenberg, A. Börner, M. Beller *Chem. Eur. J*. **2009**, *15*, 1329.

[F4] S. Saleh, E. Fayad, M. Azouri, J.-C. Hierso, J. Andrieu, M. Picquet *Adv. Synth. Catal*. 2009, **351**, 1621.

[F5] a) S. Ahrens, E. Herdtweck, S. Goutal, T. Strassner *Eur. J. Inorg. Chem*. **2006**, 1268; b) Y. Canac, N. Debono, L. Vendier, R. Chauvin *Inorg. Chem*. **2009**, *48*, 5562; c) M. Azouri, J. Andrieu, M. Picquet, H. Cattey *Inorg. Chem*. **2009**, *48*, 1236; d) J.-C. Shi, P.-Y. Yang, Q. Tong, Y. Wu, Y. Peng *J. Mol. Cat. A: Chemical* **2006**, *259*, 7; e) E. Amigues, C. Hardacre, G. Keane, M. Migaud, M. O'Neill *Chem. Comm*. **2006**, 72.

[F6] a) C. S. Consorti, G. L. P. Aydos, G. Ebeling, J. Dupont *Org. Lett*. **2008**, *10*, 237; b) J. Andrieu, M. Azouri *Inorg. Chim. Acta* **2007**, *360*, 131; c) P. J. Dyson, T. J. Geldbach, in *Catalysis by Metal Complexes-Metal Catalyzed Reactions in Ionic Liquids*, ed. B. James, P. W. N. M. van Leeuwen, Springer, Dordrecht, **2005**, Vol. 29; d) P. Wasserscheid, T. Welton, *Ionic Liquids in Synthesis*, 2nd Ed., Wiley-VCH, Weinheim, **2008**, Vol.1; e) J. Zhang, M. Dakovic, Z. Popovic, H. Wu, Y. Liu *Cat. Comm*. **2012**, *17*, 160.

[F7] a) R. Sanders, U. T. Müller-Westerhoff *J. Organomet. Chem*. **1996**, *512*, 219; b) U. T. Müller-Westerhoff, Z. Yang, G. Ingram *J. Organomet. Chem*. **1993**, *463*, 163.

[F8] O. Herd, A. Heßler, M. Hingst, M. Tepper, O. Stelzer *J. Organomet. Chem*. **1996**, *522*, 69.

[F9] a) R. P. Pinnell, C. A. Megerle, S. L. Manatt, P. A. Kroon *J. Am. Chem. Soc*. **1973**, *95*, 977; b) D. W. Allen, B. F. Taylor *J. Chem. Soc. Dalton Trans*. **1982**, *37*, 51; c) D. W. Allen, I. W. Nowell *J. Chem. Soc. Dalton Trans*. **1985**, 2505; d) A. Suarez, M. A.

Mendez-Rojas, A. Pizzano *Organometallics* **2002**, *21*, 4611; e) D. J. M. Snelders, C. van der Burg, M. Lutz, A. L. Spek, G. van Koten, R. J. M. Klein Gebbink *Chem. Cat. Chem*. **2010**, *2*, 1425; f) S. Jeulin, S. Duprat de Paule, V. Ratovelomanana-Vidal, J.-P. Genet, N. Champion, P. Dellis *Angew. Chem. Int. Ed*. **2004**, *43*, 320; g) B. Milde, M. Lohan, C. Schreiner, T.; Rüffer, H. Lang *Eur. J. Inorg. Chem*. **2011**, 5437. h) A. Jakob, B. Milde, P. Ecorchard, C. Schreiner, H. Lang *J. Organomet. Chem*. **2008**, *693*, 3821; i) B. Milde, D. Schaarschmidt, P. Ecorchard, H. Lang *J. Organomet. Chem.* **2012**, *706-707*, 52 – 65.

[F10] For example: a) O. Schuster, L. Yang, H. G. Raubenheimer, M. Albrecht *Chem. Rev*. **2009**, *109*, 3445; b) S. Diez-Gonzalez, N. Marion, S. P. Nolan *Chem. Rev*. **2009**, *109*, 3612.

[F11] F. Barriere, R. U. Kirss, W. E. Geiger *Organometallics* **2005**, *24*, 48.

[F12] G. Gritzner, J. Kuta *Pure Appl. Chem*. **1984**, *56*, 461.

[F13] B. Gorodetsky, T. Ramnial, N. R. Branda, J. A. C. Clyburne *Chem. Comm*. **2004**, 1972.

[F14] P. W. Kodding, K. A. Kerr *Acta Cryst*. **1979**, *B35*, 1261.

[F15] a) W. A. Herrmann, M. Elison, J. Fischer, C. Kocher, G. R. J. Artus *Angew. Chem. Int. Ed. Engl*. **1995**, *34*, 2371; b) A. Flahaut, K. Toutah, P. Mangeney, S. Roland *Eur. J. Inorg. Chem*. **2009**, 5422; c) X. Xu, B. Xu, Y. Li, S. H. Hong *Organometallics* **2010**, *29*, 6343.

[F16] O. V. Gusev, T. A. Peganova, A. M. Kalsin, N. V. Vologdin, P. V. Petrovskii, K. A. Layssenko, A. V. Tsvetkov, I. P. Beletskaya *Organometallics* **2006**, *25*, 2750.

[F17] B. Milde, R. Packheiser, S. Hildebrandt, D. Schaarschmidt, T. Rüffer, H. Lang, *Organometallics* **2012**, *31*, 3661.

[F18] a) J. P. Wolfe, R. A. Singer, B. H. Yang, S. L. Buchwald *J. Am. Chem. Soc*. **1999**, *121*, 9550; b) A. Zapf, A. Ehrentraut, M. Beller *Angew. Chem. Int. Ed*. **2000**, *39*, 4153; c) A. F. Littke, C. Dai, G. C. Fu *J. Am. Chem. Soc*. **2000**, *122*, 4020; d) S. D. Walker, T. E. Barder, J. R. Martinelli, S. L. Buchwald *Angew. Chem. Int. Ed*. **2004**, *43*, 1871.

[F19] a) D. Schaarschmidt, H. Lang *Eur. J. Inorg. Chem*. **2010**, 4811; b) D. Schaarschmidt, H. Lang *ACS Catalysis* **2011**, *1*, 411.

[F20] a) L. Magna, Y. Chauvin, G. P. Niccolai, J.-M. Basset *Organometallics* **2003**, *22*, 4418; b) V. K. Aggarwal, I. Emme, A. Mereu *Chem. Comm*. **2002**, 1612; c) C. J. Mathews, P. J. Smith, T. Welton, A. J. P. White, D. J. Williams *Organometallics* **2001**, *20*, 3848.

[F21] E. Gelens, F. J. J. De Kanter, R. F. Schmitz, L. A. J. M. Sliedregt, B. J. Van Steen, C. G. Kruse, R. Leurs, M. B. Groen, R. V. A. Orru *Molecular Diversity* **2006**, *10*, 17.

[F22] H. M. Colquhoun, J. Holton, D. J. Thompson, M. V. Twigg, *New Pathways for Organic Synthesis-Practical Applications of Transition Metals,* Plenum Press, New York, **1983**, pp. 383.

[F23] J. Polin, H. Schottenberger *Org. Synth*. **1996**, *73*, 262.

[F24] D. Drew, J. R. Doyle *Inorg. Synth*. **1990**, *28*, 348.

[F25] T. Imamoto, T. Oshiki, T. Onozawa, T. Kusumoto, K. Sato *J. Am. Chem. Soc*. **1990**, *112*, 5244.

[F26] H. Tomori, J. M. Fox, S. L. Buchwald *J. Org. Chem*. **2000**, *65*, 5334.

[F27] N. G. Andersen, R. McDonald, B. A. Keaya *Tetrahedron: Asymmetry* **2001**, *12*, 263.

[F28] G. M. Sheldrick *Acta Cryst., Sect. A* **1990**, *46*, 467.

[F29] G. M. Sheldrick, SHELXL-97, *Program for Crystal Structure Refinement*, University of Göttingen, **1997**.

G Imidazole Phosphines: Synthesis, Reaction Chemistry and Their Use in Suzuki-Miyaura *C,C* Cross-Coupling Reactions

Bianca Milde, Rico Packheiser, Stefanie Hildebrandt, Dieter Schaarschmidt,

Tobias Rüffer, and Heinrich Lang

Published in *Organometallics*, **2012**, *31*, 3661 – 3671.

*The platinum macrocycle **13** and the heterobimetallic platinum complex **11** were prepared and fully characterized by Dr. Rico Packheiser (Dissertation, TU Chemnitz, 2008) and Dipl.-Chem. Stefanie Hildebrandt (Diploma, TU Chemnitz, 2008). The preparation, characterization and catalytic test reactions of the phosphino imdazoles were carried out by the author.*

1 Introduction

Phosphino imidazoles represent an interesting family of molecules due to their ambivalent donor character (*P,N*) allowing their coordination to hard or soft transition metal fragments. [G1] They can be used, for example, as easily tunable ligands with good performance in palladium-catalyzed *C,C* couplings, [G1a,d,G2] as structural elements of ionic liquids in 2-phase catalytic reactions allowing facile recycling, [G1b,d,e,G2a,c,G3] or as model system for mimicking the catalytically active site in bio-inorganics. [G1c,G4] In contrast to mono-phosphino imidazoles, diphosphino imidazoles were investigated in conjunction with chirality. [G2d,G5]

Discrete molecular architectures can be designed and synthesized by molecular recognition using, for example, organic and metal-organic or organometallic compounds as building blocks containing the structural information to construct the appropriate self-assembled 2D or 3D architectures. [G6] Such structures include for instance molecular rods, squares, hexagons and boxes of which the transition metal-based squares were among the first successfully synthesized examples. [G6f,g] *Exo*-bidentate metal-organic units including nitrogen donors and mainly palladium and platinum metals have been employed as edges, while as linking components generally organic units are applied. [G6] Examples for metallo-supramolecular

squares are $[\{Pt(\mu\text{-}4,4'\text{-bpy})(dppp)\}_4]^{8+}$ [G6f] or $[\{Pt\text{-}\mu\text{-}C{\equiv}C\text{-}C{\equiv}C)(dcpe)\}_4]^{4+}$ [G7] (dppp = bis(diphenylphosphino)propane, dcpe = bis(dicyclohexylphoshino)ethane). Applications of such metallamacrocycles include homogeneous catalysis [G8] and host-guest chemistry. [G6i]

This prompted us to combine the two topics phosphino imidazoles and metallamacrocycles. In addition, the use of the appropriate phosphines in Suzuki-Miyaura *C,C* cross-coupling reactions is reported.

2 Results and Discussion

2.1 Synthesis and Characterization of Phosphino Imidazoles and Metallamacrocycles

Diphosphino imidazoles 1-(4-PR_2-C_6H_4)-2-PR'_2-4,5-Me_2-1*H*-C_3N_2 (R = Ph: **6a**, R' = Ph; **6b**, R' = Cy; **6c**, R' = Fur; R = Cy: **6d**, R' = Ph; **6e**, R' = Cy; **6f**, R' = Fur) were accessible in a consecutive reaction sequence as shown in Scheme G1. Remarkable is the sensitivity of **2** toward light, hence rapid work-up is highly recommended.

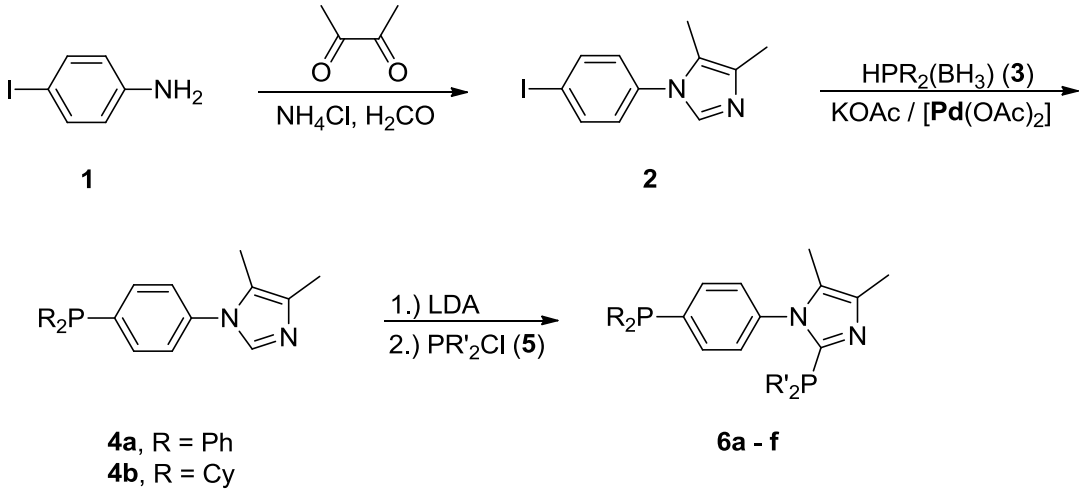

Scheme G1. Synthesis of diphosphino imidazoles **6a** – **f** (LDA = LiN(*i*-Pr)$_2$).

Palladium-promoted Stelzer coupling [G9] of 1-(4-I-C_6H_4)-4,5-Me_2-1*H*-^{c}C_3HN_2 (**2**) with $PR_2H(BH_3)$ (**3a**, R = Ph; **3b**, R = Cy) gave 1-(4-PR_2-C_6H_4)-4,5-Me_2-1*H*-^{c}C_3HN_2 (**4a**, R = Ph; **4b**, R = Cy) which on deprotonation with LiN(*i*-Pr)$_2$ followed by subsequent treatment with PR'_2Cl (**5a**, R = Ph; **5b**, R = Cy; **5c**, R = Fur) resulted in colorless diphosphines **6a** – **f** (Table G1, Experimental Section). Noteworthy is the high reactivity of phosphines **4** and **6** toward oxygen. They are rapidly oxidized to the respective phosphine oxides when exposed to air, solutions more quickly than solid materials. This also is reflected by the somewhat low yields characteristic for **4** and **6** (Table G1, Experimental Section).

Table G1. Synthesis of di-phosphino imidazoles **6a** – **f**.

Compd.	R	R'	Yield / % [a]	Compd.	R	R'	Yield / % [a]
6a	Ph	Ph	57	**6d**	Cy	Ph	60
6b	Ph	Cy	50	**6e**	Cy	Cy	46
6c	Ph	Fur	64	**6f**	Cy	Fur	65

[a] Based on **4a** or **4b**.

Phosphines **4** and **6** were characterized by elemental analysis, IR and NMR (^{1}H, ^{13}C{^{1}H}, ^{31}P{^{1}H}) spectroscopy, and high resolution ESI-TOF mass spectrometry.

The IR spectra of the mono- and diphosphino imidazoles are less expressive, while NMR spectroscopy is more meaningful. Very characteristic is the sp^2-hybridized CH imidazole proton signal at ca. 7.5 ppm for **4a** and **4b**, which upon substitution by the PR'$_2$ group (**6a** – **f**) disappears allowing the monitoring of the reaction progress. This also is possible using ^{13}C{^{1}H} NMR spectroscopy because a shift of the imidazole carbon atom in position 2 from 137 ppm in **4** (C-H) to 140 – 145 ppm in **6** (C-PR'$_2$; $^{1}J_{CP}$ = 2 – 15 Hz) occurs (Experimental Section). A further feature of **6a** – **f**, as compared to **4**, is the appearance of a doublet-of-doublets (*i. e.* **6a**: $^{3}J_{CP}$ = 3.1 Hz, $^{4}J_{PC}$ = 2.8 Hz) for the *meta*-positioned phenylene C-H unit, due to its coupling with both the PR$_2$ and the PR'$_2$ building blocks. In addition, ^{31}P{^{1}H} NMR spectroscopy is an efficient tool to control the introduction of a second phosphino moiety. While for **4** only one resonance signal is observed at 2.7 (**4a**) and -5.9 (**4b**) ppm, respectively, for **6a** – **f** two resonances between -71.7 and 2.6 ppm are characteristic, whereas the signal of the PR'$_2$ unit always appears at higher field. Nevertheless, the phosphino groups do not show phosphorus-phosphorus couplings.

Phosphino imidazoles **6a** – **f** can be applied in the Suzuki-Miyaura *C,C* cross-coupling of 2-bromo toluene with phenylboronic acid (*vide infra*) as well as in the synthesis of palladamacrocycles (Reaction G1). Molecules **6a** – **f** react quantitatively and rapidly with [PdCl$_2$(SEt$_2$)$_2$] (**7**) at ambient temperature to give air- and moisture-stable yellow complexes of type [Pd(1-(4-PR$_2$-C$_6$H$_4$)-2-PR'$_2$-4,5-Me$_2$-1*H*-C$_3$N$_2$)Cl$_2$]$_2$. Within this reaction, even using different reaction conditions, always *non*-soluble materials were obtained and hence characterization is limited. However, with **6c** as phosphino source single crystals of **8** suitable for single crystal X-ray structure studies could be obtained which allowed us to determine the structure of this complex in the solid state (Figure G1).

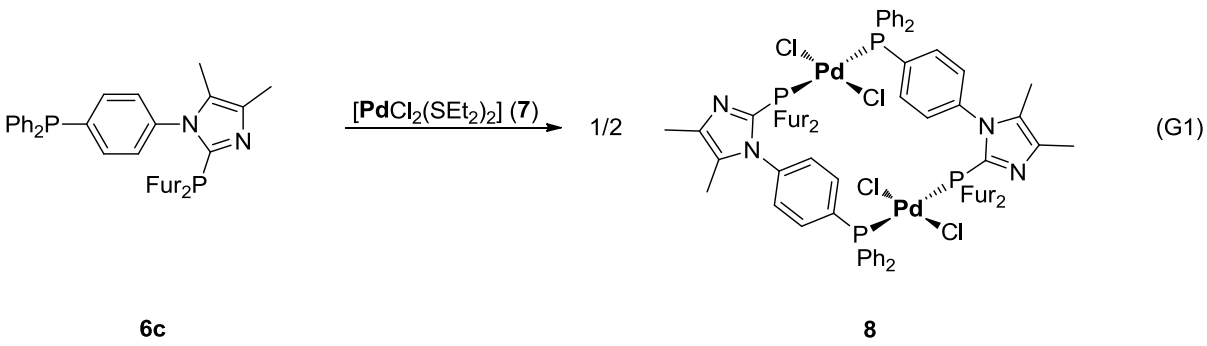

6c **8**

The very poor solubility of **8** even in common polar organic solvents precluded any reasonable NMR data. However, suitable crystals for single X-ray structure analysis were obtained by the one-step synthesis-cum-diffusion strategy at ambient temperature so that crystals could be formed in a slow reaction (*vide supra*). These crystals were subjected to single crystal X-ray structure analysis. The molecular structure of **8** is shown in Figure G1. Important bond distances (Å), bond angles (°) and torsion angles (°) are summarized in the caption of Figure G1. For crystal and structure refinement data see Experimental Section.

Cyclic **8** crystallizes in the monoclinic space group $P2_1/c$ as yellow needles. In its solid state it forms a dimeric *trans*-palladium complex with two bidentate imidazole ligands bridging two palladium dichloride units forming an 18-membered metallacycle. Compound **8** possesses a crystallographically imposed inversion symmetry with the inversion center in the middle between the palladium atoms Pd1 and Pd1A (Figure G1). The coordination at Pd is distorted square-planar with Cl1-Pd1-Cl2 and P1-Pd1-P2A angles of 168.69(4) and 174.79(4)°, respectively (r. m. s. deviation 0.0939 Å, highest deviation from planarity observed for Cl2 with 0.1199 Å), most likely attributed to ring strain. The phenylene groups are parallel oriented to each other with an interplanar distance of ca. 6.2 Å. As expected, the imidazole unit shows planarity (r. m. s. deviation 0.0094 Å) and the phenylene moiety is rotated by 70.3(5)° out of the plane of the imidazole entity. Therefore, the molecule is not planar but exhibits a structure similar to cyclophanes. [G10a] The Pd···Pd distance is 6.519 Å alluding that no direct palladium-palladium contact exists. Similar distances have been observed for $[Pd(2,5\text{-}(PPh_2)_2\text{-}C_4H_2S)Cl_2]_2$. [G10b] The bond distances of the phosphorus atom toward the furyl substituents are, as expected, shorter when compared with the P-C_{phenyl} bond length, due to the electron-withdrawing character of the furyl moieties. All other bond distances and angles correspond to related molecules, *i. e.* $[Pd(1,3\text{-}i\text{-}Pr_2\text{-}2\text{-}PPh_2\text{-}4,5\text{-}Me_2\text{-}C_3N_2)Cl_3]$ [G11] and $[Pd(2,5\text{-}(PPh_2)_2\text{-}C_4H_2S)Cl_2]_2$. [G10b]

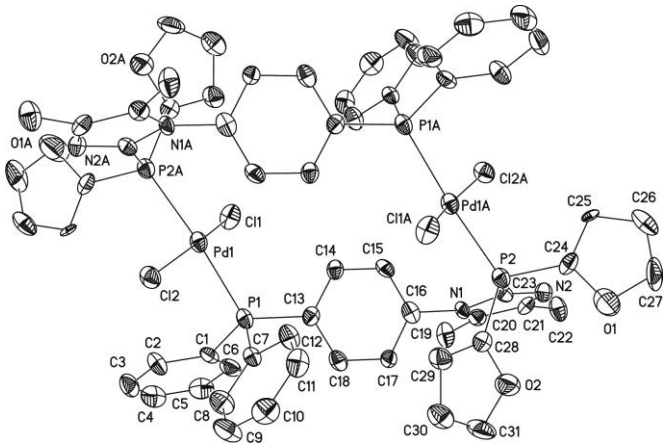

Figure G1. ORTEP diagram (50 % probability level) of the molecular structure of **8** crystallized from dichloromethane, with the atom-numbering scheme. All hydrogen atoms have been omitted for clarity. Selected bond distances (Å), angles (°) and torsion angles (°): Pd1-P1 = 2.3127(12), Pd1A-P2 = 2.3171(12), Pd1-Cl1 = 2.3008(11), Pd1-Cl2 = 2.3055(10), Pd1-P2A = 2.3171(12), C1-P1 = 1.805(4), C7-P1 = 1.814(4), C13-P1 = 1.823(4), C23-P2 = 1.796(4), C24-P2 = 1.780(5), C28-P2 = 1.799(4); Cl1-Pd1-Cl2 = 168.69(4), Cl1-Pd1-P1 = 90.80(4), Cl2-Pd1-P1 = 89.14(4), Cl1-Pd1-Cl2A = 93.61(4), Cl2, Pd1-P2A = 85.99(4), P1-Pd1-P2A = 174.79(4); C15-C16-N1-C23 = 70.3(5), C13-P1-Pd1-Cl1 = 45.28(16). (Symmetry generated atoms are indicated by the suffix A; symmetry code: -x+2, -y, -z+1.)

Supramolecular chemistry also allows the synthesis of a platinum-molecular square as given in the preparation of **13** (Scheme G2). Treatment of [Pt(dppf)Cl_2] (dppf = 1,1'-bis(diphenylphosphino)ferrocene) (**9**) and $PPh_2(C_6H_4$-4-C≡CH) (**10**) gave the bis(alkynyl)platinum complex [Pt(dppf)(C≡C-C_6H_4-4-$PPh_2)_2$] (**11**) (Scheme G1). The chelating ferrocenyl phosphine was used to enforce the required *cis*-geometry at the platinum atom. Heterobimetallic **11** gave upon reaction with [Pt$(SEt_2)_2Cl_2$] (**12**) *via* self-assembly the neutral tetra-nuclear molecular square **13** in an overall yield of 36 % (Experimental Section). Yellow **13** is poorly soluble in polar and *non*-polar solvents and is stable toward air and moisture. The neutral tetra-platinum square **13** possesses alternating edges composed of Pt(dppf) and $PtCl_2$ moieties which are connected by linear alkynyl phosphine units 4-Ph_2P-C_6H_4-C≡C.

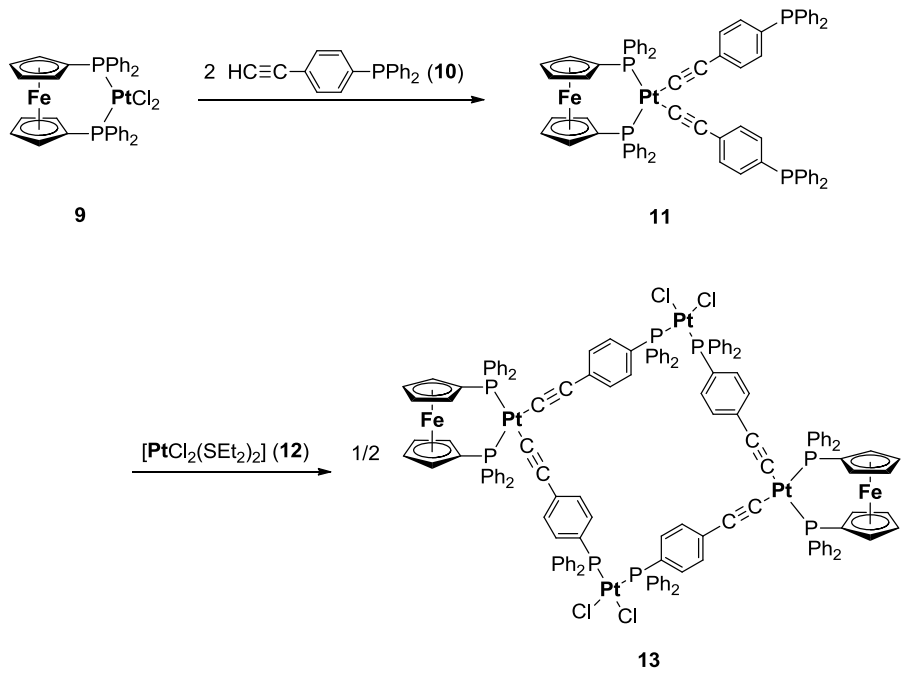

Scheme G2. Synthesis of the platinum-molecular square **13** starting from **9**.

The organometallic bis(alkynyl) platinum complex **11** and square **13** were characterized by elemental analysis, spectroscopy (IR; ^{1}H, ^{13}C{^{1}H}, ^{31}P{^{1}H} NMR) and single crystal X-ray structure analysis (Figure G2 (**11**), Figure G3 (**13**)).

Heterobimetallic **11** shows from the spectroscopic point of view no peculiarities (Experimental Section). Nevertheless, the 4-Ph_2P-C_6H_4-C≡C groups are best suited to monitor the progress of the reaction of **11** with **12** to form **13** since a shift of the phosphorus signal from -6.6 ppm in **11** to 14.7 in **13** ($PtCl_2$ edge fragment) occurs in the ^{31}P{^{1}H} NMR spectrum. Compounds **11** and **13** show a second phosphorus signal at 13.6 ppm which can be assigned to the Pt(dppf) building block with a characteristic $^{1}J_{195Pt\text{-}31P}$ coupling constant of 2380 Hz. The phosphorus-platinum coupling constant $^{1}J_{195Pt\text{-}31P}$ = 3673 Hz ($PtCl_2$) confirms the expected *cis*-arrangement at the platinum(II) center. The ^{1}H NMR spectra of **11** and **13** are easier to interpret due to their symmetrical structure (Figures G2 and G3) exhibiting the expected signals of the organic groups with distinctive AA'XX' patterns for the phenylene and the cyclopentadienyl groups. However, ^{13}C{^{1}H} NMR spectroscopy delivered no useful information due to the poor solubility of **13**. The successful formation of **11** can be IR spectroscopically controlled by the disappearance of the alkynyl C-H stretching frequency in the course of the reaction of **9** with **10** (Experimental Section). The alkynyl units in **11** and **13** are characterized by strong C≡C vibrations at 2112 (**10**) and 2114 cm^{-1} (**11**, **13**), respectively.

Single crystals of **11** and **13** could be grown by slow diffusion of *n*-hexane into a dichloromethane solution containing **11** at ambient temperature or slowly cooling of a saturated dichloromethane-**13** solution from 50 °C to ambient temperature. The molecular structure of **11** in the solid state is shown in Figure G2, while the one of **13** is depicted in Figure G3. Important bond distances (Å) and bond angles (°) are summarized in the captions of Figures G2 and G3, respectively. For crystal and structure refinement data see Experimental Section.

Complex **11** crystallizes in the monoclinic space group C_2/c and exhibits a square-planar geometry around Pt1 (r. m. s. deviation 0.0062 Å, highest deviation from planarity observed for Pt1 with -0.0156 Å) with a P1-Pt1-P2 bite angle of 97.11(6)° and a C35-Pt1-C55 angle of 90.4(3)°. The ferrocene moiety exhibits a staggered conformation (-35.2°) and the D1-Fe1 and D2-Fe1 separations are with 1.642(3) and 1.640(3) Å (D1, D2 = centroids of C_5H_4) similar to those of related compounds. [G12a] The cyclopentadienyl rings are with 5.7(5)° deviated from parallelism. The Pt-C≡C-C_{Ph} units are almost linear with Pt1-C35-C36, C35-C36-C37, Pt1-C55-C56 and C55-C56-C57 angles of 174.1(6), 173.8(7), 177.5(6) and 172.0(8)° (Figure G2). The Pt-$C_{C\equiv C}$ distances of 1.985(7) and 2.013(7) Å and the C≡C bond lengths with 1.219(9) and 1.186(9) Å reflect the formal bond order of these units. [G6b,G12a] Furthermore, complex **11** exhibits intra-molecular T-shaped and sandwich π,π interactions (Figure G2). [G12b] The C35-Pt1-C55 angle (see above) provides best preconditions for the formation of molecular squares.

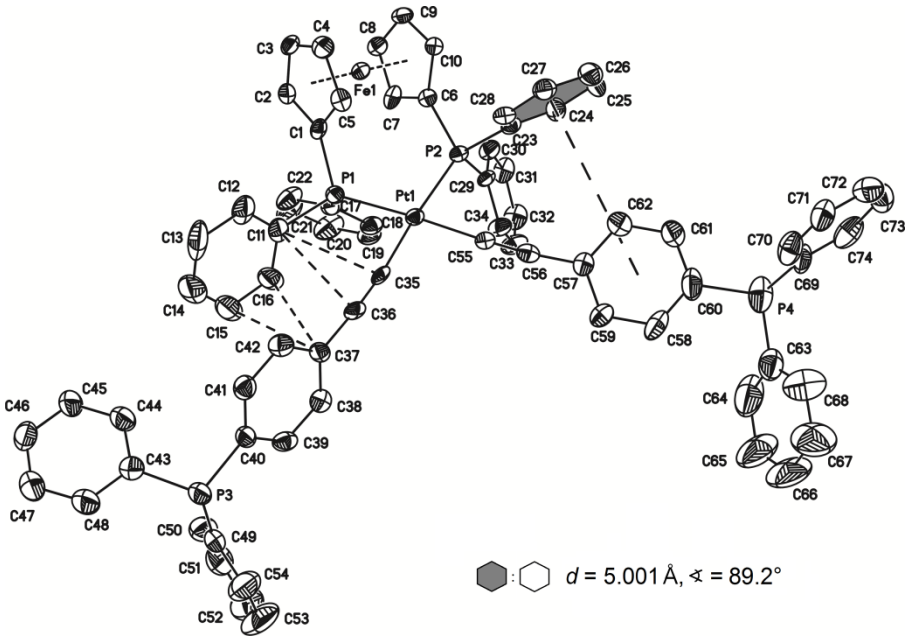

Figure G2 ORTEP diagram (50 % probability level) of the molecular structure of **11** with the atom-numbering scheme. All hydrogen atoms and one molecule of chloroform have been omitted for clarity. The T-shaped π,π interaction between the aromatic C_6 rings C23-C28 and C57-C62 are indicated with a dashed line, whereby *d* refers to the geometrical centroid to geometrical centroid distance and ∢ to the interplanar angle. Further π interactions are indicated by dashed lines, carbon-carbon distances are in the range between 3.109 (C11-C35) to 3.495 Å (C16-C37). Selected bond distances (Å) and angles (°): C35-C36 = 1.219(9), C55-C56 = 1.186(9), C35-Pt1 = 1.985(7), C55-Pt1 = 2.013(7), P1-Pt1 = 2.3010(18), P2-Pt1 = 2.3287(17), D1-Fe1 = 1.643, D2-Fe1 = 1.642; C36-C35-Pt1 = 174.1(6), C56-C55-Pt1 = 177.5(6), C35-Pt1-C55 = 90.4(3), C35-Pt1-P1 = 86.92(18), C55-Pt1-P1 = 177.06(19), C35-Pt1-P2 = 175.86(19), C55-Pt1-P2 = 85.60(19), P1-Pt1-P2 = 97.11(6), D1-Fe1-D2 = 177.5 (D1, D2 = denote the centroids of C_5H_4 at Fe1). (D1, D2 = denote the centroids of C_5H_4 at Fe1).

Complex **13** crystallizes in the monoclinic space group P_2/n and possesses a crystallographically imposed inversion symmetry with the inversion center in the middle between the platinum atoms Pt1 and Pt1A as well as Pt2 and Pt2A, respectively (Figure G3). The 32-membered metallamacrocycle consists of four platinum atoms at the corners of which two are coordinated by a chelating dppf and two monodentate PPh_2 moieties. The geometry around Pt1 and Pt2 is distorted square planar with C35-Pt1-C74, P1-Pt1-P2, P4-Pt2-P3 and Cl1-Pt2-Cl2 angles of 85.7(7), 98.24(17), 96.44(18) and 86.20(18)° (Pt1: r. m. s. deviation 0.0250 Å, highest deviation from planarity observed for Pt1 with 0.0484 Å; Pt2: r. m. s. deviation 0.1528 Å, highest deviation from planarity observed for P3 with 0.1890 Å). The Pt-C≡C-C_{Ph} units are essentially linear with Pt1-C35-C36, C35-C36-C37, Pt1-C74-C73 and C74-C73-C70 angles of 177.4(17), 169(2), 173(2) and 174.1(18)° and C≡C distances of 1.23(2) and 1.14(2) Å, respectively. The ferrocenyl moieties exhibit a staggered conformation (-35.8°) with the cyclopentadienyl rings virtually parallel oriented to each other (4.6°). In addition, complex **13** exhibits intra-molecular T-shaped, parallel-displaced and sandwich π,π interactions (Figure G3). [G12b] The Pt1···Pt1A and Pt2···Pt2A distances are 11.9350(4) and 16.2205(4) Å, respectively, allowing, for example, the emplacement of small molecules or group 11 cations as already described for [{Pt-μ-C≡C-C≡C)(dppe)}$_4$] (dppe = bis(diphenylphosphine)ethane). [G6b] Complex **13** crystallizes with eleven molecules of chloroform as packing solvent of which four are located in the cavity. However, the molecule

is not planar due to the geometry of the phosphorus atoms P3 and P4. All other structural parameters are similar to those of related molecules, *e. g.* [Pt(dppf)(C≡CPh)$_2$] [G12a] and [{Pt-μ-C≡C-C≡C)(dcpe)}$_4$]$^{4+}$ [G7] (dcpe = bis(dicyclohexylphoshino)ethane).

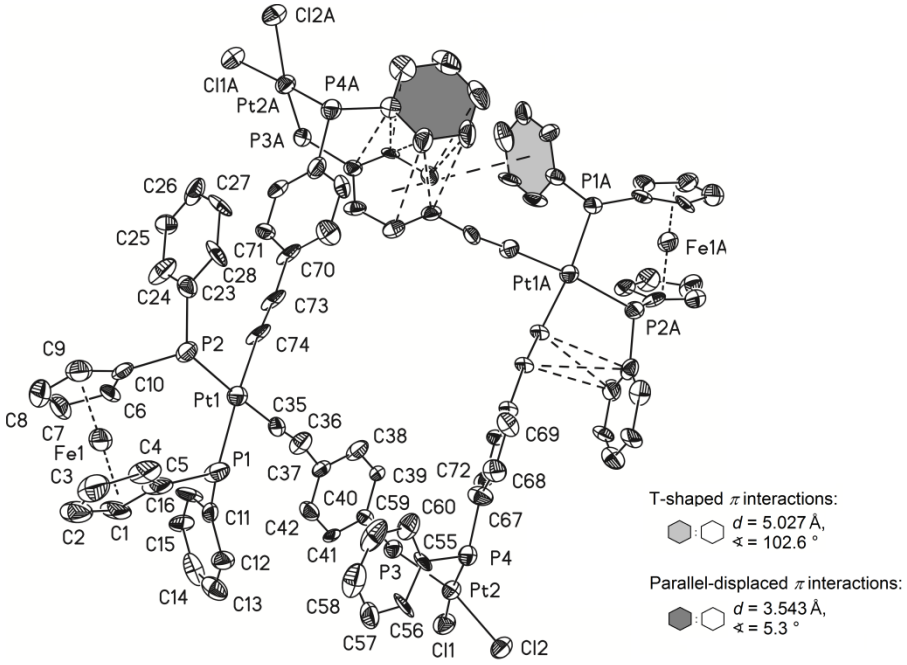

Figure G3. ORTEP diagram (50 % probability level) of the molecular structure of **13** with the atom-numbering scheme. All hydrogen atoms, the packing solvents chloroform and the phosphorus bonded phenyl groups, which are not involved in π,π interactions have been omitted for clarity. The T-shaped π,π interaction between the aromatic C_6 rings C11-C16 and C37-C42 are indicated with a dashed line, at which *d* refers to the geometrical centroid to geometrical centroid distance and ∢ to the inter-planar angle. Further parallel-displaced and sandwich π,π interactions are indicated by dashed lines. Carbon-carbon distances are in the range between 3.024 (C23-C74) to 3.502 Å (C42-C58). Selected bond distances (Å) and angles (°): C35-C36 = 1.23(2), C73-C74 = 1.14(2), C35-Pt1 = 1.996(17), C74-Pt1 = 2.030(18), P1-Pt1 = 2.290(5), P2-Pt1 = 2.311(4), P3-Pt2 = 2.264(5), P4-Pt2 = 2.239(6), Cl1-Pt2 = 2.352(5), Cl2-Pt2 = 2.361(5), D1-Fe1 = 1.646, D2-Fe1 = 1.641; C36-C35-Pt1 = 177.4(17), C73-C74-Pt1 = 173(2), C35-Pt1-C74 = 85.7(7), C35-Pt1-P1 = 87.0(5), C74-Pt1-P1 = 172.4(5), C35-Pt1-P2 = 173.2(6), C74-Pt1-P2 = 88.9(5), P1-Pt1-P2 = 98.24(17), P4-Pt2-P3 = 96.44(18), P4-Pt2-Cl1 = 173.00(17), P3-Pt2-Cl1 = 88.51(19), P4-Pt2-Cl2 = 90.01(18), P3-Pt2-Cl2 = 166.45(18), Cl1-Pt2-Cl2 = 86.20(18), D1-Fe1-D2 = 178.9. (D1, D2 = denote the centroids of C_5H_4 at Fe1; symmetry generated atoms are indicated by the suffix A; symmetry codes: -x+1/2, y, -z+3/2; -x+3/2, y, -z+3/2)

2.2 Suzuki-Miyaura *C,C* Cross-Coupling Reactions

Initially, mono- (**4a**, **4b**) and diphosphino imidazoles (**6a** – **f**) were applied in the palladium-mediated Suzuki-Miyaura coupling of 2-bromo toluene with phenylboronic acid *in situ* generating the catalytic active species by applying mixtures of [Pd(OAc)$_2$] and **4a**, **4b** or **6a** – **f** in the ratio of 1:2 (Reaction G2) to test the new phosphino imidazoles. The catalytic reactions were carried out in 1,4-dioxane-water mixtures of ratio 2:1 in presence of potassium carbonate as base at 100 °C using 0.5 mol% of the mono-phosphine and 0.25 mol% of the appropriate di-phosphine, respectively, and 0.25 mol% of the palladium source. Acetyl ferrocene as standard was added to the appropriate reaction solution to determine the rate of conversion by ^{1}H NMR spectroscopy. The obtained conversions equal ^{1}H NMR spectroscopic yields and are based on the respective aryl halides.

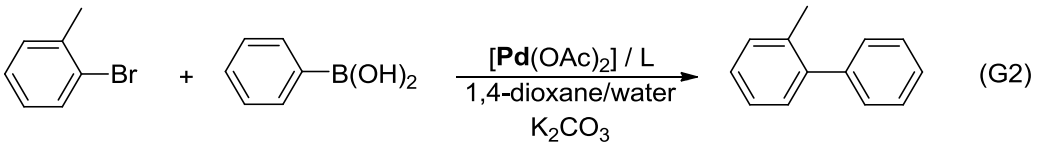

As it can be seen from Figure G4, all compounds are catalytically active, whereas phosphines **6a** – **f** are more productive and active than **4a** and **4b**. Due to the more electron-rich and bulky cyclohexyl groups, mono-phosphine **4b** is more active than **4a** featuring phenyl groups. While **4b** produces 2-methyl biphenyl in a yield of 59 %, with **4a** only a conversion of 18 % is achieved (Figure G4) which is comparable with the performance of triphenylphosphino ligands in *C,C* couplings. [G13]

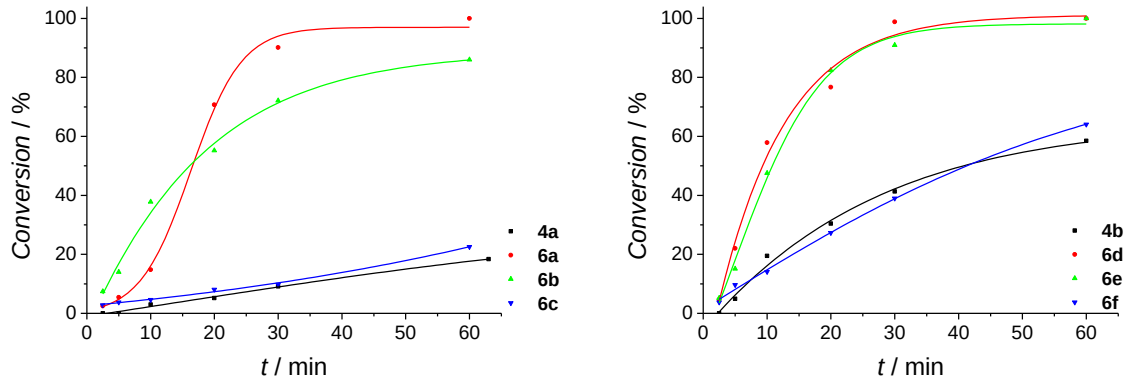

Figure G4. Kinetic investigation of **4a** and **6a** – **c** (left) and **4b** and **6d** – **f** (right) in the Suzuki-Miyaura *C,C* cross-coupling of 2-bromo toluene with phenylboronic acid to give 2-methyl biphenyl (0.5 mol% mono- or 0.25 mol% di-phosphine, 0.25 mol% [Pd(OAc)$_2$], conversion time 0 – 60 min); reaction condition based on reference [G14].

In general, the phenyl (**6a**, **b**) and cyclohexyl (**6d**, **e**) functionalized diphosphino systems show a significantly higher activity and productivity than the furyl (**6c**, **f**) derivatives. Furthermore, from Figure G4 it can be seen that the performance of the catalysts **6c** and **6f** with furyl substituted diphosphines is similar to the catalytic behavior of the complexes carrying mono-phosphines **4a** and **4b**. This result can be explained by the weak σ donating ability of the furyl phosphino group and hence has a smaller influence on the active species. Also, the catalysts based on diphosphines **6a**, **b**, **d** and **e** show a similar catalytic behavior reaching 86 – 100 % conversion after 1 h (Figure G4). Apparently, the second phosphino group featuring stronger σ donors has a positive effect on the stabilization of the active species visible by the higher activity. However, the difference of the nature of the phosphino group (phenyl *vs*. cyclohexyl) is less decisive. Nevertheless, the catalytic systems featuring phosphines **6d** and **6e** show a somewhat higher activity compared to **6a** and **6b**.

We also investigated the catalytic behavior of our systems *i*) in the coupling of *non*-activated 4-chloro toluene with phenylboronic acid using 0.01 mol% [$Pd(OAc)_2$] and *ii*) in the synthesis of sterically hindered biaryls at 50 °C. To achieve comparable results with literature-known systems, we changed to *non*-aqueous reaction conditions including potassium phosphate as base and toluene as solvent.

From Table G2 it can be seen, that the Suzuki-Miyaura coupling of 4-chlorotoluene with phenylboronic acid to give 4-methyl biphenyl using phosphines **4a** and **6b** in combination with [$Pd(OAc)_2$] gave 64 and 89 % conversion, respectively (Table G2, entries 1, 2). Especially diphosphine **6d** (TON: 8900) shows similar results, when compared to the *tert*-butyl substituted mono-phosphino benzimidazole (TON: 8600) reported by Beller *et al*. [G2b] and the cyclohexyl phosphino imidazole (TON: 8800) reported earlier by our group[G2f] (Table G2, entries 3, 4). In summary, excellent results were obtained, when compared to the cyclohexyl-functionalized phosphino imidazole (TON: 1500 – 6600) by Beller and co-workers[G2b] (Table G2, entry 5). Compared to the biphenyl ligand by Buchwald [G15a,d] a significantly higher conversion can be achieved when using 0.01 mol% palladium (Table G2, entry 6). [G15b] However, compared to trialkyl phosphino based catalysts by Fu [G15c] and Beller [G15b] (Table G2, entries 8, 9) catalyst system **6d**/[$Pd(OAc_2$] showed under the equivalent reaction conditions a somewhat lower conversion. [G15b]

The preparation of sterically hindered biaryls still represents a challenge in organic synthesis, especially under mild reaction conditions. Therefore, we investigated the coupling of *ortho*-substituted aryl bromides with phenylboronic acid in the presence of potassium

phosphate as base and [$Pd_2(dba)_3$] (dba = dibenzylideneacetone) as palladium source at 50 °C. From Table G2 it can be seen that the coupling of aryl bromides with one or two *ortho*-substituents proves successful with a palladium loading of only 0.05 mol% (Table G2, entries 6 – 9). Even the coupling of the sterically demanding 1,3,5-tri-*iso*-propyl-2-bromo benzene achieves good results with a conversion of 78 % (Table G2, entry 9). When compared to other catalytic systems suitable for these reactions, *e. g.* Fe(η^5-(1-(4-*t*-Bu-C_6H_4)-2-P(*o*-Tol)$_2C_5H_3$))(η^5-C_5H_5)/[$Pd_2(dba)_3$], [G15] only half the amount of palladium is required to achieve quantitative conversion. Compared to the established biphenyl-based catalyst by Buchwald [G15d] (Table G2, entry 14) longer reaction times and higher catalyst loadings are required, however, the catalytic reaction proceeds at considerably lower temperature (50 °C *vs.* 100 °C). Nevertheless, compared to previously reported 1-(4-I-C_6H_4)-2-PCy_2-4,5-Me_2-1*H*-C_3N_2/[$Pd_2(dba)_3$] [G2f] no enhanced catalytic activity, based on the second phosphino group, could be observed.

Table G2. Suzuki-Miyaura coupling of 4-chloro toluene and sterically hindered aryl bromides.

Entry	Aryl Halide	Ligand	Catalyst / mol%	Conversion / %	TON
1	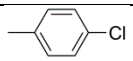	**4a**	0.01	64 [a)]	6400
2		**6d**	0.01	89 [a)]	8900
3		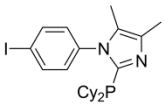	0.01	88 [a,b)]	8800
4		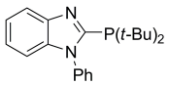	0.01	86 [a,c)]	8600
5		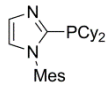	0.01	15 – 66 [a,c)]	1500 – 6600
6		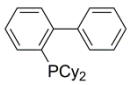	0.05	99 [d,e)]	1860
7			0.01	47 [d,e)]	4700
8		P(*t*-Bu)$_3$	0.01	92 [d,e)]	9200
9		P(*n*-Bu)Ad_2	0.01	94 [d,e)]	9400
10	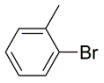	**6d**	0.05	100 [f)]	2000
11	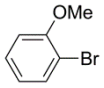	**6d**	0.05	100 [f)]	2000
12	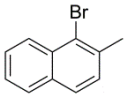	**6d**	0.05	100 [f)]	2000

13	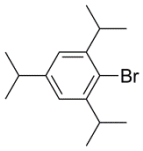	**6d**	0.05	78 [f)]	1560
14	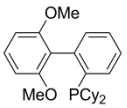		0.01	97 [f,g)]	9700

a) Reaction conditions [G2b]: 4-chloro toluene (3.0 mmol, 1.0 eq), phenylboronic acid (4.5 mmol, 1.5 eq), K_3PO_4 (6.0 mmol, 3.0 eq), toluene (6 mL), [$Pd(OAc)_2$]/phosphine (0.01 mol% [Pd], 0.1 mol% mono- or 0.05 mol% diphosphine, 100 °C, 20 h; b) Ligand from reference [G2f]; c) Ligand from reference [G2b]; d) Ligands from reference [G15b]; e) Reaction conditions [G15b]: 4-chloro toluene (3.0 mmol, 1.0 eq), phenylboronic acid (4.5 mmol, 1.5 eq), K_3PO_4 (6.0 mmol, 3.0 eq), toluene (6 mL), [Pd]:P = 1:2, 100 °C, 20 h; f) Reaction conditions [G16]: aryl halide (1.0 mmol, 1.0 eq), phenylboronic acid (1.5 mmol, 1.5 eq), K_3PO_4 (3.0 mmol, 3.0 eq), toluene (2 mL), [$Pd_2(dba)_3$]/phosphine (0.05 mol% [Pd], 0.1 mol% phosphine, 50 °C, 24 h; g) Ligand from reference [G15d], T = 100 °C, 16 h.

3 Conclusions

It has been shown that mono- and bidentate phosphino imidazoles of type 1-(4-PR_2-C_6H_4)-4,5-Me_2-1*H*-C_3HN_2 (R = Ph, Cy) and 1-(4-PR_2-C_6H_4)-2-PR'_2-4,5-Me_2-1*H*-C_3N_2 (R = Ph: R' = Ph, Cy, Fur; R = Cy: R' = Ph, Cy, Fur) can be prepared in straightforward synthesis methodologies including Stelzer coupling [G9] and selective metallation at position 2 of the imidazole unit. The diphosphino imidazoles gave upon reaction with [$PdCl_2(SEt_2)_2$] palladamacrocycles of composition [Pd(1-(4-PR_2-C_6H_4)-2-PR'_2-4,5-Me_2-1*H*-C_3N_2)Cl_2]$_2$ which, unfortunately, are insoluble in common organic solvents. However, it appeared that the derivative with R = Ph and R' = Fur allowed the growth of single crystals suitable for X-ray structure analysis using the synthesis-cum-diffusion strategy. The structure of the latter molecule in the solid state shows the formation of a neutral 18-membered metal-organic cycle with two *trans*-configurated palladium centers. A further metallamacrocycle was accessible by treatment of [Pt(dppf)(C≡C-C_6H_4-4-PPh_2)$_2$] (dppf = 1,1'-bis(diphenylphosphino)-ferrocene) with [$Pt(SEt_2)_2Cl_2$] to give [(Pt(dppf)(C≡C-C_6H_4-4-PPh_2))$PtCl_2$]$_2$ by molecular recognition. X-ray Structure determination of this compound confirmed the molecular square architecture composed of Pt(dppf) and $PtCl_2$ corner units and 4-Ph_2P-C_6H_4-C≡C linkers. Similar compounds are known and well described. [G6a,f,i,G7] Furthermore, the mono- and bidentate phosphino imidazoles 1-(4-PR_2-C_6H_4)-4,5-Me_2-1*H*-C_3N_2 and 1-(4-PR_2-C_6H_4)-2-PR'_2-4,5-Me_2-1*H*-C_3N_2, respectively, were used in the palladium-catalyzed Suzuki-Miyaura cross-coupling of, for example, 2-bromotoluene with phenylboronic acid using potassium carbonate as base under aqueous reaction conditions. [G14] All *in situ* generated phosphino

palladium species showed moderate to high catalytic activity toward the formation of 2-methyl biphenyl. It was found that the mono-phosphine species were less active and productive than the catalysts based on diphosphines. The diphosphino systems featuring phenyl and cyclohexyl groups show a similar activity and productivity with conversions of 86 – 100 %, the ones carrying weak σ donating furyl groups show productivities comparable to the appropriate mono-phosphines. However, best results were obtained with diphosphines carrying strong σ donating substituents. In addition, we investigated the catalytic behavior of 1-(4-PPh_2-C_6H_4)-4,5-Me_2-1*H*-C_3HN_2 and 1-(4-PCy_2-C_6H_4)-2-PPh_2-4,5-Me_2-1*H*-C_3N_2 in the Suzuki-Miyaura coupling of 4-chloro toluene with phenylboronic acid under *non*-aqueous conditions [G2b] at which especially the diphosphine showed excellent productivities with TONs up to 8900. Furthermore, 1-(4-PCy_2-C_6H_4)-2-PPh_2-4,5-Me_2-1*H*-C_3N_2 was applied in the synthesis of *ortho*-substituted biaryls with a palladium loading of 0.05 mol% at 50 °C under *non*-aqueous conditions [G16] showing good to excellent conversions. Compared to other catalytically active species [G2b,f,15,16] reported by Fu, Beller and Buchwald our systems show at least the same or higher productivities but at lower catalyst loadings and lower reaction temperatures.

4 Experimental Section

4.1 General Procedures

All reactions were carried out under an atmosphere of argon using standard Schlenk techniques. Tetrahydrofuran and dichloromethane were purified by distillation from sodium/benzophenone and calcium hydride, respectively; di-*i*-propylamine was purified by distillation from potassium hydroxide. Column chromatography was carried out using Silica with a particle size of 40 – 60 μm (230 – 400 mesh (ASTM), Becker) or alumina with a particle size of 90 μm (standard, Merck KGaA). For filtrations Celite (purified and annealed, Erg. B.6, Riedel de Haen) was used.

NMR spectra were recorded at 298 K with a Bruker Avance 250 or a Bruker Avance III 500 spectrometer. The ^{1}H NMR spectra were recorded at 250.13 or 500.3 MHz, the $^{13}C\{^1H\}$ at 125.7 MHz and the $^{31}P\{^1H\}$ NMR spectra at 101.249 or 202.5 MHz, respectively. Chemical shifts are reported in δ units (parts per million) downfield from tetramethylsilane with the solvent as reference signal (^{1}H NMR: standard internal $CDCl_3$, δ 7.26; $^{13}C\{^1H\}$ NMR: standard internal $CDCl_3$, δ 77.16; $^{31}P\{^1H\}$ NMR: standard external rel. 85 % H_3PO_4, δ 0.0; $P(OMe)_3$, δ 139.0). High resolution mass spectra were recorded with a Bruker Daltonik

micrOTOF-QII spectrometer (ESI-TOF). ESI-TOF mass spectra of **11** were recorded on an Applied Biosystems spectrometer. Elemental analyses were carried out with a Thermo FlashAE 1112 series instrument. Melting points of analytical pure samples were determined by a Gallenkamp MFB 595 010 M melting point apparatus. FT IR spectra were recorded with a Thermo Nicolet IR 200 spectrometer using KBr pellets or NaCl plates. All starting materials were obtained from commercial suppliers and used without further purification. 1-(4-Iodophenyl)-4,5-dimethyl-1*H*-imidazole (**2**), [G2f] borane-diphenylphosphine **3a**, [G17] borane-dicyclohexylphosphine **3b**, [G18] chlorophosphines **5b** [G19] and **5c**, [G19] $[PdCl_2(SEt_2)_2]$, [G20] $[PtCl_2(dppf)]$ [G21] and $HC{\equiv}C\text{-}C_6H_4\text{-}4\text{-}PPh_2$ [G22] were prepared according to published procedures.

4.2 Synthesis of 1-(4-(diphenylphosphino)phenyl)-4,5-dimethyl-1*H*-imidazole (4a)

Compound **2** (0.50 g, 1.68 mmol), potassium acetate (0.20 g, 2.04 mmol, 1.2 equiv) and $[Pd(OAc)_2]$ (3.8 mg, 1.0 mol%) were dissolved in dimethylacetamide (40 mL). Then borane-diphenylphosphine **3a** (0.34 g, 1.70 mmol) was added in a single portion and the reaction mixture was stirred for 3 h at 130 °C. After cooling to ambient temperature, the reaction mixture was poured into water (50 mL) and extracted twice with dichloromethane (20 mL). The dichloromethane solution was then washed five times with water (30 mL) and dried over magnesium sulfate. The solvent was removed in membrane-pump vacuum and the crude product was purified by column chromatography on Silica (column size: 3.5 × 15 cm) using a mixture of *n*-hexane-diethyl ether (ratio 1:1, *v*:*v*). Phosphine **4a** could be isolated as a colorless solid. Yield: 0.31 g (0.87 mmol, 52 % based on **2**). Anal. Calcd. for $C_{23}H_{21}N_2P$ (356.40 g/mol): C, 77.51; H, 6.23; N, 7.86. Found: C, 77.13; H, 5.97; N, 7.80. Mp.: 162 °C. IR (KBr, $\tilde{\nu}$/cm^{-1}): 1432 (m, P-C), 1500 (s, N=C), 1574/1594 (m, C=C), 2912/2942/2998 (w, C-H), 3052 (w, =C-H). ^{1}H NMR (500.30 MHz, $CDCl_3$, δ): 2.11 (s, 3 H, CH_3), 2.22 (s, 3 H, CH_3), 7.22 (dpt, $^3J_{HH}$ = 8.4 Hz, $^4J_{HH}$ = 1.9 Hz, $^4J_{HP}$ = 1.1 Hz, 2 H, H^m/C$_6H_4$), 7.33 – 7.40 (m, 12 H, H^{o,m,p}/C$_6H_5$+H^o/C$_6H_4$), 7.50 (s, 1 H, H^2/C$_3H$N$_2$). ^{13}C{^{1}H} NMR (125.81 MHz, $CDCl_3$, δ): 8.9 (s, *C*H$_3$), 12.1 (s, *C*H$_3$), 122.6 (s, C^{4,5}/*C*$_3$HN$_2$), 125.0 (d, $^3J_{CP}$ = 6.7 Hz, C^m/*C*$_6$H$_4$), 128.4 (d, $^3J_{CP}$ = 7.1 Hz, C^m/*C*$_6$H$_5$), 128.8 (s, C^p/*C*$_6$H$_5$), 133.5 (d, $^2J_{CP}$ = 19.8 Hz, C^o/*C*$_6$H$_5$), 133.8 (s, C^{4,5}/*C*$_3$HN$_2$), 134.3 (d, $^2J_{CP}$ = 19.6 Hz, C^o/*C*$_6$H$_4$), 134.7 (s, C^p/*C*$_6$H$_4$), 136.2 (d, $^1J_{CP}$ = 10.9 Hz, C^i/*C*$_6$H$_5$), 136.6 (s, C^2/*C*$_3$HN$_2$), 137.8 (d, $^1J_{CP}$ = 13.7 Hz, C^i/*C*$_6$H$_4$). ^{31}P{^{1}H} NMR (202.5 MHz, $CDCl_3$, δ): -5.9 (s). HRMS (ESI-TOF) $C_{23}H_{21}N_2P$ $[M+H]^+$ *m/z*: calcd.: 357.1515,

found: 357.1516; $[M+Na]^+$ *m/z*: calcd.: 379.1335, found: 379.1325; $[2M+Na]^+$ *m/z*: calcd.: 735.2777, found: 735.2815.

4.3 Synthesis of 1-(4-(dicyclohexylphosphino)phenyl)-4,5-dimethyl-1*H*-imidazole (4b)

To a dimethylacetamide solution (40 mL) containing **2** (0.50 g, 1.68 mmol), potassium acetate (0.20 g, 2.04 mmol, 1.2 equiv) and $[Pd(OAc)_2]$ (3.8 mg, 1.0 mol%), borane-dicyclohexylphosphine **3b** (0.36 g, 1.70 mmol) was added in a single portion and the reaction mixture was stirred for 3 h at 130 °C. Afterward, the reaction mixture was cooled to ambient temperature, poured into water (50 mL) and extracted twice with dichloromethane (20 mL). The dichloromethane solution was washed five times with water (30 mL) and dried over magnesium sulfate. After removal of all volatiles in membrane-pump vacuum, the crude product was purified by column chromatography on Silica (column size: 3.5 × 15 cm) using a mixture of *n*-hexane-diethyl ether (ratio 1:1, *v*:*v*). Phosphine **4b** could be isolated as a colorless solid. Yield: 0.30 g (0.81 mmol, 48 % based on **2**). Anal. Calcd. for $C_{23}H_{33}N_2P$ (368.50 g/mol): C, 74.97; H, 9.03; N, 7.60. Found: C, 74.46; H, 8.87; N, 7.52. Mp.: 97 °C. IR (NaCl, $\tilde{\upsilon}$/cm^{-1}): 1447 (m, P-C), 1499 (s, N=C), 1595 (m, C=C), 2849/2932 (s, C-H), 3032 (w, =C-H). ^{1}H NMR (500.30 MHz, $CDCl_3$, δ): 0.99 – 1.07 (m, 2 H, C_6H_{11}), 1.11 – 1.39 (m, 8 H, C_6H_{11}), 1.63 – 1.73 (m, 6 H, C_6H_{11}), 1.79 – 1.82 (m, 2 H, C_6H_{11}), 1.88 – 1.98 (m, 4 H, C_6H_{11}), 2.14 (s, 3 H, CH_3), 2.24 (s, 3 H, CH_3), 7.25 (dpt, $^3J_{HH}$ = 8.2 Hz, 2 H, H^m/C_6H_4), 7.52 (s, 1 H, H^2/C_3HN$_2$), 7.57 -7.50 (m, 2 H, H^o/C_6H_4). ^{13}C{^{1}H} NMR (125.81 MHz, $CDCl_3$, δ): 9.3 (s, CH$_3$), 12.8 (s, CH$_3$), 26.4 (s, C_6H$_{11}$), 26.9 (d, J_{CP} = 7.4 Hz, C_6H$_{11}$), 27.2 (d, J_{CP} = 12.5 Hz, C_6H$_{11}$), 28.8 (d, J_{CP} = 7.2 Hz, C_6H$_{11}$), 30.0 (d, J_{CP} = 16.2 Hz, C_6H$_{11}$), 32.6 (d, J_{CP} = 12.1 Hz, C_6H$_{11}$), 122.7 (s, C^{4,5}/C_3HN$_2$), 124.6 (d, $^3J_{CP}$ = 7.3 Hz, C^m/C_6H$_4$), 134.7 (s, C^{4,5}/C_3HN$_2$), 135.1 (d, $^2J_{CP}$ = 20.5 Hz, C^o/C_6H$_4$), 135.1 (s, C^p/C_6H$_4$), 135.6 (d, $^1J_{CP}$ = 19.6 Hz, C^i/C_6H$_4$), 137.3 (s, C^2/C_3HN$_2$). ^{31}P{^{1}H} NMR (202.5 MHz, $CDCl_3$, δ): 2.7 (s). HRMS (ESI-TOF) $C_{23}H_{33}N_2P$ $[M]^+$ *m/z*: calcd.: 369.2454, found: 369.2447.

4.4 General Synthesis Procedure for Phosphines 6a – f

To 0.30 g of **4a** (0.84 mmol) or **4b** (0.81 mmol) dissolved in in dry diethyl ether (40 mL) one equivalent of a 2.0 M solution of lithium di-*i*-propylamide was added dropwise at -30 °C. After warming the reaction mixture to ambient temperature, it was again cooled to -30 °C and one equivalent of the appropriate pure chlorophosphine (**5a** – **c**) was added dropwise. The

reaction mixture was stirred at ambient temperature for 2 h and the solvent was removed in vacuum. The crude product was purified by column chromatography on Silica and dried in vacuum.

4.4.1 Synthesis of 1-(4-(diphenylphosphino)phenyl)-2-(diphenylphosphino)-4,5-dimethyl-1*H*-imidazole (6a)

Following the synthesis procedure described above, **4a** (0.30 g, 0.84 mmol) was reacted with lithium di-*i*-propylamide (0.42 mL, 0.84 mmol) and the chlorophosphine **5a** (0.15 mL, 0.84 mmol). The resulting residue was purified by column chromatography on Silica (column size: 15 × 2.5 cm) using a mixture of *n*-hexane-diethyl ether (ratio 1:1, *v*:*v*) as eluent. Phosphine **6a** was obtained as a colorless solid. Yield: 0.26 g (0.48 mmol, 57 % based on **4a**). Anal. Calcd. for $C_{35}H_{30}N_2P_2$ (540.57 g/mol): C, 77.76; H, 5.59; N, 5.18. Found: C, 77.91; H, 5.76; N, 5.10. Mp.: 96 °C. IR (KBr, $\tilde{\upsilon}$/cm^{-1}): 1435 (s, P-C), 1479/1498 (m, N=C), 1593 (w, C=C), 2863/2918/2966 (w, C-H), 3051 (w, =C-H). ^{1}H NMR (500.30 MHz, $CDCl_3$, δ): 1.97 (s, 3 H, CH_3), 2.25 (s, 3 H, CH_3), 7.00 (dpt, $^3J_{HH}$ = 8.4 Hz, 2 H, H^m/C$_6H_4$), 7.25 – 7.28 (m, 8 H, C$_6H_5$), 7.32 – 7.38 (m, 10 H, H^o/C$_6H_4$ + C$_6H_5$), 7.40 – 7.45 (m, 4 H, C$_6H_5$). ^{13}C{^{1}H} NMR (125.81 MHz, $CDCl_3$, δ): 9.7 (s, *C*H$_3$), 13.2 (s, *C*H$_3$), 127.1 (s, C^{4,5}/C_3N_2), 128.2 (dd, $^3J_{CP}$ = 3.1 Hz, $^4J_{CP}$ = 2.8 Hz, C^m/C_6H_4), 128.4 (d, $^3J_{CP}$ = 7.4 Hz, C^m/C_6H_5), 128.7 (d, $^3J_{CP}$ = 4.2 Hz, C^m/C_6H_5), 128.8 (s, C^p/C_6H_5), 129.2 (s, C^p/C_6H_5), 133.8 (d, $^2J_{CP}$ = 20.7 Hz, C^o/C_6H_5), 134.0 (d, $^2J_{CP}$ = 19.7 Hz, C^o/C_6H_5), 134.1 (d, $^2J_{CP}$ = 19.6 Hz, C^o/C_6H_4), 136.3 (d, $^3J_{CP}$ = 6.2 Hz, C^{4,5}/C_3N_2), 136.5 (d, $^3J_{CP}$ = 1.9 Hz, C^p/C_6H_4), 136.7 (d, $^1J_{CP}$ = 10.9 Hz, C^i/C_6H_5), 137.5 (d, $^1J_{CP}$ = 1.9 Hz, C^i/C_6H_5), 138.5 (d, $^1J_{CP}$ = 13.0 Hz, C^i/C_6H_4), 144.0 (d, $^1J_{CP}$ = 1.9 Hz, C^2/C_3N_2). ^{31}P{^{1}H} NMR (202.5 MHz, $CDCl_3$, δ): -27.9 (s, {C_3N_2*P*Ph$_2$}), -5.5 (s, {C_6H_4*P*Ph$_2$}). HRMS (ESI-TOF) $C_{35}H_{30}N_2P_2$ [M+H]$^+$ *m/z*: calcd.: 541.1957, found: 541.1915.

4.4.2 Synthesis of 1-(4-(diphenylphosphino)phenyl)-2-(dicyclohexylphosphino)-4,5-dimethyl-1*H*-imidazole (6b)

As described earlier, **4a** (0.30 g, 0.84 mmol) was reacted with lithium di-*i*-propylamide (0.42 mL, 0.84 mmol) and chlorodicyclohexylphosphine **5b** (0.19 mL, 0.86 mmol). The crude product was purified by column chromatography on Silica (column size: 15 × 2.5 cm) using a mixture of *n*-hexane-diethyl ether (ratio 2:1, *v*:*v*) as eluent. Phosphine **6b** was obtained as a colorless solid. Yield: 0.23 g (0.42 mmol, 50 % based on **4a**). Anal. Calcd. for $C_{35}H_{42}N_2P_2$

(552.67 g/mol): C, 76.06; H, 7.66; N, 5.07. Found: C, 75.79; H, 7.73; N, 4.93. Mp.: 144 °C. IR (KBr, $\tilde{\upsilon}$/cm^{-1}): 1433 (m, P-C), 1497 (m, N=C), 1591 (w, C=C), 2847/2918 (s, C-H), 3046/3068 (w, =C-H). ^{1}H NMR (500.30 MHz, $CDCl_3$, δ): 0.94 – 1.22 (m, 10 H, C_6H_{11}), 1.52 – 1.65 (m, 10 H, C_6H_{11}), 1.87 (s, 3 H, CH_3), 2.01 – 2.06 (m, 2 H, H^1/C_6H_{11}), 2.18 (s, 3 H, CH_3), 7.02 (dpt, $^{3}J_{HH}$ = 8.2 Hz, 2 H, H^m/C_6H_4), 7.25 – 7.29 (m, 12 H, H^o/C_6H_4 + C_6H_5). ^{13}C{^{1}H} NMR (125.81 MHz, $CDCl_3$, δ): 9.7 (s, CH_3), 13.0 (s, CH_3), 26.4 (s, C_6H_{11}), 26.8 (d, J_{CP} = 8.3 Hz, C_6H_{11}), 26.9 (d, J_{CP} = 11.8 Hz, C_6H_{11}), 29.4 (d, J_{CP} = 7.8 Hz, C_6H_{11}), 30.4 (d, J_{CP} = 17.0 Hz, C_6H_{11}), 34.3 (d, $^{1}J_{CP}$ = 8.0 Hz, C^1/C_6H_{11}), 125.3 (s, $C^{4,5}/C_3N_2$), 128.6 (d, $^{3}J_{CP}$ = 7.2 Hz, C^m/C_6H_5), 128.7 (dd, $^{3}J_{CP}$ = 3.1 Hz, $^{4}J_{CP}$ = 2.8 Hz, C^m/C_6H_4), 129.0 (s, C^p/C_6H_5), 133.7 (d, $^{1}J_{CP}$ = 19.5 Hz, C^o/C_6H_4), 133.9 (d, $^{1}J_{CP}$ = 19.9 Hz, C^o/C_6H_5), 135.5 (s, $C^{4,5}/C_3N_2$), 136.6 (d, $^{1}J_{CP}$ = 11.2 Hz, C^i/C_6H_5), 137.9 (d, $^{1}J_{CP}$ = 13.1 Hz, C^i/C_6H_4), 138.0 (d, $^{3}J_{CP}$ = 1.8 Hz, C^p/C_6H_4), 144.7 (d, $^{1}J_{CP}$ = 13.9 Hz, C^2/C_3N_2). ^{31}P{^{1}H} NMR (202.5 MHz, $CDCl_3$, δ): -23.1 (s, $P(C_6H_{11})_2$), -5.6 (s, PPh_2). HRMS (ESI-TOF) $C_{35}H_{42}N_2P_2$ $[M+H]^+$ *m/z*: calcd.: 553.2825, found: 553.2896.

4.4.3 Synthesis of 1-(4-(diphenylphosphino)phenyl)-2-(di-2-furylphosphino)-4,5-dimethyl-1*H*-imidazole (6c)

Molecule **4a** (0.30 g, 0.84 mmol) was reacted with lithium di-*i*-propylamide (0.42 mL, 0.84 mmol) and chlorodi-2-furylphosphine **5c** (0.17 g, 0.85 mmol) as described above. The residue was purified by column chromatography on Silica (column size: 15 × 2.5 cm) using diethyl ether as eluent. Molecule **6c** was obtained as a colorless solid. Yield: 0.28 g (0.54 mmol, 64 % based on **4a**). Anal. Calcd. for $C_{31}H_{26}N_2O_2P_2$ (520.50 g/mol): C, 71.53; H, 5.03; N, 5.38. Found: C, 71.87; H, 5.19; N, 5.18. Mp.: 65 °C. IR (NaCl, $\tilde{\upsilon}$/cm^{-1}): 1006 (s, C-O), 1434 (m, P-C), 1497 (m, N=C), 1592 (w, C=C), 2919 (w, C-H), 3051 (w, =C-H). ^{1}H NMR (500.30 MHz, $CDCl_3$, δ): 1.94 (s, 3 H, CH_3), 2.25 (s, 3 H, CH_3), 6.31 (dt $^{4}J_{HP}$ = 1.6 Hz, $^{3}J_{HH}$ = 3.3 Hz, $^{3}J_{HH}$ = 1.8 Hz, 2 H, H^4/C_4H_3O), 6.71 (m, 2 H, H^3/C_4H_3O), 7.02 (m, $^{3}J_{HH}$ = 8.4 Hz, 2 H, H^m/C_6H_4), 7.30 (m, 2 H, H^o/C_6H_4), 7.35 – 7.40 (m, 10 H, C_6H_5), 7.59 (m, 2 H, H^5/C_4H_3O). ^{13}C{^{1}H} NMR (125.81 MHz, $CDCl_3$, δ): 9.5 (s, CH_3), 13.2 (s, CH_3), 110.9 (d, $^{3}J_{CP}$ = 6.6 Hz, C^4/C_4H_3O), 121.9 (d, $^{2}J_{CP}$ = 26.7 Hz, C^3/C_4H_3O), 127.5 (s, C^4/C_3N_2), 127.7 (dd, $^{3}J_{CP}$ = 2.5 Hz, $^{4}J_{CP}$ = 2.3 Hz, C^m/C_6H_4), 128.7 (d, $^{3}J_{CP}$ = 7.1 Hz, C^m/C_6H_5), 129.2 Hz, (s, C^p/C_6H_5), 133.9 (d, $^{2}J_{CP}$ = 19.9 Hz, C^o/C_6H_4), 134.1 (d, $^{2}J_{CP}$ = 19.8 Hz, C^o/C_6H_5), 136.4 (d, $^{4}J_{CP}$ = 3.8 Hz, C^5/C_3N_2), 136.6 (d, $^{1}J_{CP}$ = 10.9 Hz, C^i/C_6H_5), 137.2 (d, $^{3}J_{CP}$ = 1.2 Hz, C^p/C_6H_4), 138.7 (d, $^{1}J_{CP}$ = 13.6 Hz, C^i/C_6H_4), 140.4 (d, $^{1}J_{CP}$ = 12.5 Hz, C^2/C_3N_2), 147.6 (d, $^{4}J_{CP}$ = 2.6 Hz, C^5/C_4H_3O),

148.2 (d, $^{1}J_{CP}$ = 4.3 Hz, C^{2}/C_4H_3O). $^{31}P\{^{1}H\}$ NMR (202.5 MHz, $CDCl_3$, δ): -71.7 (s, $P(^{c}C_4H_3O)_2$), -5.6 (s, PPh$_2$). HRMS (ESI-TOF) $C_{31}H_{26}N_2O_2P_2$ $[M+H]^+$ *m/z*: calcd.: 521.1542, found: 521.1542.

4.4.4 Synthesis of 1-(4-(dicyclohexylphosphino)phenyl)-2-(diphenylphosphino)-4,5-dimethyl-1*H*-imidazole (6d)

Based on the general procedure described earlier, **4b** (0.30 g, 0.81 mmol) was reacted with lithium di-*i*-propylamide (0.41 mL, 0.82 mmol) and chlorodiphenylphosphine **5a** (0.15 mL, 0.84 mmol). The residue was purified by column chromatography on Silica (column size: 15 × 2.5 cm) using a mixture of *n*-hexane-diethyl ether (ratio 2:1, *v*:*v*) as eluent. The product **6d** was obtained as a colorless solid. Yield: 0.27 g (0.49 mmol, 60 % based on **4b**). Anal. Calcd. for $C_{35}H_{42}N_2P_2$ (552.67 g/mol): C, 76.06; H, 7.66; N, 5.07. Found: C, 75.86; H, 7.62; N, 4.94. Mp.: 155 °C. IR (NaCl, $\tilde{\upsilon}$/cm^{-1}): 1435 (m, P-C), 1497 (m, N=C), 1592 (w, C=C), 2849/2922 (s, C-H), 3051 (w, =C-H). ^{1}H NMR (500.30 MHz, $CDCl_3$, δ): 1.08 – 1.18 (m, 2 H, C_6H_{11}), 1.23 – 1.37 (m, 8 H, C_6H_{11}), 1.59 – 1.73 (m, 6 H, C_6H_{11}), 1.79 – 1.92 (m, 6 H, C_6H_{11}), 1.97 (s, 3 H, CH_3), 2.25 (s, 3 H, CH_3), 6.98 (m, $^{3}J_{HH}$ = 7.9 Hz, 2 H, H^{m}/C_6H_4), 7.24 – 7.78 (m, 6 H, H^{m,p}/C_6H_5), 7.38 -7.43 (m, 6 H, H^{o}/C_6H_4 + H^{o}/C_6H_5). $^{13}C\{^{1}H\}$ NMR (125.81 MHz, $CDCl_3$, δ): 9.7 (s, CH$_3$), 13.2 (s, CH$_3$), 26.6 (s, C_6H_{11}), 27.1 (d, J_{CP} = 7.3 Hz, C_6H_{11}), 27.4 (d, J_{CP} = 12.4 Hz, C_6H_{11}), 29.0 (d, J_{CP} = 7.1 Hz, C_6H_{11}), 30.1 (d, J_{CP} = 16.1 Hz, C_6H_{11}), 32.7 (d, J_{CP} = 12.2 Hz, C_6H_{11}), 127.2 (s, C^{4}/C_3N_2), 127.7 (dd, $^{3}J_{CP}$ = 2.8 Hz, $^{4}J_{CP}$ = 2.7 Hz, C^{m}/C_6H_4), 128.4 (d, $^{3}J_{CP}$ = 7.6 Hz, C^{m}/C_6H_5), 128.8 (s, C^{p}/C_6H_5), 134.0 (d, $^{2}J_{CP}$ = 20.7 Hz, C^{o}/C_6H_5), 135.1 (d, $^{1}J_{CP}$ = 19.3 Hz, C^{i}/C_6H_5), 135.9 (d, $^{2}J_{CP}$ = 20.1 Hz, C^{o}/C_6H_4), 136.2 (d, $^{1}J_{CP}$ = 6.6 Hz, C^{i}/C_6H_4), 136.2 (d, $^{3}J_{CP}$ = 2.0 Hz, C^{5}/C_3N_2), 137.5 (d, $^{3}J_{CP}$ = 1.8 Hz, C^{p}/C_6H_4), 144.2 (d, $^{1}J_{CP}$ = 2.8 Hz, C^{2}/C_3N_2). $^{31}P\{^{1}H\}$ NMR (202.5 MHz, $CDCl_3$, δ): -26.7 (s, PPh$_2$), 2.6 (s, $P(C_6H_{11})_2$). HRMS (ESI-TOF) $C_{35}H_{42}N_2P_2$ $[M+H]^+$ *m/z*: calcd.: 553.2883, found: 553.2896.

4.4.5 Synthesis of 1-(4-(dicyclohexylphosphino)phenyl)-2-(dicyclohexylphosphino)-4,5-di-methyl-1*H*-imidazole (6e)

Using the general synthesis methodology described above, **4b** (0.30 g, 0.81 mmol) was reacted with lithium di-*i*-propylamide (0.41 mL, 0.82 mmol) and chlorodicyclohexylphosphine **5b** (0.18 mL, 0.82 mmol). The crude product was purified by column chromatography on Silica (column size: 15 × 2.5 cm) using a mixture of *n*-hexane-diethyl ether (ratio 3:1, *v*:*v*) as eluent. Phosphine **6e** was obtained as a colorless solid. Yield:

0.21 g (0.37 mmol, 46 % based on **4b**). Anal. Calcd. for $C_{35}H_{54}N_2P_2$ (564.76 g/mol): C, 74.43; H, 9.64; N, 4.96. Found: C, 74.68; H, 9.37; N, 4.72. Mp.: 66 °C. IR (NaCl, $\tilde{\upsilon}$/cm^{-1}): 1446 (m, P-C), 1497 (m, N=C), 1594 (w, C=C), 2849/2923 (s, C-H), 3031 (w, =C-H). ^{1}H NMR (500.30 MHz, $CDCl_3$, δ): 0.95 – 1.04 (m, 4 H, C_6H_{11}), 1.08 – 1.35 (m, 16 H, C_6H_{11}), 1.60 – 1.70 (m, 16 H, C_6H_{11}), 1.77 – 1.79 (m, 2 H, C_6H_{11}), 1.83 – 1.91 (m, 4 H, C_6H_{11}), 1.94 (s, 3 H, CH_3), 2.04 – 2.09 (m, 2 H, C_6H_{11}), 2.25 (s, 3 H, CH_3), 7.09 (m, $^3J_{HH}$ = 8.0 Hz, 2 H, H^m/C_6H_4), 7.51 (m, $^3J_{HH}$ = 8.2 Hz, $^3J_{HP}$ = 1.9 Hz, 2 H, H^o/C_6H_4). ^{13}C{^{1}H} NMR (125.81 MHz, $CDCl_3$, δ): 9.8 (s, CH_3), 13.1 (s, CH_3), 26.5 (s, C_6H_{11}), 26.5 (s, C_6H_{11}), 26.9 (d, J_{CP} = 8.7 Hz, C_6H_{11}), 27.0 (d, J_{CP} = 12.1 Hz, C_6H_{11}), 27.1 (d, J_{CP} = 6.8 Hz, C_6H_{11}), 27.3 (d, J_{CP} = 12.4 Hz, C_6H_{11}), 29.0 (d, J_{CP} = 7.4 Hz, C_6H_{11}), 29.7 (d, J_{CP} = 8.1 Hz, C_6H_{11}), 30.1 (d, J_{CP} = 16.2 Hz, C_6H_{11}), 30.5 (d, J_{CP} = 16.9 Hz, C_6H_{11}), 32.7 (d, J_{CP} = 12.3 Hz, C_6H_{11}), 34.2 (d, J_{CP} = 8.4 Hz, C_6H_{11}), 125.8 (s, C^4/C_3N_2), 128.2 (dd, $^3J_{CP}$ = 7.2 Hz, $^4J_{CP}$ = 4.3 Hz, C^m/C_6H_4), 135.1 (d, $^2J_{CP}$ = 19.3 Hz, C^o/C_6H_4), 135.3 (d, $^1J_{CP}$ = 21.0 Hz, C^i/C_6H_4), 135.4 (s, C^5/C_3N_2), 138.1 (s, C^p/C_6H_4), 144.8 (d, $^1J_{CP}$ = 15.4 Hz, C^2/C_3N_2). ^{31}P{^{1}H} NMR (202.5 MHz, $CDCl_3$, δ): -22.2 (s, {$C_3N_2P(C_6H_{11})_2$}), 2.6 (s, {$C_6H_4P(C_6H_{11})_2$}). HRMS (ESI-TOF) $C_{35}H_{54}N_2P_2$ $[M+H]^+$ *m/z*: calcd.: 565.3871, found: 565.3835.

4.4.6 Synthesis of 1-(4-(dicyclohexylphosphino)phenyl)-2-(di-2-furylphosphino)-4,5-dimethyl-1*H*-imidazole (6f)

Molecule **4b** (0.30 g, 0.81 mmol) was reacted with lithium di-*i*-propylamide (0.41 mL, 0.82 mmol) and chlorodi-2-furylphosphine **5c** (0.17 g, 0.85 mmol) as described earlier. The crude product was purified by column chromatography on Silica (column size: 15 × 2.5 cm) using diethyl ether as eluent. Phosphine **6f** was obtained as a colorless solid. Yield: 0.28 g (0.53 mmol, 65 % based on **4b**). Anal. Calcd. for $C_{31}H_{38}N_2O_2P_2$ (532.59 g/mol): C, 69.91; H, 7.19; N, 5.26. Found: C, 70.15; H, 7.54; N, 4.95. Mp.: 115 °C. IR (KBr, $\tilde{\upsilon}$/cm^{-1}): 1007 (m, C-O), 1449 (m, P-C), 1500/1507 (w, N=C), 1598 (w, C=C), 2854/2930 (s, C-H), 3122/3143 (w, =C-H). ^{1}H NMR (500.30 MHz, $CDCl_3$, δ): 0.93 – 1.05 (m, 2 H, C_6H_{11}), 1.07 – 1.17 (m, 4 H, C_6H_{11}), 1.20 – 1.37 (m, 6 H, C_6H_{11}), 1.57 – 1.72 (m, 6 H, C_6H_{11}), 1.78 – 1.87 (m, 4 H, C_6H_{11}), 1.90 (s, 3 H, CH_3), 2.21 (s, 3 H, CH_3), 6.28 (dt $^4J_{HP}$ = 1.6 Hz, $^3J_{HH}$ = 3.3 Hz, $^3J_{HH}$ = 1.9 Hz, 2 H, H^4/C_4H_3O), 6.63 (m, 2 H, H^3/C_4H_3O), 6.98 (m, $^3J_{HH}$ = 8.0 Hz, 2 H, H^m/C_6H_4), 7.42 (m, $^3J_{HH}$ = 8.2 Hz, $^3J_{HP}$ = 1.9 Hz, 2 H, H^o/C_6H_4), 7.58 (m, 2 H, H^5/C_4H_3O). ^{13}C{^{1}H} NMR (125.81 MHz, $CDCl_3$, δ): 9.6 (s, CH_3), 13.2 (CH_3), 26.0 (s, C_6H_{11}), 27.1 (d, J_{CP} = 7.5 Hz, C_6H_{11}), 27.3 (d, J_{CP} = 12.2 Hz, C_6H_{11}), 28.9 (d, J_{CP} = 7.2 Hz, C_6H_{11}), 30.1 (d, J_{CP} = 16.2 Hz, C_6H_{11}), 32.6

(d, J_{CP} = 11.9 Hz, C_6H_{11}), 110.9 (d, $^3J_{CP}$ = 7.0 Hz, C^4/C_4H_3O), 122.1 (d, $^2J_{CP}$ = 27.5 Hz, C^3/C_4H_3O), 127.4 (s, C^4/C_3N_2), 127.6 (dd, $^3J_{CP}$ = 2.5 Hz, $^4J_{CP}$ = 2.3 Hz, C^m/C_6H_4), 135.3 (d, $^2J_{CP}$ = 19.6 Hz, C^o/C_6H_4), 136.6 (d, $^3J_{CP}$ = 4.2 Hz, C^5/C_3N_2), 137.2 (d, $^1J_{CP}$ = 14.9 Hz, C^i/C_6H_4), 139.7 (d, $^3J_{CP}$ = 1.7 Hz, C^p/C_6H_4), 140.4 (d, $^1J_{CP}$ = 11.7 Hz, C^2/C_3N_2), 147.7 (d, $^4J_{CP}$ = 2.5 Hz, C^5/C_4H_3O), 147.9 (d, $^1J_{CP}$ = 5.3 Hz, C^2/C_4H_3O). $^{31}P\{^1H\}$ NMR (202.5 MHz, $CDCl_3$, δ): -70.8 (s, $P(^cC_4H_3O)_2$), 2.6 (s, $P(C_6H_{11})_2$). HRMS (ESI-TOF) $C_{31}H_{38}N_2O_2P_2$ $[M]^+$ *m/z*: calcd.: 549.2440, found: 549.2430.

4.5 Synthesis of [Pd(1-(4-PPh$_2$-C$_6$H$_4$)-2-PFur$_2$-4,5-Me$_2$-1*H*-C$_3$N$_2$)Cl$_2$]$_2$ (8)

Complex **8** was synthesized *via* the synthesis-cum-diffusion strategy to ensure the formation of crystals suitable for single crystal X-ray structure analysis. Therefore, a solution of **6c** (20 mg, 0.04 mmol) in dichloromethane (2 mL) was inserted into a test tube and covered with a layer of dichloromethane (10 mL). Afterward, a solution of $[PdCl_2(SEt_2)_2]$ (**7**, 13 mg, 0.04 mmol) in dichloromethane (2 mL) was added slowly. The resulting yellow crystals were subjected to single crystal X-ray structure analysis.

4.6 Synthesis of [Pt(dppf)(C≡C-C$_6$H$_4$-4-PPh$_2$)$_2$] (11)

$[PtCl_2(dppf)]$ (**9**, 0.7 g, 0.87 mmol) was dissolved in a dichloromethane-di-*i*-propylamine mixture (100 mL, ratio 7:3, *v*:*v*), followed by the addition of [CuI] (5.7 mg, 0.1 mmol) and 2 equiv of **10** (0.5 g, 1.75 mmol). The reaction mixture was stirred for 6 h at ambient temperature and filtered through a pad of alumina. Afterward, the amount of solvent was reduced in vacuum to 5 mL and *n*-hexane (20 mL) was added. The supernatant layer was removed, the precipitate dissolved in dichloromethane (10 mL) and chromatographed on alumina (column size: 5 × 1.5 cm) using dichloromethane as eluent. After drying in vacuum, product **11** was obtained as a yellow solid. Yield: 495 mg (0.45 mmol, 51 % based on **9**). Anal. Calcd. for $C_{74}H_{56}FeP_4Pt$ (1320.05 g/mol): C, 67.33; H, 4.28. Found: C, 67.40; H, 4.50. Mp.: 183 °C (dec.). IR (KBr, $\tilde{\upsilon}$/cm^{-1}): 2114 (m, C≡C), 1432/1477 (s, P-C). ^1H NMR (250.13 MHz, $CDCl_3$, δ): 4.18 (dpt, $^3J_{HH}$ = 1.8 Hz, $^3J_{HP}$ = 1.7 Hz, 4 H, H^α/C_5H_4), 4.31 (pt, $^3J_{HH}$ = 1.8 Hz, 4 H, C_5H_4), 6.76 (dpt, $^3J_{HH}$ = 8.3 Hz, $^4J_{HH}$ = 1.7 Hz, $^3J_{HP}$ = 1.5 Hz, 4 H, H^m/C_6H_4), 6.91 – 6.95 (m, 4 H, H^p/C_6H_5), 7.20 – 7.24 (m, 8 H, $H^{o,m}/C_6H_5$), 7.28 – 7.30 (m, 20 H, $H^{o,m,p}/C_6H_5$), 7.35 – 7.38 (m, 4 H, H^o/C_6H_4), 7.80 – 7.84 (m, 8 H, $H^{o,m}/C_6H_5$). $^{13}C\{^1H\}$ NMR (125.7 MHz, $CDCl_3$, δ): 72.9 (pt, $^2J_{PC}$ = 3.3 Hz, C^β/C_5H_4), 75.7 (pt, $^2J_{PC}$ = 5.0 Hz, C^α/C_5H_4), 77.7 ($C^i/C_5H_4^{*)}$), 104.9 (d, $^2J_{CP}$ = 20.5 Hz, *C*≡C-P), 110.1 (d, $^1J_{CP}$ = 34.8 Hz, C≡*C*-P), 128.0 (pt,

$^{3}J_{CP}$ = 5.3 Hz, C^{m}/C_6H_5(dppf)), 128.5 (d, $^{3}J_{CP}$ = 6.6 Hz, C^{m}/C_6H_5), 128.6 (s, C^{p}/C_6H_5), 128.9 (s, C^{p}/C_6H_4), 130.6 (s, C^{p}/C_6H_5(dppf)), 131.6 (d, $^{3}J_{CP}$ = 7.4 Hz, C^{m}/C_6H_4), 132.7 (d, $^{2}J_{CP}$ = 19.9 Hz, C^{o}/C_6H_5(dppf)), 132.8 (pt, $^{1}J_{CP}$ = 8.9 Hz, C^{i}/C_6H_5(dppf)), 133.4 (d, $^{1}J_{CP}$ = 5.1 Hz, C^{i}/C_6H_4), 133.8 (d, $^{2}J_{CP}$ = 19.5 Hz, C^{o}/C_6H_4), 135.0 (pt, $^{2}J_{CP}$ = 5.6 Hz, C^{o}/C_6H_5(dppf)), 137.9 (d, $^{1}J_{CP}$ = 10.8 Hz, C^{i}/C_6H_5). ^{31}P{^{1}H} NMR (101.249 MHz, $CDCl_3$, δ): 6.6 (P(C_6H_5)$_2$), 13.5 ($^{1}J_{31P\text{-}195Pt}$ = 2374 Hz, dppf). MS (ESI-TOF) $C_{74}H_{56}FeP_4Pt$ [M+H]$^{+}$ *m/z*: calcd.: 1320.24, found: 1320.6(45). *) Signal concealed by $CDCl_3$.

4.7 Synthesis of [Pt(dppf)(C≡C-C_6H_4-4-PPh_2)$_2$$PtCl_2$)]$_2$ (13)

To a solution of **11** (50 mg, 0.04 mmol) in dichloromethane (10 mL) [$PtCl_2(SEt_2)_2$] (**12**, 14.2 mg, 0.04 mmol) was added in a single portion and stirred for 1 h at ambient temperature. Afterward, the amount of solvent was reduced in vacuum to 2 mL and the formed complex was precipitated by addition of *n*-pentane (10 mL). The supernatant layer was decanted and the yellow residue was washed twice with *n*-pentane (5 mL). After drying in vacuum, **13** was obtained as a yellow solid. Yield: 45 mg (0.014 mmol, 70 % based on **12**). Anal. Calcd. for $C_{148}H_{112}Cl_4Fe_2P_8Pt_4$ × ¼ CH_2Cl_2 (3172.08 g/mol): C, 55.48; H, 3.54. Found: C, 55.20; H, 3.50. Mp.: >247 °C (dec.). IR (KBr, $\tilde{\upsilon}$/cm^{-1}): 2114 (s, C≡C), 1432/1481 (s, P-C). ^{1}H NMR (250.13 MHz, $CDCl_3$, δ): 4.19 (pt, $^{3}J_{HH}$ = 2.0 Hz, 8 H, C_5H_4), 4.35 (pt, $^{3}J_{HH}$ = 2.0 Hz, 8 H, C_5H_4), 5.30 (s, CH_2Cl_2) 6.40 – 6.57 (m, 8 H, H^{m}/C_6H_4), 6.90 – 7.01 (m, 8 H, H^{p}/C_6H_5), 7.09–7.40 (m, 64 H, C_6H_5 + H^{o}/C_6H_4). 7.80 – 7.84 (m, 16 H, H^{o,m}/C_6H_5). ^{31}P{^{1}H} NMR (202.5, $CDCl_3$, δ): 13.6 ($^{1}J_{31P\text{-}195Pt}$ = 3673.3 Hz, P(C_6H_5)$_2$), 14.7 ($^{1}J_{31P\text{-}195Pt}$ = 2380.1 Hz, dppf).

4.8 General Procedure for the Suzuki-Miyaura Reaction [G14]

2-Bromo toluene (500 mg, 2.92 mmol), phenylboronic acid (470 mg, 3.85 mmol, 1.3 equiv), potassium carbonate (1.21 g, 8.76 mmol, 3 equiv) and acetyl ferrocene (111 mg, 0.49 mmol) were dissolved in a 1,4-dioxane-water mixture (10 mL, ratio 2:1, *v*:*v*). After addition of 0.25 mol% of [$Pd(OAc)_2$] and 0.5 mol% of the mono-phosphine (**4**) or 0.25 mol% of the appropriate diphosphine (**6**), the reaction mixture was stirred for 1 h at 100 °C. Samples of 1 mL were taken after 2.5, 5, 10, 20, 30, and 60 min and filtered through a pad of Silica (column size: 6 × 2.5 cm) using diethyl ether as eluent. All volatiles were evaporated under reduced pressure and the conversions were determined by ^{1}H NMR spectroscopy.

4.9 General Procedure for the Suzuki-Miyaura Coupling of Aryl Chlorides [G2b]

4-Chloro toluene (379 mg, 3.0 mmol), phenylboronic acid (550 mg, 4.5 mmol, 1.5 equiv), potassium phosphate (1.27 g, 6.0 mmol, 3 equiv) and acetyl ferrocene (114 mg, 0.50 mmol) were dissolved in toluene (6 mL). After addition of 0.01 mol% [$Pd(OAc)_2$] and 0.1 mol% of the appropriate mono-phosphine **4a** or 0.05 mol% of the diphosphine **6d**, the reaction mixture was stirred for 20 h at 100 °C. Afterward, a sample of 2 mL was taken and filtered through a pad of Celite. After evaporation of all volatiles under reduced pressure, the conversions were determined by ^{1}H NMR spectroscopy.

4.10 General Procedure for the Synthesis of Sterically Hindered Biaryls [G16]

Phenylboronic acid (183 mg, 1.5 mmol, 1.5 equiv), potassium phosphate (0.64 g, 3.0 mmol, 3.0 equiv), acetyl ferrocene (114 mg, 0.50 mmol), 0.05 mol% [$Pd_2(dba)_3$] and 0.05 mol% of **6d** were dissolved in toluene (2 mL). Afterward, the appropriate aryl bromide (1.0 mmol, 1.0 equiv) was added in a single portion and the reaction mixture was stirred for 24 h at 50 °C. Thereafter, the reaction mixture was filtered through a pad of Celite and the solvent was removed in membrane-pump vacuum. The conversions were determined by ^{1}H NMR spectroscopy.

4.11 Crystal Structure Determination

The crystal and intensity collection data for **8**, **11** and **13** are summarized in Table G3. All data were collected on an Oxford Gemini S diffractometer with graphite monochromatized Mo K_α radiation (λ = 0.71073 Å) at 110 K (**8**) and graphite monochromatized Cu K_α radiation (λ = 1.54184 Å) at 100 K (**11**, **13**). The structures were solved by direct methods using *SHELXS-91* [G23] and refined by full-matrix least-square procedures on F^2 using *SHELXL-97* [G24]. All *non*-hydrogen atoms were refined anisotropically and a riding model was employed in the refinement of the hydrogen atom positions.

Table G3. Crystal and intensity collection data for **8**, **11** and **19**.

	8	**11**	**13**
Formula weight	1395.56	2759.37	4485.04
Chemical formula	$C_{62}H_{52}Cl_4N_4O_4P_4Pd_2$	$C_{149}H_{113}Cl_3Fe_2P_8Pt_2$	$C_{159}H_{123}Cl_{37}Fe_2P_8Pt_4$
Crystal system	monoclinic	monoclinic	monoclinic
Space group	$P2_1/c$	$C2/c$	$P\ 2/n$
a (Å)	13.4466(9)	40.6012(7)	23.4813(7)

b (Å)	19.1778(10)	10.5638(3)	10.8030(5)
c (Å)	12.0298(11)	28.5311(6)	34.7075(9)
α (°)			
β (°)	109.351(9)	98.492(2)	102.178(3)
γ (°)			
V (Å³)	2926.9(4)	12102.9(5)	8606.1(5)
ρ_{calc} (mg m^{-3})	1.583	1.514	1.731
F(000)	1408	5544	4380
Crystal dimensions (mm)	0.15 × 0.10 × 0.03	0.15 × 0.05 × 0.01	0.40 × 0.05 × 0.01
Z	2	4	2
Max. and min. transmission	1.00000, 0.80718	1.00000, 0.64472	1.00000, 0.50057
Absorption coefficient (λ, mm^{-1})	0.958	8.131	13.616
Scan range (°)	2.90 – 26.00	4.09 – 61.80	4.17 – 62.50
Index ranges	-16 ≤ h ≤ 16 -23 ≤ k ≤ 17 -14 ≤ l ≤ 12	-42 ≤ h ≤ 46 -11 ≤ k ≤ 9 -32 ≤ l ≤ 31	-26 ≤ h ≤ 26 -12 ≤ k ≤ 10 -39 ≤ l ≤ 39
Total reflections	18592	36140	26442
Unique reflections	5710	9392	11727
R_{int}	0.0805	0.0627	0.1010
Data/restraints/parameters	5710 / 0 / 361	9392 / 21 / 745	11727 / 520 / 874
Goodness-of-fit on F^2	0.675	0.884	0.943
R_1[a], wR_2[a] [I 2σ(I)]	0.0373, 0.0546	0.0409, 0.0890	0.0826, 0.1819
R_1[a], wR_2[a] (all data)	0.1059, 0.0590	0.0727, 0.0980	0.1617, 0.2224
Largest differences in peak and hole peak in final Fourier map (e Å^{-3})	0.830, -0.457	2.568, -1.389	4.745, -1.340

[a] $R_1 = [\Sigma(||F_o| - |F_c|)/\Sigma|F_o|]$; $wR_2 = [\Sigma(w(F_o^2 - F_c^2)^2)/\Sigma(wF_o^4)]^{1/2}$; $S = [\Sigma w(F_o^2 - F_c^2)^2]/(n - p)^{1/2}$. n = number of reflections, p = parameters used.

5 Acknowledgement

We are grateful to the Deutsche Forschungsgemeinschaft and the Fonds der Chemischen Industrie for generous financial support. Additionally, we would like to thank Sabrina Krauße and Martina Steinert for assistance in lab.

6 Supporting Information

CCDC 867788, CCDC 867790 and CCDC 867789 contain the supplementary crystallographic data for complexes **8**, **11** and **13**. These data can be obtained free of charge from the Cambridge Crystallographic Database *via* www.ccdc.cam.ac.uk/products/csd/request/.

7 References

[G1] a) H. Willms, W. Frank, C. Ganter *Organometallic*, **2009**, *28*, 3049; b) J. Li, J. Peng, Y. Bai, G. Zhang, G. Lai, X. Li *J. Organomet. Chem*. **2010**, *695*, 431; c) S. Sauerbrey, P. K. Majhi, J. Daniels, G. Schnakenburg, G. M. Brändle, K. Scherer, R. Streubel, *Inorg. Chem*. **2011**, *50*, 793; d) Q.-X. Wan, Y. Liu, Y.-Q. Cai *Catal. Lett.* **2009**, *127*, 386; e) D. J. Brauer, K. W. Kottsieper, C. Liek, O. Stelzer, H. Waffenschmidt, P. Wasserscheid *J. Organomet. Chem*. **2001**, *630*, 177; f) S. S. Moore, G. M. Whitesides *J. Org. Chem*. **1982**, *47*, 1489; g) V. Diez, G. Espino, F. A. Jalon, B. R. Manzano, M. Perez-Manrique *J. Organomet. Chem*. **2007**, *692*, 1482; h) M. A. Jalil, S. Fujinami, T. Honjo, H. Nishikawa *Polyhedron* **2001**, *20*, 1071.

[G2] For example: a) A. Dumrath, X.-F. Wu, H. Neumann, A. Spannenberg, R. Jackstell, M. Beller *Angew. Chem. Int. Ed*. **2010**, *49*, 8988; b) S. Harkal, F. Rataboul, A. Zapf, C. Fuhrmann, T. Riermeier, A. Monsees, M. Beller, *Adv. Synth. Catal*. **2004**, *346*, 1742; c) J. Sirieix, M. Oßberger, B. Betzemeier, P. Knochel *Synlett* **2000**, *11*, 1613; d) N. Debono, Y. Canac, C. Duhayon, R. Chauvin *Eur. J. Inorg. Chem*. **2008**, 2991; e) C. Torborg, J. Huang, T. Schulz, B. Schäffner, A. Zapf, A. Spannenberg, A. Börner, Beller M. *Chem. Eur. J*. **2009**, *15*, 1329; f) B. Milde, D. Schaarschmidt, T. Rüffer, H. Lang, *Dalton Trans*. **2012**, *41*, 5377.

[G3] a) S. Saleh, E. Fayad, M. Azouri, J.-C. Hierso, J. Andrieu, M. Picquet *Adv. Synth. Catal*. **2009**, *351*, 1621; b) C. S. Consorti, G. L. P. Aydos, G. Ebeling, J. Dupont *Org. Lett*. **2008**, *10*, 237; c) J. Andrieu, M. Azouri *Inorg. Chim. Acta* **2007**, *360*, 131; d) P. J. Dyson, T. J. Geldbach in *Catalysis by Metal Complexes-Metal Catalyzed Reactions in Ionic Liquids*, ed. James, B.; van Leeuwen, P. W. N. M.; Springer, Dordrecht, **2005**, Vol. 29; e) P. Wasserscheid, T. Welton, *Ionic Liquids in Synthesis*, 2nd Ed., *Wiley-VCH*, Weinheim, **2008**, Vol.1; f) J. Zhang, M. Dakovic, Z. Popovic, H. Wu, Y. Liu *Cat. Comm*. **2012**, *17*, 160.

[G4] a) T. L. Gilchrist *Heterocyclenchemie*, ed. H. Neunhoeffer, Weinheim, Wiley-CH, **1995**, p 300; b) T. Schulz, C. Torborg, B. Schäffner, J. Huang, A. Zapf, R. Kadyrov, A. Börner, M. Beller *Angew. Chem. Int. Ed*. **2009**, *48*, 918; c) M. R. Grimmett in *Science of Synthesis-Five membered Heteroarenes with two Nitrogen or Phosphorous Atoms*, Vol.-ed. Neier, R.; Thieme, Stuttgart-New York, **2002**, Vol. 12, p 325; d) J. Liu, J. Chen, J. Zhao, Y. Zhao, L. Li, H. Zhang *Synthesis* **2003**, *17*, 2661.

[G5] a) I. Abdellah, C. Lepetit, Y. Canac, C. Duhayon, R. Chauvin *Chem. Eur. J*. **2010**, *16*, 13095; b) N. V. Artemova, M. N. Chevykalova, Y. N. Luzikov, I. E. Nifant'ev, E. E. Nifant'ev *Tetrahedron* **2004**, *60*, 10365; c) T. Benincori, E. Brenna, F. Sannicolo, L. Trimarco, P. Antognazza, E. Cesarotti, F. Demartin, T. Pilati, G. Zotti *J. Organomet. Chem*. **1997**, *529*, 445; d) Y. Canac, N. Debono, L. Vendier, R. Chauvin *Inorg. Chem*. **2009**, *48*, 5562.

[G6] For example: a) T. Baumgartner, R. Reau *Chem. Rev*. **2006**, *106*, 4681; b) M. I. Bruce, K. Costuas, J.-F. Halet, B. C. Hall, P. J. Low, B. K. Nicholson, B. W. Skelton, A. H. White *J. Chem. Soc., Dalton Trans*. **2002**, 383; c) F. Würthner, C.-C. You, C. R. Saha-Möller *Chem. Soc. Rev*. **2004**, *33*, 133; d) M. Ferrer, A. Gutierrez, M. Mounir, O. Rossell, E. Ruiz, A. Rang, M. Engeser *Inorg. Chem*. **2007**, *46*, 3395; e) M. Janka, G. K. Anderson, N. P. Rath *Organometallics* **2004**, *23*, 4382; f) P. J. Stang, D. H. Cao *J. Am. Chem. Soc*. **1994**, *116*, 4981; g) M. Fujita, J. Yazaki, K. Ogura *J. Am. Chem. Soc*. **1990**, *112*, 5645; h) C. J. Jones *Soc. Chem. Rev*. **1998**, *27*, 289; i) J. A. Whiteford, P. J. Stang, S. D. Huang *Inorg. Chem*. **1998**, *37*, 5595.

[G7] S. M. ALQaisi, K. J. Galat, M. Chai, D. G. Ray, III., P. L. Rinaldi, C. A. Tessier, W. J. Youngs *J. Am. Chem. Soc*. **1998**, *120*, 12149.

[G8] a) Z. Weng, S. Teo, L. L. Koh, T. S. A. Hor *Organometallics* **2004**, *23*, 3603; b) G. Molander, J. P. Burke, P. J. Carroll *J. Org. Chem*. **2004**, *69*, 8062; c) K. K. Hii, M. Thornton-Pett *Organometallics* **1999**, 1887; d) H. Wang, R. Zhong, X.-Q. Guo, X.-Y. Feng, X.-F. Hou *Eur. J. Inorg. Chem*. **2010**, 174.

[G9] O. Herd, A. Heßler, M. Hingst, M. Tepper, O. Stelzer *J. Organomet. Chem*. **1996**, *522*, 69.

[G10] a) C. J. Brown *J. Chem. Soc*. **1953**, 3265; b) D. M. Kang, S. G. Kim, S. J. Lee, J. K. Park, K. M. Park, S. C. Shin *Bull. Korean Chem. Soc*. **2005**, *26*, 1390.

[G11] N. Kuhn, M. Göhner *Z. Anorg. Allg. Chem*. **1999**, *625*, 1415.

[G12] a) W.-Y. Wong, G.-L. Lu, K.-H. Choi *J. Organomet. Chem*. **2002**, *659*, 107; b) M. O. Sinnokrot, E. F. Valeev, C. D. Sherrill *J. Am. Chem. Soc*. **2002**, *124*, 10887.

[G13] A. Jakob, B. Milde, P. Ecorchard, C. Schreiner, H. Lang, *J. Organomet. Chem.* **2008**, *693*, 3821.

[G14] O. V. Gusev, T. A. Peganova, A. M. Kalsin, N. V. Vologdin, P. V. Petrovskii, K. A. Layssenko, A. V. Tsvetkov, I. P. Beletskaya *Organometallics* **2006**, *25*, 2750.

[G15] a) J. P. Wolfe, R. A. Singer, B. H. Yang, S. L. Buchwald *J. Am. Chem. Soc*. **1999**, *121*, 9550; b) A. Zapf, A. Ehrentraut, M. Beller *Angew. Chem. Int. Ed*. **2000**, *39*, 4153; c) A. F. Littke, C. Dai, G. C. Fu *J. Am. Chem. Soc*. **2000**, *122*, 4020; d) S. D. Walker, T. E. Barder, J. R. Martinelli, S. L. Buchwald *Angew. Chem. Int. Ed*. **2004**, *43*, 1871.

[G16] a) D. Schaarschmidt, H. Lang *Eur. J. Inorg. Chem*. **2010**, 4811; b) D. Schaarschmidt, H. Lang *ACS Catalysis* 2011, **1**, 411.

[G17] T. Imamoto, T. Oshiki, T. Onozawa, T. Kusumoto, K. Sato *J. Am. Chem. Soc*. **1990**, *112*, 5244.

[G18] H. Tomori, J. M. Fox, S. L. Buchwald *J. Org. Chem*. **2000**, *65*, 5334.

[G19] N. G. Andersen, R. McDonald, B. A. Keaya *Tetrahedron: Asymmetry* **2001**, ***12***, 263.

[G20] D. Zim, A. L. Monteiro, J. Dupont *Tetrahedron Lett*. **2000**, *41*, 8199.

[G21] M. D. Jansen, M. Herres, L. Zsolnai, A. L. Spek, D. M. Grove, H. Lang, G. van Koten *Inorg. Chem.* **1996**, *35*, 2476.

[G22] N. T. Lucas, M. P. Cifuentes, L. T. Nguyen, M. G. Humphrey *J. Cluster Sci*. **2001**, *12*, 201.

[G23] G. M. Sheldrick *Acta Cryst., Sect. A* **1990**, *46*, 467.

[G24] G. M. Sheldrick SHELXL-97, *Program for Crystal Structure Refinement*, University of Göttingen, **1997**.

H Summary

The emphasis of this work was the synthesis and characterization of novel phosphines and their application in homogeneous catalysis, especially in palladium-catalyzed Mizoroki-Heck and Suzuki-Miyaura cross-couplings as well as in the ruthenium-catalyzed synthesis of *β*-oxopropyl esters. The applied phosphines feature characteristic electronic and steric properties and can be divided into two main categories: *i*) (ethynyl)ferrocenyl-based phosphines and *ii*) (phosphino)imidazoles or (phosphino)imidazolium salts. The electronic properties could be easily and effectively quantified by measurement of the $^{1}J(^{31}P\text{-}^{77}Se)$ coupling constants of the appropriate seleno phosphines whereat the steric properties were determined by calculation of the Tolman cone angle based on X-ray data.

All newly synthesized compounds were fully characterized by elemental analysis, IR and NMR (^{1}H, $^{13}C\{^{1}H\}$, $^{31}P\{^{1}H\}$) spectroscopy. Furthermore, high-resolution ESI-TOF mass spectrometry and single crystal X-ray structure analysis were carried out. In addition, the electrochemical (CV, SW, LSV) behavior of all ferrocenyl-containing compounds and the spectro-electrochemical behavior (*in situ* UV-Vis/NIR, *in situ* IR spectroscopy) of selected palladium complexes were determined.

The results obtained in this work are divided into five Chapters:

Chapter C: Metallocenyl Phosphine Palladium Dichlorides: Synthesis, Electrochemistry and their Application in *C,C* Coupling Reactions

Chapter D: Fundamental Study of (Ferrocenylethynyl)phosphines: Correlation of Steric and Electronic Effects in *C,C* Cross-Coupling Reactions

Chapter E: (Ethynylferrocenyl)phosphine Ruthenium Complexes in Catalytic *β*-Oxopropyl Benzoate Formation

Chapter F: Phosphino Imidazoles and Imidazolium Salts for Suzuki-Miyaura *C,C* Coupling Reactions

Chapter G: Imidazole Phosphines: Synthesis, Reaction Chemistry and Their Use in Suzuki-Miyaura *C,C* Cross-Coupling Reactions

The content of each Chapter is discussed below. The labeling of the compounds consists of a character representing the Chapter and the compound number as firstly mentioned in the respective Chapter.

Chapter C

In this Chapter the synthesis, characterization and application of ferrocenyl phosphines PR_2Fc (**C3a**, R = Ph; [C7] **C3b**, R = *o*-Tol; **C3c**, R = Fur; **C3d**, R = *t*-Bu; [C7] **C3e**, R = Cy [C7]), their appropriate seleno phosphines (**C4a** – **e**) and palladium complexes (**C9a** – **e**) are described. A first systematic investigation of the catalytic activity and productivity in the Mizoroki-Heck and Suzuki-Miyaura *C,C* cross-coupling reactions of a series of ferrocenyl phosphine palladium complexes under similar reaction conditions is presented. Thereby, the electronic properties were modified by means of specific introduction of electron-donating and -withdrawing substituents at the phosphine to allow the prediction of the catalytic performance.

The novel phosphines, seleno phosphines and appropriate palladium complexes were prepared by a straightforward synthesis methodology as depicted in Scheme H1.

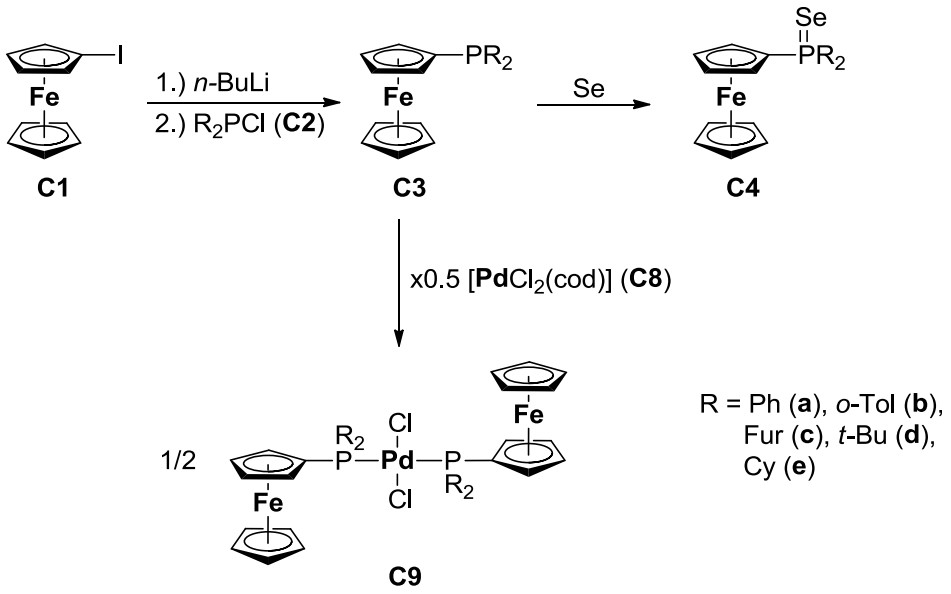

Scheme H1. Synthesis of ferrocenyl phosphines (**C3**), seleno phosphines (**C4**) and palladium complexes (**C9**).

The σ donor ability of the ferrocenyl phosphines (**C3a** – **e**) was easily determined by measuring the $^1J(^{31}P\text{-}^{77}Se)$ coupling constants of the appropriate seleno phosphines (**C4a** – **e**) indicating that the aliphatic phosphines **C4d** and **e** are more Lewis-basic than the aromatic phosphines. As expected, a linear correlation between the redox potentials of the aromatic ferrocenyl phosphine palladium complexes featuring aromatic groups with $^1J(^{31}P\text{-}^{77}Se)$ could be established representing another readily available tool for the determination of the Lewis-basicity.

The newly synthesized complexes were applied as catalysts in the Mizoroki-Heck (reaction of iodo benzene with *t*-butyl acrylate) and in the Suzuki-Miyaura cross-coupling (reaction of 2-bromo toluene and 4-chloro acetophenone with phenylboronic acid). The highest activity and productivity of the investigated palladium complexes in the Mizoroki-Heck reaction was observed for **9d**. This result is allegeable by the high σ donor capacity and bulkiness of the respective phosphine. For the Suzuki-Miyaura reaction it was found that the lower $^{1}J(^{31}P\text{-}^{77}Se)$ and hence the higher the Lewis-basicity of the phosphine, the higher is the catalytic activity. Compared to phosphapalladacyclic systems and *N*-heterocyclic carbene complexes, [C2,C4f,C7e] the ferrocenyl phosphine palladium complexes are less active but, compared to similar metallocenyl mono- and diphosphine palladium catalysts, they show higher activities under similar reaction conditions, no additional reductant is necessary and high regioselectivity is observed.

Chapter D

Within this Chapter, the preparation of a series of heterobimetallic complexes of type $[Pd(Cl)(\mu\text{-}Cl)(P(C{\equiv}CFc)R_2)]_2$ (D**6e**, R = *t*-Bu; D**6f**, R = Cy) and *cis/trans*-$[PdCl_2(P(C{\equiv}CFc)R_2)_2]$ (**D7a**, R = Ph; **D7b**, R = *o*-Tol; **D7c**, R = Mes; **D7d**, R = Fur, **D7e**, R = *t*-Bu; **D7f**, R = Cy) by reaction of $[PdCl_2(cod)]$ and $[PdCl_2(SEt_2)_2]$, respectively, with (ferrocenylethynyl)phosphines $P(C{\equiv}CFc)R_2$ (**D3a** – **f**) is presented (Scheme H2). Novel complexes **D6** and **D7** were applied successfully as catalysts in the Mizoroki-Heck reaction (treatment of iodo benzene with *t*-butyl acrylate) and Suzuki-Miyaura cross-coupling (reaction of 2-bromo toluene and 4-chloro acetophenone with phenylboronic acid). In continuation to the subject of Chapter C, an ethynyl spacer unit between the ferrocenyl moiety and the phosphorus atom was introduced to study the influence on the σ donor ability ($(Se)P(C{\equiv}CFc)R_2$ (**D4a** – **f**), $^{1}J(^{31}P\text{-}^{77}Se)$). In addition the Tolman cone angle (Θ) as a parameter for the steric hindrance was calculated [D17] from the obtained X-ray structural data of the respective palladium complexes (**D6e**, **f**, **D7a** – **c**).

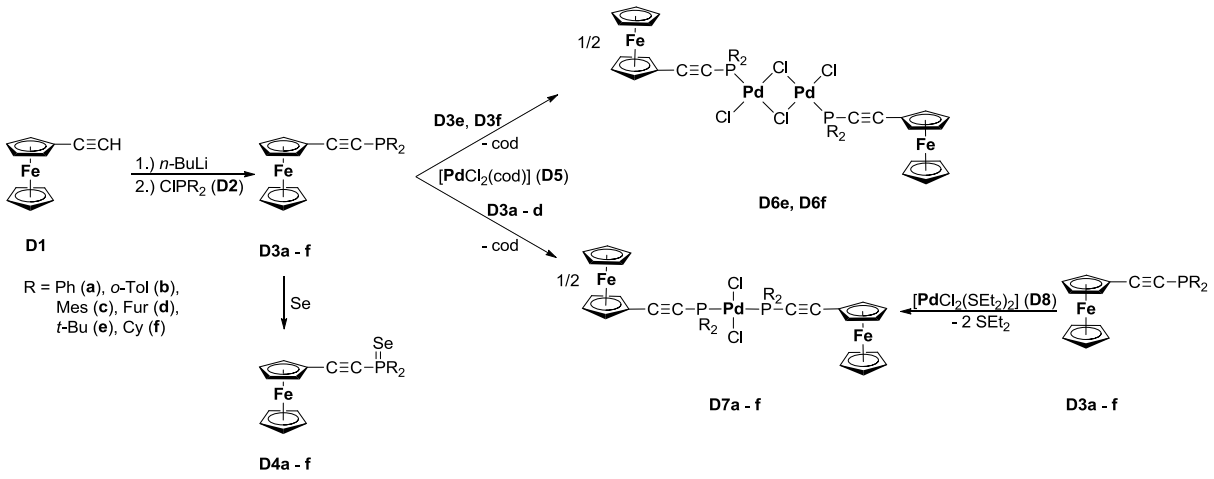

Scheme H2. Synthesis of the (ferrocenylethynyl)phosphines **D3a** – **f**, seleno phosphines **D4a** – **f** and palladium complexes **D6e**, **f** and **D7a** – **f**.

The most efficient catalysts in the Mizoroki-Heck reaction are **D7b** and **c** featuring electron-rich and bulky groups and complex **D7d** with its weak σ donor ability. Furthermore, all generated palladium catalysts are active in the Suzuki-Miyaura cross-coupling revealing the same trend as the ferrocenyl phosphino catalysts discussed in Chapter C: the lower the $^{1}J(^{31}\text{P-}^{77}\text{Se})$ coupling constant and hence the higher the Lewis-basicity of the phosphine, the higher is the catalyst activity. The dependency of the Suzuki-Miyaura reaction on steric properties is less prominent in comparison to the Mizoroki-Heck reaction due to the much higher reaction rates leading to a hindered appraisement of the catalysts. Compared to the ferrocenyl phosphino palladium dichlorides (Chapter C) the (ferrocenylethynyl)phosphino catalysts reported are marginally less active due to the electron-withdrawing character of the ethynyl spacer unit.

Electrochemical measurements of **7e** in the presence of $[(n\text{-Bu})_4\text{N}][\text{B}(\text{C}_6\text{F}_5)_4]$ as supporting electrolyte surprisingly revealed two redox processes with a peak separation of ΔE^0 = 0.165 V. *In situ* UV-Vis/NIR spectroscopy confirmed moderate electronic coupling between the (ferrocenylethynyl) units ,which occurs most probably "through space", and the complex can be classified as class II/III borderline system according to Robin and Day. [D29]

Chapter E

The synthesis, characterization and application of a series of (ethynylferrocenyl)phosphino ruthenium compounds of type $(\text{FcC}\equiv\text{C})\text{R}_2\text{P}(\text{RuCl}_2(\eta^6\text{-}p\text{-cymene}))$ (**E3a**, R = Ph; **E3b**, R = *o*-Tol; **E3c**, R = Fur; **E3d**, R = *t*-Bu; **E3e**, R = Cy) and $(\text{RuCl}_2(\eta^6\text{-}p\text{-cymene}))(\text{FcC}\equiv\text{C})\text{P-}$

$(C{\equiv}CPPh_2(RuCl_2(\eta^6\text{-}p\text{-cymene})))_2$ (**E10**) resulting from the addition of (ethynylferrocenyl)phosphines $P(C{\equiv}CFc)R_2$ (**E1a** – **e**) or $P(C{\equiv}CFc)(C{\equiv}CPPh_2)_2$ (**E9**) to $[RuCl_2(\eta^6\text{-}p\text{-cymene})]_2$ (**E2**) are described in this Chapter (Scheme H3).

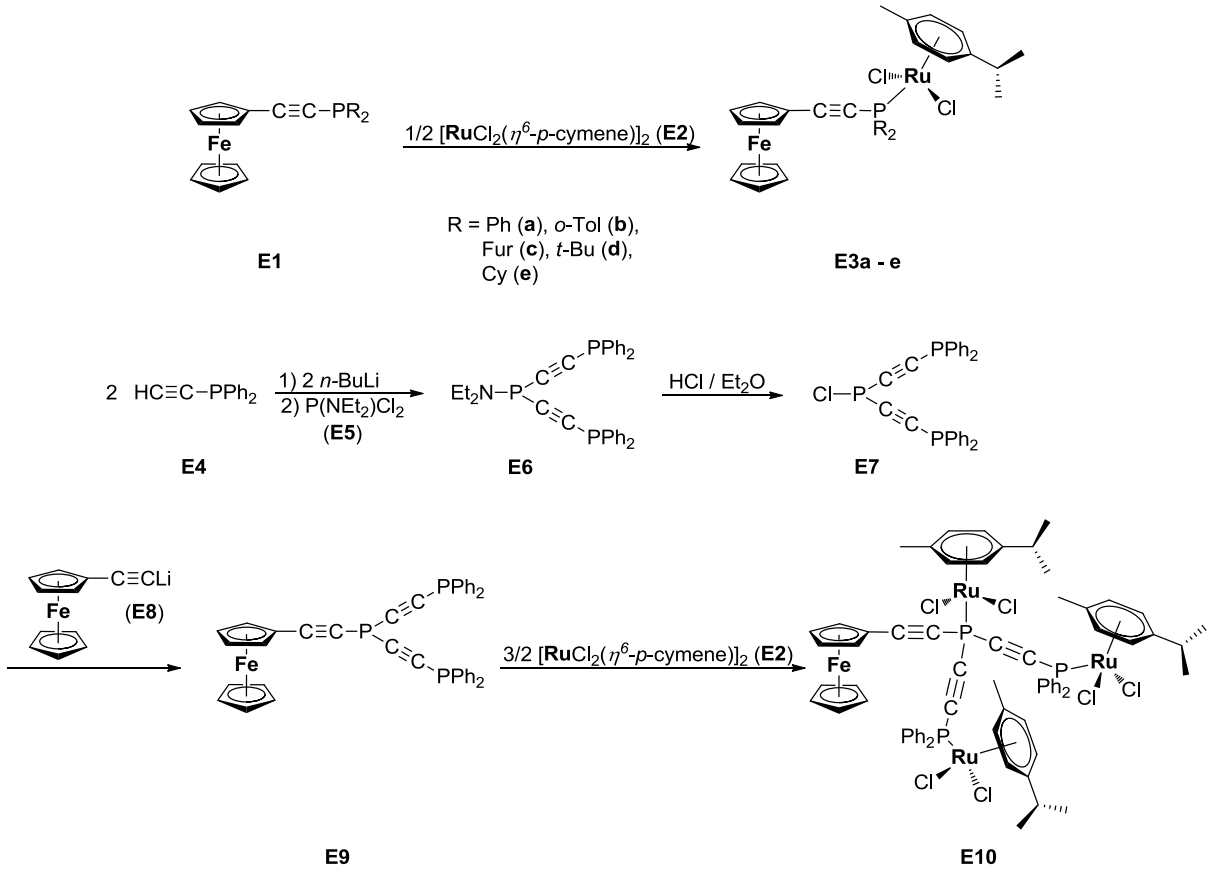

Scheme H3. Formation of heterodinuclear complexes **E3a** – **e** (top) and synthesis of tetrametallic **E10** (bottom).

To clarify whether strong or weak electron donating groups at the phosphorus atom are responsible for the activity, we applied the newly synthesized complexes as catalysts in the ruthenium-catalyzed addition of benzoic acid to propargyl alcohol for the synthesis of *β*-oxo propyl benzoate. The highest conversion was obtained with tetrametallic **10** which is most probably due to to synergistic and cooperative effects between the appropriate transition metals which improves the catalytic activity with increasing number of active centers present in one molecule. Compared to the literature-known catalysts with either Lewis-basic or electron-poor phosphines, no general trend concerning the Lewis-basicity or steric factors could be deduced. It is most probably a combination of both issues at which electron-poor ligands, however, are best suited. Moderate electron-rich species are only effective catalysts, when they possess bulky ligands.

Chapter F

This Chapter contains the synthesis, characterization and application in Suzuki-Miyaura cross-couplings of a series of imidazoles 1-(4-X-C_6H_4)-4,5-R_2-^{c}C_3HN_2 (**F3a**, X = Br, R = H; **F3b**, X = I, R = Me; **F3c**, X = H, R = Me; **F5**, X = Fc, R = H; **F7**, X = C≡CFc, R = H; **F9**, X = Ph, R = Me), phosphino imidazoles 1-(4-X-C_6H_4)-2-PR'$_2$-4,5-R_2-^{c}C_3N_2 (**F11a** – **k**; X = Br, I, Fc, FcC≡C, Ph; R = H, Me; R' = Ph, Cy, Fur), imidazolium [1-(4-X-C_6H_4)-3-R''-4,5-R_2-^{c}C_3HN_2]I (**F16a**; X = Br, R = H, R'' = *n*-Bu; **F16b**, X = Br, R = H, R'' = *n*-Oct; **F16c**, X = I, R = Me, R'' = *n*-Oct, **F16d**, X = H, R = Me, R'' = *n*-Oct) and phosphino imidazolium salts [1-C_6H_5-2-PR'$_2$-3-*n*-Oct-4,5-Me_2-^{c}C_3N_2]PF_6 (**F17a**, R' = Ph; **F17b**, R' = Cy) or [1-(4-PPh_2-C_6H_4)-3-*n*-Oct-4,5-Me_2-^{c}C_3HN_2]PF_6 (**F20**) (Scheme H4). The applied synthesis methodologies include alkylation, metallation, *P,C* coupling (Stelzer) and *C,C* cross-coupling reactions (Suzuki-Miyaura, Negishi, Sonogashira). In addition the σ donor ability was verified by $^{31}P\{^1H\}$ NMR measurement of the $^1J(^{31}P\text{-}^{77}Se)$ coupling constants of the appropriate seleno phosphines 1-(4-X-C_6H_4)-2-P(=Se)R'$_2$-4,5-R_2-^{c}C_3N_2 (**F11a-Se** – **f-Se**; X = Br, I; R = H, Me; R' = Ph, Cy, Fur).

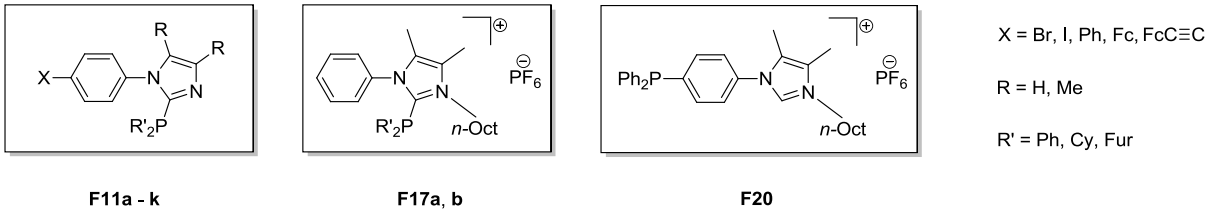

Scheme H4. Overview of the phosphino imidazoles and phosphino imidazolium salts.

All newly prepared phosphino imidazoles and imidazolium salts were applied in the Suzuki-Miyaura cross-coupling of 2-bromo toluene with phenylboronic acid as model reaction utilizing [$Pd(OAc)_2$] as palladium source. It could be observed that the more electron-rich the phosphines are, the more active and productive the catalyst system is. The phosphino imidazolium system showed higher activity and productivity compared to their neutral derivatives due to better solubility. In addition, it was observed that the halide at the phenylene unit is reactive and must be replaced by innocent organic or organometallic moieties, otherwise the appropriate C-Br or C-I bonds are involved in the catalytic reactions.

In the coupling of *non*-activated 4-chloro toluene at low catalyst loadings excellent conversions with TON values up to 8800 could be obtained by applying 1-(4-I-C_6H_4)-2-PCy_2-4,5-Me_2-^{c}C_3N_2 (**F11e**) as ligand. Furthermore, the cyclohexyl derivative **F11e** was used in the synthesis of sterically hindered biaryls at only 50 °C. Compared to the biphenyl ligand, first

described by Buchwald[F18a,d], significantly higher conversions can be achieved. In comparison with the trialkyl phosphino ligands by Fu [F18c] and Beller [F18b] conversions within the same range were observed.

The phosphino imidazolium salts were additionally tested in the coupling of 2-bromo toluene with phenylboronic acid in [BMIM][PF_6] showing lower conversion when compared to the reaction in 1,4-dioxane, recycling proved unsuccessful as well. The inactivity, most probably caused by the formation of stable 1,3-dialkylimidazole-2-ylidene palladium complexes, could not be overcome by applying [BDMIM][BF_4]. Furthermore, precipitation of metallic palladium occurred during the catalytic reaction indicating that the catalytic species is only active for a short period leading to rapid decomposition. This is most probably attributed to the lower σ donor ability of the ionic phosphines and hence insufficient stabilisation of the active species.

Chapter G

Mono- and bidentate phosphino imidazoles of type 1-(4-PR_2-C_6H_4)-4,5-Me_2-1*H*-C_3HN_2 (**G4a**, R = Ph; **G4b**, R = Cy) and 1-(4-PR_2-C_6H_4)-2-PR'_2-4,5-Me_2-1*H*-C_3N_2 (R = Ph: **G6a**, R' = Ph; **G6b**, R' = Cy; **G6c**, R' = Fur; R = Cy: **G6d**, R' = Ph; **G6e**, R' = Cy; **G6f**, R' = Fur) can be synthesized following straightforward synthesis methodologies as depicted in Scheme H5. The reaction of the diphosphino imidazoles with [$PdCl_2(SEt_2)_2$] gave palladamacrocycles of type [Pd(1-(4-PR_2-C_6H_4)-2-PR'_2-4,5-Me_2-1*H*-C_3N_2)Cl_2]$_2$ which are, however, insoluble in common organic solvents.

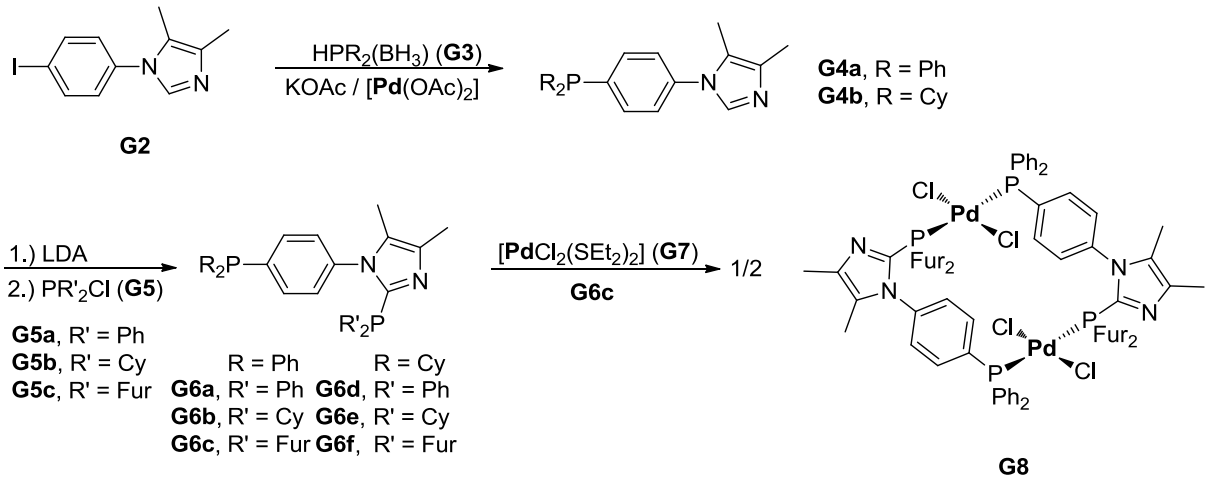

Scheme H5. Synthesis of diphosphino imidazoles **6a** – **f** and macrocyclic **8**.

The mono- and bidentate phosphino imidazoles **G4** and **G6** were applied in the palladium-catalyzed Suzuki-Miyaura reaction of 2-bromo toluene with phenylboronic acid as model reaction. All *in situ* generated phosphino palladium species showed moderate to high catalytic activity toward the formation of 2-methyl biphenyl, however, the mono-phosphines being less active and productive. Similar activities are observed for the phenyl and cyclohexyl diphosphine systems. Diphosphines carrying weak σ donating furyl groups show productivities comparable to the appropriate mono-phosphines. Molecule 1-(4-PCy_2-C_6H_4)-2-PPh_2-4,5-Me_2-1*H*-C_3N_2 (**G6d**) was applied as ligand in the coupling of 4-chloro toluene with phenylboronic acid and showed excellent productivities with TONs up to 8900. Furthermore, the diphosphine **G6d** was applied in the synthesis of *ortho*-substituted biaryls with a palladium loading of 0.05 mol% at 50 °C showing good to excellent conversions which shows, compared to other catalytically active species [G2b,f,G15,G16] reported by Fu, Beller and Buchwald, at least the same or higher productivities at lower catalyst loadings and lower reaction temperatures.

Acknowledgement/Dank

I'm done! ☺ Die Arbeit ist fertig! ☺ Das Werk vollbracht! ☺

Das wäre jedoch nicht ohne Hilfe und Unterstützung möglich gewesen. Daher möchte ich an dieser Stelle all denen Danken, die mir in den letzten Jahren unterstützend und aufmunternd zur Seite standen. Wen ich vergessen haben sollte: Sorry!

Danke an…meinen Chef Prof. Dr. H. Lang für die Aufnahme in die tolle Arbeitsgruppe, für die Freiheiten die er mir bei der Wahl des Themas gelassen hat, das gewährte Vertrauen, die Unterstützung, die hilfreichen Diskussionen und die Möglichkeit im Ausland zu forschen.

Danke an…Prof. Dr. S. Spange für die Anfertigung des Zweitgutachtens und an seine Mitarbeiter Dr. A. Seifert und Dr. R. Lungwitz für die Aufnahme von Festkörper-NMR Spektren und für das Ein oder Andere „Leihen" von Chemikalien zu Testzwecken.

Danke an…Prof. Dr. A.J. Arduengo, III für die freundliche Aufnahme in seine Arbeitsgruppe und die Unterstützung während meines Aufenthaltes in Tuscaloosa/USA.

Danke an…Dr. P. Ecorchard, D. Schaarschmidt und Dr. T. Rüffer für das Anfertigen der Einkristallröntgenstrukturanalysen und ihrer Hilfe bei der Auswertung.

Danke an…U. Stöß und J. Fritzsch für das Messen der Elementaranalysen.

Danke an…B. Kempe und Dr. R. Buschbeck für die Aufnahme der Massenspektren.

Danke an…N. Rüffer, D. Grimm, U. Stöß und J. Rutter für ihre organisatorische und nicht-chemische Unterstützung.

Danke an…Dr. U. Siegert und Dr. H. Petzold für ihre Hilfestellung bei NMR Problemen.

Danke an…Dr. Roy und Dieter für das Korrekturlesen dieser Arbeit.

Danke an…meine Nicht-mehr-Mitstreiter und Kommilitonen Dr. Ron, Dr. Sascha und Dr. Alex für die zahlreichen, fruchtbaren Diskussion, sowohl in chemischen als auch nicht-chemischen Bereichen.

Danke an…meine lieben (Ex)Laborkollegen FrÄnk, Domi, Claus, Chrischi und Dirki-in der B113 hat das Arbeiten echt Spaß gemacht.

Danke an…meine (Ex)Kollegen und Freunde aus den anderen Laboren (AJ (:-*), Colin, Mani (Muppi), Mombi, Ric, Ron (9 Jahre!), Roy, Uwe, …) für ihre Unterstützung, die vielen fruchtbaren chemischen Diskussionen, die fröhlichen Grillabende und den Spaß innerhalb und außerhalb der Chemie.

Danke an…die gesamte AG Lang für das tolle Arbeitsklima und die stete Hilfsbereitschaft.

Danke an…meine außeruniversitären Freunde und meine Familie, die mir immer unterstützend zur Seite standen und zum Glück nix mit Chemie zu tun haben.

Publications, Oral Presentations, Poster

Publications

1.) **Electrochemical and DFT-studies of Substituted Thiophenes.**

M. Al-Anber, B. Milde, W. Alhalash, H. Lang, R. Holze *Electrochim. Acta* **2008**, *53*, 6038 – 6047.

2.) **Palladiumdichloride (ferrocenylethynyl)phosphanes and their Use in Pd-catalyzed Mizoroki-Heck and Suzuki-Miyaura Carbon–Carbon Cross-Coupling Reactions.**

A. Jakob, B. Milde, P. Ecorchard, C. Schreiner, H. Lang *J. Organomet. Chem.* **2008**, *692*, 3821 – 3830.

3.) Metallocenyl Phosphine Palladium Dichlorides: Synthesis, Electrochemistry and their Application in *C,C* Coupling Reactions.

B. Milde, M. Lohan, C. Schreiner, T. Rüffer, H. Lang *Eur. J. Inorg. Chem*. **2011**, 5437 – 5449.

4) **Fundamental Study of (Ferrocenylethynyl)phosphines: Correlation of Steric and Electronic Effects in *C,C* Cross-Coupling Reactions.**

B. Milde, D. Schaarschmidt, P. Ecorchard, H. Lang *J. Organomet. Chem*. **2012**, *706-707*, 52 – 65.

5) **(Ethynylferrocenyl)phosphine Ruthenium Complexes in Catalytic *β*-Oxopropyl Benzoate Formation**.

B. Milde, T. Rüffer, H. Lang *Inorg. Chim. Acta* **2012**, 387, 338 – 345.

6) **Phosphino Imidazoles and Imidazolium Salts for Suzuki-Miyaura *C,-C* Coupling Reactions.**

B. Milde, D. Schaarschmidt, T. Rüffer, Heinrich Lang *Dalton Trans*. **2012**, 41, 5377 – 5390.

7) **Synthesis, Electrochemistry, Spectro-electrochemistry and Solid State Structures of Palladium Biferrocenylphosphines and Their Use in *C,C* Cross-Coupling Reactions.**

M. Lohan, B. Milde, S. Heider, J. M. Speck, S. Krauße, D. Schaarschmidt, T. Rüffer, H. Lang *Organometallics* **2012**, 31, 2310 – 2326.

8) **Imidazole Phosphines: Synthesis, Reaction Chemistry and Their Use in Suzuki-Miyaura *C,C* Cross-Coupling Reactions.**

B. Milde, R. Packheiser, S. Hildebrandt, D. Schaarschmidt, T. Rüffer, H. Lang *Organometallics* **2012**, 31, 3661 – 3671.

Oral Presentations

1.) **Metallorganische Chemie – Organometallische Chemie: Eine Arbeitsgruppe stellt sich vor.**

B. Milde, H. Lang, Doktorandenseminar TUC, 12.06.2008, Chemnitz/Germany.

2.) **Ethynylferrocenyl Phosphine-based Catalysts for Cross-Coupling Reactions.**

B. Milde, H. Lang, International Main-Group-Element and Organometallic Meeting, 24. – 27.09.2009, Bad Schandau/Germany.

3.) **Homogeneous Catalysis: New Aspects In Carbon–Carbon Bond Forming Reactions.**

B. Milde, H. Lang, 1st Symposium for Global Challenges for Sustainable Development 2010, 25. – 26.02.2010, Rennes/France.

Posters

1.) **Metallodendrimere und multimetallische Übergangsmetall-Komplexe als Katalysatoren für Mizoroki-Heck- und Suzuki-Miyaura-Kreuzkupplungs-reaktionen.**

C. Schreiner, B. Milde, D. Friedrich, A. Jakob, A. Nicolai, H. Lang, 40. Jahrestreffen Deutscher Katalytiker, 14. – 16.03.2007, Weimar/Germany.

2.) **Ferrocenyl Phosphine-based Catalysts for Suzuki-Miyaura Cross-Coupling Reactions.**

B. Milde, S. Tripke, D. Schaarschmidt, A. Jakob, H. Lang, 7th Ferrocene Colloquium, 16. – 18.02.2009, Düsseldorf/Germany.

3.) **Ferrocenyl Phosphine-based Catalysts for Suzuki-Miyaura Cross-Coupling Reactions.**

B. Milde, S. Tripke, D. Schaarschmidt, A. Jakob, H. Lang, 42. Jahrestreffen Deutscher Katalytiker, 11. – 13.03.2009, Weimar/Germany.

4.) **Imidazol-basierende Katalysatoren für Kohlenstoff–Kohlenstoff-Kreuzkupplungs-reaktionen.**

B. Milde, H. Lang, 43. Jahrestreffen Deutscher Katalytiker, 10. – 12.03.2010, Weimar/Germany.

5.) **Metallocenyl-based Catalysts for *C,C* Coupling Reactions.**

B. Milde, M. Lohan, H. Lang, 44. Jahrestreffen Deutscher Katalytiker, 16. – 18.03.2011, Weimar/Germany.

Curriculum Vitae

Personal Information

Name:	Bianca Milde
Date of Birth:	17.08.1983
Place of Birth:	Lichtenstein
Nationality:	German

Education

10/2007 to present	Ph. D. Thesis, Chemnitz University of Technology, Chemnitz/ Germany, Department of Inorganic Chemistry (Prof. Dr. Heinrich Lang) Thesis: (Ethynyl-)Ferrocenyl Phosphine Palladium Complexes and (Bis-)Phosphinoimidazol(e/ium) Compounds and their Application in Homogeneous Catalysis
09/2008 – 11/2008	Visiting Scholar, University of Alabama, Tuscaloosa/USA, Department of Organic Chemistry (Prof. Dr. A. J. Arduengo, III) Funded by a short-time fellowship for Ph.D. students (DAAD)
02/2006 – 03/2006	Practical Training, J. Heyrovsky Institute of Physical Chemistry, Prague/Czech Republic, Department of Organometallic Catalysis (Dr. Jiri Ceijka/Dr. Karel Mach)
10/2002 – 09/2007	Diploma in Chemistry, Technical University of Chemnitz, Chemnitz/Germany Thesis: Übergangsmetallkomplexe für die Homogene Katalyse (Prof. Dr. Heinrich Lang)
09/1994 – 07/2002	Prof. Dr. Max Schneider Gymnasium, Lichtenstein/Germany, A Levels
08/1990 – 08/1994	Heinrich-von-Kleist Grundschule, Lichtenstein/Germany

Selbstständigkeitserklärung

Hiermit erkläre ich an Eides statt, dass ich die vorliegende Promotionsarbeit mit dem Titel „(Ethynyl-)Ferrocenyl Phosphine Palladium Complexes and (Bis-)Phosphinoimidazol(e/ium) Compounds and their Application in Homogeneous Catalysis“ selbstständig und ohne unzulässige Hilfsmittel angefertigt habe. Alle wissentlich verwendeten Textausschnitte, Zitate oder Inhalte anderer Verfasser wurden ausdrücklich als solche gekennzeichnet. Die Arbeit hat in dieser oder ähnlicher Form noch keiner anderen Prüfungsbehörde vorgelegen.

Chemnitz, den 03.04.2012

Appendix

Appendix #1

(*Eur. J. Inorg. Chem.* **2011**, 5437 – 5449)

Metallocenyl Phosphine Palladium Dichlorides: Synthesis, Electrochemistry and their Application in *C,C* Coupling Reactions

Bianca Milde, Manja Lohan, Claus Schreiner, Tobias Rüffer, and Heinrich Lang

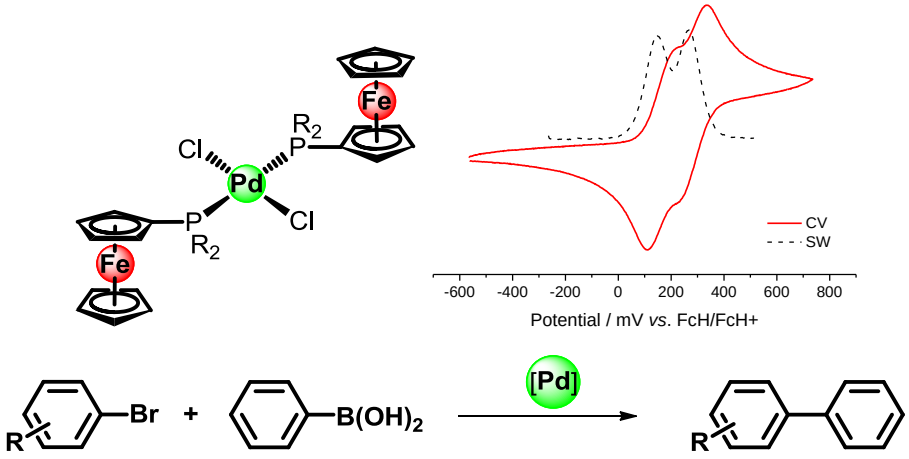

Abstract

The synthesis and characterization of a series of metallocenyl phosphines of type PR_2Mc / $Se{=}PR_2Mc$ (Mc = Fc = Fe(η^5-C_5H_4)(η^5-C_5H_5): **3a**/**4a**, R = Ph; **3b**/**4b**, R = *o*-Tol; **3c**/**4c**, R = Fur; **3d**/**4d**, R = *t*-Bu; **3e**/**4e**, R = Cy. Mc = Rc = Ru(η^5-C_5H_4)(η^5-C_5H_5): **6a**/**7a**, R = Ph; **6b**/**7b**, R = *o*-Tol; **6c**/**7c**, R = Fur; **6d**/**7d**, R = Cy) and their palladium complexes $[PdCl_2(PR_2Mc)_2]$ (Mc = Fc: **9a**, R = Ph; **9b**, R = *o*-Tol; **9c**, R = Fur; **9d**, R = *t*-Bu; **9e**, R = Cy. Mc = Rc: **10a**, R = Ph; **10b**, R = *o*-Tol; **10c**, R = Fur; **10d**, R = Cy) is reported. The structure of **4b** in the solid state confirms the tetrahedrally distorted geometry at phosphorus with the *ortho*-tolyl groups indicating steric congestion, as confirmed by ^1H and $^{13}C\{^1H\}$ NMR spectroscopy. Phosphines **3**, **4** and **9** were characterized by cyclic voltammetry using $[(n\text{-Bu})N_4][B(C_6F_5)_4]$ as

supporting electrolyte. In general, the first oxidation occurs at the phosphine metallocenyl unit(s), although the appropriate Pd complexes are oxidized at more positive potentials. Depending on the phosphines and seleno phosphines follow-up reactions occur which are discussed. In contrast, the palladium complexes show a reversible redox behavior. UV-Vis/NIR spectro-electrochemical studies carried out with **9b** indicated an electrostatic interaction among the two terminal ferrocenyls. All palladium compounds were examined as catalysts in the Mizoroki-Heck and Suzuki-Miyaura *C,C* cross coupling showing high catalytic activities, at which the results of these investigations can be correlated with electronic ($^{1}J(^{31}P\text{-}^{77}Se)$) parameters of the seleno phosphines.

Appendix #2

(*J. Organomet. Chem*. **2012**, *706-707*, 52 – 65)

Fundamental Study of (Ferrocenylethynyl)phosphines: Correlation of Steric and Electronic Effects in *C,C* Cross-Coupling Reactions

Bianca Milde, Dieter Schaarschmidt, Petra Ecorchard, and Heinrich Lang

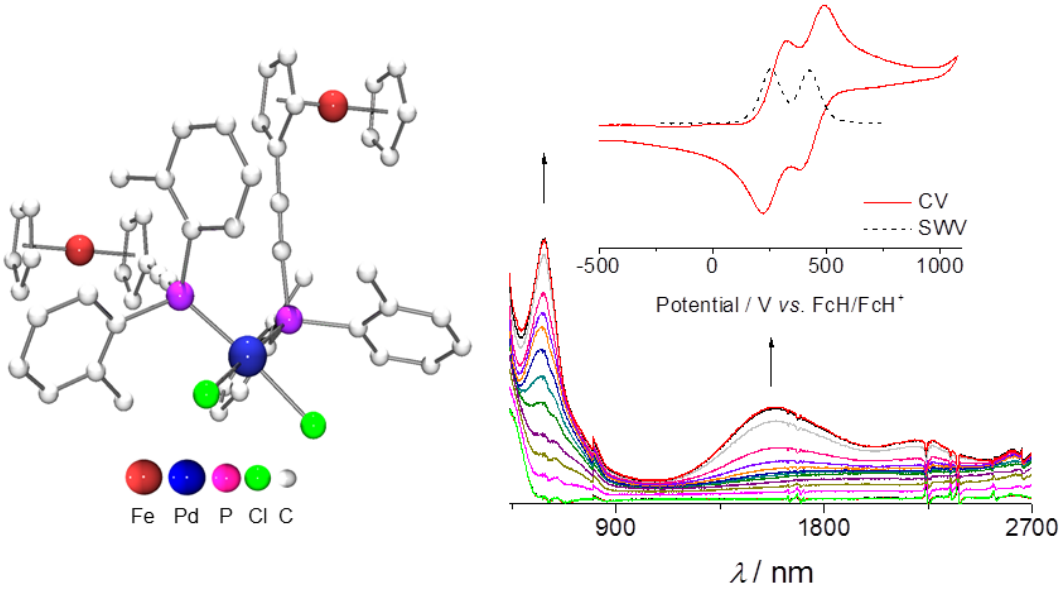

Abstract

Complexes [Pd(Cl)(μ-Cl)(P(C≡CFc)R_2)]$_2$ (Fc = Fe(η^5-C_5H_4)(η^5-C_5H_5); **6a**, R = *t*-Bu; **6b**, R = Cy) and [$PdCl_2$(P(C≡CFc)R_2)$_2$] (**7a**, R = Ph; **7b**, R = *o*-Tol; **7c**, R = Mes; **7d**, R = Fur; **7e**, R = *t*-Bu; **7f**, R = Cy) are accessible by the reaction of P(C≡CFc)R_2 (**3a** – **f**) with either [$PdCl_2$(cod)] (**5**) (cod = cyclo-1,5-octadiene) or [$PdCl_2(SEt_2)_2$] (**8**). The spectroscopic, mass-spectrometric and cyclovoltammetric data of **6** and **7** were investigated and the structures of four complexes (**6a**, **6b**, **7b**, **7c**) in the solid state determined. Complexes **7a** – **f** are mono-nuclear with palladium in a square-planar environment and show a *cis*- (**7b**) or *trans*-configuration (**7c**) with linear FcC≡CP moieties in the solid state. In contrast, **6a** and **6b** are forming dimers with a planar $Pd_2P_2Cl_2$(μ-Cl)$_2$ core of which the ethynyl ligands are above and below this plane positioned. Electrochemical studies of phosphines **3a** – **3f** and the

appropriate seleno phosphines **4a** – **4f** show after oxidation follow-up reactions, while a reversible behavior is found for the corresponding palladium complexes **6** and **7**. UV-Vis/NIR and IR spectro-electrochemical measurements of **7f** indicate moderate electronic interactions between the ferrocenyl units. All complexes are catalytically active in Mizoroki-Heck (reaction of iodo benzene with *tert*-butyl acrylate) and Suzuki-Miyaura (2-bromo toluene or 4-chloro acetophenone with phenyl boronic acid) *C,C* cross-couplings. The activity of the respective palladium catalysts can be predicted by the size of the Tolman cone angle and the electronic properties as verified by $^{31}P\{^{1}H\}$ NMR spectroscopy ($^{1}J(^{31}P\text{-}^{77}Se)$) of the phosphine ligands.

Appendix #3

(*Inorg. Chim. Acta* **2012**, *387*, 338 – 345)

(Ethynylferrocenyl)phosphine Ruthenium Complexes in Catalytic *β*-Oxopropyl Benzoate Formation

Bianca Milde, Tobias Rüffer, and Heinrich Lang

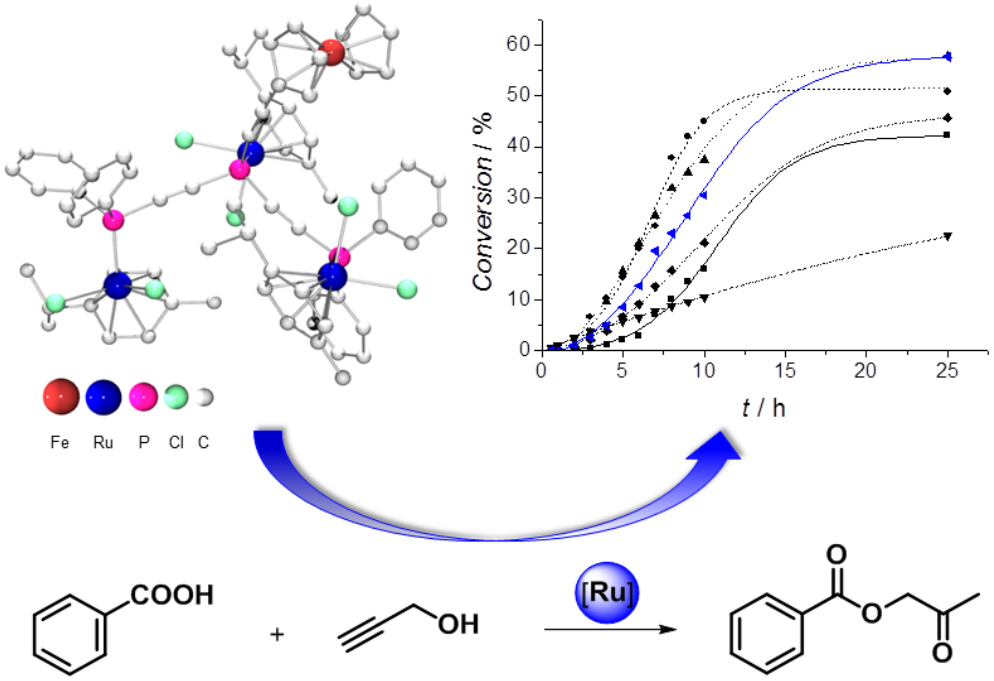

Abstract

The synthesis of a series of (ethynylferrocenyl)phosphino ruthenium compounds of type (FcC≡C)R_2P(RuCl_2(η^6-*p*-cymene)) (**3a**, R = Ph; **3b**, R = *o*-Tol; **3c**, R = Fur; **3d**, R = *t*-Bu; **3e**, R = Cy; *p*-cymene = 1-*i*-Pr-4-Me-C_6H_4; Fc = Fe(η^5-C_5H_4)(η^5-C_5H_5)) and (RuCl_2(η^6-*p*-cymene))(FcC≡C)P(C≡CPPh_2(RuCl_2(η^6-*p*-cymene)))$_2$ (**10**) resulting from the addition of ferrocenylphosphines P(C≡CFc)R_2 (**1a** – **1e**) or P(C≡CFc)(C≡CPPh_2)$_2$ (**9**) to [RuCl_2(η^6-*p*-cymene)]$_2$ (**2**) is described. The structures of **3b**, **3c** and **10** in the solid state are reported confirming the expected tetrahedral coordination sphere about the phosphorus as well as the

ruthenium atoms. Ruthenium complexes **3** and **10** are catalytically active under mild conditions in the alkyne-to-carboxylic acid coupling as it was shown for the reaction of propargyl alcohol with benzoic acid. A comparison with literature known [$Ru(PR_3)Cl_2(\eta^6$-*p*-cymene)] catalysts is presented.

Appendix #4

(*Dalton Trans.* **2012**, *41*, 5377 – 5390)

Phosphino Imidazoles and Imidazolium Salts for Suzuki-Miyaura *C,C* Coupling Reactions

Bianca Milde, Dieter Schaarschmidt, Tobias Rüffer, and Heinrich Lang

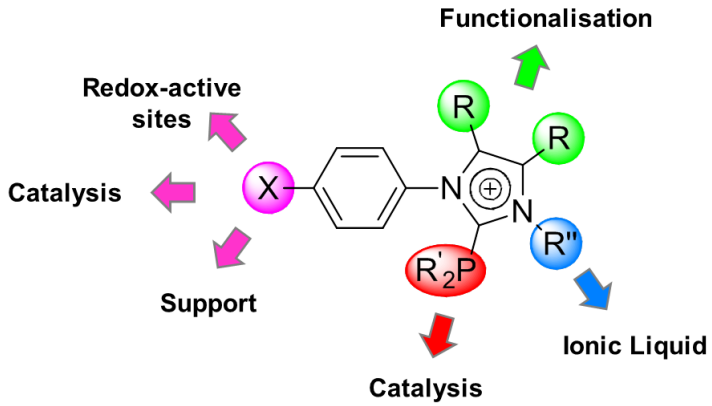

Abstract

The consecutive synthesis of imidazoles 1-(4-X-C_6H_4)-4,5-R_2-^{c}C_3HN_2 (**3a**, X = Br, R = H; **3b**, X = I, R = Me; **3c**, X = H, R = Me; **5**, X = Fc, R = H; **7**, X = C≡CFc, R = H; **9**, X = Ph, R = Me; Fc = Fe(η^5-C_5H_4)(η^5-C_5H_5)), phosphino imidazoles 1-(4-X-C_6H_4)-2-PR'$_2$-4,5-R_2-^{c}C_3N_2 (**11a** – **k**; X = Br, I, Fc, FcC≡C, Ph; R = H, Me; R' = Ph, Cy, Fur), imidazolium salts [1-(4-X-C_6H_4)-3-R''-4,5-R_2-^{c}C_3HN_2]I (**16a**; X = Br, R = H, R'' = *n*-Bu; **16b**, X = Br, R = H, R'' = *n*-Oct; **16c**, X = I, R = Me, R'' = *n*-Oct, **16d**, X = H, R = Me, R'' = *n*-Oct) and phosphino imidazolium salts [1-Ph-2-PR'$_2$-3-*n*-Oct-4,5-Me_2-^{c}C_3N_2]PF_6 (**17a**, R' = Ph; **17b**, R' = Cy) or [1-(4-PPh_2-C_6H_4)-3-*n*-Oct-4,5-Me_2-^{c}C_3HN_2]PF_6, (**20**) and their selenium derivatives 1-(4-X-C_6H_4)-2-P(=Se)R'$_2$-4,5-R_2-^{c}C_3N_2 (**11a-Se** – **f-Se**; X = Br, I; R = H, Me; R' = Ph, Cy, Fur) are reported. The structures of **11a-Se** and [(1-(4-Br-C_6H_4)-^{c}$C_3H_2N_2$-3-*n*-Bu)$_2$$PdI_2$] (**19**) in the solid state were determined. Cyclovoltammetric measurements were performed with the ferrocenyl-containing molecules **5** and **7** showing reversible redox events at E^0 = 0.108 V (ΔE_p = 0.114 V) (**5**) and E^0 = 0.183 V (ΔE_p = 0.102 V) (**7**) indicating that **7** is more difficult to

oxidise. Imidazole oxidation does not occur up to 1.3 V in dichloromethane using [(*n*-Bu)$_4$N][B(C$_6$F$_5$)$_4$] as supporting electrolyte, whereas an irreversible reduction is observed between -1.2 and -1.5 V. The phosphino imidazoles **11a** – **k** and the imidazolium salts **17a**,**b** and **20**, respectively, were applied in the Suzuki-Miyaura *C*,*C* cross-coupling of 2-bromo toluene with phenylboronic acid applying [Pd(OAc)$_2$] as palladium source. Depending on the electronic character of **11a** – **k**, **17a**,**b** and **20** the catalytic performance of the *in situ* generated catalytic active species can be predicted. As resume, more electron-rich phosphines with their higher donor capability show a higher activity and productivity. Additionally, **11e** was applied in the coupling of 4-chloro toluene with phenylboronic acid showing an excellent catalytic performance when compared to catalysts used by Fu, Beller and Buchwald. Furthermore, **11e** is eligible for the synthesis of sterically hindered biaryls under mild reaction conditions. *C*-*C* Coupling reactions with the phosphino imidazolium salts **17b** and **20** in ionic liquids [BMIM][PF$_6$] and [BDMIM][BF$_4$] were performed, showing less activity than in common organic solvents.

Appendix #5

(*Organometallics* **2012**, *31*, 3661 - 3671)

Imidazole Phosphines: Synthesis, Reaction Chemistry and Their Use in Suzuki-Miyaura *C,C* Cross-Coupling Reactions

Bianca Milde, Rico Packheiser, Stefanie Hildebrandt, Dieter Schaarschmidt, Tobias Rüffer, and Heinrich Lang

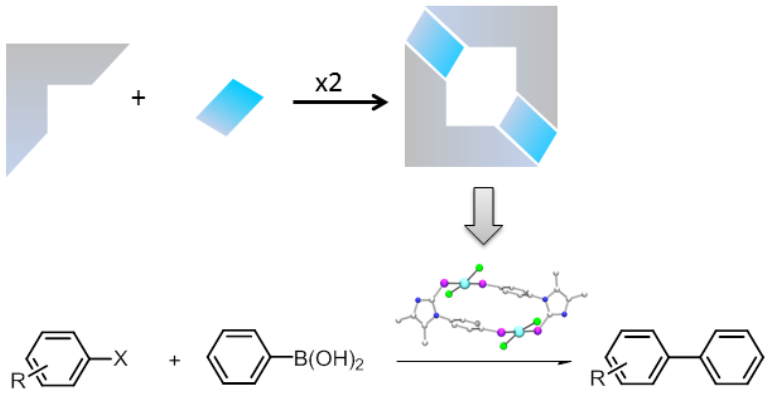

Abstract

A straightforward consecutive synthesis methodology for the preparation of phosphino imidazoles 1-(4-PR_2-C_6H_4)-4,5-Me_2-1*H*-C_3HN_2 (**4a**, R = Ph; **4b**, R = Cy) and 1-(4-PR_2-C_6H_4)-2-PR'$_2$-4,5-Me_2-1*H*-C_3N_2 (R = Ph: **6a**, R' = Ph; **6b**, R' = Cy; **6c**, R' = Fur; R = Cy: **6d**, R' = Ph; **6e**, R' = Cy; **6f**, R' = Fur) is presented. Phosphino imidazoles **6a** – **f** were reacted with [$PdCl_2(SEt_2)_2$] (**7**) giving [Pd(1-(4-PR_2-C_6H_4)-2-PR'$_2$-4,5-Me_2-1*H*-C_3N_2)Cl_2]$_2$. Single crystals of [Pd(1-(4-PPh_2-C_6H_4)-2-$PFur_2$-4,5-Me_2-1*H*-C_3N_2)Cl_2]$_2$ (**8**) suitable for single crystal X-ray structure analysis could be obtained by using the synthesis-cum-diffusion strategy confirming the formation of a neutral 18-membered Pd_2P_4 cycle with two trans-configurated palladium centers. A Pt_4P_4 cyclic compound, accessible by molecular recognition, was obtained via treatment of [Pt(dppf)(C≡C-C_6H_4-4-PPh_2)$_2$] (dppf = 1,1'-bis(diphenylphosphino)ferrocene) (**11**) with [$PtCl_2(SEt_2)_2$] (**12**). The structure of **13** in the solid state was

confirmed by crystal structure determination proving the formation of a neutral molecular square composed of Pt(dppf) and $PtCl_2$ corner units and 4-Ph_2P-C_6H_4-C≡C linkers. In addition, compounds **6a** – **f** were applied in the palladium-promoted Suzuki-Miyaura cross-coupling of 2-bromo toluene with phenylboronic acid using potassium carbonate as base. All *in situ* generated phosphino imidazole palladium species showed high catalytic activity at which the diphosphino systems featuring phenyl and cyclohexyl groups achieved the best results. Additionally, phosphine **6d** was applied in the coupling of 4-chloro toluene with phenylboronic acid and in the synthesis of sterically hindered biaryls under mild reaction conditions showing an excellent performance. In comparison with other catalytically active species, *i. e.* Beller, Fu and Buchwald, equal or higher productivities where obtained using lower catalyst loadings and lower reaction temperatures.